

The Application of Trace Element and Isotopic Analyses  
to the Study of Celtic Gold Coins and their Metal  
Sources.

Chris Bendall



Johann Wolfgang Goethe University-Frankfurt 2003

**The Application of Trace Element and Isotopic Analyses to the Study of Celtic  
Gold Coins and their Metal Sources.**

**Dissertation  
zur Erlangung des Doktorgrades  
der Naturwissenschaften**

**vorgelegt beim Fachbereich Geowissenschaften  
der Johann Wolfgang Goethe-Universität  
in Frankfurt am Main**

**Von  
Chris Bendall  
Oxford**

**Frankfurt (2003)**

**vom Fachbereich Geowissenschaften der  
Johann Wolfgang Goethe-Universität als Dissertation angenommen**

**Dekan:**

**Gutachter:**

**Datum der Disputation:**

I would firstly like to thank those people and institutions which provided coins and gold samples for analysis, they include:

Celtic coins:

S. Berger; Historisches Museum, Frankfurt

Dr. K.-J. Gilles; Rheinisches Landesmuseum, Trier

Johan van Heesch; Cabinet des Medailles, Biblioteque Royale, Brussels

Gino Languini; Wallendorf

Francois Reinert, M.A. ; Musée National d'Histoire et d'Art, Luxemburg

Dr. David Wigg-Wolf ; Fundmünzen der Antike, Johann Wolfgang Goethe-Universität (Includes the coins excavated from the Martberg, Sanctuary site)

Gold Samples:

Bruno van Eerdenbrugh; Belgium

Dr. Beda Hofmann; Naturisches Museum Bern, Switzerland

Werner Störk; AG Minifossi, Stuttgart

Secondly, I would like to thank everyone within the Institute of Mineralogy, Uni-Frankfurt, who have all helped in one way or another to make the study possible.

And last but not least my beautiful family Adi and Avi who are more amazing and wonderful than anything else.

## Table of Contents

<b>Abstract (English)</b>	<b>1</b>
<b>Abstract (German)</b>	<b>3</b>
<b>German Summary</b>	<b>5</b>
<b>I. Introduction</b>	<b>13</b>
<b>II. Aims</b>	<b>14</b>
<b>III. Synopsis</b>	<b>14</b>
<b>1.0 Numismatic Context and Ancient Metallurgical Methods</b>	<b>16</b>
<b>1.1 Numismatics</b>	<b>16</b>
<b>1.1.1 Celtic society</b>	<b>16</b>
<b>1.1.2 The Celts and their coins: origins and use</b>	<b>16</b>
<b>Phase 1 (3<sup>rd</sup> century B.C.)</b>	<b>19</b>
<b>Phase 2 (c.200-125 B.C.)</b>	<b>20</b>
<b>Phase 3 (125-60BC)</b>	<b>20</b>
<b>Phase 4 (60-20 BC)</b>	<b>21</b>
<b>1.2 Metallurgy and the Colour of Money</b>	<b>22</b>
<b>1.3 Metal Refining Processes</b>	<b>24</b>
<b>1.3.1 Gold Refining</b>	<b>24</b>
<b>1.3.2 Silver</b>	<b>24</b>
<b>1.3.3 Copper</b>	<b>25</b>
<b>1.4 Casting and Striking</b>	<b>26</b>
<b>2.0 Analytical Methods Chapter</b>	<b>28</b>
<b>2.1 Introduction</b>	<b>28</b>
<b>2.2 Sample preparation</b>	<b>28</b>
<b>2.3 EPMA</b>	<b>29</b>
<b>2.3.1 Coins</b>	<b>30</b>
<b>2.4 Trace Element Fingerprinting by LA-ICPMS</b>	<b>33</b>
<b>2.4.1 Element Fractionation</b>	<b>35</b>
<b>2.4.2 Standardisation</b>	<b>36</b>
<b>a) Nebulised Solution Calibration</b>	<b>36</b>
<b>b) 100% normalisation</b>	<b>36</b>
<b>2.4.3 Quantification</b>	<b>37</b>
<b>a) Using solution standards</b>	<b>37</b>

b) Choosing the Internal Standard	39
c) Data Reduction	39
d) The precision and accuracy of the method	39
2.4.4 Limitations of the technique	40
2.4.5 Conclusion:	41
2.5 Pb Isotopes	41
2.5.1 Solution Procedure	42
2.5.2 Laser Ablation Method	44
2.6 Cu Isotopes	46
2.6.1 Chromatographic and Mass Bias Considerations	47
a) Chromatographic considerations	47
b) Correcting for Instrument Mass Bias	48
c) Spike addition and measurement procedure	49
d) Reproducibility	49
2.6.2 Laser Method	51
2.6.3 Conclusions	53
2.7 Silver and Copper coinages	54
2.7.1 Sample preparation	54
2.7.2 EPMA	54
2.7.3 Isotopic analyses	55
2.8 Natural Gold Samples	56
2.8.1 Sample Preparation	56
2.8.2 EPMA	56
2.8.3 Trace Elements	56
3.0 Coin Chapter	57
3.1 Coin Weights	57
3.2 Coin Alloys	59
3.2.1 Scheers 23	63
3.2.2 Scheers 18	63
3.2.3 Scheers 16	64
3.2.4 Rainbow Cups	65
3.2.5 Scheers 30/I	66
3.2.6 Scheers 30/IV	67

3.2.7	Series 30/V POTTINA	68
3.2.8	Scheers 30/VI ARDA	69
3.2.9	Flans	70
3.2.10	Silver and Copper coinages	71
3.2.11	Discussion	74
3.3	Evidence for Techniques from Metallographic Studies	75
3.4	Trace Elements	78
3.4.1	Determining Useful Traces	78
3.4.2	Observing changes in metal sources	79
3.4.3	Correlations	80
	a) The correlation of Te with Ag	80
	b) The correlation of Sb and Ni with Cu	82
	c) The Pt and Au correlation	84
3.4.4	Summary	86
3.5	Pb Isotopes	87
3.5.1	Results	87
3.5.2	Controls on mixing lines	88
3.5.3	Regional comparison	90
3.6	Cu Isotopes	91
3.7	Discussion	93
3.8	Summary	96
3.9	Recommendations for future work	98
4.0	Geochemistry of Gold Sources	99
4.1	Introduction	99
4.2	Gold Deposits Types and Classification	99
4.3	Placer gold; characteristics and classification	101
4.3.1	Gold Morphology and Classification	101
4.3.2	Gold Compositions.	102
4.3.3	Gold Rimming	102
	a) Previous Studies	102
	b) Observations from this study	106
4.3.4	Inclusions	107

<b>4.4</b>	<b>Trace Elements</b>	<b>109</b>
4.4.1	Selecting elements unaffected by transport effects	110
4.4.2	Visualising the data	114
4.4.3	Summary	114
<b>4.5</b>	<b>Gold Sample Localities</b>	<b>114</b>
4.5.1	Germany	114
	a) The Rheingold	114
	b) Eder, Hessen (M-7)	118
	c) Schwarza, Thüringen (M-17)	118
4.5.2	Switzerland	119
4.5.3	France	122
4.5.4	Belgium	125
4.5.5	Scotland and Italy	126
<b>4.6</b>	<b>Discussion</b>	<b>126</b>
<b>4.7</b>	<b>Pb Isotopes</b>	<b>128</b>
4.7.1	Results	130
4.7.2	Conclusions	131
<b>4.8</b>	<b>Gold Chapter; Summary and Conclusions</b>	<b>132</b>
	<b>References</b>	<b>139</b>
	<b>Appendices</b>	<b>127</b>
	<b>Curriculum Vitae</b>	<b>141</b>
	<b>On CD-Rom -</b>	
	<b>Appendix 1 : Coin Catalogue</b>	
	<b>Appendix 2: Gold Samples</b>	
	<b>Appendix 3: Averaged EPMA results of the coin alloys</b>	
	<b>Appendix 4: EPMA results of gold samples</b>	
	<b>Appendix 5: Trace element data; gold coins</b>	
	<b>Appendix 6: Trace element data; gold samples</b>	
	<b>Appendix 7: Pb isotope data; coins and the gold samples</b>	
	<b>Appendix 8: Cu isotope data; coins and the gold samples</b>	



## **The application of trace element and isotopic analyses to the study of Celtic gold coins and their metal sources.**

The focus of this study were Celtic gold coins excavated from the Martberg, a Celtic *oppidium* and sanctuary, occupied in the first century B.C. by a Celtic tribe known as the Treveri. These coins and a number of associated coinages, were characterised in terms of their alloy compositions and their geochemical and isotopic signatures so as to answer archaeological and numismatic questions of coinage development and metal sources. This required the development of analytical methods involving; Electron Microprobe (EPMA), Laser Ablation-ICP-MS, solution Multicollector-ICP-MS and LA-MC-ICP-MS.

The alloy compositions (Au-Ag-Cu-Sn) were determined by EPMA on a small polished area on the edge of the coins. A large beam size, 50µm (diameter), was used to overcome the extreme heterogeneity of these alloys. These analyses were shown to be representative of the bulk composition of the coins. The metallurgical development of the coinages was defined and showed that the earlier coinages followed a debasement trend, which was superseded by a trend of increasing copper at the expense of silver while gold compositions remained stable. This change occurred with the appearance of the inscribed "POTTINA" coinage, Scheers 30/V. Two typologically different coinages, Scheers 16 and 18 ("Armorican Types") were found to have markedly different compositions which do not fit into the trends described above. A Flan for a gold coin, which may indicate the presence of a mint at the Martberg, was found to have an identical weight and composition as the Scheers 30/I coins, which preceded the majority of the coins found at the Martberg in the coin development chronology.

The trace element analyses were made by Laser Ablation-ICPMS using an Aridus™ desolvating nebuliser to introduce matrix matched solution standards to calibrate the measurements, which were then normalised to 100%. Quantitative results were obtained for the following elements:

Sc, Ti, Cr, Mn, Co, Ni, Cu, Zn, Se, Ru, Rh, Pd, Ag, Sb, Te, W, Ir, Pt, Pb, Bi.

The remaining elements remain problematic as they produced incorrect standardisations mainly due to chemical effects in solution such as adsorption onto the beaker walls or oxidation : V, Fe, Ga, Ge, As, Mo, Sn, Re, Os, Hg.

Changes in the sources of Au, Ag and Cu were observed during the development of the coinages through the variation of trace elements, which correlate positively with the major components of the coin alloys. Changes in the Pt/Au ratios show that the Scheers 23 coins contain distinctly different gold from the later coinages and that the Scheers 18 gold source was also different. Te/Ag was used to show that the Sch.23 coins also contained different silver and some subgroups were observed in the Sch. 30/V coins. A major change in copper source is indicated by the sudden increase of Sb and Ni with the introduction of the Sch. 30/V coins (POTTINA), which can be linked to a similar change in copper observed in the contemporary silver coinage, Sch. 55 (with a ring).

Lead isotopic analyses were made by solution- and Laser Ablation – MC-ICP-MS, The laser technique proved to be in good agreement with the solution analyses with

precisions between 1 and 0.1‰ (per mil). The development of the laser method opens the way for easy and virtually non-destructive Pb isotopic determinations of ancient gold coins. The results showed that Sch. 23 is very different from the following coinages, Sch. 16 and 18 are also different, forming their own group, and all the later “Eye” staters (Sch. 30/I-VI) lie on a mixing line controlled by the addition of copper from a Mediterranean source, probably Sardinia or Spain. An indication of gold and silver sources should be possible with further analyses of the Sch. 23 and Rainbow Cup gold coins and the Sch. 54 and 55 silver coinages.

Copper Isotopic analyses were made by solution- and Laser Ablation – MC-ICP-MS. Both techniques require further development to produce more reproducible results. The results show that there appears to be a trend to more positive  $\delta\text{Cu}65$  values for the later coinages and that the link between the copper used in the Sch. 30/V (POTTINA) coins and the silver Sch. 55 (with a ring) coins is also shown by similarly positive  $\delta\text{Cu}65$  values.

The full suite of analyses were also made on samples of gold from the region. They were mostly composed of “placer gold”, alluvial gold found in rivers. It was found that when a study is restricted to a limited number of deposits or areas then it is possible to distinguish between deposits based on the concentration of those elements which are least affected by transport related alteration processes. These elements include; the PGE’s, due to their refractory nature, and those elements which are usually present in high enough concentrations to remain relatively unaffected, eg: Cu, Pb and Sb. Due to the nature of the coin alloy it is not possible to link the gold used in the coins studied here with gold deposits, as the large amounts of Ag and Cu, added to the coin alloys, have masked the Au signature. However, further Pb isotopic analyses of gold deposits should prove useful in determining from which regions Celtic gold was derived.

## The application of trace element and isotopic analyses to the study of Celtic gold coins and their metal sources.

### Zusammenfassung

Ziel dieser Arbeit war die Charakterisierung keltischer Goldmünzen, die am Martberg, einem keltischen *oppidum* und Kultstätte, ausgegraben wurden; diese Fundstelle wurde im ersten Jahrhundert vor Christus vom keltischem Stamm der Treveri bewohnt. Die Münzen und mit ihnen assoziierte Münzfunde wurden im Hinblick auf ihre Legierungszusammensetzung, ihre geochemischen und ihre Isotopen-Signaturen untersucht, um archäologische und numismatische Fragen der Münzentwicklung und der Rohstoffquellen zu klären. Dies geschah unter Zuhilfenahme analytischer Methoden; im Genaueren sind die Elektronenstrahlmikrosonde (EPMA), Laser-Ablation (LA-) Inductively Coupled (IC)-Mass Spectrometry (MS), Lösungs-Multicollector (MC)-ICP-MS und LA-MC-ICP-MS.

Die Zusammensetzungen der Legierungen im System Gold-Silber-Kupfer-Zinn wurden durch EPMA an einer kleinen, planpolierten Stelle an den Rändern der Münzen durchgeführt. Durch Verwendung eines auf 50 µm aufgeweiteten Strahldurchmessers konnten räumlich gemittelte Analysen erstellt werden, die große Heterogenitäten der Proben kompensieren, und mit *Bulk*-Analysen der Münzen übereinstimmen. Die metallurgische Entwicklung der Münzen konnte so erkannt werden; bei späteren Prägungen wurde zunächst der Goldanteil zugunsten eines erhöhten, festen Silber/Kupferanteils abgesenkt. Im Anschluss hieran gefertigte Prägungen zeigen erhöhte Kupfer/Silber-Verhältnisse bei konstantem Goldanteil. Dieser Wechsel ereignete sich mit dem Aufkommen der beschrifteten ‚Pottina‘-Münzen, Scheers 30/V. Zwei typologisch unterschiedliche Münzgruppen, Scheers 16 und 18 (‚Armorica‘-Typ) fallen aus dem beschriebenen Trend heraus. Auch ein Rohling einer Goldmünze wurde am Martberg entdeckt und deutet so auf eine mögliche Prägestätte an diesem Ort hin, zudem dieser das gleiche Gewicht und die gleiche chemische Zusammensetzung wie die Scheers 30/I-Münzen aufweist. Diese stellen in einer zeitlichen Abfolge die Vorläufer der Hauptfunde am Martberg dar.

Die Spurenelemente wurden durch LA-ICP-MS mit einem Aridus™ Zerstäuber analysiert, der Matrix-angepasste Standardlösungen zur Kalibrierung der Messungen einbrachte. Im Anschluss wurden die Ergebnisse durch die EPMA-Analytik auf 100% normalisiert. Quantitativ wurden folgende Elemente bestimmt:

Sc, Ti, Cr, Mn, Co, Ni, Cu, Zn, Se, Ru, Rh, Pd, Ag, Sb, Te, W, It, Pt, Pb, Bi

Die weiteren analysierten Elemente waren aufgrund falscher Standardisierungen problematisch; was vor allem auf physikalisch-chemische Lösungseffekte wie Adsorption an Gefäßwänden und Oxidation multivalenter Kationen zurückzuführen ist. Ihre Liste umfaßt:

V, Fe, Ga, Ge, As, Mo, Sn, Re, Os, Hg.

Veränderungen der Gold-, Silber- und Kupferquellen im Laufe der Münzentwicklung wurden durch die Variation der Spurenelemente belegt, die mit den Hauptelementen der Münzlegierungen positiv korreliert sind. Ein Wandel des Platin/Gold-Verhältnisses zeigt, dass die Scheers 23 Münzen eine deutlich von späteren

Prägungen verschiedene Goldquelle beinhalten, ebenso ist die Herkunft der Scheers 18 Münzen eine andere. Das Tellur/Silber-Verhältnis kann aufzeigen, dass bei den Scheers 23 Proben auch eine andere Silberquelle benutzt wurde; ähnliche Schlüsse können aus der graphischen Auswertung bei einigen Untergruppen der Scheers 30/V Münzen gefunden werden. Ein deutlicher Wechsel der Kupferlagerstätte ist durch den signifikanten Anstieg der Antimon- und Nickelgehalte bei den Scheers 30/V Münzen („Pottina“) aufgezeichnet; dieser stimmt mit ähnlichen Veränderungen der Kupferkomponente bei zeitgleichen Silbermünzen überein (Probe Scheers 44 (mit Ring)).

Die Blei-Isotopie wurde durch Lösungs- und LA-MC-ICP-MS analysiert. Laser- und Lösungstechniken zeigen gute Übereinstimmung mit einer Präzision zwischen 0,1 und 1<sup>0</sup>/<sub>00</sub>. Die erstmalige Entwicklung adäquater Protokolle zur Bestimmung der Blei-Isotopie mittels Laser-Ablation eröffnet einen einfachen und quasi zerstörungsfreien Weg zur Charakterisierung antiker Goldmünzen. Die Ergebnisse zeigen einen deutliche Unterschied zwischen Scheers 23 und späteren Münzprägungen. Ähnlich hierzu Scheers 16 und 18, die eine eigene Gruppe bilden, und alle „Eye-staters“-Münzen (Scheers 30/I-VI), die auf einem Mischbereich aufspannen, der durch die Zugabe von Kupfer aus einer mediterranen Quelle – Sardinien oder Spanien – erzeugt wird. Hinweise auf die Gold- und Silberlagerstätten sollten in Zukunft möglich sein, wenn die Scheers 23 und „Rainbow cup“-Münzen wie auch die Scheers 54 und 55 Silbermünzen genauer untersucht werden.

Kupferisotopische Analysen wurden durch Lösungs- und LA- MC-ICP-MS durchgeführt. Beide Techniken verlangen der Weiterentwicklung, um reproduzierbarere Ergebnisse zu erhalten. Die bisherigen Resultate zeigen einen Trend der späteren Prägungen zu erhöhten  $\delta^{65}\text{Cu}$ -Werten. Die bereits erwähnte Verbindung zwischen Scheers 55 (mit Ring) und den Scheers 30/V (Pottina)-Prägungen wird durch ähnliche  $\delta^{65}\text{Cu}$ -Werte bestätigt.

Alle erwähnten analytischen Techniken wurden auch verwandt, um Goldproben aus der Region zu untersuchen. Meist handelt es sich hierbei um Goldseifen, alluviale Vorkommen in Flüssen. Es konnte gezeigt werden, dass eine Studie einer limitierten Anzahl von Lagerstätten oder Gebieten eine Unterscheidung zulässt, wenn man die Elemente betrachtet, die bei transportbedingten Alterierungsprozessen am wenigsten verändert werden. Diese umfassen neben den refraktären und inerten Platingruppenelementen die Elemente, die in solch hoher Konzentration auftreten, dass Alterierung sie nur unwesentlich beeinflusst, d.h. Kupfer, Blei und Antimon. Aufgrund der genutzten Legierungen ist es jedoch nicht möglich, das Gold der Münzen mit dem der Lagerstätte zu korrelieren, da die großen Beimengungen von Silber und Kupfer die Goldsignatur überlagern. Mit weiteren blei-isotopischen Analysen der Goldlagerstätten könnten jedoch weitere Rückschlüsse auf die Herkunft des keltischen Goldes gezogen werden.

## Zusammenfassung der Dissertationsschrift

### A. Einleitung

Die typologische Entwicklung antiker Münzen ist oftmals mit metallurgischen Fortschritten bei Ihrer Herstellung verknüpft. Veränderungen der Typologie gingen z.B. häufig mit neuen Legierungen wie auch veränderten Münzgewichten einher. Daher spielen metallurgische Untersuchungen an Münzen eine zentrale Rolle in unserem Verständnis der geschichtlichen Entwicklung; gerade das Zusammenspiel von Spurenelement- und Isotopenanalytik eignet sich, zwischen jüngeren und älteren wie auch gleich alten Prägungen benachbarten Regionen zu unterscheiden.

Im Rahmen dieser Arbeit wurden analytische Methoden entwickelt, die Rohstoff-Herkunft wie auch Aspekte der Münzentwicklung und –produktion aufklären. Als Proben wurden hierbei keltische Goldmünzen verwandt. Im Mittelpunkt steht hierbei eine Ausgrabung am Martberg an der Mosel, einer Siedlung und Kultstätte, die bereits im ersten Jahrhundert vor Christus vom keltischen Stamm der Treveri bewohnt worden war. Dort wurden zwischen 1994 und 1999 zahlreiche Grabungen im Rahmen des Forschungsprogramms ‚Romanisierung‘ der DFG und des Landesamtes für Denkmalpflege in Rheinland Pfalz durchgeführt. Inmitten einer Siedlung aus der späteren Eisenzeit förderten die Grabungen eine große Kultstätte zutage, inmitten der sich, von einer Umfriedung umgeben, eine Reihe von Tempeln und weiteren Bauwerken befand. Die dort gefundenen Goldmünzen wurden der archäologischen Spät-Latène, vornehmlich D2a und D2b, zugeordnet und entsprechen dem ‚Ostern Augen Staters‘-Typus. Ihre Einteilung erfolgt nach Scheers (1977) und Haselgrove (1999) in folgende typologische Gruppen:

Scheers 30/IV ohne Inschrift  
Scheers 30/V mit Inschrift (POTTINA)  
sowie  
Scheers 30/VI mit Inschrift (ARDA).

Außerdem wurden die bedeutendsten Münzen der umliegenden Region untersucht, die vor Scheers 30 IV-VI geprägt worden waren: Scheers 23, 18, 16 und 30/1. Diese entstammen alle dem Rheinland bzw. dem Westufer des Rheins. Sie sind außerdem mit den ‚Regenbogenschusselchen‘ -Münzen assoziiert, da sie der gleichen Region entstammen und die sich in zwei Gruppen einteilen lassen: Eine ältere Süddeutsche und eine jüngere Hessische.

Die Zielsetzung der Arbeit wird im Folgenden kurz skizziert und im Anschluß diskutiert.

1. Charakterisierung der Münzen in Bezug auf die Zusammensetzung ihrer Legierungen mit Ermittlung geochemischer Signaturen. Hierbei kamen folgende analytische Verfahren zum Einsatz:

a) Mikrosondenanalytik an polierten Münzrändern zur Ermittlung der Gesamtzusammensetzung einer Münze

b) Quantitative, orts aufgelöste Spurenelementanalytik mittels LA-ICP-MS (Laser Ablation – Inductively Coupled Plasma – Mass Spectrometry)

- c) Extraktion von Blei- und Kupferseparaten für die Isotopenanalytik per MC-ICP-MS (Multi-Collector-ICP-MS)
- d) Blei und Kuper-Isotopenanalytik mit LA-MC-ICP-MS

- 2.) Datenauswertung zur Ermittlung oder Überprüfung
- der chronologischen Münzentwicklung in der Region (zeitliche Veränderungen bei Verwendungen von Gold-Silber-Kupfer-Legierungen)
  - inwieweit verschiedene Lagerstätten abgebaut wurden
  - einer eventuellen Prägung direkt am Martberg; hierfür wurden Signaturen eines dort gefundenen Münzrohlings mit denen andere Münzen verglichen
  - eventueller Recyclingprozesse zur Münzgewinnung unter Verwendung älterer Münzen oder anderer Artefakte
  - einzelner Goldabbaugebiete, die Rohstofflieferanten für die Prägung gewesen sein könnten

## B. Analytik

Zur Ermittlung von Spurenelementkonzentrationen wie auch von Isotopenverhältnissen einzelner Elemente sind hochsensitive Messtechniken erforderlich. Insbesondere die ICP-Massenspektrometrie hat sich hierfür als geeignet erwiesen, wie die präzisen und genauen Messungen sowohl der Konzentrationen als auch der Blei- und Kupferisotopie an den keltischen Münzen aufzeigen. Einen Überblick der Meßgrößen und der zu ihrer Ermittlung verwandten Geräte zeigt folgende Tabelle:

Daten	Analytische Technik
Hauptelemente (Au, Ag, Cu, Sn & Pb)	Elektronenstrahlmikrosonde (Jeol 8900)
Mikrostrukturelle Untersuchungen	Elektronenstrahlmikrosonde (Jeol 8900)
Spurenelemente	LA-ICP-MS (Finnigan Element)
Pb-Isotopie	MC-ICP-MS (Finnigan Neptune)
Cu-Isotopie	MC-ICP-MS (Finnigan Neptune)

### Hauptelemente und Mikrostrukturelle Untersuchungen

Die Hauptelementkonzentrationen wie auch mikrostrukturellen Untersuchungen wurden mit der Elektronenstrahlmikrosonde durchgeführt. Zuerst wurde eine kleine Fläche an den Ecken der Münzen planpoliert, so dass die zu messende Legierung frei von korrodierter Oberfläche ist und ein Silber- wie auch Kupferverlust auszuschließen ist. Diese hohen Silber- und Kupferanteile in den Legierungen sind sehr heterogen verteilt, so dass ein aufgeweiteter Elektronenstrahl von 50 µm nötig ist, um eine räumlich gemittelte, aussagekräftige Analyse zu erhalten. Strukturelle Untersuchungen (Auftreten von mehreren Legierungen durch Entmischung etc.) wurden mit Rückstreuелеktronenbildern durchgeführt, die unterschiedliche Phasen optisch auflösen kann.

### Spurenelemente

Die im Rahmen dieser Arbeit entwickelte Methode zur Ermittlung von Spurenelementkonzentrationen besteht aus einer Kombination einer Standardisierung mit externem Lösungsstandard (Pickhardt et al. 2000) und einer

Normalisierung (Gratuze et al. 1993) auf 100%. Ein Satz von Matrix-angepaßten Standardlösungen wurde erstellt – da keine Festkörperstandards verfügbar sind - und durch einen Zerstäuber zur ICP-MS geführt. Standard- und ‚Blank‘-Messungen wurden zu Beginn jeder Messreihe erstellt. Ein Standard wurde während eines Messtages mehrfach gemessen, um instrumentellen Drift aufzuzeichnen. Mitsamt des Kupfers und des Silbers ist so eine Gruppe von etwa 30 Spurenelementen gemessen worden.

Die erhaltenen Ergebnisse wurden standardisiert. Dies geschah unter der Annahme, dass die Summe aller gemessenen Konzentrationen der Gesamtsumme abzüglich des Goldgehalts entspricht. Dieser wurde durch Mikrosondenmessung ermittelt und dann als interner Standard zur Normalisierung (100%) der Ergebnisse verwandt.

Das oben beschriebene Arbeitsverfahren zur Standardisierung der Laserablation-Analysen erlaubt Quantifizierung für folgende Elemente:

Sc, Ti, Cr, Mn, Co, Ni, Cu, Zn, Se, Ru, Rh, Pd, Ag, Sb, Te, W, Ir, Pt, Pb, Bi.

Die übrigen untersuchten Elemente verhalten sich problematisch, da sie inkorrekte Standardisierungen ergeben. Dies ist hauptsächlich aufgrund chemischer und physikalischer Effekte in den Lösungen (wie Adsorption an den Becherwänden oder Oxidation multivalenter Elemente) zurückzuführen und betrifft die Elemente

V, Fe, Ga, Ge, As, Mo, Sn, Re, Os, Hg.

### **Blei-Isotopie**

Die Blei-Isotope wurden sowohl mittels Lösungs- wie auch Laser Ablation-ICPMS gemessen. Für die Analyse der Lösungen wurde ein im Rahmen dieser Arbeit modifiziertes chromatographisches Trennverfahren angewandt, welches auf einem zweistufigen Prozeß basiert. In einer erste Stufe werden die Gold- und Silberbestandteile in der Legierung der Münzen entfernt, während in der zweiten Stufe Blei- und Kupferionen in zwei separate Lösungen aufgetrennt werden.

Hier wurde erstmalig ein Protokoll zur Beprobung Goldmünzen per Laserablationsmethode erstellt. Dies beinhaltet Zugabe einer elementaren Thalliumspike Lösung mittels des Aridus<sup>TM</sup> Zerstäubers (während der Ablation der Münzen), um auftretende Massenschwankungen zu korrigieren. Die Laserablation und Lösungs-Messungen weisen eine hervorragende Übereinstimmung (hinsichtlich der Präzision) zwischen 1 und 0.1<sup>0</sup>/<sub>00</sub> auf. Die Laserablation konnte so als schnelle und effiziente Methode zur Ermittlung der Blei-Isotopie der Goldmünzen eingeführt werden, welche zudem die Zerstörung und das Risiko einer chemischen Kontamination im Gegensatz zur traditionellen Lösungstechnik vermeidet.

### **Kupfer-Isotopie**

Die Lösung, die das Kupfer-Separat enthält, fällt als Beiprodukt der Blei-Chromatographie ab und bietet so zusätzliche die Möglichkeit zur Analyse der Kupfer-Isotope. Die Realisierbarkeit eines Protokolls mit *Nickel-spiked* Lösung zur Korrektur von Massenschwankungen wurde überprüft und mit der Standard-Probe-Standard Methode (*sample bracketing technique*) durch eine Kupfer-Standardlösung verglichen. Das neue Protokoll mit *Nickel-spike* erwies sich als

ausgezeichnet und lieferte exaktere Ergebnisse als das alte Verfahren. Die Laserablations-Methode wurde hier auch angewandt und zeigte zu den Lösungsmethoden vergleichbare Resultate auf, allerdings wiesen Messungswiederholungen eine große Varianz auf, so dass die Anwendung von LA-MC-ICP-MS der Weiterentwicklung bedarf.

### C. Die Münzen

Die unter Zuhilfenahme der im vorherigen Kapitel aufgeführten Verfahren erstellten Datensätze können nun zusammenfassend im Hinblick auf die Numismatik zusammengefaßt werden. Durch kombinierte Anwendung von Legierungs-, Spurenelement- und Blei-Isotopen- Datensätzen ist es möglich, die Änderung der zur Herstellung der Münzen genutzten Metallvorkommen in einem zeitlichen Kontext zu beschreiben.

Die Untersuchungen der Legierungszusammensetzung haben gezeigt, daß eine Abreicherung des Goldgehalts durch Hinzufügen einer Silber-Kupfer Komponente fester Stöchiometrie erfolgte, wie man an Sch23, Sch 30/Ia und Sch. 30 IV Münzen erkennen kann. Dieser wurde von einer zusätzlichen Entwicklung zu erhöhtem Kupfer/Silberverhältnis bei gleichbleibendem Goldgehalt bei Sch. 30/V und Sch 30/VI begleitet. Ausnahmen hiervon stellen Sch. 16 und Sch. 18 vom „Armorikanischen“ Typ dar, Fig 1.

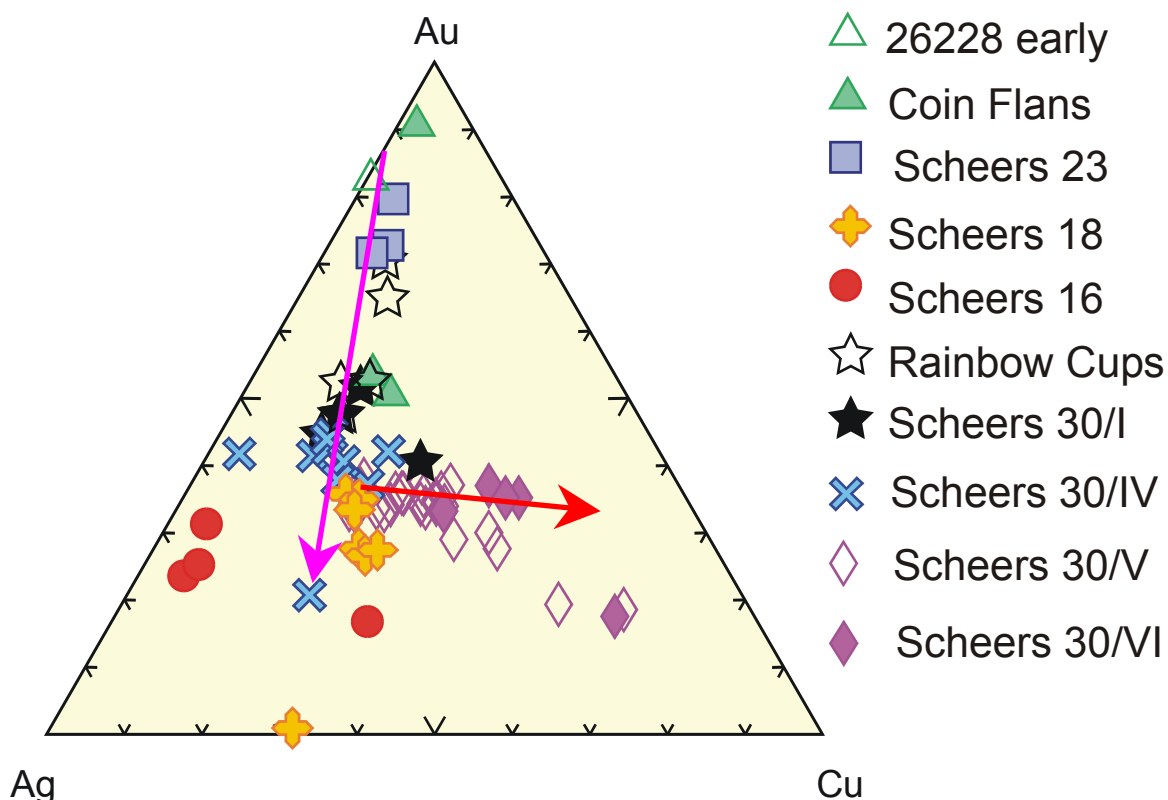


**Fig 1:** The purple line shows the progressive chronological debasement of the earlier coinages, with the red line representing the change to more copper rich alloys, which occurred during the Sch. 30/V (POTTINA) coinage.



Die Überprüfung von Korrelationen der Spurenelemente untereinander erfolgt durch graphische Auswertung, durch Auftragen von z.B. Pt/Au, Sb/Cu und Ni/Cu können Veränderungen der Metallvorkommen aufgezeigt werden. Die Goldquelle verändert sich von hohen Pt/Au Gehalten bei Sch.23 zu moderat hohen Pt/Au Gehalten bei Sch. 18 bis hin zu dem niedrigen Pt/Au Verhältnis von Sch. 16 und den Augenstater, bei denen keine weiteren distinkten Unterschiede der Goldquelle detektiert werden konnten. Hohe Pt, Os, Ir und Ru-Gehalte in den Scheers 23 Münzen können mit den von Manching untersuchten Münzen verglichen werden, bei denen mehr als ein Drittel Osmiridium Einschlüsse enthielten und von denen ein Ursprung aus einem griechischen Vorkommen vermutet wird (Gebhard et al., 1999).

Analysen unterschiedlicher Typen von Goldvorkommen (placer, Goldadern, s. nächster Abschnitt) zeigen, daß die meisten Vorkommen ausreichend Platin enthalten, um eine Konzentration, wie sie in den meisten Münzen gefunden wird, zu erzielen; dies gilt selbst für Scheers 23 Münzen mit ihren hohen Platingehalten.

Eine genauere Zuordnung der Münzen zu einer Goldquelle ist unter Nutzung der anderen Spurenelementdaten nicht möglich, da die Beimischung von Silber und Kupfer die originäre Goldsignatur zu sehr überlagert hat und lediglich Platin- und evtl. Palladiumdaten als klar zum Gold korreliert betrachtet werden können.

Untersuchungen der Te/Ag Verhältnisse deuten darauf hin, daß es eine gleichbleibende Silberquelle gegeben haben könnte, da eine lineare Korrelation ersichtlich ist. Dies trifft vor allem auf einige spezielle Münzen und Untergruppen, wie z.B. Sch. 30/Vc, zu.

Der Korrelation, die in der Veränderung der Legierungszusammensetzung von Sch. 30/IV zu 30/V erkennbar ist, wird durch den plötzlichen Wechsel in der Kupferzusammensetzung mit erhöhten Antimon- und Nickelgehalten verstärkt, der sich bis zu Sch.30/IV hinzieht. Dies korreliert mit einem ähnlichen Wechsel im Sb/Cu Verhältnis in Sch. 55 (mit Ring), einer Silberprägung, von der anzunehmen ist, daß sie aus typologischen Merkmalen mit diesen Goldmünzen zeitgleich ist. Die Spurenelementdaten erlauben daher eine konkrete Verknüpfung zwischen Silber- und Goldmünzen.

Die so gewonnenen Erkenntnisse werden durch die Blei-Isotopendaten gestützt. Diese zeigen auf, daß die Sch 23, Sch 18 und Sch 16 Münzen jeweils anderen Trends als die Hauptmenge der Münzen entsprechen. Ausnahme hiervon bildet nur die Fö105 Münze, die zwar zur Gruppe Sch18 gehört, aber am niedrigen Ende des Sch 23 Felds liegt. Die ,Regenbogenschusselchen Münzen liegen am kupferarmen Ende eines linearen Mischungsbereiches, der von den ‚Augen stater‘-Münzen beschrieben wird. Dieser Bereich wird durch Zunahme von Kupfer mit hohen  $^{207}\text{Pb}/^{206}\text{Pb}$  und  $^{208}\text{Pb}/^{206}\text{Pb}$ -Verhältnissen bestimmt. Das Kupfer scheint einem sardischen Vorkommen zu entstammen, wohingegen die Silber- und Goldvorkommen nicht identifiziert werden konnten, Fig 2.

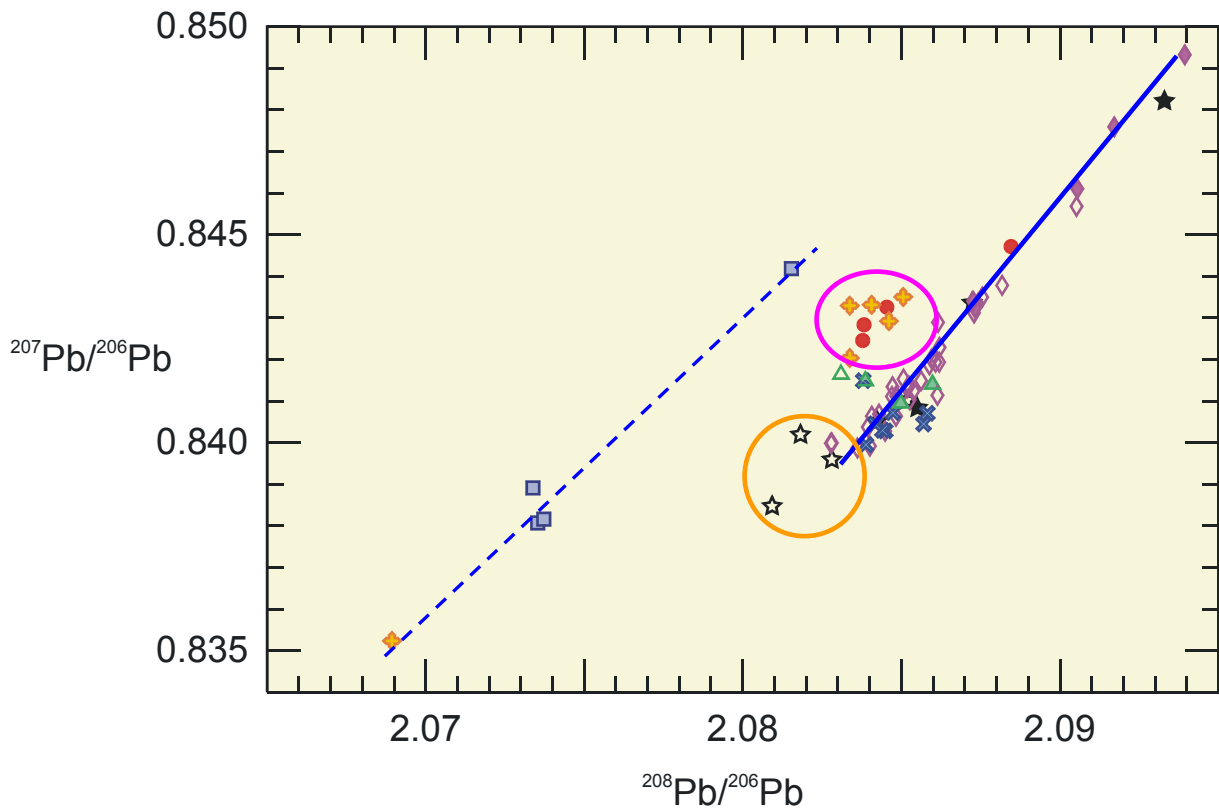


**Fig 2:** The dashed blue line highlights a possible mixing line produced by the Sch. 23 coins and the Sch. 18 coin Fö105. The purple ellipse represents the Armorikanischen type coins, Sch. 16 and 18, while the orange ellipse surrounds the Southern Regenbogenschusselchen coins. The solid blue line defines the mixing line produced by the Augen staters, which is controlled by the addition of copper with higher lead isotopic ratios.

Zusammengefasst bieten Pb-isotopische Untersuchungen die beste Methode, um mögliche Ursprungsgebiete der Münzen zu identifizieren. Mit Anwendung von Laser-Ablationsmethoden sollte in Zukunft eine große Menge von Münzen für die Analyse zugänglich gemacht werden. Die Spurenelementanalysen liefern weitergehende Detailinformationen über Änderungen der Vorkommen innerhalb einer einzelnen Region, die zuerst durch Blei-Isotope definiert wurde. Prägungen von für die lokale Geschichte besonderem Interesse sind Sch 30/I, Sch. 23 und die Regenbogenschusselchen -Münzen. Für die Sch 16 und Sch 18 Münzen ist eine weitergehende, vergleichende Untersuchungen mit anderen Münzen vom Armorikanischen -Typ interessant. Der Aufbau einer ausführlicheren Datenbank mit Blei-Isotopen-Daten, die sich auf einzelne Goldvorkommen bezieht, ist wünschenswert.

#### D. Gold

Goldminen, die dem Keltischen Kulturkreis zugeordnet werden, sind in Frankreich durch die Arbeit von Cauuet (1989) untersucht worden, erste analoge Untersuchungen bezüglich frühzeitlicher Goldgewinnung in Belgien sind ebenso durchgeführt (V. Hurt, pers. komm.) worden. Der größte Teil keltischer Goldminen, die primäre Lagerstätten in Westen Europas erschlossen haben, ist bisher aber noch nicht genauer untersucht worden. Aus diesem Grund wurden im Rahmen

dieser Arbeit auch sekundäre (Seifen-)Lagerstätten untersucht, da deren Beprobung generell leichter ist und sie zudem seit Alters her zur Goldgewinnung genutzt wurden.

Hier stellen sich zwei grundsätzliche Fragen:

Sind primäre und speziell sekundäre Lagerstätten anhand ihrer Spurenelementzusammensetzung zu unterscheiden?

und

Gibt es eine Verbindung zwischen den Goldlagerstätten und keltischen Goldmünzen?

Die untersuchten Goldlagerstätten sind die Goldseifen des Rheintales, sowie primäre Lagerstätten des Rheinischen Schiefergebirges, speziell der belgischen Ardennen. Die meisten Proben wurden von privaten Sammlern und Organisationen, die sich mit der Lagerstättenprospektion beschäftigen, zur Verfügung gestellt. Neben den Proben aus den oben genannten Gebieten entstammen noch einige dem Osten Deutschlands, Italien, der Schweiz, Frankreich und den Britischen Inseln.

Die Seifenlagerstätten wurden hierbei ausführlicher untersucht, da ihnen der größte Teil der Proben entstammt. Neben der Beschreibung der Beprobungspunkte wurde eine Charakterisierung der einzelnen Proben durch ihre Spurenelementgehalte und Isotopenverhältnisse durchgeführt.

### **Zusammenfassung:**

- 1) Jeder legierende Zusatz bei einer Goldmünze macht eine Zuordnung der Proben zu einer Goldquelle unmöglich, da Silber, Kupfer, Blei und Antimon zum einen die wichtigsten Legierungsbestandteile sind, zum anderen aber auch die zentralen Verunreinigungen der Goldquelle darstellen: Es können daher nur nichtlegierte Artefakte herangezogen werden, um sie so ihrer Herkunft zuzuordnen.
- 2) Solche Untersuchungen können nur dann aussagekräftig sein, wenn es sich um Artefakte aus lokaler Produktion handelt, für die nur wenige Lagerstätten zur Verfügung standen. Besonders zu beachten ist hierbei das Überlappen der geochemischen Signaturen bei Seifenlagerstätten, das hier Zuordnungen erschwert.
- 3) Refraktäre Elemente oder Elemente von generell hoher Konzentration erwiesen sich als besonders hilfreich zur Charakterisierung von primären und auch sekundären Lagerstätten. Dies betrifft vor allem die Platingruppenelemente (speziell Pt) sowie Kupfer, Antimon und Blei. Die Platingruppenelemente eignen sich sehr gut, da sie inert genug sind, um nicht zu alterieren oder sich mit anderen Elementen zu verbinden. Kupfer, Antimon und Blei kommen generell in solch hohen Konzentrationen vor, daß Alterierung ihre Gehalte nur unwesentlich verändert.
- 4) Spezielle Vergesellschaftungen von Spurenelementen in Seifengold können Hinweise auf das Muttergestein der Primären Lagerstätte liefern und die

physikalisch-chemischen Bedingungen, die während der Abscheidung des Golds herrschten, liefern.

Durch die kombinierte Anwendung der Haupt- und Spurenelementdaten wie auch der Blei- und Kupferisotopendaten ist es möglich, die Entwicklung antiker Münzprägungen zu rekonstruieren, wie sie aufgrund veränderter Prägungstechniken wie auch der Erschließung neuer Lagerstätten auftritt. Die Verbindung von Laser-Ablation- und Single- wie auch Multicollector-ICP-MS erlaubt solche Untersuchungen quasi zerstörungsfrei. Die Entwicklung adäquater Protokolle zur Standardisierung ermöglicht hierbei eine genaue und präzise Datenermittlung. Weiterhin konnte gezeigt werden, dass große Veränderungen der Münz-Typologie oftmals von deutlichen Veränderungen der Spurenelementkonzentrationen wie auch der Blei-Isotopensignatur begleitet werden, was auf unterschiedliche Metallquellen und deren Ausbeutung durch verschiedene Münzhersteller hinweist. Aufgrund fehlender lokaler Lagerstätten mag dies große Veränderungen der sozopolitischen Zugehörigkeit der Einwohner der Rhein-Mosel-Region in der späten Eisenzeit reflektieren.

#### Literatur:

Cauuet, B., 1999a, L'exploitation de l'or en Gaule à l'Age du Fer, In: L'or dans l'Antiquité. De la mine à l'objet, Cauuet, B. ed, Aquitania suppl. 9 (Toulouse), 31-86.

Gebhard, R., Lehrberger, G., Morteani, G., Raub, Ch., Steffgen, U., Wagner, U., 1999, Production techniques of Celtic gold coins in Central Europe, In: L'or dans l'Antiquité. De la mine à l'objet, Cauuet, B. ed, Aquitania suppl. 9 (Toulouse), 217-233.

Gratuze, B., Giovagnoli, A., Barrandon, J.N., Telouk, Ph. et Imbert, J.L., 1993, Apport de la méthode ICP-MS coulée à l'ablation laser pour la caractérisation des archéomatériaux, Rev. d'Archéométrie, 17, 89-104.

Pickhardt, C., Becker, J.S., Dietze, H-J., 2000, A new strategy of solution calibration in laser ablation inductively coupled plasma mass spectrometry for multielement trace analysis of geological samples, Fresenius J Anal Chem, 368, 173-181.

## I. Introduction

The typological and metallurgical development of ancient coins are often closely linked; changes in typology were frequently accompanied by a change of alloy and change of weight. Therefore metallurgical studies of ancient coinages have an important part to play in understanding these developments. Metallurgical, trace element and isotopic studies have the potential to show how coins are related to each other, to coinages both earlier and younger in their respective chronologies and to contemporary coinages from neighbouring areas.

This thesis describes techniques developed to acquire data for such studies from a suite of Celtic gold coins and to answer questions of coinage development, production and metal sources

The focus of this study are the Celtic gold coins excavated on the Martberg, an *oppidium* and sanctuary believed to have been occupied in the first century B.C. by the Celtic tribe of the Treveri, and associated coinages. It is situated on a 55-hectare plateau, 190m above Pommern on the Mosel River in Western Germany and is one of several *oppida*, including the Titelberg and Wallendorf, associated with the Treveri. The site was first excavated from 1885-90 by J. Klien and has been the focus of recent excavations from 1994-1990 as part of a research program titled, “*Romanisierung*”, funded by the Deutschen Forschungsgemeinschaft through the Landesamt für Denkmalpflege Rheinland Pfalz. Within a late Iron Age settlement the excavations revealed a large sanctuary containing several temples within an enclosure, and a number of associated buildings. Two inscriptions suggest that Mars was worshipped here, the principle deity of the Treveri. The gold coins are thought to be associated with the archaeological periods of the Latène, in particular D2a and D2b. Many of the inscribed Pottina coinage, were found within the Sanctuary precinct and had been “sacrificed” by being cut in half as religious offerings.

The gold coinages represented at the Martberg are those known collectively as the Eastern “Eye” Staters, which were classified, by Scheers (1977) and Haselgrove (1999) into the following typological groups:

Scheers 30/IV, uninscribed,  
Scheers 30/V, inscribed (POTTINA),  
and Scheers 30/VI, inscribed (ARDA)

Also studied were the most important coinages found in the region, which were minted before Scheers 30 IV-VI: Scheers 23, Scheers 18, Scheers 16 and Scheers 30/I, all of which are associated with the Rhineland or the left bank of the river, and the rainbow cups, which can be divided into two groups, the earlier series from Southern Germany, and a later series from Hessen.

Typological developments are linked both temporally and spatially to changes in the coinages of neighbouring tribes. Interaction between coin producing tribes can be seen in the utilisation of similar motifs, weights and alloy compositions. When studying coins it is vital to study both earlier coins from the area and from neighbouring regions to provide a context in which metallurgical, geochemical and isotopic changes can be observed. Whether these coins also share similar metal

sources is one of the questions that can be answered by techniques developed during this study.

## **II. Aims:**

- 1) To characterise the coinages in terms of their alloy compositions and their geochemical and isotopic signatures. This involved the following analytical development;
  - a) A method of Electron Microprobe analysis on polished areas of the coin edges, which provides representative alloy compositions of the coins.
  - b) A method of quantitative trace element analysis by Laser Ablation ICPMS
  - c) A method for extracting lead and copper separates for isotopic analysis by solution MC-ICPMS
  - d) A method of lead and copper isotope analysis by Laser Ablation MC-ICPMS.
- 2) To use this information to;
  - a) Define the chronology of coin development in the area in terms of changes to the Au-Ag-Cu alloy.
  - b) To investigate changes in metal sources through time, between coinages and during coinages
  - c) To investigate the possibility that a mint was located at the Martberg by comparing the signatures of an unstruck flan for a gold coin found there, with those of the coinages.
  - d) To investigate if recycling of previous coinage or other metal artefacts can be detected.
  - e) To also study the possible gold sources to see if a particular gold producing region can be associated with the coins.

## **III. Synopsis**

The following chapter is a literature review of coin development in Western Europe in the Late Iron Age and in particular the coinages studied here. This is followed by a review of what is known about metallurgical refining and coin production methods probably employed by the Celts.

Chapter two describes the analytical techniques and discusses their accuracy and precision with examples from the data.

Chapter three documents and discusses the alloy, trace element and lead and copper isotopic data.

Chapter four documents the investigation of gold deposits from the region and discusses the application of trace element and lead isotopic studies to determining the gold sources of ancient artefacts.

This is followed by a final summary, conclusions and recommendations for future studies.

## **1.1 Numismatic Context and Ancient Metallurgical Methods,**

This literature review describes the numismatic development and chronology of the coins studied and provides information on the metallurgical methods of refining and coin production, which is pertinent to the investigation of the coin alloys, and trace element signatures.

## **1.2 Numismatics**

### **1.2.1 Celtic society**

A generalised model of Celtic society throughout Western Europe in the first few centuries B.C. is difficult to make due to its fragmentary nature and the cultural diversity that resulted from this. A major challenge in the study of Celtic society and material culture is the distinct lack of literature produced by the Celts themselves. However, the sources from the Mediterranean cultures provide some information; observations, which Posidonius made in the early first century BC, were often cited by later authors such as Atheneaus, Diodorus Siculus and Strabo, and also those of Julius Caesar himself who recorded his, in his commentary *De Bello Gallico* (Gallic wars of 58-51 B.C.)(Cunliffe,1988). To a certain extent many of these general models are supported by Irish vernacular literature recorded as late as the 8<sup>th</sup> century AD (Creighton, 2000).

### **1.2.2 The Celts and their coins: their origins and use.**

The Greeks of Asia Minor in the seventh century B.C. with the use of coinage starting to spread into Central and Western Europe in the late-fourth century B.C., and becoming well established by the second century B.C invented coinage. The term Celtic coinage is applied to the coinages struck in an area stretching from the Pyrenees and Northern Italy to Southeast Britain, and from Armorica across Central Europe to the Carpathian Mountains, although not all areas were inhabited by peoples generally regarded as "Celtic".

A broad regional classification of Celtic coins can be made based on the type of the primary metal, which was used. Fig. 1.1 shows the distribution of the initial Celtic gold, silver and bronze coinages, and the Greek and Roman precursors, which they imitated (from Allen, 1980).

This project is concerned specifically with the coins of Northwest Europe, and therefore the so called „Gold Belt“. The Gold belt can be divided into two sectors, Eastern and Western, based on the different prototype coins that were used. The area east of the Rhine used the gold stater of Alexander III of Macedon while to the west in an area centred on Gaul the gold stater of Phillip II of Macedon was mainly used.



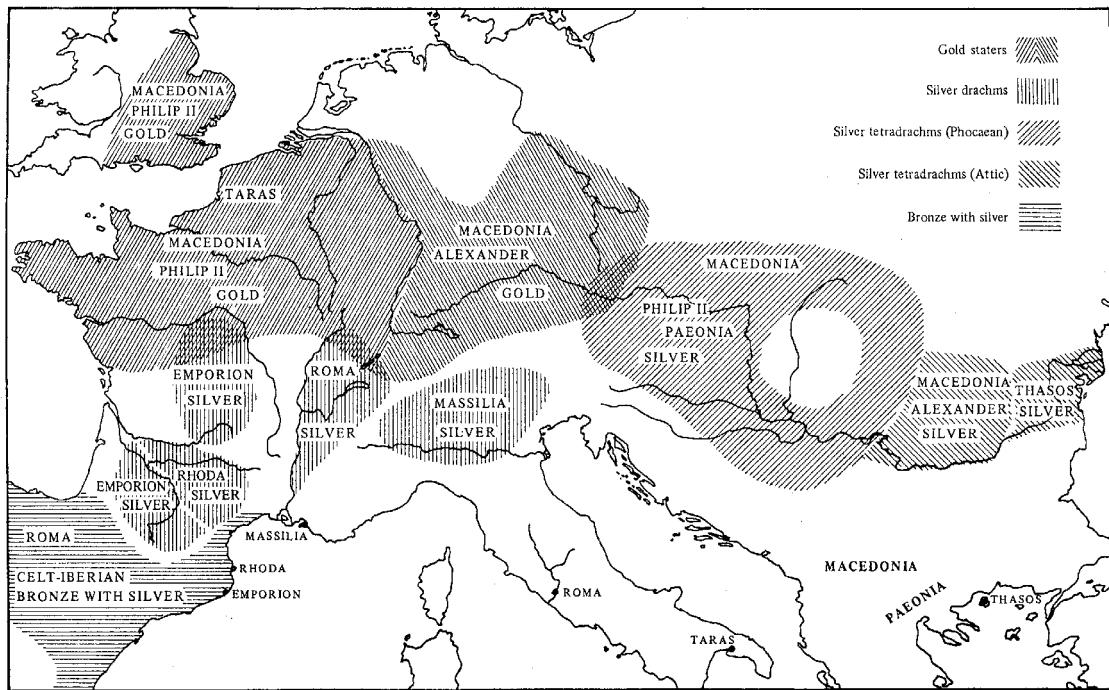


**Fig 1.1:** Distribution of Celtic coinages (Allen 1980)

The Celtic people were probably first introduced to coinage during their forays as mercenaries in the armies of the Mediterranean nations. Gold had always played an important part in Celtic culture and they were often depicted wearing an array of golden jewellery, torcs and armbands as they ferociously went into battle (Nash 1981). It is well known that while many of Mediterranean mercenaries accepted payment in baser coinages such as silver, the Celtic warriors of North western Europe, and in particular the Belgae, probably insisted on payment in gold. The gold coins paid to them and carried back to their homelands may have been initially remelted into torcs and other forms of Celtic gold work, but eventually the concept of coinage and its ability to easily exchange wealth took hold (Cunliffe, 1988). The gold stater of Phillip II of Macedon depicts a chariot drawn by four horses and the head of Apollo on the obverse. Elements of this motif can be recognised on most Celtic gold coins for the entire period of their production, from the first Celtic coinage minted, sometime in the 3<sup>rd</sup> century, until the Roman period. The motif evolves over time, the number of horses reduced to one, sometimes with wings or a human head, and the head can grow medusa like tentacles or becomes a study of only the eye, and in one case disappears entirely. The horse is a constant, however, and perhaps the main reason the original motif was accepted and prevailed in one form or another for so long, is the Celtic people's obsession with the horse as a symbol of the Earth and its power to give life, take life or make someone a king (Creighton, 2000).

Numismatic studies of coinages produced by the Celts of Gaul and Southwest Germany relied for many years on the chronology proposed by J.B. Colbert de Beaulieu (1973) and for Belgic Gaul the descriptive studies and interpretations of Simone Scheers (1977) are also of great importance. Central to Colbert de Beaulieu's chronology is the suggestion that Celtic gold coinages did not become widespread until the late 2<sup>nd</sup> cent. B.C. The major silver coinages in Northern Gaul then began to appear towards the mid-1<sup>st</sup> cent. B.C.

To a large extent these earlier chronologies were based purely on an interpretation of artistic development and historical considerations, and have been superseded as new coins have been recovered from well-defined archaeological contexts allowing many issues to be more reliably dated. Haselgrove (1999) has summarised recent work on an alternative approach in light of this new archaeological evidence, concentrating on Belgic Gaul. He argues that Colbert de Beaulieu's chronology is in need of review, and that the work of Scheers, while providing a wealth of data on the coinages, suffers in the interpretation as it attempts to equate the changes in the coinages to known historical events and to tying particular Celtic coinages to Roman precursors. He proposes instead that developments should be considered in terms of five broad periods spanning from the 3<sup>rd</sup> cent. B.C. to the early-1<sup>st</sup> cent. A.D, and that gold was already widespread in the late 3<sup>rd</sup> cent. B.C. Silver then began in the late 2<sup>nd</sup> cent. B.C.

Haselgrove is critical of the traditional method of assigning coinages to Celtic tribes. This method is based mainly on information on the location of these tribes during Caesar's Gallic Wars and the Roman period, and especially as Caesar's own testimony implies that the area was culturally and politically unstable, and settlement continuity from the 3<sup>rd</sup> cent. B.C. to the 1<sup>st</sup> cent. A.D. was unlikely.

This is also the view of Nash (1981) who notes: "No coinage can be expected to spread itself evenly over a political territory, because the distribution of coinage depends on the pattern of settlement and land use of the society using it, a fact which makes the use of distribution patterns of Celtic coinage to establish the probable territories of Celtic peoples a very unreliable tool."















Many of the earlier coin types also exhibit diffuse, overlapping distributions, which make their assignation to a particular tribe untenable. Haselgrove instead divides Belgic Gaul into Central, Southern, Western and Eastern zones.

Haselgrove's Eastern zone was the focus of this project and is centred on the area traditionally associated with the Celtic tribe of the *Treveri*, whose territory is said to have reached from the Rhine to the Maas. Recent work has focused on important tribal centres such as the Titelberg *oppidum*, Wallendorf, and above all the Martberg, where some 2000 Celtic coins have been excavated since 1994 (Wigg, 2000). Less archaeological research has been done on the right bank of the Rhine, but the numismatic framework has been well established thanks to work by Heinrichs (in print) and Schulze-Forster (in print; see also Wigg and Riederer 1998).

The main body of coin material studied here came from recent excavations at the Martberg; however, the study area was extended to cover a region spanning both banks of the Rhine. This is designed to take into account the fact that some of the earliest coinages in the region are found both east and west of the river (e.g. Scheers 16 and 23). Furthermore the 'triquetrum' gold rainbow cups from Hessen are closely related to the gold coinage of Southern Germany, which has been studied in detail by Hartmann (1976), Lehrberger (1995) and Gebhard et al (1999), providing a broader context for the results of the analyses proposed here.

Loscheider (1998), Metzler (1995), Schulze-Forster (in print) and Wigg (2000; Wigg and Riederer 1998) have looked at the coinage of the study area in more detail.

The following is a short history of the development of coinage in Belgic Gaul with special attention on the eastern sector and the coinages attributed to the Treveri. It is mostly drawn from the most recent review by Haselgrove (1999) and also highlights some of the important cultural changes and historical events, which occurred during this period. The chronology of the coinages studied is summarised in Fig. 1.2.

	West of the Rhine		East of the Rhine		
	Gold	Silver	Gold	Silver	
Phase 1 (LTC); to late-2nd cent.	 Sch. 23 ↑↑↑↑?		 Sch. 23 <i>Central Hesse</i>	<i>South Hesse</i>	<i>Central Hesse</i>
Phase 2 (LTD1); late-2nd. cent. – c. 90/85 B.C.	 Sch. 16-20	 Sch. 54	 dIT. 9439	 Sch. 56	↑↑↑↑
Phase 3 (LTD2a); c. 90/85 B.C. – c. 60 B.C.	 Sch. 30/IV ↑↑↑↑?	 Sch. 55 (o. Ringel)	 dIT. 9441	 Sch. 57/I	↑↑↑↑
Phase 4 (LTD2b); c. 60 B.C. – c. 20 B.C.	 Sch. 30/VI	 Sch. 30a	 dIT. 9442	 Sch. 57/II	↑↑↑↑

**Fig. 1.2:** Chronology of the main gold and silver coinages in the Middle Rhine region (from: Wigg and Riederer [1998])

### Phase 1 (3<sup>rd</sup> century B.C.)

As mentioned above, the Celts first experience of coinage was in the armies of Mediterranean Kings, in particular those of Macedon, and that their coinages closely imitated the Macedonian precursors.

Therefore, the earliest indigenous Gaulish coinages, which began in the Eastern and Western zones, closely imitated the philippus coinage struck by Phillip II of Macedon and his successors from c.340 B.C. onwards.

Coins found near the Moselle valley were early copies of staters minted for Phillip III at Lampsacus c.323-315 B.C. and weigh 8.1g (the originals 8.6g). Somewhat later derivatives of the phillipus have been found in a late third century B.C. context at Ribemont-sur-Ancre (Somme).

### **Phase 2 (c.200-125 B.C.)**

During this period gold coinage began to be struck over a much larger area and in greater numbers, with coins being found in hoards and settlements. It also saw the introduction of cast potin (high tin bronze), which appears at this time in the Southern and Eastern zones.

The Gold Staters of this period weigh between 8.0 and 7.0g with broader flans, c.23-27mm, than earlier phillipus imitations. The important coinages of this period include:

Scheers 8 (Gallo-Belgic A) Classes I-V with 76% to 77% gold and Classes VI-VIII with 71% to 73% gold

For the Eastern zone the Scheers 23 ¼ stater with winged Pegasus on the reverse is important occurring frequently along both banks of the Rhine (79% Gold).

Other major coinages are:

Scheers 34 janiform head and devolved philippus style horse

Scheers 32-33 backward looking horse

Scheers 16-20 Armorican type with human headed horse.

### **Phase 3 (125-60BC)**

Phase 3 saw the development of two main groups of gold, one based on the original biface stater Scheers 9 and a second based on the "eye" staters, Scheers 30/I.

The gold coins decreased in weight to more 6.0g than 7.0g and with smaller 16-18mm flans. Meanwhile the potin is of higher quality.

The entire eye series was originally attributed to the Treveri but now it is clear from the distribution of the coins that they can be divided into two separate groups. The Scheers 30/I-III eye staters belonging to the Southern Zone, and the Scheers 30/IV-VI staters to the Eastern Zone, the area inhabited by the Treveri. The typology and weight of the Class IV coins indicate that they were directly derived from the Scheers 30/I coins (Fig 1.3).

Some constraint on the date of the Scheers 30/I coins (the Southern "eye" coinages) is possible in light of recent finds. Sch. 30/I Coins have been found in a La Tène D1b pit at Condé-sur-Suippe and at the fortified site of St Thomas (Aisne), which was abandoned around the La Tène D2a/D2b transition. This indicates that the Scheers 30/I were in circulation by the first decade of the first century.

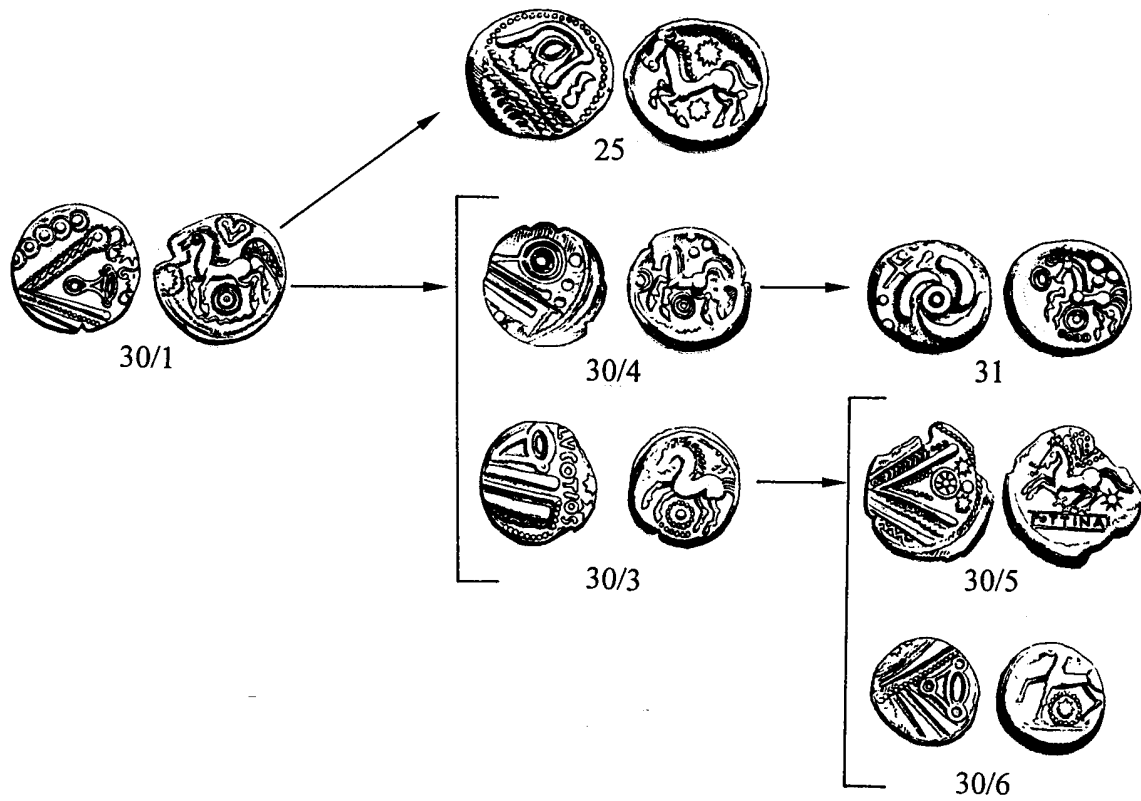


**Fig 1.3:** Chronology of the eye staters as proposed by Haselgrove (1984)

The Scheers 30/IV coinage is the first gold coinage to appear at the site of the Martberg, which is the focus of this study. The timing of this coinage is believed to be well before the end of stage 3 and that, although it is derived from Scheers 30/I, it may have been produced at a similar time to its prototype (Haselgrove, 1999).

In general, this is a period when many of the large central settlements (oppida) appeared and began to grow, and this phase sees the production of more prolific and consistent coinages. Coins found from this period also tend to be found more in settlement sites rather than scattered throughout the landscape, as was previously the case (Nash, 1981).

#### **Phase 4 (60-20 BC)**

Phase 4 covers the archaeological period from the end of La Tène D2 and into the beginning of the Roman period. It is marked by the appearance of “struck bronze” which superseded the potin coinages, and the use of legends, in mostly Roman but also Greek alphabets, which are also found on the gold coinages. Two examples from this study are the coinages of *Pottina* and *Arda*, Scheers 30/V and 30/VI respectively. Although, the *Pottina* coinage came before the *Arda*, it is not possible to fix dates to these coinages more firmly than to say they were produced late during Stage 4 and maybe related to events during and after the Roman conquest. The *Pottina* coins show a marked drop in weight and a change in alloy. The number of dies associated with 30/V is 83, double that of the 30/IV coinage (43) (Scheers,

1977) indicating that they were minted in some quantity. Although it is tempting to relate the *Pottina* coinage to events of the Gallic war, there is no specific evidence. It is known that the Treveri, the tribe that most likely produced this coinage, along with their neighbours the Remi, initially welcomed the Romans. There are suggestions in the ancient literature that subsidies were paid to friendly kings by Rome (Creighton, 2000), but whether or not this can be seen in the development of the coinage is a matter of interpretation.

The Arda coinage, Scheers 30/VI, is noticeably more localised with finds restricted to the two main *oppida*, the Titelberg and the Martberg. As mentioned above it is difficult to pin point the date of its production. However, bronze coins with the same legend are dated on the basis of Roman prototypes to the 40s-30s B.C., and a date early in this range is likely for the gold coins. Closely linked silver and bronze issues typify this issue and the contemporary issues of the region. The weights of the gold and bronze coinages are little different to the previous coinages (Scheers 30/V, Scheers 55) however; the gold coinages obviously contain much more copper giving them a reddish hue.

This brings us to the end of the coinage development and relevant history, which sets the stage for the current project. The metallurgical considerations of metal refining and coin production are now described.

## 1.2 Metallurgy and the Colour of Money

A major part of modern Celtic numismatics is based on the analysis of the metal alloys used in coinages and comparing this data with groups of coins determined through die studies (Northover, 1992, Cowell, 1998). However, the study of Celtic refining and minting techniques remains relatively untouched. This section describes previous metallurgical studies of Celtic coinages and is followed by a review of the metal refining and coin manufacture techniques that were employed by the ancients and possibly by the Celts.

Although we commonly refer to coinages as Gold, Silver or Copper, they are in fact hardly ever made of the pure element. Gold artefacts and in particular the coinages are often in reality composed of a ternary Au-Ag-Cu alloy with significant traces of other elements such as antimony, tin and lead.

The purity of Celtic gold coins can be approximately determined by colour. It has been shown that in Britain copper and silver were often added to electrum to alter its colour more towards that of pure gold (Northover, 1992). Figure 1.4 shows the colour produced by the range of Au-Ag-Cu alloys, the stippled areas show the composition of the majority of Celtic coins from Britain, which have been analysed (modified from Northover 1992). These analyses have shown that the original British Celtic coinages have compositions closer to the broad-flan staters of Phillip II of Macedon, upon which they were based. The latter were produced from refined gold containing 98-99% gold (Northover, 1992). This analytical survey of the British Celtic gold coinage including data from Cowell (1998), shows that the Gallo-belgic (A,B,C,E) are linked by a common debasement mechanism, which seems to involve successive additions of a fixed proportion of silver and copper. A trend line was fitted to the linear correlation on the ternary plot, which indicated that the proportions of silver to copper were about 2:1.

Eg: Natural gold ~ 85/15% Au/Ag% + 10% Ag-Cu eutectic mixture 2:1 65/35%

The same debasement trend has also been observed in the Central Gaulish coins studied by Nieto and Barrandon, (2002).

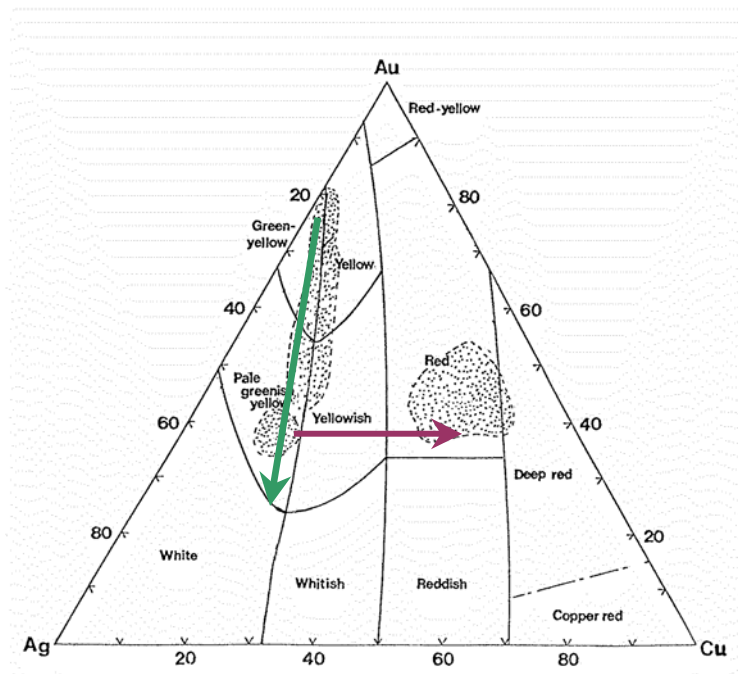


**Fig 1.4:** The Au-Ag-Cu alloy system showing the colours of the various alloys. The trend of debasement followed by the Gallo-Belgic A-E<sub>IV</sub> (Green) and then the change to copper rich coinages with constant gold contents, Gallo-Belgic E<sub>VI</sub> (purple). Modified from Northover (1999).

Northover goes on to suggest that sophisticated refining methods such as salt cementation (see gold refining section below) were unknown to the Celts of this period and it is not until the Roman domination of North western Europe that the effect of producing coinage from Roman refined gold can be seen. This is based on the consideration that during the period of the Roman occupation of Western Europe, the debasement trend described above came to an end for the British Gallo-Belgic coins and they became increasingly copper rich at the expense of silver with gold concentrations remaining relatively constant (Fig 1.4). Such a trend cannot be achieved through a debasement mechanism and requires the addition of refined gold (i.e.: free of the usual major components of native gold, Ag, Hg and Cu). However, in a recent study, fragments of crucibles from the Iron Age site of Cros Gallet (Le Chalard, Haute-Vienne) in Central France were examined by neutron activation analysis (Gratuze, 1999). The vitrified part of the crucibles were found to be enriched in silver which would indicate that salt cementation and cupellation processes may have been used to refine gold.

### 1.3 Metal Refining Processes

An understanding of the refining of gold, silver and copper, is necessary for the interpretation of trace element and isotopic signatures observed in the gold coinages. The following section summarises these processes.

#### 1.3.1 Gold Refining

Gold may occur in two general types of deposit

i) As primary mineralisation as native gold associated with quartz +/- calcite, and sulphide veins or contained within the sulphides themselves.

Or,

ii) As secondary placer deposits in rivers and streams

Gold refining techniques had been used in the Mediterranean for over 300 years before gold coinage began to be used by the Celts. Evidence of salt cementation refining has been found near the ancient birthplace of gold coinage, Lydia in Eastern Turkey (Craddock, 1995).

Salt cementation involves packing a mixture of salt and some silicate material (usually brick dust) into a parting vessel or crucible. This formed the cement which, when heated carefully with gold grains or beaten foils, converted the silver into silver chloride leaving the gold behind.



The silver could then be recovered via cupellation (Halleux 1985, Craddock 1995).

#### 1.3.2 Silver

Silver may occur in several different forms:

Native silver

„Dry Ores“ AgCl Cerargyrite or horn silver, Ag<sub>2</sub>S argentite or silver glance, and mixed ores: Ag<sub>3</sub>SbS<sub>3</sub> pyrargyrite, proussite Ag<sub>3</sub>AsS<sub>3</sub>, stephanite Ag<sub>5</sub>SbS<sub>4</sub>

Silver from electrum or copper

Silver in pyrite ores e.g. in: FeS<sub>2</sub>, CuFeS<sub>2</sub>, FeAsS<sub>2</sub>

Complex partially oxidised sulphate jarosite ores associated with enrichment zones between gossans and primary deposits

Argentiferous Lead ores PbS galena, PbCO<sub>3</sub> cerussite, PbSO<sub>4</sub> anglesite

The richer native silver and dry ores were probably exhausted by the iron age and the major sources of silver would have been argentiferous lead, jarosites and the de-silvering of copper ores, Craddock, (1995).

Native silver is rather pure Cu<0.5%, Au and Pb<0.1%, while “Dry” silver ores can contain up to 0.5% Au and 2.5% Pb (Gale and Stos-Gale, 1981)

Silver refining is the result of two steps (Bayley, J., Eckstein, K)



1. Smelting, a reducing process and
2. Cupellation, an oxidising process

Lead plays a major role in the refining of silver because molten lead and silver are highly soluble in each other and most silver ores in antiquity were in fact argentiferous lead sulphides.

An argentiferous lead bullion is produced from the first smelting step, which is cupelled to remove the lead.

During cupellation the bullion is placed on a shallow cupellation hearth and melted under oxidising conditions so that a lead oxide „Litharge“ is formed. Lead oxidises under conditions where silver remains metallic.

In antiquity the cupellation hearth was lined with porous calcium rich material like burnt and pulverized bones (bone ash) and/or clay lime mixtures. The litharge soaked into the lining forming the litharge cakes that are commonly found at archaeological excavations. The high surface tension of the molten metal allows it to remain on the surface until all the lead is oxidised leaving a pure silver button.

Litharge cakes may also contain the oxides of copper and tin, which oxidise along with the lead especially as Ag-Cu-Sn alloys were often being recycled for their silver.

Some silver can be lost during this process as the formation of  $\text{Cu}_2\text{O}$  (cuprite is miscible with silver and drops of this mixture were absorbed by the litharge). More lead is needed to avoid this. Many Roman finds show this loss and they either did not notice or did not mind the small loss.

Silver cupelled with Pb, would contain a residual Pb component of between 0.05 and 2.5%, less than 0.05% would therefore indicate no cupellation, although more than this could also be the result of Ag from PbS.

Therefore ancient silvers separated from non-plumbic ores will have the Pb isotopic signature of the Pb added during cupellation.

Other important traces include:

Zn would not survive this process and its presence would therefore indicate no cupellation.

Ag from PbS often has 0.5% Cu and between 0.1 to 1.0% Bi.

Au contents of Ag from PbS is between 0.001 to 0.1 %.

Au in Ag from jarosites and oxidised ores up to several % smelting of these ores would result in the Cu, As, Sb and Bi going into the litharge with Au and most of the Bi going into the Silver (Pernicka and Bachmann 1983).

### 1.3.3 Copper

Copper can occur as native copper in the supergene zones of copper mineralised systems, as various oxide and carbonate minerals above this zone and as sulphides below it. Copper sulphide mineralisation represents the primary occurrence and may occur in a variety of mineralisation types including sedimentary or volcanic hosted massive sulphides, magmatic sulphides, porphyry copper and skarn deposits.

During the copper refining process the gangue needs to be fluxed to remove it from the copper as a liquid “slag”. If the gangue is high in silica this requires iron or manganese oxides, if low in silica and high in iron (sulphides), it requires the addition of silica as sand.

In both cases fayalite  $\text{Fe}_2\text{SiO}_4$ , or its isomorph in which Mn replaces some of the Fe, is produced. These phases have relatively low melting points (1150-1200°C) and a low capacity to dissolve copper; therefore the slag carries all the gangue away leaving the copper metal behind.

The effect of using different fluxes on the trace element signatures was investigated via a series of experiments made by Tylecote (1977). Trace elements which are commonly found to remain after refining with concentrations over 10 ppm are;

Pb, Sb, Se, As, Ge, Zn, Ni, Fe, S, Si, Ag, Mg, Mn

NB: Mn only present where Mn oxide was used as flux

The amount of As and Sb can be drastically altered by working techniques (Mckerrrel & Tylecote, 1972). Although direct reduction smelting will retain a high proportion of these elements it is clear that bismuth is useless as a provenancing element as it segregates badly (Charles and Slater, 1970) and is extremely volatile in oxide and sulphide smelting techniques.

However, Ni, Ag and Au would be very reliable indicators of source as the Cu/Ni and Cu/Ag ratios will be the same for both ore and metal.

High As and Sb may represent direct reduction of oxide ores as Cu produced from sulphide ores requires an extra step of roasting in which the As and Sb content should be drastically reduced. In contrast, oxide ores only require reducing and fluxing to produce the copper metal thereby preserving most of the Sb and As.

#### **1.4 Casting and Striking**

To produce blanks of appropriate weight, molten metal was poured into open or two-part closed clay moulds. Experimentation has shown that, with practice, pouring into open moulds or even simply onto a flat surface can be controlled accurately enough to produce blanks within acceptable weight tolerances. However, some scholars, disagree that such methods would have been used to produce flans for gold or silver coins, and it has been suggested that metal beads or granules of the correct weight were placed in a mould, which was then put into a furnace to melt the granules (Wickens 1996). Work carried out on the site of Manching, a Celtic *oppidium* located on the Danube in Southern Germany (Lehrberger, 1995; Gebhard et al, 1999) produced a variety of detailed analyses of coins; coin moulds and kiln fragments, which lends weight to the second hypothesis. They were found at the site during excavations from 1955 to 1973 and are thought to represent the remains of gold workshops dated at 150 to 100 B.C. It was determined that gold and silver alloys were melted in coin moulds under reducing conditions, possibly achieved with a covering of charcoal, at temperatures of 1100-1250°C, produced with the aid of bellows (Gebhard et al, 1999). The indication that bellows were used was based on

the observation of a fan of gold and silver particles all dispersed in the same direction from each depression in the coin mould. This adds weight to the conclusion that the measuring out of the metals into the crucibles occurred the prior to melting.

Coins made from copper alloys, such as bronze, were cast using open or closed moulds in which a chain of mould hollows were connected by channels. Clear evidence for this method can be seen on the coins, which display flanges on opposite edges of the coins where the runners connecting the coins in the chain would have been (Wickens, 1996). One further step often required before the flan could be struck would be to remove any impurities that may have risen to the top of the flan owing to oxidation during open casting. The flan could have been washed in some form of organic acid or pickle; in some cases the impurities seem to have been scraped off (Wickens, 1996). For gold coins this step may have been done by reheating the coin under reducing conditions prior to striking, the hot flan also being easier to strike.

## 2.0 Analytical Methods Chapter

### 2.1 Introduction

The application of trace element and isotopic analyses to Celtic gold coins required considerable analytical development. In particular the use of a laser ablation sampling system connected to single and multi-collector inductively coupled plasma mass spectrometers, for the measurement of quantitative trace element data and precise and reproducible Pb and Cu isotopic signatures. The following chapter describes the methods used in this study and examines the questions of accuracy, precision and reproducibility with examples from data acquired during the project. The bulk of the data will be presented in later chapters within the context of the aims of the study. The techniques are described with reference to the gold coinages, differences in the analytical techniques used for the natural gold samples and the silver and copper coinages will be described at the end of the chapter. The data required and the analytical techniques used are summarised in Table 2.1

Data Required	Analytical Technique
Major Components (Au,Ag,Cu,Sn &Pb)	Electron Microprobe (Jeol 8900)
Micro textural studies	Electron Microprobe (Jeol 8900)
Trace elements	LA-ICP-MS (Element Finnigan)
Pb Isotopes	MC-ICP-MS (Neptune Finnigan)
Cu Isotopes	MC-ICP-MS (Neptune Finnigan)

**Table 2.1:** The data required and the analytical techniques used.

### 2.2 Sample preparation

Two thousand years of burial can cause significant alteration of the coin surfaces (Figure 2.1), therefore abrasion and polishing of the surface is required to remove this altered layer.

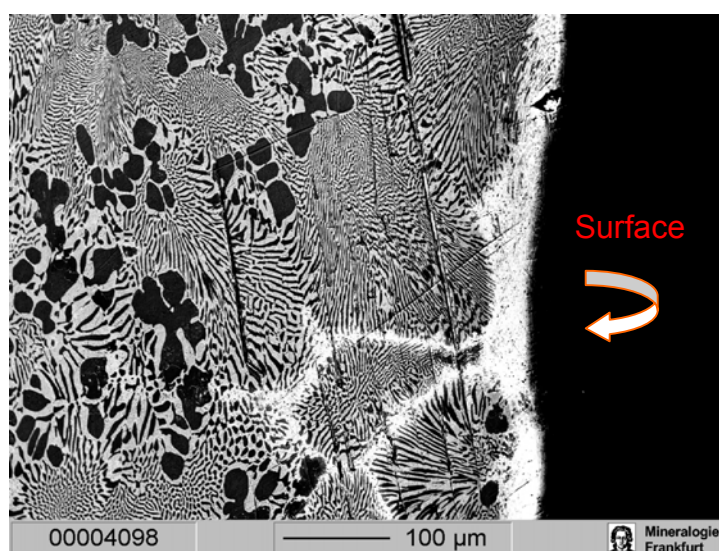
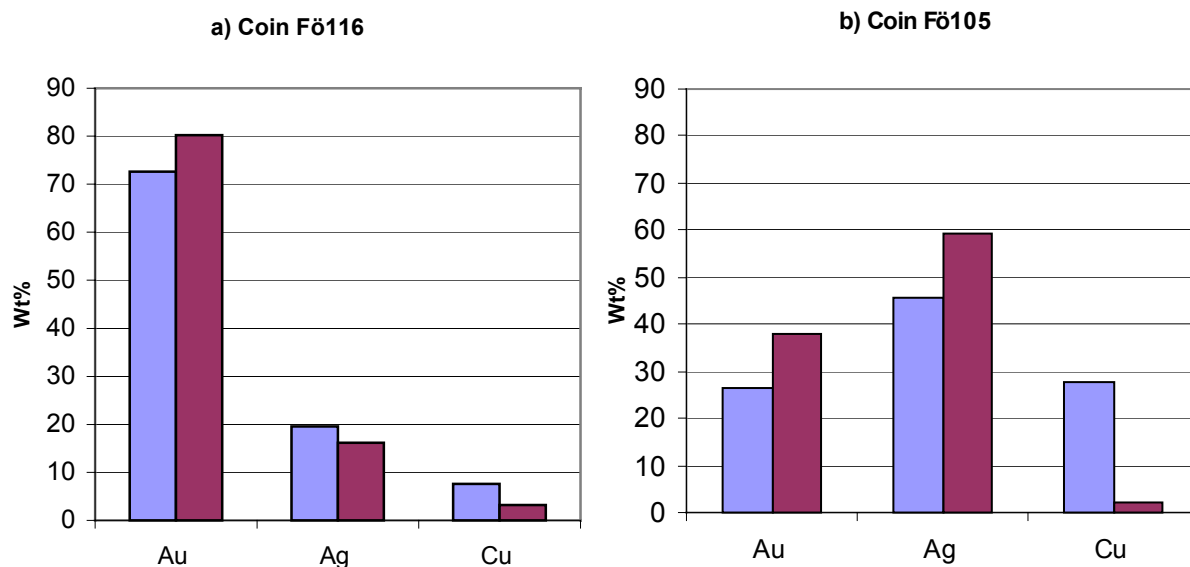


**Figure 2.1** An EPMA compositional picture of a polished area on the edge of a coin. In Figure 2.1 the effects of weathering and Cu loss can be seen (the brighter zone at the surface) and these must be avoided when acquiring measurements. The surface

alteration has been recorded down to an average depth of 50µm; deeper development along grain boundaries to more than 200µm has also been observed. Dark Cu-rich dendritic phases have also been observed surrounded by the Zebra like eutectic texture formed by intergrown Cu and Ag rich phases. Occasionally Ag as well as Cu is lost from the surface, Figures 2.2a and 2.2b. However, usually more Cu is lost leading to an enrichment in Au and Ag. The coins we see today actually appear much more golden than when they were made, which is important to consider if an understanding of the cultural significance of a coinages colour is to be gained.



**Figures 2.2a & b:** Variation of Au, Ag and Cu between the surface (Purple) and the polished areas (blue) of coins Fö116 (left) and Fö105 (right).

The altered surface layer therefore needs to be removed prior to analysis. Each coin was first abraded on the edge with P320 grade sand paper, followed by a second finer grade (P1200) paper and finally polished on a felt lapping mat with the aid of Super Pol Blue metal-polishing paste. This created a flat polished area of approximately 2-3 mm<sup>2</sup> in area. The edge of the coin is the best place to polish the coin as it allows for the maximum penetration into the coin over a smaller area and leaves the designs on the faces of the coins undamaged. The coins were then washed in an ultrasonic bath with petrol-benzin followed by distilled water and dried with lint less paper and a blast of clean nitrogen gas. How the coins were mounted for analysis is discussed in the context of each analytical technique below.

### 2.3 EPMA

Electron microprobe analyses of the Coins and Natural gold samples were made to determine the major components (Au, Ag, Cu and Sn) of the alloys present and the Pb concentration. This data was used not only to discuss archaeological alloy groups but also to determine how much sample would be required for dissolution prior to Pb and Cu isotope analyses (section 2.5 and 2.6). Finally these concentrations are also used for internal standardisation and quantification of the trace element data (see section 2.4).

A Jeol 8900 Superprobe was used for these measurements. Measurements were made using a 30nA beam current, 50µm beam diameter and 20Kv accelerating

voltage. Table 2.2 gives the details of the measuring conditions for each element and the Limit Of Detection (L.O.D.) calculated from the analyses.

Element	Spectral Line	Crystal	Time (secs)	L.O.D. (ppm)
Sb	La	PETJ	20	13
As	La	TAP	60	26
Pb	Ma	PETJ	30	28
Cu	Ka	LIFH	20	14
Bi	Ma	PETJ	30	34
Sn	La	PETJ	20	21
Ni	Ka	LIFH	40	11
Ag	La	PETJ	30	19
S	Ka	PETJ	30	6
Mn	Ka	LIFH	40	6
Zn	Ka	LIFH	20	17
Fe	Ka	LIFH	20	9
Au	Ka	LIFH	30	59

**Table 2.2:** The measuring conditions and LOD for each element analysed by electron microprobe.

### 2.3.1 Coins

The most important feature of the gold coin alloys is that many of them are alloyed to a large degree with Ag and Cu. Microprobe measurements therefore concentrated on the analysing the Au, Ag, Cu and Sn, representing over 99% of the coin compositions. The nature of the alloy has important effects, not only on the colour and weight of the coinages but also on the analytical methodology, which must be employed to acquire data. Some of the results of the coin measurements are presented here to explore the accuracy of the method employed.

After the coins were prepared by abrasion and polishing they were mounted vertically so that the polished edge could be observed with the electron microprobe. The first most striking feature of the many of coinages and especially the series Sch. 30/I-VI and the Scheers 16 and 18 coins, is their inhomogeneity. This feature is highlighted in Figure 2.3, a and b, showing a compositional scan of two coins from series 30/V. The high amounts of silver and copper, which are not soluble in each other at these concentrations, produce a eutectic texture during cooling. Depending on the initial composition of the alloy mix, the alloy will either nucleate silver or copper rich primary phases, depending on whether the original alloy mix lay on the Cu or Ag side of the eutectic, see figure 2.4a and b, (Scott, 1991). These dendritic phases grow until the remaining melt reaches the eutectic composition. The melt freezes as soon as this point is reached, thereby producing the intricate patterns of interlayered silver and copper rich plates (eutectic texture) interstitial to the original dendrites. The picture of 20409 (Figure 2.3a) shows that each dendrite forms the core of an alloy crystal with the eutectic mixture forming on the periphery. The crystal (grain) boundaries can be easily seen in this case as they are highlighted by a relative enrichment of Au and Ag at the edges. This enrichment is a secondary

weathering effect produced by the loss of the more soluble Cu during burial. This process is enhanced along the more porous grain boundaries.

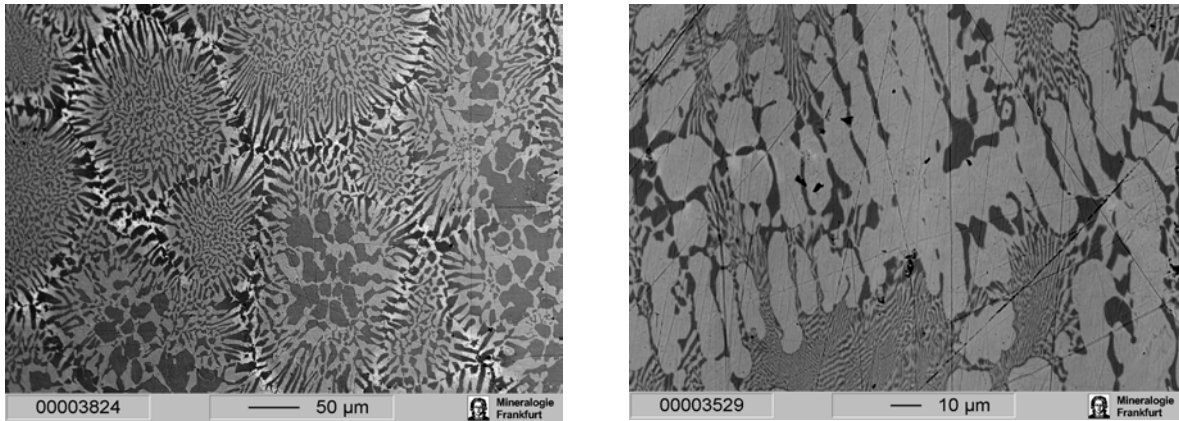


**Fig 2.3a & b:** These two series 30/V coins, 20409(Cu-rich, right) and 32243(Ag-rich, left) show the typical features of these ternary alloys. The light phases are silver rich and the dark phases are copper rich.

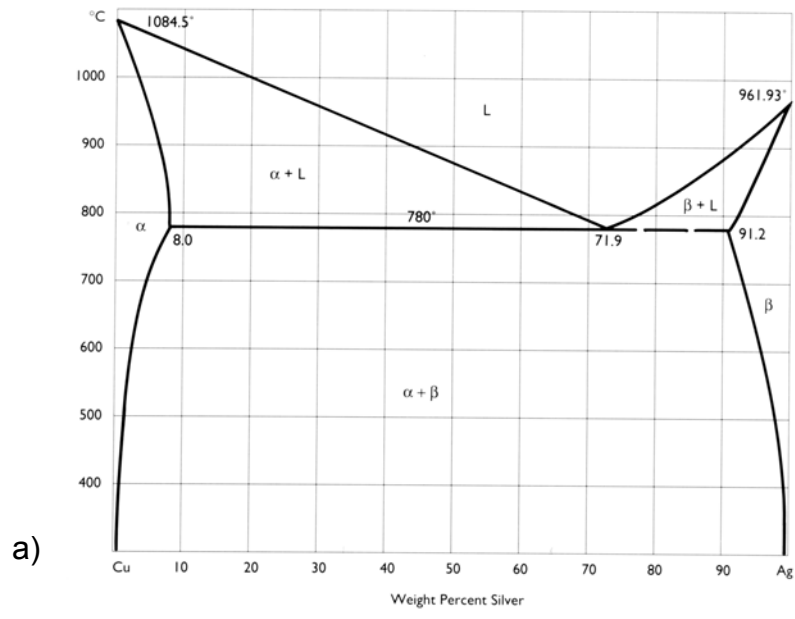


**Fig 2.4:** a) Shows the phase diagram for the Cu-Ag system with the eutectic point at 71.9 % Ag. (From Scott, 1991)

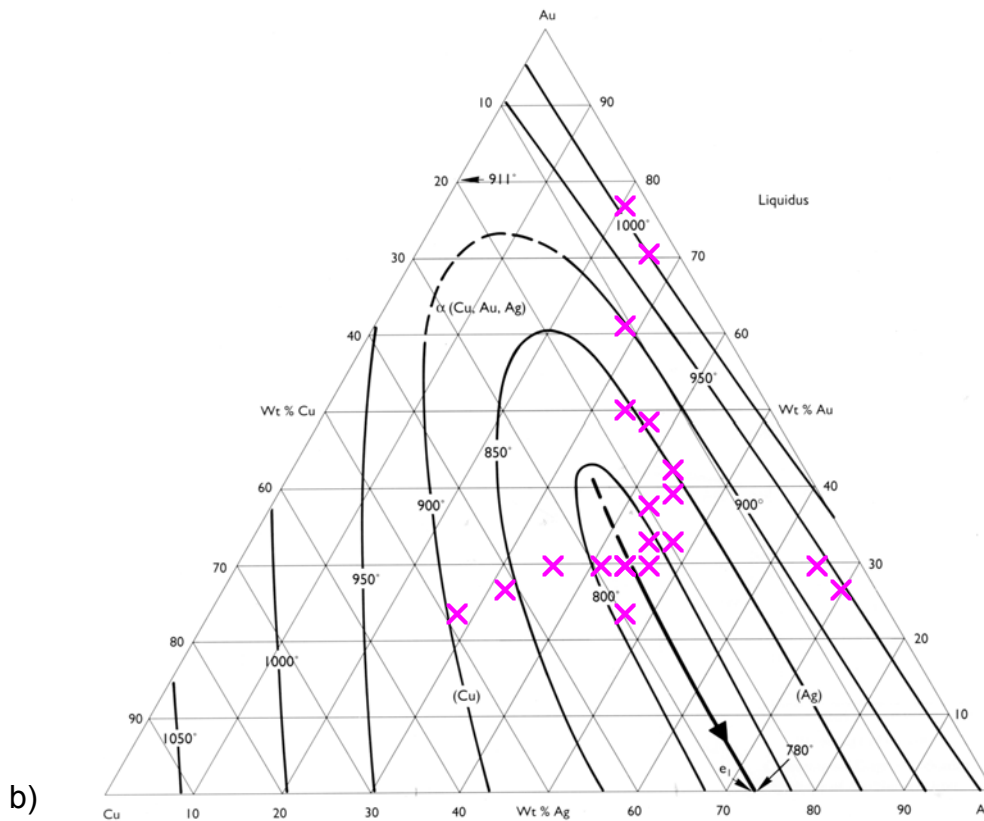


**Fig 2.4:** b) shows the phase diagram of the Cu-Ag-Au system with crosses representing the typical alloy compositions measured from the coins. Gold is soluble in both copper and silver and causes the eutectic point to shift so that coins, with an alloy composition of 34%Au, 40% Ag and 26% Cu, sit right on the eutectic. (From Scott, 1991)

The amount of eutectic mix, relative to dendritic crystals that is present, depends on how close the original mixture was to the eutectic. For an alloy with 30% Au the eutectic point will be at 45% Ag and 25% Cu, see figure 2.2b. The closer to the eutectic the more eutectic texture will be present. This heterogeneity produced by the exsolution of silver and copper rich phases means that a large electron beam size must be used so to acquire data, which is more representative of the original metal mix. It is obvious that a larger beam will provided a more representative bulk composition, however technical considerations do not allow a beam any bigger than 50 $\mu$ m. Ten measurements are acquired from each coin. The data is then averaged and the standard deviation calculated. Coins with larger dendritic growths of Ag or Cu rich phases are therefore associated with higher errors than coins with bulk compositions closer to the eutectic mixture and limited growth of primary dendritic phases.

An important consideration, which has bearing on the validity of the analytical methods both by EPMA and Laser, is whether the near surface analyses are representative of the whole coin. To investigate this one of the series V coins 22007 was sacrificed, cut in half, mounted and polished.

Gold, silver and copper measurements acquired from a line analysis of the coin from one edge to another are shown in Figure 2.5. It shows the strong heterogeneity, which is typical of these alloys. A rise in Ag concentration is accompanied by a



complementary fall in Cu vice versa. The Au composition remains fairly stable due to its solubility in both the Ag and Cu rich phases. A comparison of measurements made on the polished edge of the coin and the core are shown in Table 2.3, revealing that the results agree with each other very well within the variation dictated by the heterogeneous alloy

### 22007 Line Analysis

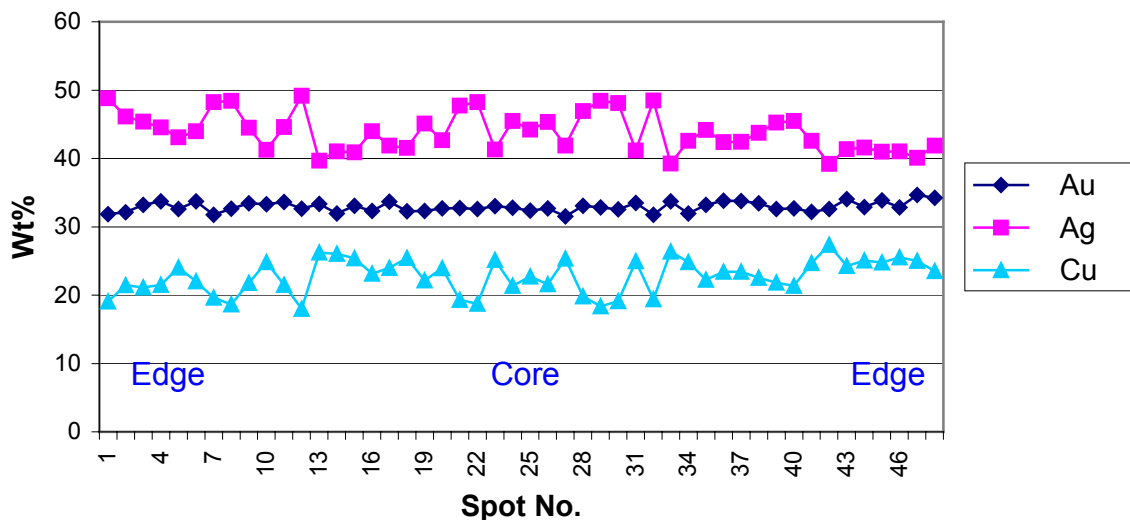


**Fig 2.5:** A line of analysis for the major components acquired from coin 22007, which had been cut in half and polished. Each spot represents a circular area with a diameter of 30µm, which overlap to form a continuous section of the coin from one side of the coin to the other

	Au wt%	Ag wt%	Cu wt%
Polished Surface	32.9 +/- 1.9	43.3 +/- 4.8	23.0 +/- 4.2
Polished Core	33.2 +/- 0.7	44.1 +/- 2.7	22.9 +/- 2.5

**Table 2.3** Shows the averages of ten analyses made on the polished surface of the coin and on the polished core. The results agree with each other very well although the analyses of the polished surface areas show greater variation.

A complete table of the Au, Ag, Cu, Pb and Sn analyses by EPMA can be found in the appendix.

## 2.4 Trace Element Fingerprinting by LA-ICPMS

Watling et al (1994), established a semi-quantitative method, using laser ablation ICP-MS, for fingerprinting gold and other metal sources using their trace elements. This technique is based on the understanding that the hydrothermal fluids, from which the gold precipitates, can be derived from a variety of rock types, undergo various modifications during migration and be caused to precipitate the gold in a number of ways. The technique was originally used for tracing stolen gold bullion from mines in Western Australia. This is a qualitative method, which used the relative intensities of a large suite of elements to distinguish between mines and mineralising events based on the presence or absence of various element

associations. The trace element fingerprinting concept has since been used in a number of studies to provenance the source of gold used in archaeological artefacts in South Africa, Central France and the British Isles (Grigorova et al 1998a, 1998b, Gondonneau et al 1996, Taylor et al, 1995) and also in the study of placer gold (Outridge et al, 1998).

Initially different gold signatures were distinguished by a simple visual comparison of the spectra but later studies (Outridge et al, 1998) used multivariate statistical methods such as Spearman coefficients to show correlations and groups. One of the most useful and representative methods of visualising the data is to make tri-plots (ternary diagrams) of the relative intensities of the different isotopes measured (Taylor et al, 1995) or their calculated concentrations (Gondonneau et al, 1996). Element associations which have been used to construct these plots include; La-Sr-Ba, Ge-La-Ga, As-Co-Hg, Sb-Cd-Sn, Bi-Cu-Sn, Cu-Sb-Ag, Pt-Cd-As, Pt-Pd-Ag, Pd-Pt-Rh. Gondonneau et al (1996) showed that the Phillipus stater imitations of Gaul contained less PGE's than the Greek originals.

All these studies have used qualitative and semi-quantitative data based on the relative intensities of the elements measured. Unfortunately, there are several problems with acquiring quantitative trace element data from gold by laser ablation:

- a) Laser and ICP induced "Matrix effects"
- b) Lack of external standards
- c) Limited choice of internal standard as Au is monoisotopic.

Element fractionation, where some elements appear to be preferentially vaporised and ionised over others is matrix dependent and requires the use of several solid and homogenous external standards. Unfortunately there are no commercially available standards with the required suite of trace elements. Au is monoisotopic and it is not possible to measure at high concentrations without damaging the detectors. The choice of internal standard is therefore limited to the polyatomic AuAr<sup>+</sup> species, at 237 atomic mass units (amu). This was considered by Watling et al (1994), but the variations in coupling behaviour between different types of gold and the laser were thought to be too variable and internal standardisation untenable. As the method relies on distinguishing gold signatures by the presence or absence of various elements, the lack of quantitative data was not considered a problem. Gratuze et al (1993), however, did take the method a step further to quantification by utilising the AuAr<sup>+</sup> polyatomic species as an internal standard and normalising the results to 100%.

A major problem of this present study is that the artefacts to be studied, Celtic gold coins of the 1<sup>st</sup> century BC are heavily alloyed with Ag and Cu, which bring their own suite of trace elements along with them. Initial studies based on semi-quantitative methods did not produce any definite indication of which elemental associations might be useful for identifying the gold sources and merely showed that the elemental signature of the coins was controlled by the addition of copper. Quantitative measurements were therefore considered a desirable goal, firstly to see if the concentrations of the elements could provide an extra tool for unravelling the relative amounts of trace elements provided by the three components of the alloy, Au-Ag-Cu, and secondly to create a quantitative database which would be of use to later studies.

As mentioned above the standardisation of the analyses to acquire quantitative data, from the Laser Ablation process, is problematic. The efficiency of both the laser ablation sampling and the ionisation of the sample by the ICP can vary considerably from day to day and during a measurement session, especially when analysing materials with variable matrices. The following discussion highlights the problems related to the quantitative measurement of trace elements in metals by LA-ICPMS and details the trace element standardisation method used in this study.

#### **2.4.1 Element Fractionation**

There are three main causes of element fractionation (Jackson & Günther, 2003):

- 1) Differential volatilisation and condensation processes at the ablation site
- 2) Fractionation during sample transport via the partitioning of elements into particulate and vapour phases, which are differentially transported.
- 3) Fractionation in the ICP due to incomplete vaporisation and ionisation of particulates

The laser ablation process involves the absorption of laser energy by “Quasi-free” electrons above the sample surface. The energy absorbed is transferred by collision from the electrons to the atoms in the sample causing the exploding ablation process to begin. At the same time, a plasma breakdown occurs in the surrounding gas caused by thermal electrons escaping from the sample. The plasma is also heated by laser absorption. Propagation of “The Shockwave” with the ablated material and the evaporation of ejected sample particles in the gas plasma are important processes for the composition of the aerosol particles which are formed after recombination and cooling of the plasma. (Koch et al, 2002)

Preferential evaporation of some elements may occur at this stage if, during the rapid cooling, the vapour pressures of the sampled elements are very different. For example Zn and Cu.

The use of He instead of Ar as the carrier gas of the laser-ablated aerosols provides a 3-5 times increase in sensitivity over Ar and helps to restrict element fractionation. Laser induced plasma in He is significantly smaller than in Ar and He is more thermally conductive, allowing for the faster spread of thermal energy away from the sampling and hence a quicker end to the growth of particles through condensation. This limits the amount of elemental fractionation, which can occur at this stage (Horn & Günther, 2002).

Jackson and Günther (2003), conducted experiments to monitor the effect of particle size on elemental and isotopic fractionation in the ICP. They found that larger particles, over 0.5µm, are not completely ionised by the plasma allowing for the preferential vaporisation of some elements. The use of He is therefore doubly important as it reduces the particle size, which are more easily ionised by the ICP (Horn & Günther, 2002). Element and isotopic fractionation is further reduced by the use of a glass wool filter in the tubes between the ablation cell and the plasma, removing the larger more troublesome particles (Jackson, 2003).

The fractionation process can be reduced, monitored and corrected for by using matrix matched external standards (standards with the same Au, Ag and Cu composition and containing similar levels of the trace elements of interest) in conjunction with an internal standardisation method (Kogan, 1994). As there are no commercially available solid standards, which match the matrices of the coins and natural gold samples, attempts were made to make in-house standards. Unfortunately the production of homogeneous standards was not achieved and another method, employing solution standards, was used.

#### **2.4.2 Standardisation**

The method developed in this study involved a combination of external solution standardisation (Pickhardt et al, 2000) combined with a 100% normalisation method, which assumes that all the constituents of the coins are analysed (Gratuze et al, 1993).

##### **a) Nebulised Solution Calibration**

Pickhardt et al (2000) described a calibration method that uses solution standards to calibrate laser ablation analyses. The solution was introduced into a LA system utilising a desolvating nebuliser. During calibration the standard solutions were nebulized and carried through the Laser cell while ablating a lithium borate blank. During the analysis of the samples (which were fused into a lithium borate glass) a 2% HNO<sub>3</sub> solution was nebulised. Calibration was made with the use of three standard solutions. Two internal standards were utilised; Zn and Nd, both providing results which agreed very well with the reference material (< 12% variation) for most elements.

Whether solid or solution standards are used, internal standardisation is an important tool. Usually a minor isotope of a major element is used for which the concentration is independently known eg. by electron microprobe analysis. This allows variations in the ablation process or nebulization of the sample to be adjusted for and reduces the affects of matrix and laser parameter matching between calibration samples and unknowns.

The technique used in this study is somewhat different from the one described by Pickhardt. The standard solution was not introduced through the laser ablation cell. Instead it was carried by the Ar (sample gas) and mixed with the He later, see figure 2.6.

##### **b) 100% normalisation**

An alternative method of quantification, in opposition to the internal standardisation method, was developed by Gratuze et al, (1993), and assumes that all the constituents of the material are analysed and therefore add up to 100%. The method used the AuAr<sup>+</sup> polyatomic species, which was monitored to estimate the Au concentration, and then the results of the major elements, Au, Ag and Cu were summed together and normalised to 100%, thereby calculating relative concentrations of the trace elements.

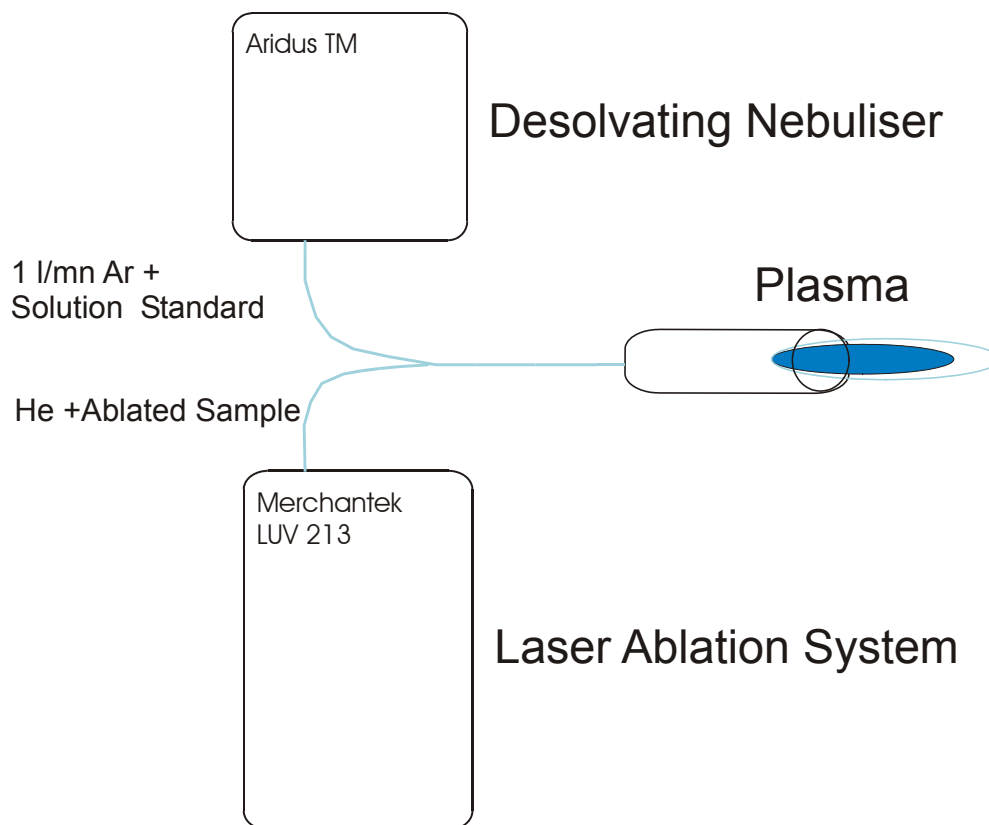


**Fig 2.6:** Schematic diagram of the standard and sample introduction system used in this study. The solution standards are introduced through the desolvating nebuliser with the Ar sample gas, which is mixed with the sample carrier gas from the laser ablation system before entering the plasma. During analysis of the samples a solution of 2% HNO<sub>3</sub> is provided in the place of the standard.

### 2.4.3 Quantification

#### a) Using solution standards

The method developed in this study involved a combination of external solution standardisation (Pickhardt et al, 2000) combined with 100% normalisation (Gratuze et al, 1993).

First a set of solution standards were produced. The concentration of the solutions were calculated based on the average concentration of the major element compositions of the samples and on the volume of material ablated by the laser. Three solutions were made with trace element concentrations, which would mimic the ablation of a solid sample with 1, 10, and 100ppm trace element concentrations.

1. A calculation was made to estimate the amount of material (in ppm) which is ablated from a sample during laser analysis and therefore the concentration of the major components of the sample material, which would be expected to be delivered to the plasma
2. For each major component this value was divided by the Uptake of the Aridus<sup>TM</sup> desolvator (ml/mn) times the total acquisition time (eg; the time it takes to make the analysis).

For example:

A coin alloy contains 40%Au, 40%Ag and 15% Cu

The volume of the hole ablated (80µm diameter and 200µm width) is 0.000001 cm<sup>3</sup>

The amount of Au ablated is 40000ppm X 0.000001 cm<sup>3</sup> = 0.402ppm

Considering that the Adridus uptake is 0.08 ml/min

And the analysis acquisition time is ~2 min

Then the amount of Au that should be dissolved in a solution to deliver the same amount of Au to the plasma as the laser is:

$$0.402 / (0.08 * 2) = 2.51 \text{ ppm}$$

The same calculations were made for Ag, Cu and then 1 ppm, 10 ppm and 100 ppm concentrations of the trace elements.

The basic concept of the method is that the concentration is directly proportional to the counts per second acquired by the ICPMS. So that the intensities (cps) measured can be directly related to a concentration in ppm with reference to a line produced by plotting cps vs. ppm.

With three solutions of different trace element concentrations this is true for most of the elements of interest such as Ni in Fig 2.7. However other elements are more problematic showing no such correlation and therefore cannot be reliably used. Elements which cannot be used include As, Ga, Ge, Re, Os, Hg. For most of these elements the problem arises as they are not stable in the standard solution, either because of their volatility in oxidising solutions (e.g.; Os) or because they are absorbed onto the sides of the plastic container (e.g.; Hg) (Y. Lahaye, pers. comm.).

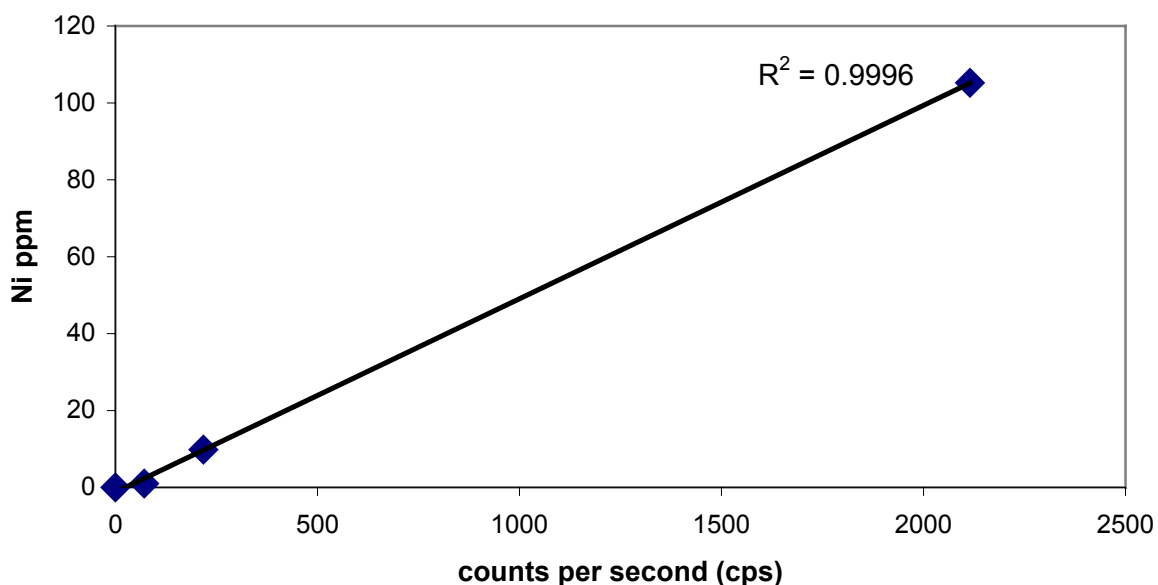


**Fig 2.7:** Plot of counts per second (cps) vs. the concentration (ppm) of Ni added to the standard solutions. The points represent standard solutions of 0, 1, 10 and 105 ppm.

## **b) Choosing the Internal Standard**

Au would be the most useful as it is more evenly distributed in the coin alloys than Cu or Ag and therefore would reduce the effect of fractionation effects between Cu and Ag rich phases. However, as Au has only one isotope it is unmeasurable on the ICPMS, as it would overload the detectors and either the AuAr<sup>+</sup> polyatomic species would need to be used as a proxy, or the Au would have to be measured in an off-peak mode. Both of these alternatives do not provide a 100% correlation with real Au concentration.

Therefore, a different method was considered. Instead of measuring the Au, everything else is measured including all the Ag and Cu (eg. both isotopes of each element, this is possible as the signal for these elements is effectively halved, distributed over two isotopes, allowing the total Cu and Ag to be measured). Then utilising the EPMA results, all these elements are equated to the percentage of the sample they represent, less the Au content.

Effectively after calibrating the data with the standard solutions, all the elements (except Au) are summed together.

Eg. If X% Au was measured by EPMA then the concentration of the summed together elements must represent 100-X%.

The total concentration of all the elements with Au can then be calculated and everything normalised to 100%. The dataset thereby acquired shows all the elements in percent %, which is then converted to ppm.

## **c) Data Reduction**

The results acquired from the analyses represent the cps for each isotope analysed over the ~2min acquisition time.

With the GLITTER™ software the results are processed to subtract the blank. One feature of the software displays the cps measured versus the acquisition time as a time resolved analysis. The software allows you to select the ablation period to be considered as data and to select the pre-ablation blank to make the individual blank corrections for each analysis.

The averaged and blank corrected results are then processed with a Microsoft Excel macro program to produce concentrations in ppm relative to regression lines produced from the analysis of three standard solutions representing 1, 10 and 100ppm levels of trace elements, as described above.

## **d) Precision and Accuracy of the Method**

Figure 2.8 shows repeated measurements of coin 22007 from two different days and three different measurement sessions. It shows that the measurements are in good agreement. However, elements such as Zn, Sn, Sb and Re should be handled with care when using them to discriminate between different coin populations.

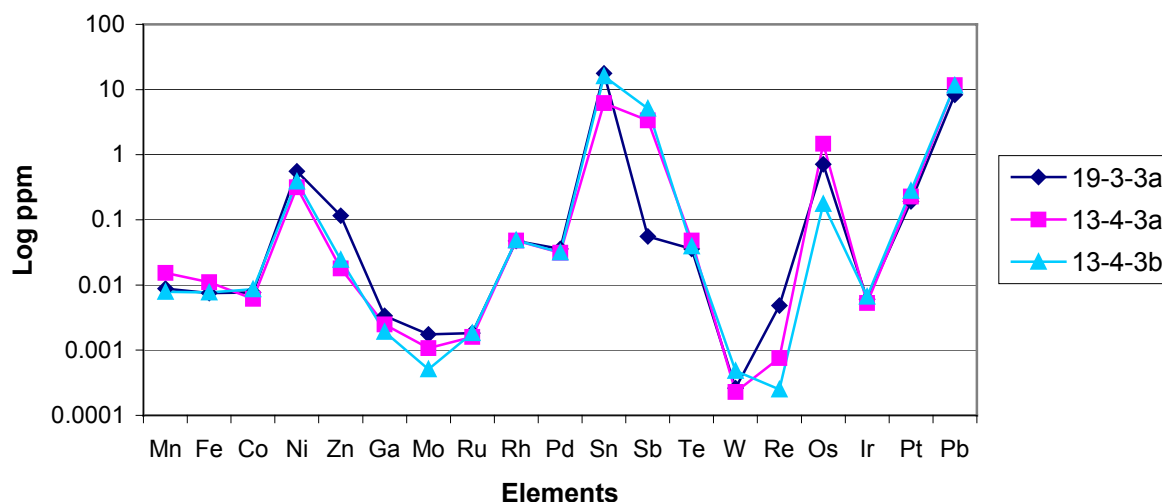


**Fig 2.8:** Trace element reproducibility for sample 22007 analysed on two different days (19-3-3 and 13-4-3).

#### 2.4.4 Limitations of the technique

There are a number of elements which would be desirable to measure but which have presented problems that have made them unusable. There are three categories of these elements:

- i) those with poor standardisation, i.e.: unstable elements.
- ii) those with polyatomic interferences.
- iii) and those affected by the “tailing” effects of more concentrated elements such as Au, Ag and Cu.

Poor standardisation effects those elements which are more volatile or which have precipitated from the solution, absorbing onto the sides of the beaker in which the standard is stored. These include: Fe, Zn, Ge, As, Se, Sn, Os, Hg and Bi.

Polyatomic interferences are produced by elements combining with ubiquitous elements such as Ar, O, N and H, which are present in the sample gas and ambient air (air enters the system as the laser ablation cell and the ICP are not under vacuum). For instance  $^{63}\text{Cu}$  and  $^{65}\text{Cu}$  combined with  $^{40}\text{Ar}$  to produce polyatomic species with masses of 103 amu and 105 amu respectively, thereby overlapping with  $^{103}\text{Rh}$  and  $^{105}\text{Pd}$ . Therefore other isotopes of these elements need to be measured to acquire the true concentration of these elements and not merely a reflection of the copper concentration.

Tailing effects occur when one element such as silver is present in such high amounts that the bottom of the peak overlaps with its neighbouring masses. In the case of silver, it has two isotopes  $^{107}\text{Ag}$  and  $^{108}\text{Ag}$ , producing tailing effects on  $^{106}\text{Pd}$ ,  $^{108}\text{Pd}$  and  $^{110}\text{Pd}$ . In effect this means that whenever the concentration of Ag increases so does the measured Pd.



It is therefore important to select the isotopes of the elements of interest, which are free of both polyatomic and tailing overlap.

Unfortunately the tailing effect of Ag was not noticed until all the analyses had been made and so although the isotopes of Pd 106, 108 and 110 were selected to monitor the effects of the CuAr<sup>+</sup> polyatomic mass on Pd105, none of them could be used. Pd is a potentially very useful element for discriminating gold sources as it would not be seriously altered during weathering and is present in relatively high concentrations in comparison with all the other PGE's (Ru, Ir and Os) except for Pt. Variations in the Pt/Pd ratio might provide a means of discriminating between gold deposits. However, the applications of this will have to be investigated in later studies where Pd104 is also analysed.

#### **2.4.5 Conclusion**

The procedure described above for standardising laser ablation analyses with the use of solution standards allows quantitative results to be obtained for the following elements:

Sc, Ti, Cr, Mn, Co, Ni, Cu, Zn, Se, Ru, Rh, Pd, Ag, Sb, Te, W, Ir, Pt, Pb, Bi.

The remaining elements remain problematic as they produced incorrect standardisations mainly due to chemical effects in solution such as adsorption onto the beaker walls or oxidation: V, Fe, Ga, Ge, As, Mo, Sn, Re, Os, Hg.

Pd requires special attention, it has the potential to be very useful as a discriminating element given its noble nature and relatively high abundance compared to other PGE's (except Pt), however, for the types of matrices studied here, tailing and polyatomic affects need to be avoided, and this requires analysis of all the isotopes of Pd, most importantly <sup>104</sup>Pd which represents 11.44% of Pd in nature and should not be affected by tailing effects from Ag.

#### **2.5 Pb Isotopes**

Lead is distributed widely through out the earth and also forms its own minerals in which radiogenic Pb has been separated from its parent isotopes of U and Th. These minerals include Galena, Pb-sulfosalts, Pb oxides and carbonates. It also occurs as a trace element in most sulphides and native gold. It is therefore also present in significant amounts in ancient metallurgical artefacts made from ores containing these minerals.

The isotopic compositions of Pb in rocks and ore deposits display complex patterns of variation that reflect the multitude of chemical environments in which the lead may have resided and passed through before being sampled.

The study of "common" lead isotopic ratios, is Pb that occurs in minerals whose U/Pb and Th/Pb ratios are so low that the Pb isotopic composition does not change very much with time.

Nier et al (1941) first reported isotopic analyses of Pb extracted from galena's from different ore deposits showing conclusively that such leads have variable isotopic

compositions resulting from variable mixing of radiogenic lead with primeval Pb prior to deposition. Archeometric studies of common lead use the linear correlations of Pb ratios, which result from mixing leads of different isotope compositions in varying proportions.

Lead isotopic studies have been increasingly used to provenance metal artefacts from the ancient world, focussing mostly on the Bronze Age (Pernicka et al, 1990, 1997; Stos-Gale et al, 1997). In particular the base metal sources of the Aegean, Mediterranean and Eastern Europe have been intensively studied. In recent years the Oxford Isotrace Laboratory has produced a database of lead isotope measurements of European base metal ores (Stos-Gale, 1996, 1998; Gale, 1997).

The Pb isotopic signature that we see may not always represent a distinct source and may well be the result of mixing several sources, especially when the recycling of metal is considered. This is particularly true for the Gold (Au-Ag-Cu) coinages, with up to 40% copper, and the Silver coinages, which typically contain around 6% Cu and some more than 30% Cu. This problem can be investigated by the consideration of a Pb Isotopic Mixing Model. When diagrams of Pb-Pb isotope ratios are plotted they typically form linear arrays known as isochrons. However, when the Pb isotopic signature is a result of mixing different sources then a curvi-linear array is also formed, which is not an isochron. This line can be used to estimate the end member of the array. The end member signatures can then be compared with the Pb isotopic data from the metal deposits in order to identify the sources.

Multi-Collector ICP-MS isotopic analyses of common lead provide precise and accurate measurements. Watkins (1993) and Longreich (1987) have shown that by employing a mass bias correction through the use of thallium as an internal spike, a significant improvement was made compared to conventional TIMS analyses, which is only surpassed by double- or triple-spike TIMS techniques. The added advantage of the ICP-MS method being an overall reduction in instrument time and overall labour, making it much better suited to the determination of Pb isotopic compositions for a large number of samples.

This study also sought to develop a method of sampling the gold coins by Laser Ablation. Some LA-ICPMS measurements of silver coins were made by (Guerra et al 1999), however they were using a single collector ICPMS and so the results lacked accuracy and precision. The combination of using Laser Ablation with a Multi-Collector ICPMS is described below showing that it is a viable technique for the type of studies undertaken in Archeometry.

### **2.5.1 Solution Procedure**

First the coins are drilled along their edges, on the spot that has already been polished for the EPMA analyses. Any contaminating affects from the coin surface are therefore avoided. The samples then undergo weighing, dissolution and chromatographic separation of Pb from the sample matrix, as described in table 2.4. The amount of sample required is calculated from the Pb concentration measured by electron microprobe.

<b>Sample Dissolution</b>	<b>Chromatography Dowex 1X8</b>
Weigh Sample Dissolve in 1ml Aqua Regia Ultrasonic bath for 60mn Heat at ~80°C for 2 hours Ultrasonic bath for 60mn Dry Add 1ml 6M HCl Centrifuge and remove AgCl precipitate.	Condition Column with 0.5ml 6M HCl Load the sample in 2 x 0.5ml 6M HCL Elute with 4 x 0.5 ml 6M HCL Add 0.5ml H <sub>2</sub> O Collect everything  Dry down the 3.5ml of solution  Dissolve in 1ml 0.6M HBr Condition column with 0.5ml 0.6M HBr Load the sample in 2 x 0.5ml 0.6M HBr Elute with 3 x 0.5ml 0.6M HBr Collect everything (Cu separate) Change beaker  Elute and collect 4 x 0.5ml 6M HCL (Pb Separate) You now have two beakers, one with Cu in HBr and one with Pb in HCL

**Table 2.4:** The chemistry involved in the separation of Pb and Cu separates from a gold rich matrix.

This two stage chromatographic process is required as the gold and silver rich matrix seems to restrict the amount of lead recovered from the more usual one step HBr/HCl method. The recovery rates are still not perfect but do allow enough lead to be recovered for analysis. The first HCl only separation is designed to remove the Au and Ag from the matrix. Firstly, AgCl precipitates and is easily removed by centrifuge, it is necessary to remove the liquid and add fresh HCl before centrifuging again so that as much of the Pb and Cu as possible is removed. Secondly the Dowex resin holds onto the AuCl<sup>-</sup> anions very strongly and efficiently removes the gold while allowing the lead and copper to pass through. The copper elution is actually more complicated and in fact the method is not optimised for sufficient recovery of copper, this is discussed in greater detail in section 2.6. The second chromatographic step produces two solutions. Firstly the Cu is collected in 0.6M HBr and then the lead is washed through with 6M HCl.

The white precipitate after dissolving the sample in aqua regia was positively identified as AgCl via the following steps.

1. Sample 22006 was spun for 15 min and 13400 rpm, the fluid was pipetted off and another 50µl added.
2. It was vibrated ultra-sonically for one minute (the fluid still appeared a little yellowish), so it was then centrifuged for another 7 min, fluid removed.
3. This last step was repeated with another 50µl.

4. The white precipitate was dried overnight and then crushed and mounted on a boric acid pellet for XRF analysis which showed distinct Ag and Cl peaks with no copper or gold detected. As the sample was very small any lead that might have been there would have been too low to detect. The AgCl turned purple after bombardment with X-rays.

The Pb isotopic analyses were made with a Finnigan Multi-Collector ICPMS. To correct for mass bias the sample solution is mixed into a 50ppb natural Tl standard solution (Alpha ICP-Std). The natural  $^{205}\text{Tl}/^{203}\text{Tl}$  ratio of 2.3871 (Dunstan et al, 1980) was used to correct for instrumental mass bias of the Pb isotope ratios, applying the exponential law of Russell et al (1978).  $^{204}\text{Pb}$ ,  $^{206}\text{Pb}$ ,  $^{207}\text{Pb}$  and  $^{208}\text{Pb}$  are measured simultaneously along with  $^{205}\text{Tl}$  and  $^{203}\text{Tl}$ .  $^{202}\text{Hg}$  is also measured so as to monitor the interference of  $^{204}\text{Hg}$  on  $^{204}\text{Pb}$ .

The results are presented in the following relevant chapters. Some of the data is presented here in order to assess the reproducibility of the technique.

### 2.5.2 Laser Ablation Method

Due to the inherent cultural and metallic value of the gold coinages, many of the coins procured from the Museums and Coin collections of Belgium, Luxembourg and Germany, could not be drilled to provide material for dissolution and analysis by solution MC-ICPMS. The EPMA results for the coins showed that sufficiently high amounts of Pb were present to make sampling by Laser Ablation a viable option. The method of making isotopic analyses with a LA-MC-ICPMS system is essentially the same for Pb and Cu isotopes and is described in general below followed by the details of the two methods.

Firstly, a way of making the mass bias correction needs to be found. This can be done in one of two ways.

- i) An elemental spike, such as Tl, can be added to the system during the measurement using a desolvating nebuliser in a similar configuration as was used for the trace element acquisition procedure (Fig. 2.6).
- ii) Each sample can be bracketed, before and after by the measurement of a standard, "Sample Bracketing".

To add a Tl spike, during Laser Ablation analysis, a desolvating nebuliser (Cetac, Aridus<sup>TM</sup>) was used. The He carrying the sample from the laser cell and the Ar carrying the Tl from the Aridus<sup>TM</sup> are mixed before entering the ICP. The set up is the same as for the trace element analyses (Fig 2.6) except the Tl spike is continuously added through the desolvating nebuliser.

This method of desolvating the Tl solution was used here and a Pb isotopic standard was only measured before and after each measurement session (not each sample) to monitor the accuracy of the machine. The reproducibility of the method can be seen in the following two figures, which compare the Laser analyses with solution analyses of the same coins and also replicate laser analyses of these coins during measurement sessions and over a period of several months. Coin 22007 that had been cut in half and described above provides a suitable in-house standard for routinely checking the analyses.

### Comparing Replicate Laser Analyses

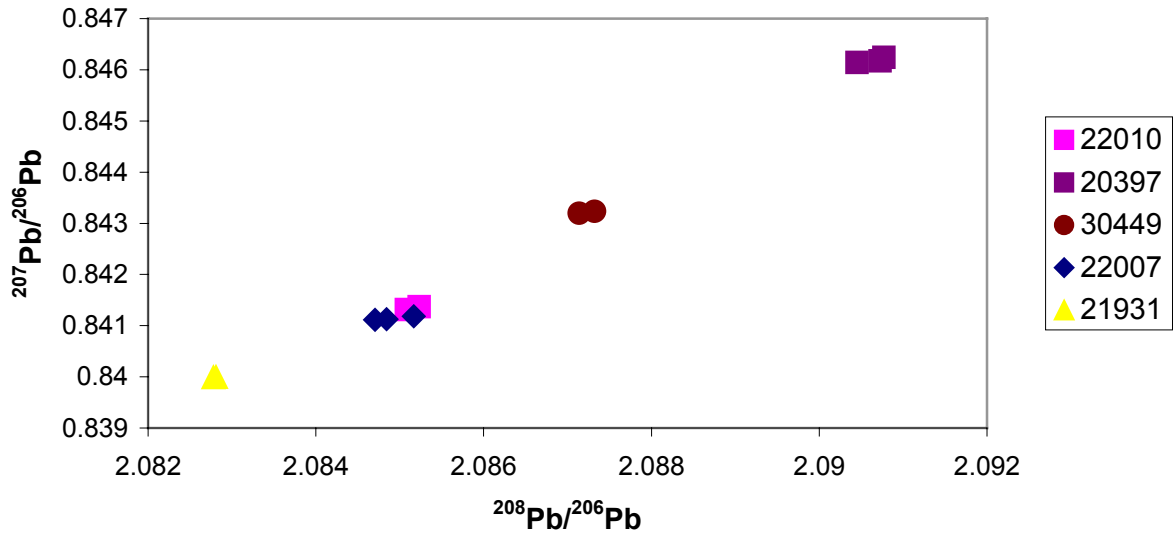


**Fig 2.9:** This figure shows replicate Pb isotope analyses by Laser Ablation MC-ICPMS; the individual error for each point is smaller than the symbol.

### Comparing Pb isotope analyses by Solution and Laser

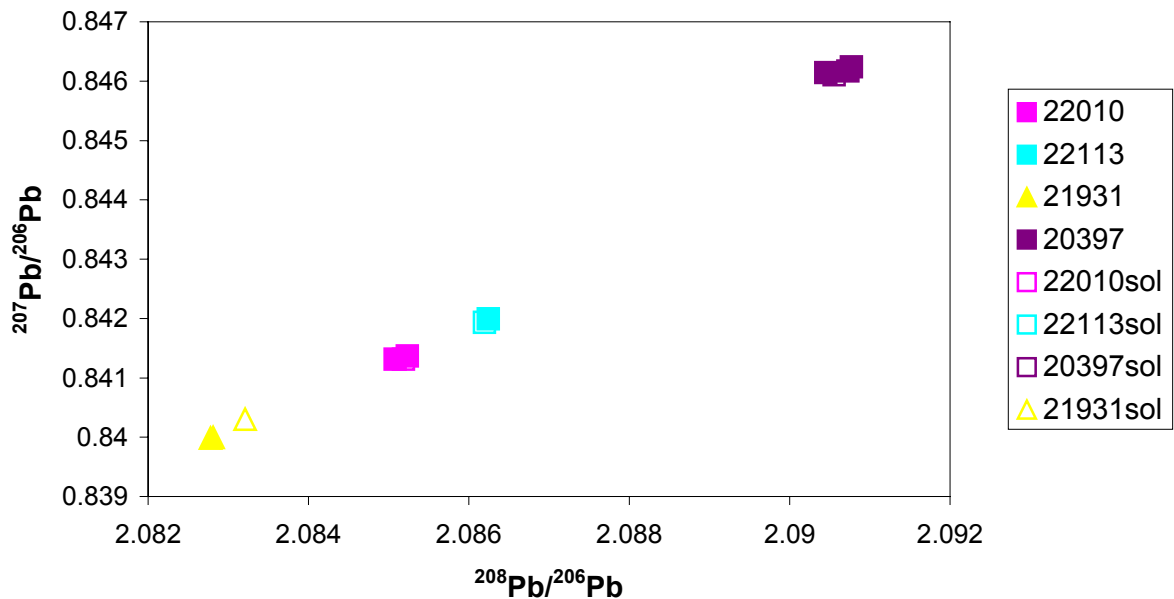


**Fig 2. 10:** The analyses by laser are compared to those made by solution.

Figure 2.9 shows the reproducibility of the laser ablation-MC-ICPMS method is between 1 and 0.1‰ (per mil) on the  $^{208}\text{Pb}/^{206}\text{Pb}$  ratio. Figure 2.10 shows that the results acquired by laser are in good agreement with those acquired by solution. Actually the 21931 laser analyses are almost identical while the 21931 solution analysis sits at some distance from them. This is a result of a particularly bad chemistry blank, of 0.24ppb Pb, for the batch that included preparation of solution sample 21931 and suggests that the laser analyses were more accurate. This

shows that, for these types of samples with more than sufficient lead, LA-MC-ICPMS is the method of choice, providing accurate results of sufficient precision, whilst avoiding chemistry blank problems, the drilling of the coins and many hours of lab work. However, the major disadvantage of this method is that only the  $^{207}\text{Pb}/^{206}\text{Pb}$  and the  $^{208}\text{Pb}/^{206}\text{Pb}$  ratios can be used.

## 2.6 Cu Isotopes

The possibility of using Cu isotopes as possible geochemical traces, that could be applied to the provenancing of archaeological artefacts, has been investigated by Gale et al (1999). They found that archaeological copper objects, such as the copper oxide ingots found in Crete, Cyprus and Sardinia, showed  $^{63}\text{Cu}/^{65}\text{Cu}$  ratios differ from the isotopic composition of the NIST (SRM) 976 copper isotope standard by up to several per mil. Also, an initial study on the effect of smelting and refining concluded that the copper isotopic composition is not altered by these processes. A pure copper separate solution is a by-product of the lead separation technique described above and therefore it was decided to investigate the variation of the copper isotope ratio of the samples from this study.

Several investigations to determine a suitable and reproducible analytical technique, utilising a MC-ICPMS, have been made and show the existence of isotopic variations between natural samples of native copper, Cu-carbonate and Cu-sulphides (Maréchal et al 1999, Zhu et al 2000). Copper isotopic ratios are reported as a delta value via the following equation:

$$\delta^{65}\text{Cu} = \left[ \frac{(^{65}\text{Cu}/^{63}\text{Cu})_{\text{sample}}}{(^{65}\text{Cu}/^{63}\text{Cu})_{\text{NIST 976}}} - 1 \right] \times 1000 \quad \text{or} \quad \varepsilon^{65}\text{Cu} = \left[ \frac{(^{65}\text{Cu}/^{63}\text{Cu})_{\text{sample}}}{(^{65}\text{Cu}/^{63}\text{Cu})_{\text{NIST 976}}} - 1 \right] \times 10000$$

Zhu et al (2000), have reported that copper minerals which form through low temperature aqueous fluids, such as native copper and Cu-carbonates, in the supergene zones of ore deposits, typically show an enrichment in  $^{65}\text{Cu}$  with  $\delta^{65}\text{Cu}$  values ranging from -3.31 to +15.85. Cu-sulphides and Cu-Fe-sulphides, such as chalcopyrite and bornite, from igneous-hosted ore deposits, show a relatively small variation from -6.17 to +3.98. However, the same minerals from active hydrothermal vent sites on the seafloor (the precursors of Volcanic Hosted Massive Sulphide deposits-VHMS) show a much broader range from -4.81 to +11.47 and are also highly variable within individual localities. This is probably due to the fact that they are formed during the interaction of hot hydrothermal fluids and cold seawater. However, subsequent hydrothermal diagenesis of seafloor sulphides may induce isotopic homogenisation within the sulphides producing both a shift towards lower and less variable  $^{65}\text{Cu}$  values.

The  $\delta^{65}\text{Cu}$  values for different types of copper minerals as reported by Zhu et al (200) and by Gale et al (1999) are shown in figure 2.11.

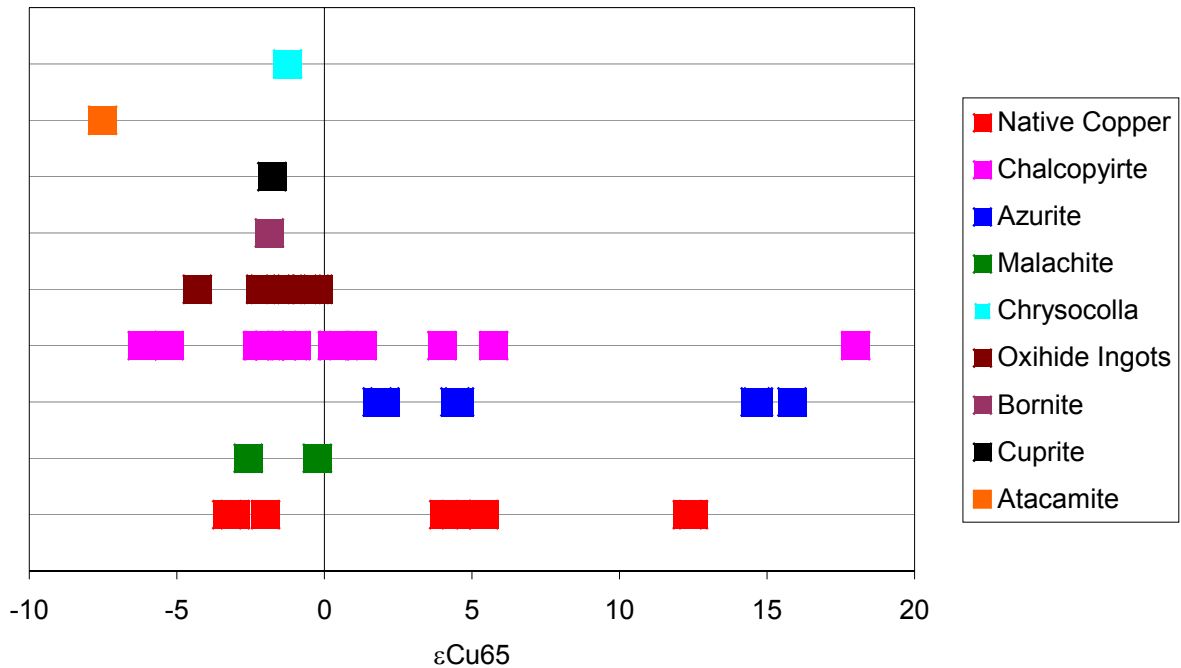


**Fig: 2.11:** The  $\epsilon_{65}\text{Cu}$  values for different types of copper minerals as reported by Zhu et al (2000) and by Gale et al (1999).

Although, copper from igneous hosted deposits may show a regional variation, copper from the oxidised and supergene zones of these same deposits will display much more varied isotopic compositions. Therefore it may be possible to distinguish copper artefacts produced from oxidised and supergene ores from those produced from Cu-sulphide ores. However, the range of values for individual deposits has not been studied in depth and it is possible that individual deposits do not retain a particular signature but rather a range of values which may overlap with other deposits to a large degree, making provenance studies based on Cu isotopes alone untenable. A recent study by Klein et al (in press), has shown that the combined use of Cu and Pb isotopes for the provenance study of Roman copper coinages is a powerful tool for helping to distinguish between copper producing areas with overlapping Pb isotopic compositions.

### 2.6.1 Solution: Chromatographic and Mass bias Considerations.

#### a) Chromatographic considerations

Both Solution and Laser sampling methods were investigated for the coins. However, it must be stressed that the copper separate solutions are a by-product of the Pb separation method which is optimised for Pb recovery with chemical blanks as low as possible. This method does not recover all the copper and may produce incorrect  $\delta\text{Cu}^{65}$  values due to chemical fractionation induced by the chromatographic method. Maréchal and Albarède (2002), have studied the chemical fractionation of copper isotopes in anion exchange columns in some detail and found that with column volumes of 1.6ml and using 7M HCl to elute the copper, 30mls of acid were needed to recover the full yield of copper. The lighter isotope is preferentially retained by the resin

and therefore when copper recovery is not complete then  $\delta^{65}\text{Cu}$  acquired will be erroneously positive.

To examine the recovery of copper, from a Au and Ag rich matrix with 6M HCl through a 0.5ml column volume, a gold, silver and copper metal mix was weighed out to simulate the average matrix of the gold coins and dissolved in the same way as the coin samples. The anion chromatographic method with 6MHCl was then tested with every 0.5ml eluted being separately collected for measuring by solution ICPMS. Consideration of the data provided by Maréchal and Albarède (2002), suggested that 9-10mls would be sufficient to recover all the copper. The amount of solution usually collected during the separation of Pb is 4.5mls (red dashed line), represented by the ninth measurement (Fig 2.12) which equates to 91.7% of the total Cu .

### Chromatographic Cu recovery with 6M HCl

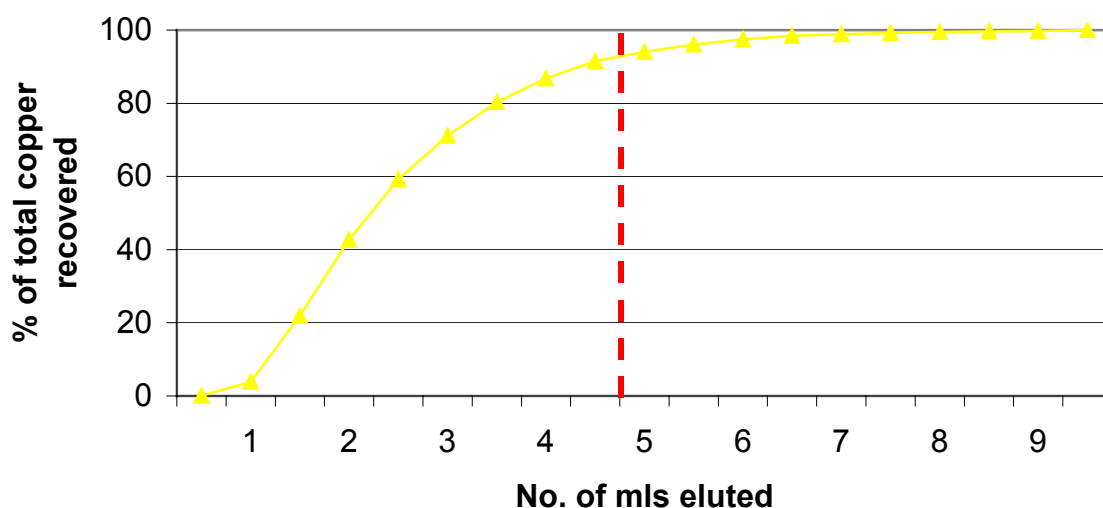


**Fig 2.12:** Copper elution (% of total recovered) versus the amount of 6M HCl eluted (in ml)

The same procedure now needs to be made with a dissolved sample of the SRM 976 copper standard to see how much the copper isotopes are fractionated by the above process.

#### b) Correcting for Instrument Mass Bias

An important feature of ICPMS measurements is the instrument discrimination (here after referred to as mass bias) which allows heavier masses transmitted by the mass spectrometer with higher efficiency than lighter masses thereby effectively causing the artificial fractionation of the isotope system under investigation. There are two ways to deal with this:

1. Sample Bracketing
2. Measuring an isotopic spike at the same time as measuring the sample

Both methods were employed here for comparison. For the sample bracketing method a Cu standard 976 was measured before and after each sample while for



the isotopic spike method a 1ppm solution of Ni was used. Previous studies (Maréchal et al, 1999 and Zhu et al, 2000) used a Zn spike and it was shown that Cu and Zn isotopes do not fractionate in the same way (Maréchal et al, 1999). It was thought that the instrumental fractionation of Ni could be more similar to that of Cu than Zn as the ionisation potential of Ni is more similar to Cu. Repeated measurements of the standard employing both sample bracketing and spike techniques are compared and discussed below.

### **c) Spike addition and measurement procedure**

1. The copper solution from the Pb separation chemistry is evaporated and then diluted with a 1ppm Ni solution (Ni standard) to produce a solution with 400ppb Cu. The difference in isotopic abundances between the Cu isotopes and the Ni isotopes means that more Ni is required to produce a similar signal (same voltage at the detector) than an equivalent concentration of Cu.
2. After the measurement of the chemistry blank, each sample was then measured bracketed by the measurement of the Cu standard; SRM 976.

If the instrument mass bias for both Ni and Cu follow the same law (exponential or power law) then all measurements should define a linear array (Figure 2.11) with a slope of 1 (Maréchal et al, 1999). The correlation coefficient of 0.9742 (and slope of 0.9964), shown here, indicates that instrument mass bias for the Ni and Cu is the same and therefore Ni can be used to correct for this while measuring the unknown copper isotope ratios of the samples.

### **d) Reproducibility**

Figures 2.13 and 2.14 show the reproducibility of the analytical method with variations of ~0.05 per mil for the spiked mass bias corrections and up to 0.15 per mil for the sample bracketed correction. Figure 2.15 also shows that the sample bracketing method can produce inaccurate results of up to 0.1 per mil. This is in agreement with previous studies of Zhu et al (2000), which employed zinc as an elemental spike and showed that the spiked technique provided more accurate and precise results than the standard bracketing technique.

Examining the fractionation of the  $^{62}/^{60}\text{Ni}$  ratio relative to the  $^{65}/^{63}\text{Cu}$  ratio

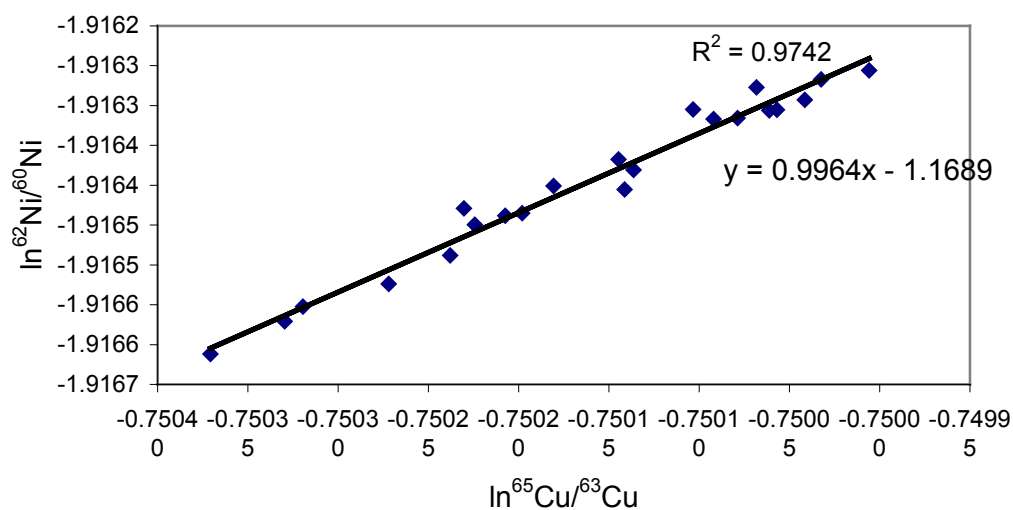


**Fig 2.13:**  $\ln^{65}/^{63}\text{Cu}$  ratio vs the  $\ln^{62}/^{60}\text{Ni}$  ratio. If the isotopes of Ni are fractionated by the mass bias of the instrument in the same way then this plot should produce a straight line with a slope close to 1.

Comparing replicate measurements of three coins by solution on the same day

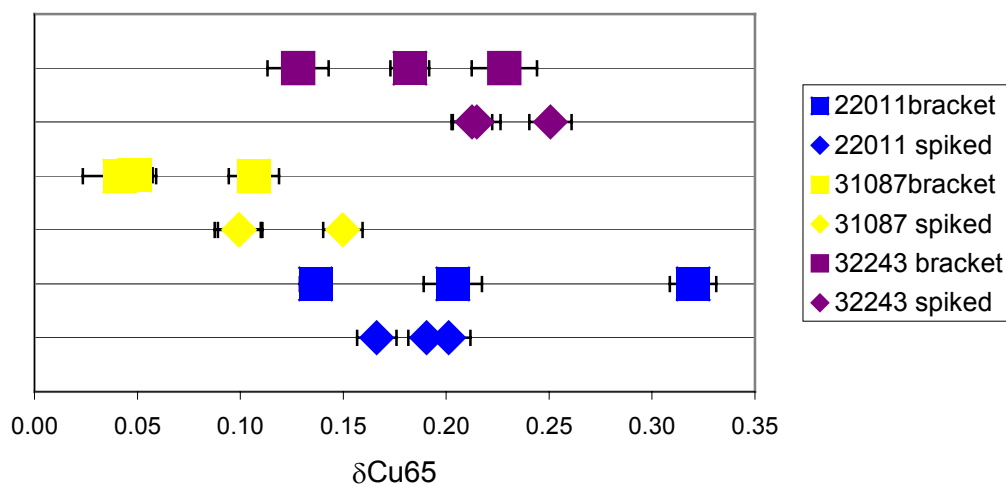


**Fig 2.14:**  $\delta\text{Cu}65$  values acquired from three repeated solution measurements of three samples using both a spike and sample bracketed correction for the mass bias. The spread of the results for the sample bracketed analyses is larger than for the analyses which were spiked.

Bracketed  $\delta\text{Cu65}$  vs Spiked  $\delta\text{Cu65}$

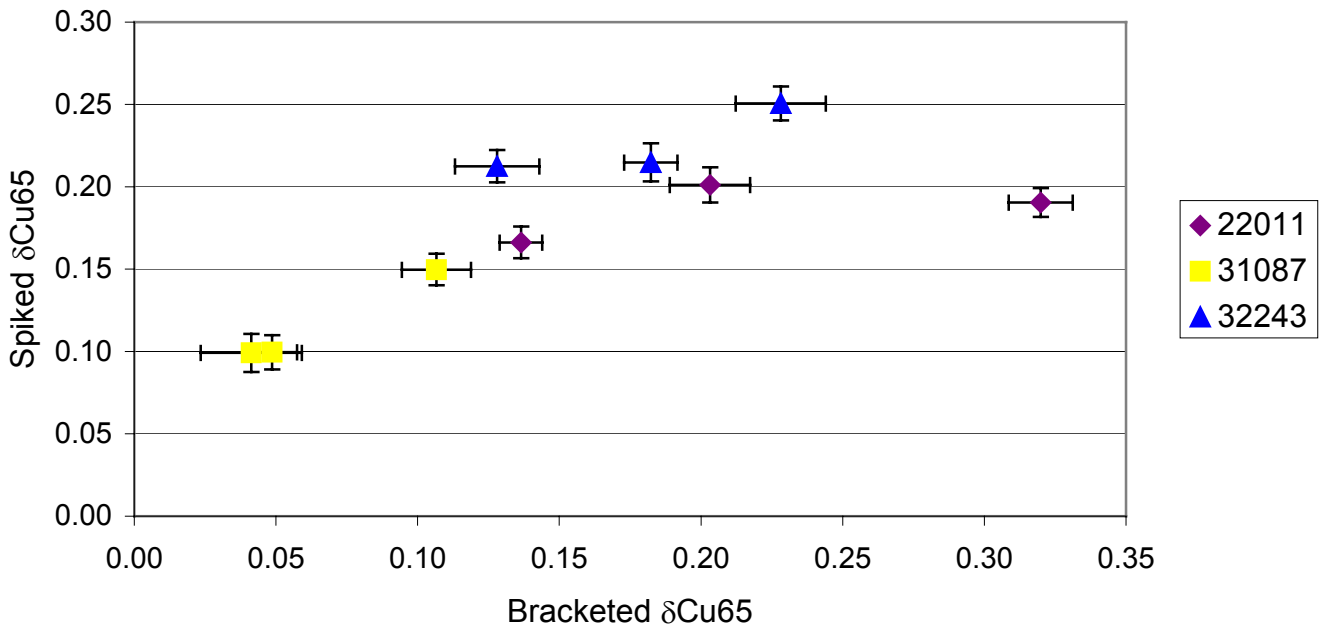


**Fig 2.15** : Sample bracketed results vs. the spiked results. It shows that for samples 22011 and 32243 there are measurements that do not lie on the expected correlation line. These two points show variation parallel to the x-axis, indicating that the accuracy of the sample bracketed method is not reliable.

### 2.6.2 Laser Method

A preliminary study to measure Cu isotopes by laser was also made using both the Ni spike and sample bracketing techniques. Introduction of the Ni spike utilised the same configuration as was used for the Pb isotopic and trace element analyses (Fig 2.6) with a Ni spike solution introduced through the Aridus™ desolvating nebuliser. The standard bracketing technique involved the ablation of the solid copper standard; SRM 976, between each sample analysis.

The variation of repeated analyses of individual samples, by laser ablation, is much larger than by solution with variations up to 2 per mil (Fig 2.15). This may be related to fractionation of the copper isotopes on or near the surface of the coins. It has been shown earlier in this chapter that Cu loss can occur up to 200µm into the coin. The results from 22007 were all made from the middle of this coin as it has been cut in half and polished. They show a tighter grouping of the results, although still not comparable to the solution analyses.

Fig 2.16 shows the comparison of laser and solution analyses, while the analyses for coin 31087 compare very well, those for the others do not. Considering the range of values acquired for the repeated analysis of coins by laser (see previous figure and 21931 on this one) then it is not surprising that differences between the two techniques occur. This can also be seen for the solid copper standard, Figure 2.17. More work is required for the laser ablation technique, perhaps the utilisation of a glass wool filter as suggested by Jackson (2003), will improve the analyses.

Comparison of repeated  $\delta\text{Cu}65$  measurements by laser ablation

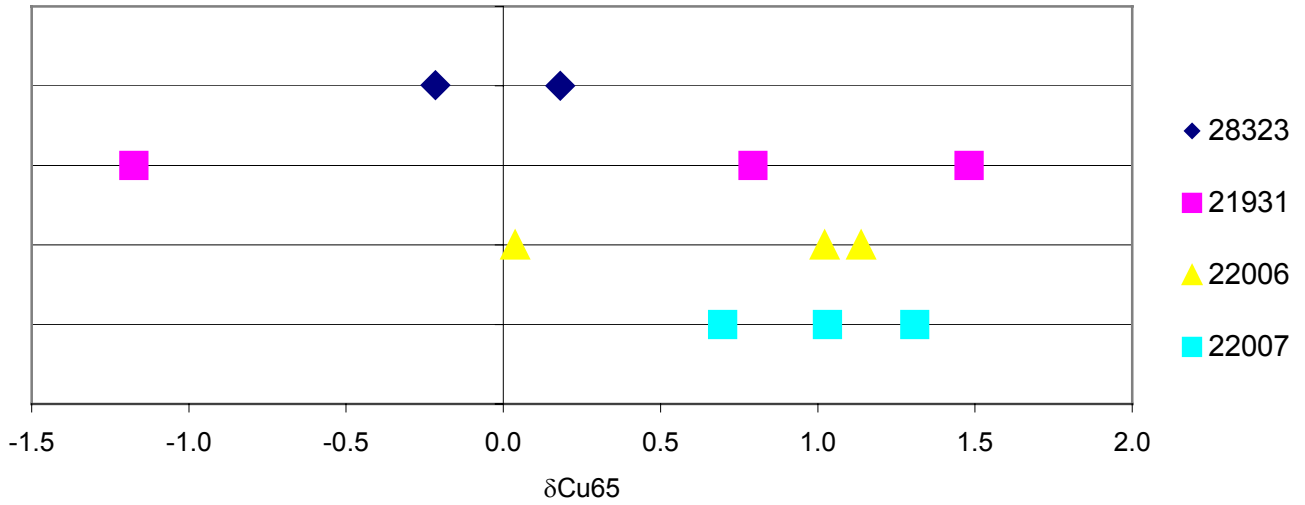


**Fig 2.14.** : Repeated measurements of four coins by laser ablation.

Comparing solution and laser  $\delta\text{Cu}65$  analyses

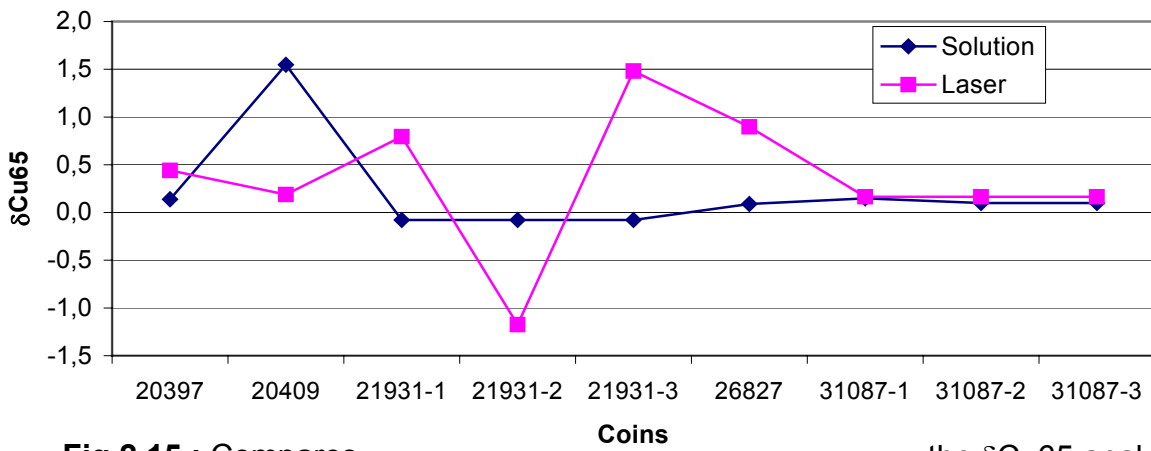


**Fig 2.15** : Compares the  $\delta\text{Cu}65$  analyses of five coins by solution and laser. Two of the coins have been measured repeatedly, 21931 has been measured three times by laser and 31087, three times by solution.

### Repeat Measurements of Solid Copper Standard by LA

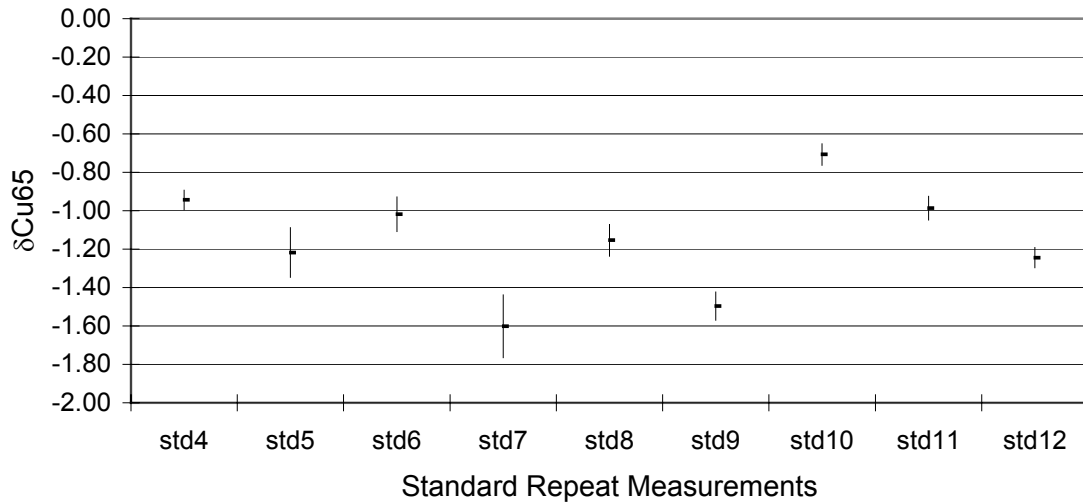


**Fig 2.16** : Repeat measurements of solid copper standard NIST 976 by LA-MC-ICPMS indicating that the ~ 1-2 per mil variations observed for the coins is also seen here and that it is the laser ablation method and probably not heterogeneities in the  $\delta\text{Cu65}$  of the material which is to blame.

### 2.6.3 Conclusions

- i. Instrument mass bias for Ni and Cu is the same and therefore a Ni spike can be used to correct for this while measuring the unknown copper isotope ratios of the samples.
- ii. The Ni spike technique provides more accurate and precise results than the standard bracketing technique.
- iii. The Laser Ablation technique produces comparable results but requires more development to improve reproducibility of the results.

## 2.7 Silver and Copper coinages

Because Silver and copper represent major components of the Celtic gold coinages, a small suite of silver and copper based coinages were investigated to determine the contribution of silver and copper to the chemical and isotopic signatures of the gold coins. This included the full range of analyses that were made on the gold coins, however, the trace element analyses by LA-ICPMS were purely qualitative as quantitative analyses were not required and quantification would have required extra development. Differences in Pb and Cu isotopic solution preparation also exist between the base metal coinages and the gold coinages and these methods are described below.

### 2.7.1 Sample preparation

The polishing and drilling of the coins is the same as for the Gold coins described in section 2.2.

### 2.7.2 EPMA

Electron microprobe analyses were made on the polished edges as with the gold coins, see section 2.3. The accuracy of the method with respect to these types of alloys is discussed below with reference to data collected during measurement.

Figure 2.17 shows the struck bronze alloy from a compositional scan. The exsolution of most of lead into the crystal boundaries can be seen. It makes the acquisition of accurate data with a maximum beam of 50µm very difficult, either a too high or too low Pb concentration is recorded. Also it is obvious that the Sb segregates mostly into the Pb phase.

Figure 2.18. shows analyses made with a <1µm electron beam on the bright spots (Pb and Sb blebs), the light zones (crystal boundaries) and the dark zones pictured in photo 2.4. It shows that all the Pb is segregated into the bright spots with most of the Sb while lower amounts (0.6 to 1 Wt% Sb) are present in the light zones and less than 0.2 wt% in the dark zones.

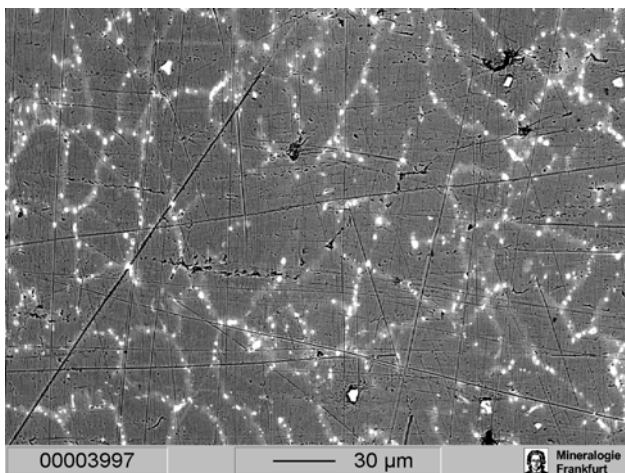


**Fig 2.17:** This compositional EPMA scan shows Pb and Sb are concentrated in the light zones which highlight the crystal boundaries. Pb and Sb are concentrated in even higher amounts within the 1-2µm bright spots within these light zones and also occasional ~5µm blebs.

The struck bronze and potin coins would benefit more from solution analysis of dissolved drillings, which would provide a more representative composition of the alloy than can be acquired by EPMA.

### Pb vs Sb coin 20411

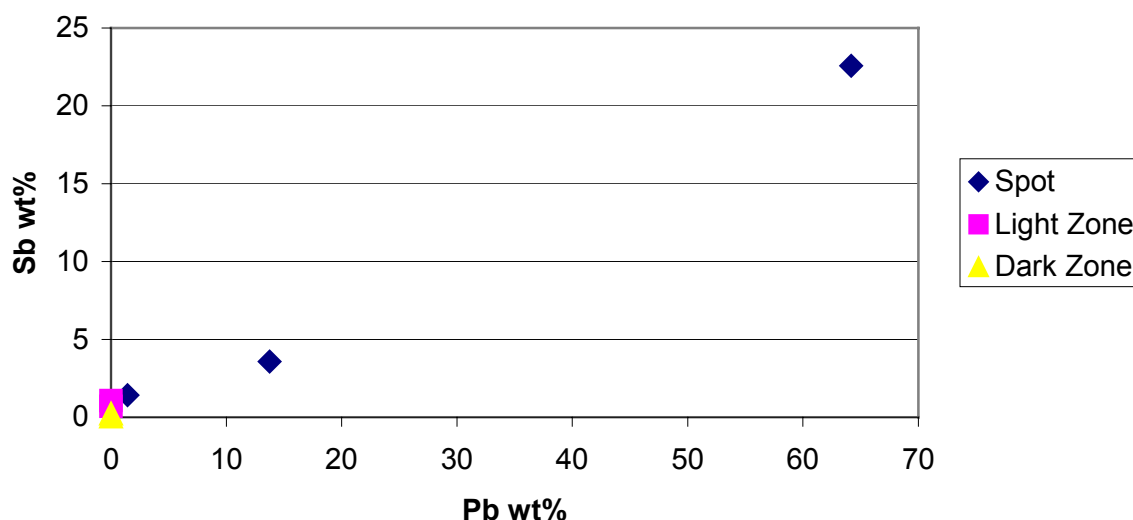


**Fig 2.18** : Pb wt% vs. Sb wt% of coin 20411 (struck bronze) shows the correlation of Pb with Sb.

### 2.7.3 Isotopic analyses

Due to the absence of gold, the chromatographic method required only one chromatographic step, which is the same as the second chromatographic stage used for the gold based matrices.

However, initial sample dissolution is as follows:

Silver: 1 ml 6M HNO<sub>3</sub> is added to the sample and left to dissolve overnight. Much of the silver typically remains but is dissolved during the last stage of evaporation.

The HNO<sub>3</sub> is evaporated and then another 1ml of 6M HNO<sub>3</sub> is added to this,

Finally, 0.5 ml of 6M HCL is added to make sure that the Pb and Cu are in solution, This causes the precipitation of AgCl.

Copper:

The copper samples are dissolved in 1ml 6M HNO<sub>3</sub> and 0.5ml 6M HCl is added, as for silver.

After dissolution the solution is dried down and 0.5ml 0.6M HBr is added. This solution is put in the ultrasonic bath for 30 min to make sure everything is in solution (except the silver chloride which is insoluble) and then the sample is loaded on preconditioned columns (with 0.6M HBr) and washed through with -2mls of 0.6M HBr to collect the copper and then 4mls of 6MHCL to collect the Pb.

## 2.8 Natural Gold Samples

### 2.8.1 Sample Preparation

The gold samples are photographed to record their size and morphology and then embedded in epoxy for polishing .

### 2.8.2 EPMA

The EPMA analyses are made using the same measuring program as for the gold coins (section 2.3) although a 7 $\mu$ m beam size was used instead of 50 $\mu$ m. The largest affect on the analyses of the natural gold samples is the porosity of the gold grains which produces low totals of up to 6-7% loss, this can be adjusted using the 100% normalisation function of the EPMA software. Also the grains are not homogenous and are commonly rimmed with a zone of almost pure gold. If the grain is only partially polished this will appear to be present throughout the grain as if the whole grain is composed of high purity gold. Therefore care must be taken to analyse the unaltered cores of the gold grains.

### 2.8.3 Trace Elements

For the natural gold samples the process of assigning the Au wt% as an internal standard became a little complicated as the EPMA results for each of the numerous individual grains in each sample were not noted. A method was used to assign Au values to each ablation based on the relative response of the AuAr<sup>+</sup> polyatomic species, which was matched with the Au concentrations measured by EPMA for each sample set of gold grains. The results from the LA-ICPMS and EPMA have simply been sorted from highest to lowest so that matches could be made. Figure 2.19 shows a correlation between the two types of results, which is sufficient to assign the gold concentrations measured by EPMA to the correct gold grain analysed by LA-ICPMS

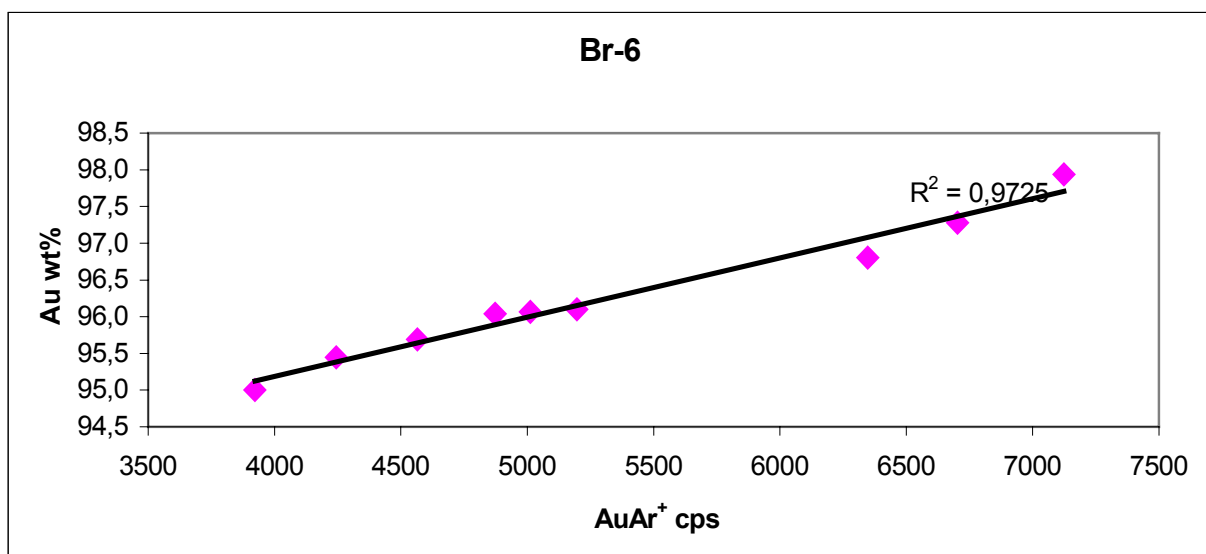


**Fig 2.19:** shows a plot of AuAr<sup>+</sup> (cps) vs. Au wt% for a sample of gold nuggets.



### 3.0 Coin Chapter

The study focused on the gold coinages excavated from the Martberg oppidum. This includes coins found there during excavations over the last ten years and coins from private collectors and national collections which are considered to be related to the coinages of the Martberg and the people who manufactured them. Whether or not all the coinages studied here were the product of the *Treveri* is a matter for debate, especially as probably only the “eye” staters can be definitely linked to them. The coinages which existed in the area before the “eye” staters, Scheers 23, 18 and 16 do not show any particularly strong stylistic relationship to the later eye staters and may have been the product of an earlier tribe which inhabited the area. The coins studied are listed in Table 3.1 and the find locations of the coins are shown on Map 3.1 covering an area centered around the Moselle valley.

This chapter summarises the data and observations acquired during the study of the coins. This includes the coin alloy compositions and characteristics and their trace element and Pb and Cu isotopic signatures. Firstly, the observations and data acquired by electron microprobe will be presented, followed by the trace element data and the Pb and Cu isotopic analyses. Each data set is discussed separately with the broader picture being considered at the end of the chapter.

#### 3.1 Coin Weights

Table.3.1 presents the coins grouped together in their respective coinages, in roughly chronological order, considering the numismatic history of the coins discussed in Chapter 1. Many of the coins that were found within the sanctuary of the Martberg, representing coinages Scheers 30/V and 30/VI, were sacrificed. They were notched or halved as religious offerings (Figures 3.1a and b). The sacrificing of coins seems to be restricted to these two coinages and therefore only a relatively small number of the coins from these two series are representative in terms of weight.

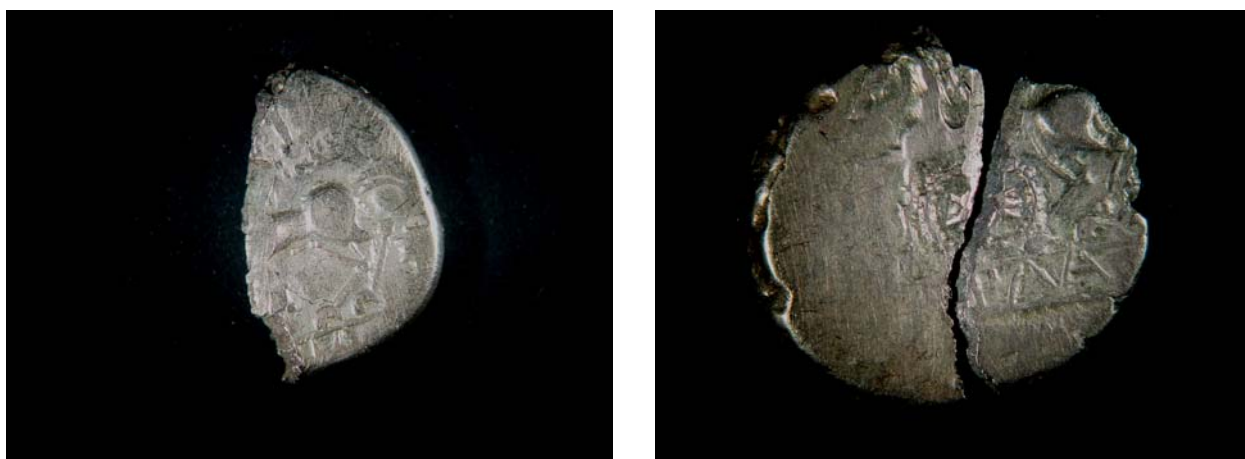
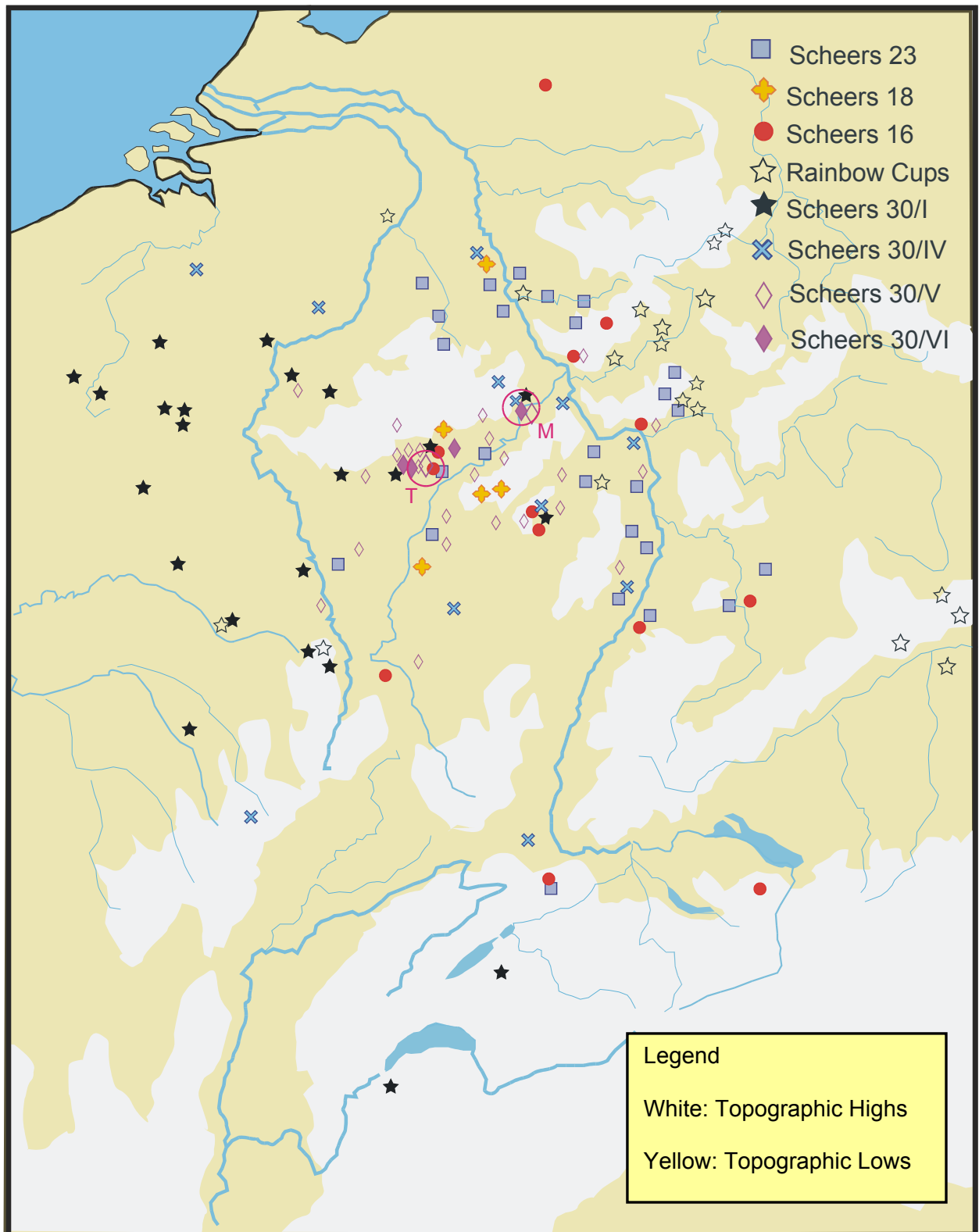


**Fig: 3.1 a & b)** On the left is coin 22010 from series 30/V showing the backend of the horse. This coin was sacrificed, chopped in half, as an offering in the sanctuary of the Martberg oppidum. The coin on the right 20397 is from series 30/VI and was initially merely notched, however its high copper composition makes this coin very brittle and it has since broken into two pieces.



**Map 3.1:** A distribution map of the coinages studied with the two main oppida of the Treveri; the Martberg (M) and the Titelberg (T).

### 3.2 Coin Alloys

The most striking feature of the gold coin alloys is that all of them are alloyed to a large degree with Ag and Cu. Microprobe measurements therefore concentrated on analysing the Au, Ag, Cu and Sn compositions of the coins. The nature of the alloy has important affects, not only on the colour and weight of the coinages but also on the analytical methodology which must be employed to acquire data which is accurate and precise enough to use. This is not only important for the microprobe measurements but also the LA analyses and is discussed in detail in Chapter 2. This section presents the alloy data acquired by electron microprobe and discusses the groups that occur with reference to their numismatic classification. The die sets used for striking the coinages have not been the focus of rigorous study, however, when obvious differences have been observed they are noted.

The Au, Ag and Cu compositions of the coins are summarised in Fig 3.1. A complete table of the Au, Ag, Cu, Pb and Sn analyses by EPMA can be found in the appendix along with standard deviation calculations for each measurement.

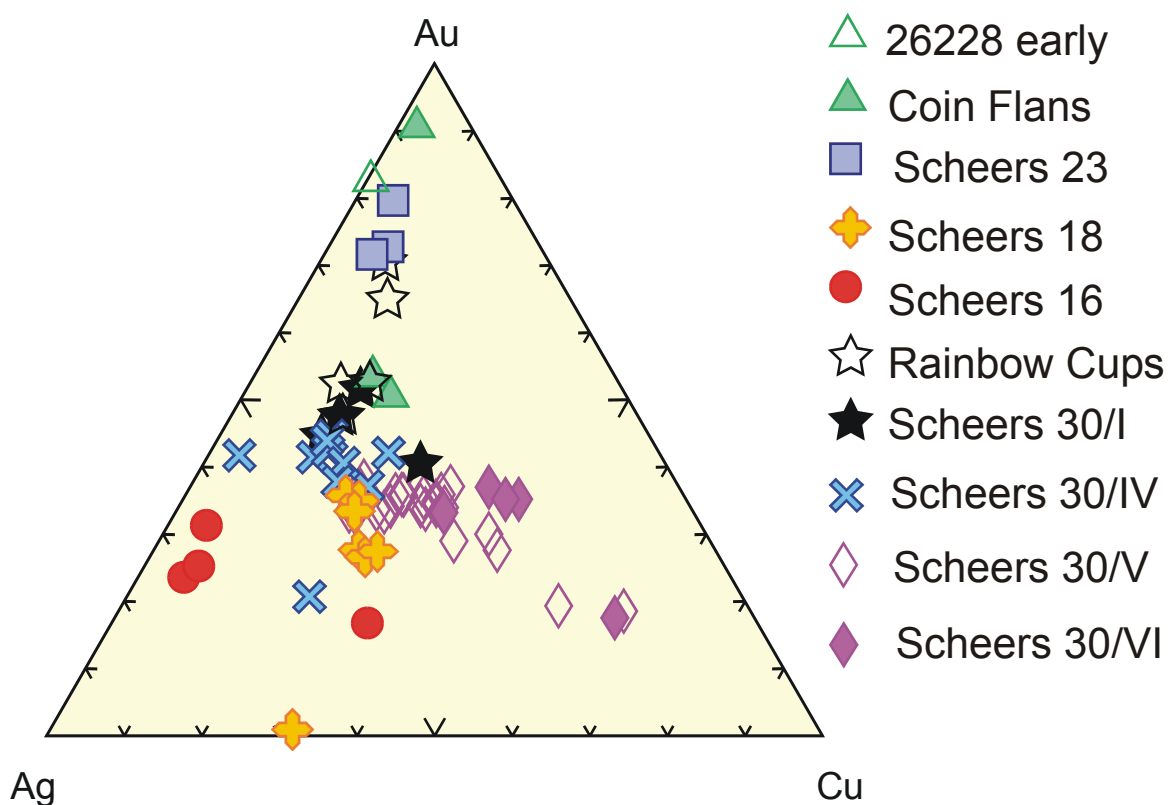


**Fig 3.1:** is a ternary Au-Ag-Cu plot of the results which show a general trend of decreasing Au content which comes to halt around the time of the series 30/IV coins and stays relatively constant as copper increases. The Scheers 18 and 16 coins are not part of this trend, typified with lower gold contents than the other coinages. Sn has been added to the copper as its presence is probably due to the addition of recycled bronze (coins 21931 and 22008, see Table 3.1).

The following sections note important characteristics of each coinage.

**Table 3.1: Classifies the coins within their respective coinages and includes their weights and Au-Ag-Cu compositions**

Coin Type	Identification	Weight (g)	Au wt%	Ag Wt%	Cu wt%	Note
<b>Early unknown</b>	26228	0.87	78.9	16.2	0.5	Plated ? Possibly Sch. 16?
<b>Scheers 23</b>	Fö117	2.04	79.6	15.5	4.8	Quarter Stater
	Robiano	1.94	71.5	22.2	6.1	Quarter Stater
	Fö116	1.92	72.6	19.6	7.6	Quarter Stater
<b>Scheers 18a</b>	FU G122	7.21	27.4	43.6	28.9	
	Fö105	7.11	26.5	45.5	27.7	
	3321	7.06	27.6	45.9	26.4	
<b>Scheers 18b</b>	Stw4	1.89	33.4	43.6	23.0	Quarter Stater
	FU G121	1.75	34.9	42.2	22.8	Quarter Stater
	2950	7.31	35.7	43.5	20.7	
	87150	5.78	0.9	67.3	31.0	3.34 wt% Sn
<b>Scheers 16</b>	FU G93	5.81	25.1	67.4	6.9	
	FU G77	6.43	16.75	50.18	32.84	
	Stw4a	6.36	31.24	63.66	4.90	
	9800b	6.20	23.53	70.43	5.84	
<b>Rainbow Cups</b>	SFLAN1045	7,51	70.30	21.04	8.40	Bavarian IIIa
	8543	7.45	52.46	32.01	15.38	Bavarian IIe
	6124	7.31	64.82	23.59	11.46	Bavarian IIc
	Regen	7.08	47.62	38.00	14.34	Hessen
	Fö124	6.84	52.22	35.89	11.76	Hessen
<b>Scheers 30/1</b>	LT8799	6.11	47.46	38.40	14.00	
	Lux 7	5.75	44.56	42.19	13.14	
	SFLAN507	6.10	51.55	33.75	14.65	
	22011	3.64	40.46	31.55	27.93	Plated
<b>Scheers 30/IV</b>	22809	5.89	41.41	44.89	13.63	
	22807	5.94	43.89	40.29	14.17	
	30IV586	5.87	43.80	41.86	14.18	
	87149	5.90	42,29	42,48	15,10	

Coin Type	Identification	Weight (g)	Au wt%	Ag Wt%	Cu wt%	Note
	30IVG176	5.91	40.46	41.32	17.97	
	30IV329	5.88	37.69	43.47	18.57	Wallendorf
	30IV575	5.76	36.99	39.88	22.83	
	30IV582	5.82	41.97	34.82	23.02	
	32243	3.64	20.72	55.96	23.62	
	31433	1.60	40.52	52.78	3.90	Plated, broken
<b>Scheers 30/Va</b>	30V542	5.41	36.58	41.23	21.99	Ag-rich
	31087	5.48	37.82	40.15	22.00	Ag-rich
	Fö106	5.49	33.34	44.13	22.24	Ag-rich
	28323	1.79	34.90	41.80	22.29	Ag-rich, Halved
	22007	3.04	32.94	43.29	22.91	Ag-rich, Halved
<b>Scheers 30/Vb</b>	20163	5.58	33.45	40.45	25.55	Eutectic composition
	22009	5.42	33.28	39.83	26.88	Eutectic composition
	Lux 3	5.39	34,03	38,48	27,15	
	6719	5.36	35,77	37,09	27,02	
	30VG179	5.50	35.77	36.15	27.82	Cu-rich
	Lux 4	5.36	35,71	36,07	28,10	
<b>Scheers 30/Vc</b>	20409	2.06	37.42	32.88	29.68	Cu-rich Halved
	12325	5.48	35,40	33,57	30,81	
	Lux 2	5.45	34,14	34,57	31,00	
	30V549	5.50	33.60	34.22	31.86	Cu-rich
	Lux 5	5.47	33.77	31.55	34.14	
	26827	2.55	35.39	30.73	32.51	Cu-rich Halved
	22006	1.80	33.71	32.14	32.57	Cu-rich Halved
	22113	3.62	34.83	32.30	32.64	Cu-rich Halved
	22010	2.60	36.89	29.33	33.40	Cu-rich Halved
<b>Scheers 30/Vd</b>	21931	2.57	19.28	24.29	56.28	Halved 4.61% Sn
	22008	5.06	18.57	16.43	65.34	2.05% Sn
	8544	4.25	28,18	28,71	45,20	Plated

Coin Type	Identification	Weight (g)	Au wt%	Ag Wt%	Cu wt%	Note
	19698	3.68	30.26	27.88	41.60	Plated
	19697	4.40	28.52	32.62	38.48	Plated
<b>Scheers 30/VI</b>	26227	5.41	33.12	32.10	34.51	
	30449	2.37	36.98	24.46	38.53	Halved
	Lux 1	5.22	35,05	23,21	41,47	
	20397	4.93	35.10	21.57	43.20	Notched, broken
	Lux 6	4.98	17.48	17.92	64.25	Plated
	SFLAN1451	4.58	0.81	1.11	88.29	10.25% Sn Bronze
	SFLAN617	4.98	----	----	78.45	20.43% Zn Brass
<b>Coin Blanks (Flans)</b>	SFLAN3000	2.29	90.21	7.00	2.45	Possible Flan
	SFLAN1148	5.49	50.35	30.33	19.14	Possible Flan
	FLAN	6.14	53.12	31.01	15.23	Flan

**Table 3.1:** All the Gold alloy coins studied are listed here, grouped together in their respective coinages, which are roughly arranged in the accepted chronological order of development (Haselgrove, 1999). Included in the table are the coin weights and the major components of the alloys, Au, Ag, Cu and Sn, as measured by electron microprobe. Many of the coin weights are not representative of the coinages as they are coins which were sacrificed by halving in the sanctuary of the Martberg oppidium. Coin 20397 was merely notched at that time but was found broken into two pieces. The Scheers 30/V coinage can be divided into a number of groups based on the composition of the coins. Where Sn has been measured in excess of 0.5 wt% it has been included as part of the copper component, on the assumption that it represents recycled bronze. The Au-Ag-Cu compositional data listed here is plotted in Fig 3.1.

### 3.2.1 Scheers 23



**Fig 3.2:** Scheers 23, the earliest coinages studied with the head of Apollo and the winged Pegasus.

The three examples of this coinage studied are all quarter staters with thickness of no more than 1mm (Figure 3.2). They are the most Au rich of the coins studied and hence their alloys are more homogenous. Two coins Fö116 and Sch23 Robiano have very similar alloys while Fö117 is markedly different with higher Au content (Table 3.1).

### 3.2.2 Scheers 18



**Fig: 3.3:** Scheers 18; one of the “American” type coinages with the head of Apollo and a human headed horse.

This group contains a total of seven coins (Fig. 3.3), two quarter staters, four full staters and a rather odd stater with broken edges which is made from a Ag:Cu alloy, 67:31wt% respectively, approximately 3% Sn and less than 0.5% Au.

This coinage can be divided into two groups by its Au composition (Fig 3.4). The

higher Au group represents the two quarter staters and a stater which is a little heavier than the staters from the lower Au group.

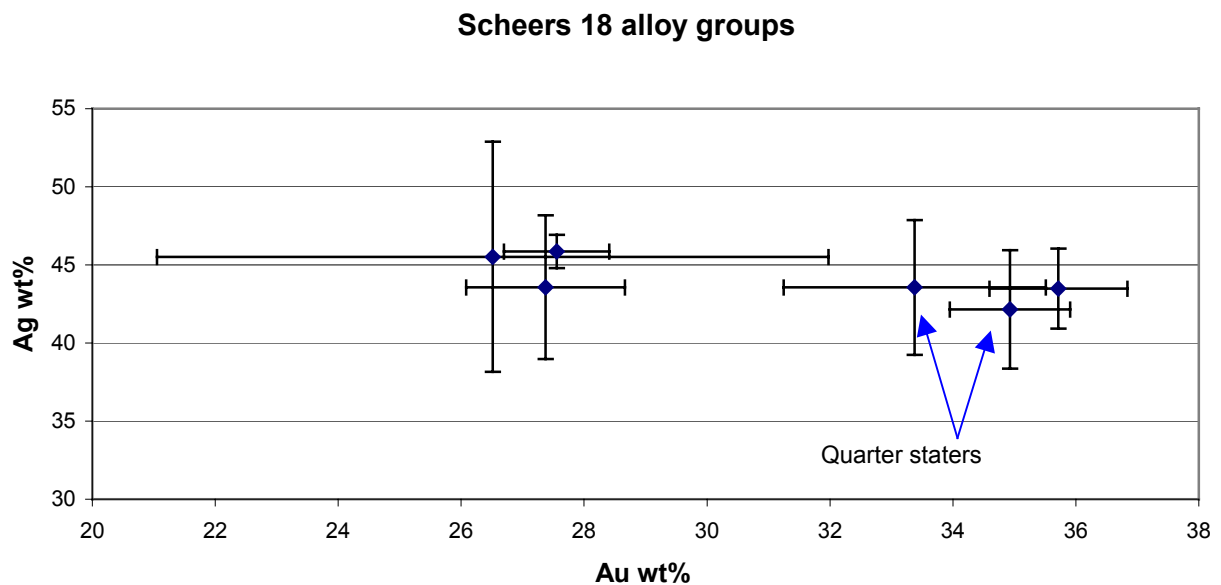


**Fig 3.4:** A Au wt% vs. Ag wt% plot showing the two alloy groups represented in the Scheers 18 coinage.

### 3.2.3 Scheers 16



**Fig. 3.5:** Scheers 16 supersedes the Scheers 18 and also belongs to the “Armorican” type coinages.

This Silver rich coinage supersedes Scheers 18 in the chronology and typology. They are smaller in size but have lower weights (Fig. 3.5).

Figure 3.6 shows that they form a consistent alloy group, except for coin FUG77, which is distinctly different with lower Au and Ag in favour of Cu. This coin also has a large error associated with its analysis which is probably a result of extreme heterogeneity produced by the enhanced phase separation of a Cu-rich phase due to the low Au content. In contrast, the other three coins of this series have relatively low errors as there Ag:Cu ratio is high enough that it has suppressed the



### Scheers 16 alloy groups

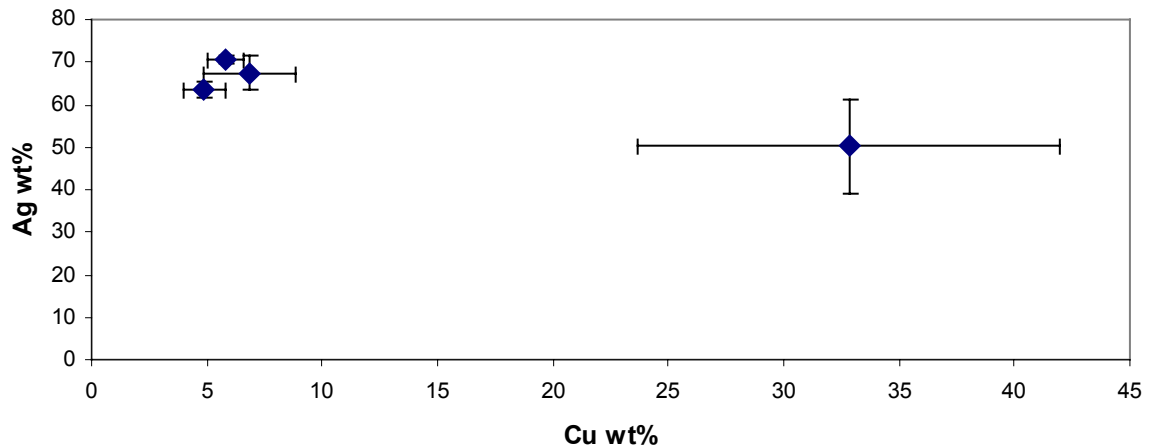


**Fig 3.6:** Cu wt% vs. Ag wt% reveals the main group and the Cu-rich coin FUG77.

### Coin 26228

This coin is quite small and because of the many peculiarities associated with it, it is dealt with separately. By its size it may have been a quarter stater and although it is very dirty and malformed, making its identification very difficult, it has been classified as Scheers 16. Of all the alloys it is the most pure with no addition of Cu although its Ag content puts it in the range of the Scheers 23 coinages. It also gives the appearance of being plated but it is difficult to be certain without damaging it too much

### 3.2.4 Rainbow Cups

The four coins from this coinage actually represent four different types which can be divided into Southern and Northern numismatic groups, Figure 3.7.

### Rainbow Cups

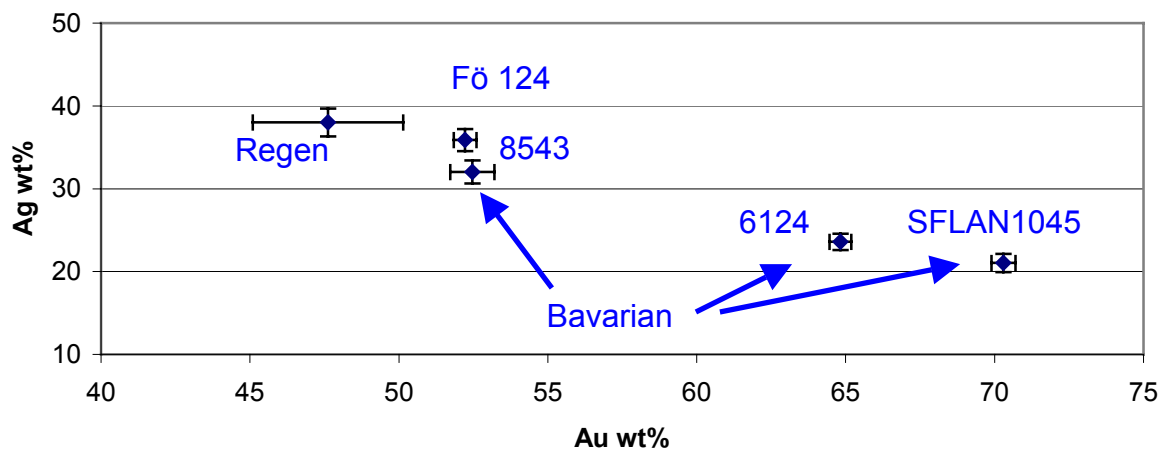


**Fig 3.7:** This shows the Au-Ag composition of the ternary alloy for the rainbow cup coins.

The Northern group is localised around an area east of the Rhine immediately adjacent to the Treveran lands of the Moselle valley, while the Southern group is centred around the Danube river in Bavaria. Two general stylistic groups are represented by the Southern Rainbow cup coins (8543, 6124, and SFLAN1045, belonging to the Bavarian series, IIe, IIc and IIIa respectively). The alloy compositions of the rainbow cup coins agree with earlier studies made by Hartmann (1976).

### 3.2.5 Scheers 30/I



**Fig. 3.8:** Scheers 30/I is the first of the “Eye” stater series.

The first of the “Eye” stater series (Figure 3.8), its alloy is not particularly consistent (Figure 3.9), although the coinage can not be truly characterised by only three real coins. The forth, 22011 is a plated coin with an alloy mix closer to that of the Scheers 30/V series

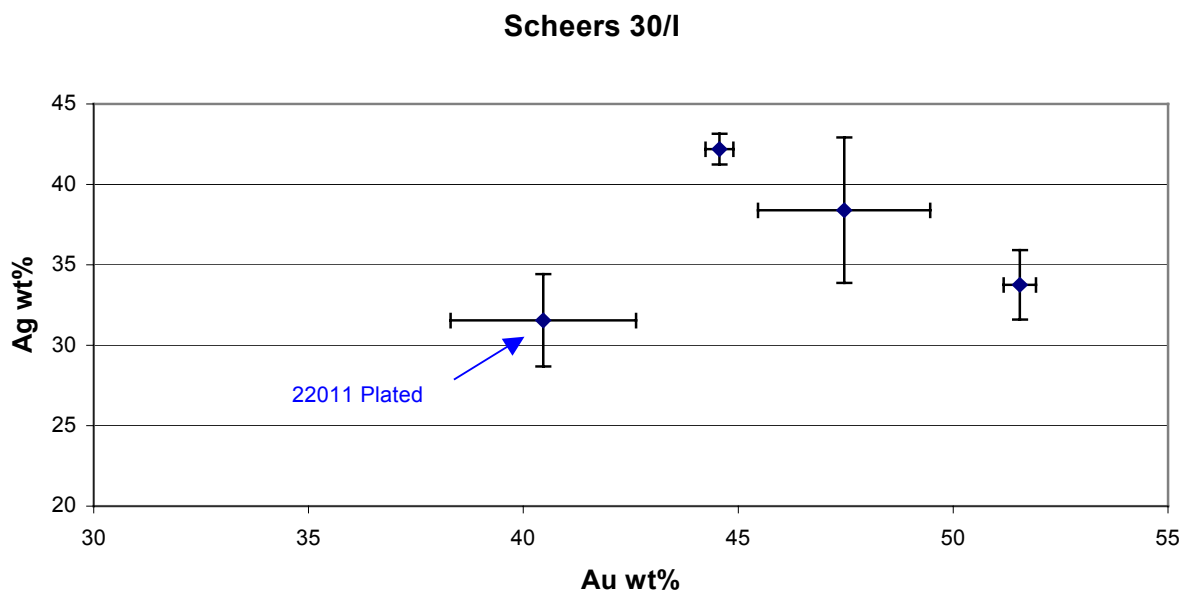


**Fig 3.9:** Showing the four coins from the Sch. 30/I series. Coin 22011 is highlighted as it is a plated coin with the Au and Cu composition of the plating shown here. The core of the coin is 99% pure copper.

### 3.2.6 Scheers 30/IV



**Fig. 3.10:** Scheers 30/IV the second of the “Eye” stater series represented in the study area.

This coinage is the first Gold coinages represented at the Martberg. Of the coins found there, two are of anomalous composition. One is a plated copper core, 32243, with plating containing very low amounts of Cu, although retaining the same relative amounts of Ag and Au, whilst the other, 31433, has a similar amount of Cu as the others but the Ag content has increased at the expense of Au. These two coins are excluded from the graph below (Figure 3.11). There seems to be the possibility of three subgroups but only two can be really given any confidence. Coins 30IV575 and 30IV582 (blue ellipse) seem to form a higher Cu subgroup and they are also slightly lighter than the others.

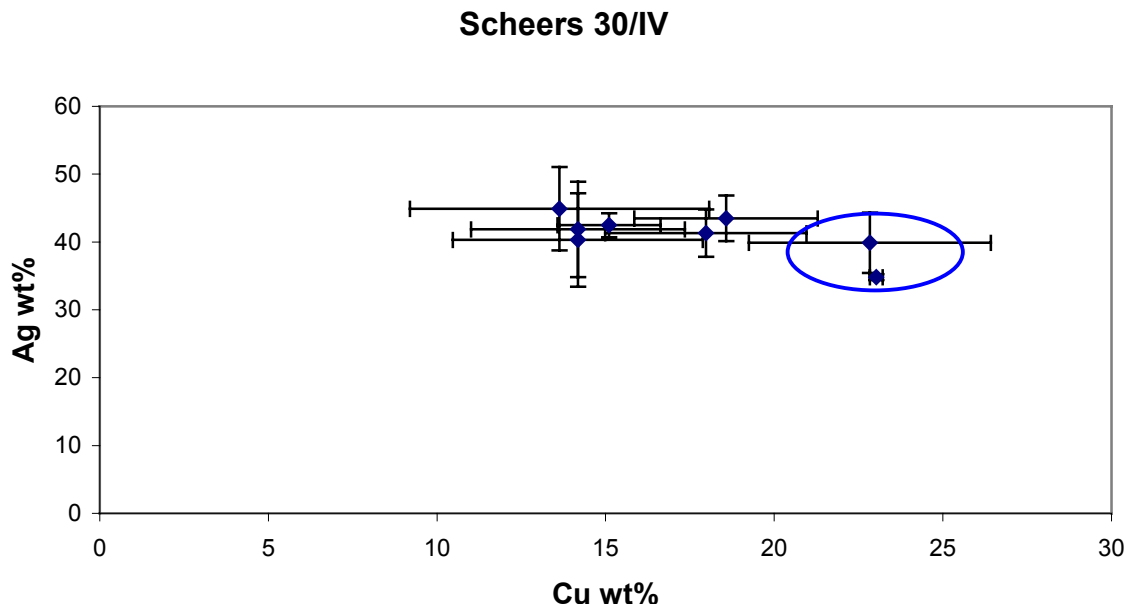


**Fig 3.11:** A plot of Cu wt% vs. Ag wt%. The error involved in the measurement of these coins makes it unclear if there are any real subgroups represented in this coinage.

**NB:** Coinages Sch 30/IV - 30/VI are better observed on Cu vs. Ag plots than Au vs. Ag plots as examination of the Tri-plot, Fig 3.1, shows the development of the coinage as progressing horizontally across the graph with little change in Au content.

### 3.2.7 Series 30/V POTTINA



**Fig 3.12:** The first inscribed coinage of the area, carrying the legend POTTINA.

This coinage is the most prolific of those studied, not only is it the most common gold coinage found at the Martberg but also the most common of those found in the area (Fig. 3.12). It is also the first inscribed coinage of the area, carrying the legend POTTINA, and is the first coinage to be sacrificed with many of the coins broken in half. See section Coin Weights.

### Series 30V subgroups

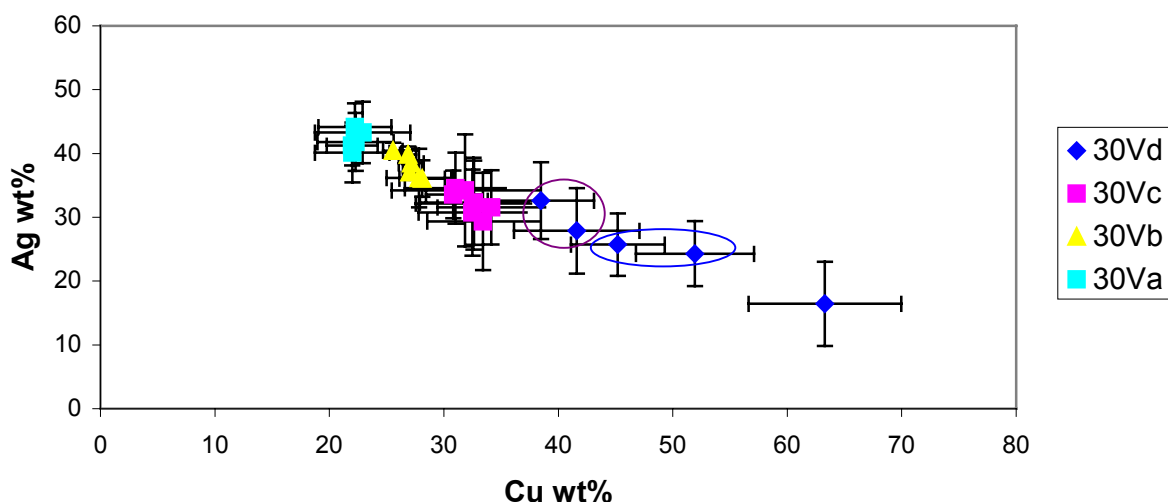


**Fig 3.13:** Here is a Plot of Cu vs. Ag for the Series 30/V coins, showing the subgroups into which it can be divided based on Alloy composition.

This coinage can be divided into four groups based on the Cu composition of the coins, Fig 3.13. Group 30/Va is silver rich in that it lies on the silver side of the

eutectic (See Fig 2.4b Analytical Methods Chapter). Group 30/Vb is also relatively silver rich, however it lies on and a little to the copper side of the eutectic. The very low error which is seen in some of these coins is a result of having compositions close to that of the eutectic mixture which results in the formation of very finely interspersed plates of Cu and Ag rich phases which allow for a more homogeneous result to be measured with a 50µm beam size (Section 2.3). The error tends to increase the further away from the eutectic the alloy lies as then larger and coarser primary dendrites can form whilst decreasing the amount of fine eutectic mixture which can form.

The striking of group 30/c is distinctly different from the first two groups, although it is uncertain whether a slightly different design of die is used (possibly without the diagonal rope design on the obverse, what is clear is that all the coins from this group are all badly struck. Also, it maybe possible to further divide this subgroup as the plot shows two concentrations of points. However, the error caused by the inhomogeneity of the alloy does not allow this to be confidently made.

Group 30/Vd contains coins with anomalously high copper compositions. Two of the these coins, 21931 and 22008 (represented in the blue ellipse), also contain significant amounts of Sn (2-4%) and suggest that recycled bronze was used in their manufacture in instead of refined copper. They also have a distinctive black patina from oxidation during burial.

There are also two plated coins with almost pure copper cores, 19697 and 19698, in the purple ellipse. The alloy mix used in the plating is consistent between the two, within error. Another coin from subgroup 30/Vd is also plated, however this coin (8544) is much more copper rich.

### 3.2.8 Scheers 30/VI ARDA

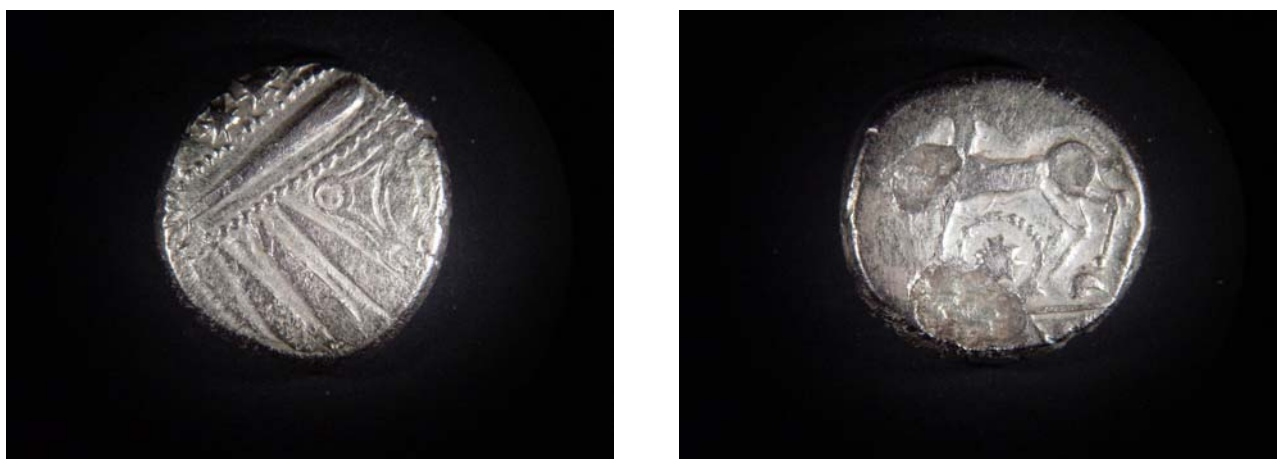


**Fig 3.14:** The Scheers 30/VI coins carry the legend ARDA

This coinage carries the legend ARDA and immediately supersedes the POTTINA coinage (Fig. 3.14). It is not a prolific coinage with only around 10 actual gold coins found.

The coins have an average Cu composition of 40% (Fig. 3.15). Coin 26227 is somewhat different with a composition and weight (5.41g) which resembles more

the Series 30/Vc coins, although as most of the 30/VI coins are either broken, or plated, it is difficult to be certain what the weight of these coins should be.

Coins SFLAN1451 and SFLAN617, found at the Wallendorf oppidium, are completely different from everything else. They have motifs consistent with the gold coinage but one is brass while the other is bronze (Table 3.1).

### Scheers 30/IV ARDA

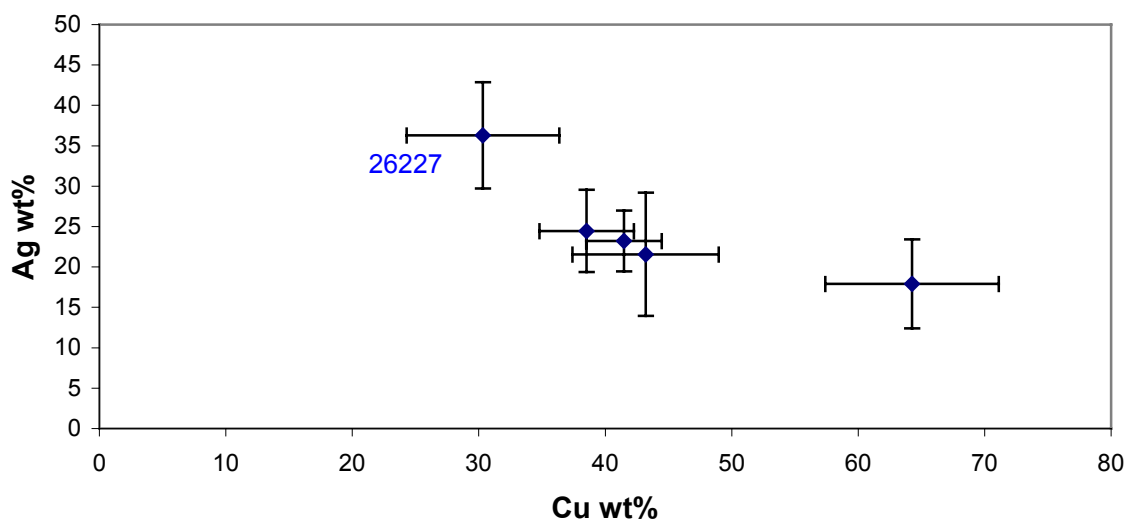


**Fig 3.15.:** The Cu vs. Ag plot shows that while three of the coins are in good agreement two of them are quite different and in fact one of them, 26227, has a similar alloy to the Series 30/Vc.

### 3.2.9 Flans

The metal objects grouped together here are Au-Ag-Cu alloys which may have been destined to become coins (pictures can be found in the Appendix: Coin Catalogue). The one named Flan was found at the Martberg and is clearly a real flan which has been hammered flat prior to striking. Of the other two, (both found at the Wallendorf oppidium) SFLAN1148 is more likely to be coin material than SFLAN3000, as its alloy mix closely resembles that of the first Flan while the other is very gold rich and does not resemble any of the coins studied here (Fig 3.16). The Flan and SFLAN1148 (the protoflan) both have alloy mixes which are similar to coins from Scheers 30/I and also some of the Rainbow cups, however the weight of SFLAN1148 is far to low, resembling more the weight of the POTTINA series. The Flans weight is very similar to that of coins from Scheers 30/I. Table 3.2.

	Weight g	Au wt %	Ag wt%	Cu wt%
Flan	6.14	53.12	31.01	15.23
SFLAN507 (30/I)	6,10	51.55	33.75	14.65

**Table 3.2** The Flan and the series 30/1 coin SFLAN507 are practically identical in weight and alloy.

### Comparing Flans with Sch 30/I and the Rainbow Cups

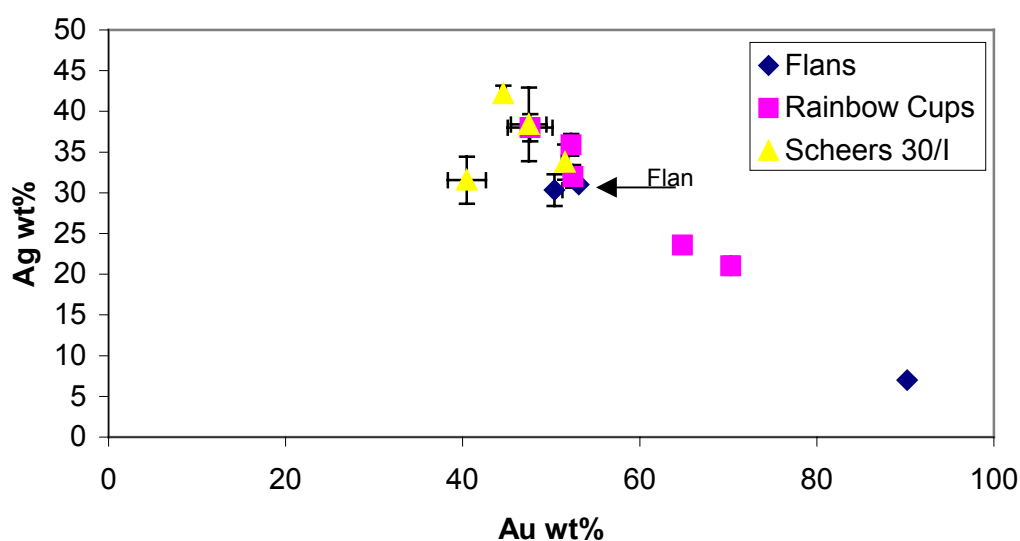


**Fig 3.16:** A Au vs. Ag plot of the Flans and the Scheers 30/I and Rainbow Cup coins to which they show compositional similarities.

#### 3.2.10 Silver and Copper coinages

A suite of contemporary silver and copper coinages were also examined to help in determining what affect the addition of silver and copper had on the trace element and isotopic signatures of the gold coin alloys. This included the full range of analyses that were made on the gold coins (see section 2.7).

The silver coinages represented include coins from Scheers 54, Scheers 55 and Scheers 55 with a ring motif. Their compositions, determined by electron microprobe analysis, are summarised in Table 3.3. According to Wigg and Riederer (1998)(see Fig 1.2) Sch. 54 is contemporary with the gold coinages Sch.16 and 18, while the Sch. 55 are associated with the Sch. 30/IV and Sch. 55 (with a ring) with Sch. 30/V.

Analyses by Riederer (Wigg and Riederer, 1998), which were made on 54 silver coins from these groups have shown that there are two groups of alloys for the Sch 55 with ring, one, identical to the Sch 55, represented by coin 15654, and the second with over twice as much copper represented by coins 15666 and 20794. Riederer's analyses also show a steep increase in Sb with the second Sch. 55 with ring group, from below a detection limit of 0.02 wt% to over 0.1 wt% Sb, which has important implications for the source of Cu in the gold coins as the change from Sch 55 without a ring to Sch 55 with a ring is contemporary with the change from Sch 30/IV to Sch. 30/V with a similar steep increase in Sb content.

The copper based coinages analysed represent two basic groups, one is the Potin coinages and the other is the Struck Bronze. Potin, as the name suggests is a high tin bronze which was typically cast as chains of coins in a mould with the design carved into it. The Struck Bronze coins are a little confusingly named as they

<b>Comment</b>	<b>Ag wt%</b>	<b>Cu wt%</b>	<b>Pb wt%</b>	<b>Sb wt%</b>	<b>As wt%</b>	<b>Bi wt%</b>	<b>S wt%</b>	<b>Mn wt%</b>	<b>Zn wt%</b>	<b>Fe wt%</b>	<b>Au wt%</b>
<b>15666-55R</b>	85.92	13.31	0.27	0.01	0.00	0.02	0.00	0.02	0.00	0.01	0.44
<b>20794-55R</b>	86.97	12.35	0.18	0.15	0.05	0.01	0.00	0.01	0.00	0.01	0.26
<b>15654-55R</b>	93.53	5.51	0.54	0.00	0.00	0.08	0.02	0.02	0.01	0.00	0.30
<b>20160-55</b>	92.01	7.25	0.12	0.00	0.00	0.04	0.01	0.02	0.01	0.00	0.54
<b>20792-55</b>	93.19	5.90	0.44	0.00	0.00	0.06	0.01	0.02	0.00	0.00	0.37
<b>20793-55</b>	93.38	5.77	0.54	0.00	0.00	0.07	0.01	0.01	0.00	0.00	0.21
<b>20791-54</b>	96.67	2.65	0.39	0.00	0.00	0.07	0.00	0.02	0.01	0.00	0.18
<b>20143-54</b>	96.68	2.69	0.53	0.00	0.00	0.06	0.01	0.01	0.00	0.01	0.00
<b>20988-54</b>	97.25	2.25	0.13	0.00	0.00	0.02	0.01	0.02	0.01	0.01	0.31
<b>24829?</b>	83.54	3.19	0.22	0.00	0.00	0.04	0.02	0.02	0.00	0.04	1.38
<b>29867?</b>	87.88	4.22	0.03	0.00	0.00	0.03	0.01	0.02	0.01	0.01	0.87

**Table 3.3:** Table of Silver coins investigated. There are three coinages represented, Scheers 55, Scheers 55 with a ring motif and Scheers 54 (each coin has a sample number with the coinage number noted after the hyphen, R denotes the presence of the ring design and a ? mark shows that it is unknown which coinage they belong to). The two coins of uncertain type seem to fit with the Scheers 55 with a ring.



Coin No.	Cu wt%	Pb wt%	Sb wt%	As wt%	Bi wt%	Ag wt%	Ni wt%	Sn wt%	Mn wt%	S wt%	Fe wt%
<b>23039p</b>	67.65	7.59	0.21	0.09	0.20	0.10	0.10	18.88	0.01	0.06	0.00
<b>29650p</b>	72.34	7.98	1.18	0.12	0.00	0.15	0.10	19.98	0.01	0.05	0.00
<b>29476p</b>	78.18	3.33	0.68	0.23	0.02	0.17	0.14	17.24	0.01	0.06	0.02
<b>1299p</b>	79.11	5.14	0.32	0.16	0.01	0.08	0.09	15.80	0.01	0.03	0.01
<b>23040p</b>	79.79	10.66	0.25	0.12	0.04	0.14	0.09	8.80	0.01	0.02	0.00
<b>19696s</b>	89.90	5.03	0.24	0.04	0.01	1.14	1.33	0.08	0.01	0.01	0.00
<b>20189s</b>	95.36	3.00	1.09	0.10	0.02	0.24	0.17	0.01	0.01	0.01	0.00
<b>24861s</b>	96.60	1.02	0.71	0.05	0.01	0.24	0.08	0.00	0.01	0.01	0.00
<b>21825s</b>	97.97	0.95	0.17	0.01	0.01	0.09	0.85	0.03	0.01	0.09	0.01
<b>20416s</b>	98.07	1.46	0.52	0.02	0.02	0.15	0.00	0.05	0.01	0.00	0.00
<b>20186s</b>	98.42	0.80	0.30	0.01	0.01	0.26	0.06	0.36	0.01	0.00	0.00
<b>24619s</b>	99.14	0.91	0.16	0.02	0.01	0.18	0.01	0.09	0.01	0.00	0.00
<b>26657s</b>	99.56	0.06	0.02	0.02	0.03	0.06	0.01	0.02	0.01	0.00	0.01
<b>20411s</b>	99.58	0.31	0.39	0.04	0.01	0.19	0.10	0.02	0.01	0.00	0.00

**Table 3.4:** Shows the major and trace element composition of the copper based coinages, measured by electron microprobe (see section methods). The Potin coins are denoted by p and the Struck Bronze with s.

contain no Sn, instead they contain significant amounts of Pb ~1%. The distribution of lead between the Cu crystals aids in the flow of the metal for casting and striking. As with the Potin, these coins were cast as chains, however, unlike the Potin coins the mould did not contain the impression of the design. These coins were merely cast in plain moulds and were struck afterwards to produce the design, hence the term "Struck". The copper coin compositions and major trace elements, as

### **3.2.11 Summary of Major Element Compositions:**

Studies of coin alloy mixtures are important as they reveal subgroups within coinages which probably reflect different mintings. They also show the metallurgical development of coinages through processes such as progressive debasement and allow theories to be made as to the type and amount of metal that was available to the Celtic people.

Considering the tri-plot of Au-Ag-Cu compositions of the coins (Fig: 3.1), a trend line can be imagined that leads down from the earlier Sch 23 coins through the Rainbow cups to the Sch 30/I and Sch 30/VI coinages (as in Fig 1.4. Chapter 1). Such a trend would follow the same pattern observed for the development of the British Gallo-Belgic (Northover, 1999) and Central Gaulish coinages (Nieto and Barrandon, 2002), which is considered to be the result of progressive debasement of native gold sources and previous gold coinages through the addition of an approximately 2:1 mixture of Ag:Cu. (65%:35%).

The problem with the chronology of the coins presented here is there is a large gap in the trend where one would have thought Sch. 18 and Sch.16 to fit. Instead their compositions are extremely gold poor in comparison to their predecessors and to the coins that came after.

After Sch30/IV, there was a change from the possible debasement chronology, to one where coins must have been made with sources of refined gold on hand, as the gold content remains relatively stable while more copper is added at the expense of silver. The step from Sch. 30/IV to Sch. 30/Va can still be achieved via a debasement with a 40%:60% Cu:Ag mixture. However, the next step to Sch. 30/Vb requires the addition of refined gold and copper because merely debasing the coinage would lead to lower Au compositions, which instead stay relatively stable.

A cursory examination of the coin motifs and comparisons of the distances between and shape of the motifs elements, indicates that whenever there is a change in alloy this is accompanied by a change in die set. A rigorous study of the die sets is required to see if the alloy subgroups shown here also share the same dies. With respect to the Sch. 30/V coins Scheers (1983) recorded 82 die sets from 90 coins.

With reference to the question of a mint at the Martberg and the Flan that was found there, both the alloy and the weight of the Flan shows that it is almost identical to coins from the Scheers 30/I coinage. Only one of these were found at the Martberg, 22011, and that one was plated. In fact the Flan seems to most closely resemble the Sch. 30/I coin SFLAN507 which was found at the Wallendorf oppidium where the

### 3.3 Evidence for Manufacture Techniques from Metallographic Studies

Coin 22007 was cut in half and polished to compare analyses of the polished edge and the core of the coin (see section 2.3.1) so as to determine the validity of the analytical method. It also allowed a more detailed metallographic study to be made of the coin which led to the following proposal of how the coins were treated during manufacture. Figures 3.18 a,b,c and d are Back Scattered Electron (BSE) scans of the coins cross-section made on the electron microprobe. They all show the intense heterogeneity of the alloys with the exsolution of a primary Ag-rich phase followed by the Cu-rich phase. The Ag phase forms initially as dendritic crystal growths which can become deformed when the coin alloy is hammered flat prior to striking and during the striking itself. The photos show these effects and also the effect that reheating of the coin can have .

It can be seen that although hammering involved in the coins manufacture caused many of the dendrites to be flattened it has not caused any recrystallisation in the centre of the coin. On the contrary, recrystallisation seems only to be present near the coin surface. A closer look, photos b, c and d show some interesting patterns , where the coin has been struck and a depression created deformation of the dendrites can be seen to follow the curves of the stamp. However on the upper flat surface the dendrites are not flattened and only those towards the centre of the coin are.

The observations can be explained in the following way (Fig. 3.17):

- 1) the metal for the coins was melted
- 2) Then the flan was hammered flat (Causing flattening of initial dendrites)
- 3) The coin was reheated (perhaps under reducing conditions to remove the black oxide would probably form if the metal mix with this much copper was melted under oxidising conditions, Gebhard et al, 1999, or merely to allow easier striking)

This could cause the recrystallisation of the surface of the coin

- 4) Then the coins are struck, perhaps aided by the heat of the coin (“hot struck”), this would cause deformation in the high pressure zones (the areas of most squashing) while the upper flat areas, which would not have suffered so much from the force of the strike, preserved the recrystallised zone which was produced during the reheating of the flan prior to striking.

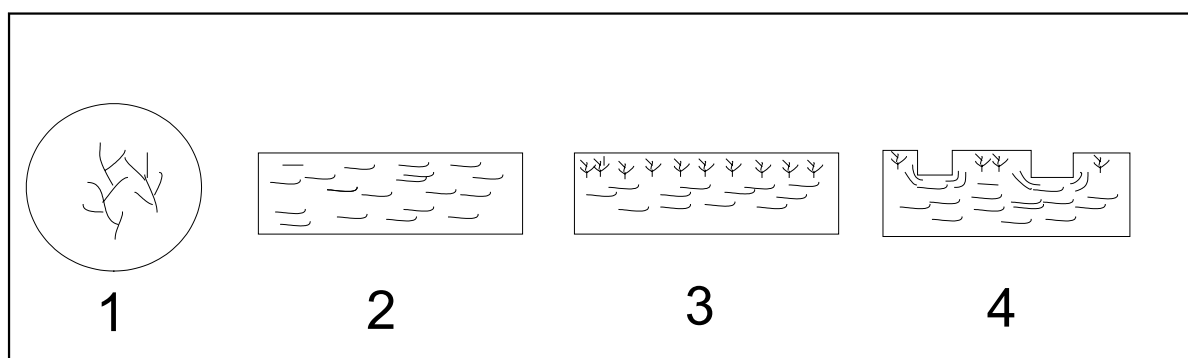


**Fig 3.17:** Dendrite deformation during, hammering (2), reheating (3) and striking (4).

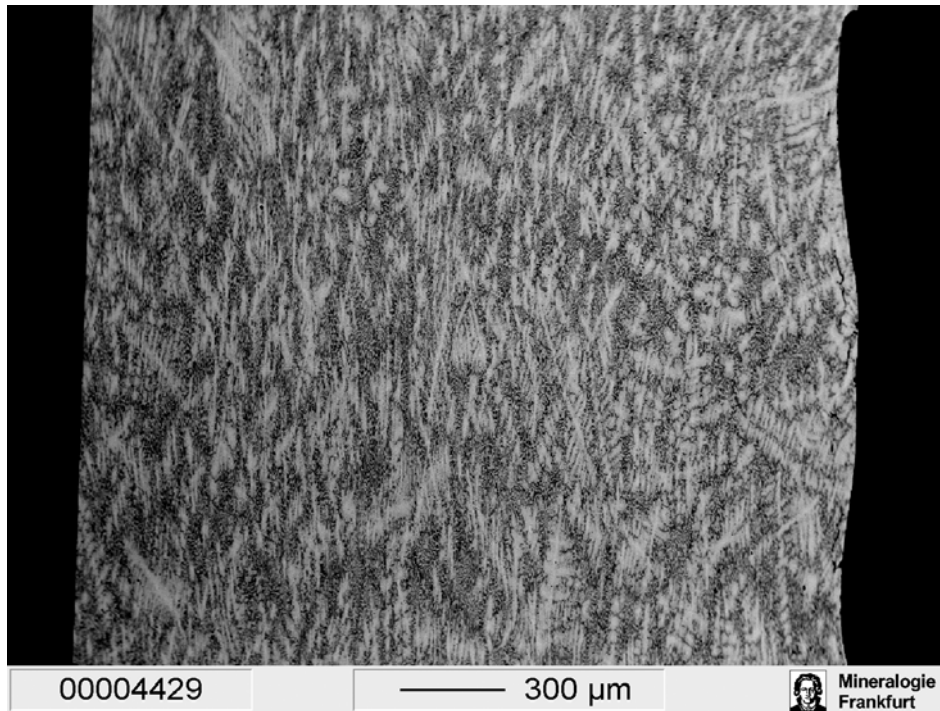


**Fig: 18 A)** This BSE image of the cut and polished 22007 shows the predomination of flattened Ag rich dendrites in the centre of the coin with relatively unflattened dendrites at the edges.

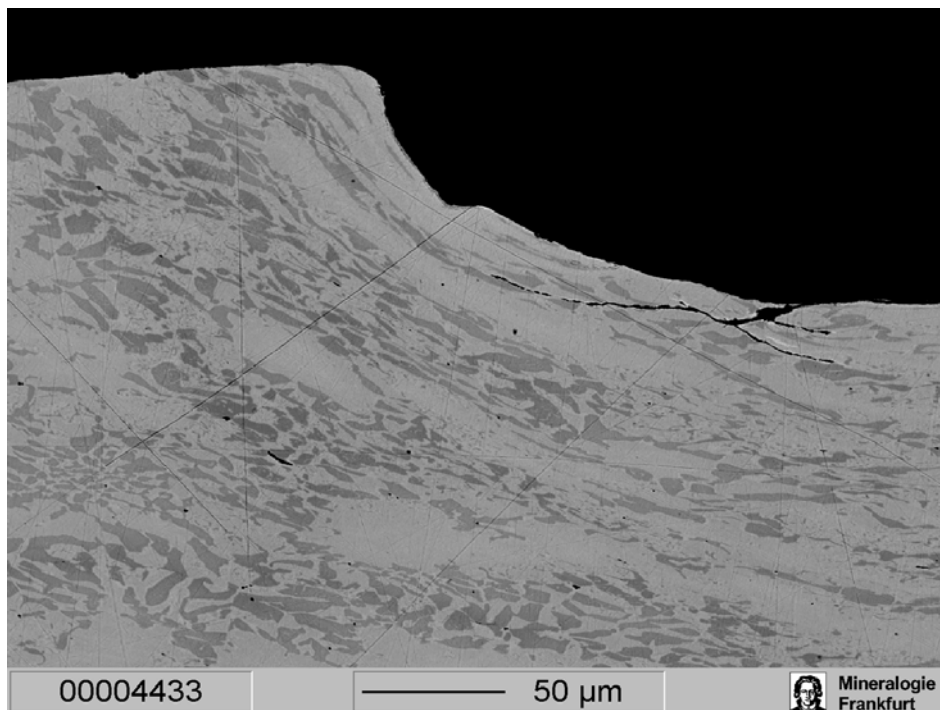


**Fig: 18 B)** This is a close up of an area from the same coin where the striking of the motif can be seen to have caused the curved flattening of the dendrites in a zone which would have experienced the most compaction during striking.

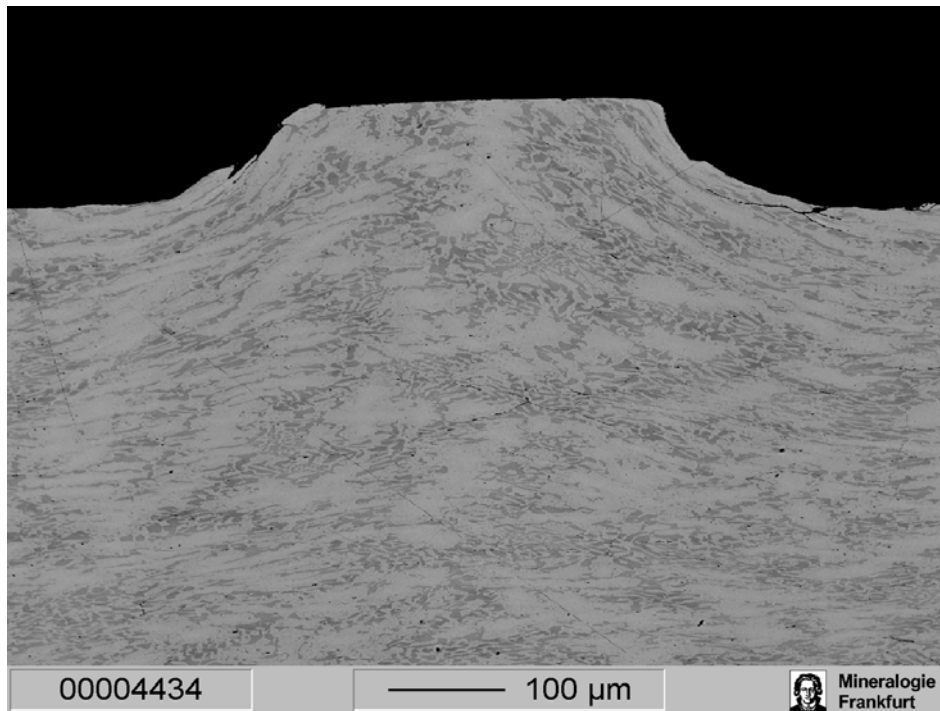


**Fig: 18 C)** This picture shows the same thing, however the high area between the indentations does not show the strong development of the flattened dendrites.

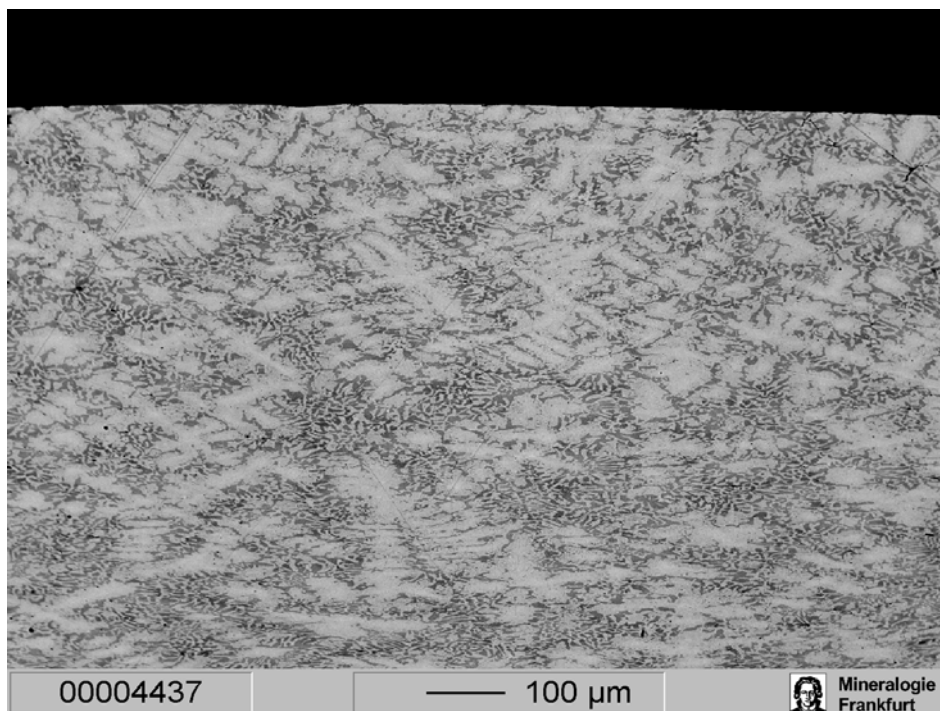


**Fig: 18 D)** This is an area where no indentation occurred, the flattened dendrites do not occur in the top few 100µm

## Evidence of Sulphide Ores

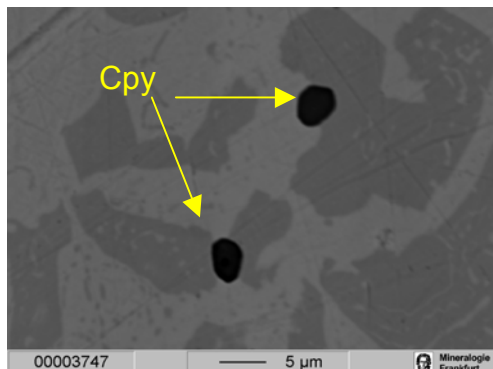


**Fig. 3.19:** Is a compositional scanned image of coin 30449, sulphide droplets with a composition similar to chalcocopyrite (Cpy) were observed.

This indicates that copper sulphide ores were probably used as a source of the copper.

### 3.4 Trace Elements

The trace element analyses of the coinages is used to examine the geochemical relationships which exist between the coins and coinages and to determine if metal sources have changed through time. From the alloy data we know that the coins are related to each other by the amounts of Au, Ag and Cu they contain, but it does not tell us if the same sources of metal were used or if the metal for a coinage was recycled. Also, for most of the coinages the alloy mix falls into a number of subgroups and the question is, if these subgroups are different sub issues and if so, do they derive their metal from different sources.

#### 3.4.1 Determining Useful Traces

The first step in considering the trace element data is to first scrutinise the quality of the data, selecting an initial suite of elements which hold enough integrity to be useful discriminators (see section 2.4.4). This is mainly related to the heterogeneity of the elements within each sample.

Figure 3.20 gives an idea of which elements show the least internal variation (i.e.: the least variation within a particular coin) for all the coins studied and therefore, which elements are most useful as discriminators. Usually the higher %RSD's (%Relative Standard Deviations= average/standard deviation x 100), those over 60, are a result of the concentration of that element being too low. For the other elements the separate Cu-rich and Ag-rich phases are a major cause of the heterogeneous distribution of the trace elements. The same is shown for sample SFLAN3000 a gold rich Protoflan. Due to its low silver (7%) and copper (2.45%) composition it is a very homogenous sample and hence the lower %RSD's for many of the elements measured.

For the next step only Co, Ni, Zn, Ga, Ru, Sn, Sb, Te, W, Ir, Pt, Pb and Bi have low enough %RSD's (~40 or lower) to be considered.

### %RSD Comparison

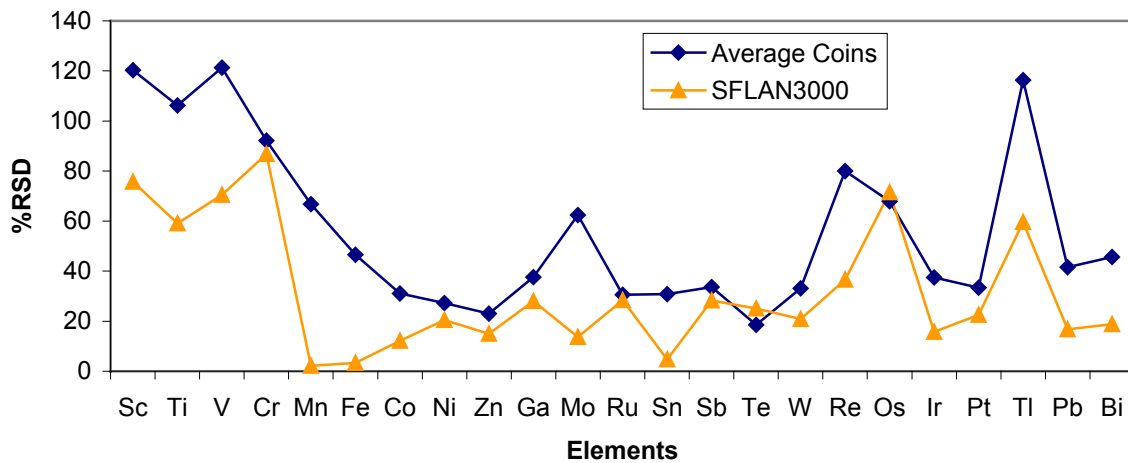


**Fig 3.20:** For this figure the %RSD for each element of each coin was found (Appendix 5) and then the average of each element for all the coins was calculated. The line for SFLAN3000 is shown for comparison with a Au-rich alloy (i.e.: more homogenous).

#### 3.4.2 Observing changes in metal sources of ternary alloys

The second step is to begin plotting an array of x,y and tri-plots of various element associations, firstly to see if correlations exist between the major elements (Au, Ag and Cu) and the traces, and secondly to see which elemental associations show meaningful groups. Correlations of trace elements with major components allow characteristics of the individual metal sources to be differentiated independent of the other two major components of the alloy. The basic premise of this method is that, if a trace element shows a correlation with one of the major components of the alloy, and not with the others, then it can be used to observe changes in that metal's source.

When an x,y plot is made, of one element versus another, what we see is a graphical representation of the element ratios. The relationships we observe can come in three general forms.

- i. **The positive correlation:** If for instance one of the trace elements shows a positive correlation to one of the major components of the alloy then it can be assumed that the presence of that trace element is controlled by the addition of the major element. It is possible that the trace element may correlate positively with more than one of the major components. The chance of trace elements correlating with both Au and Ag is high as Au and Ag can both come from the same source, especially for alloys with less than 30% Ag as natural gold can easily have up to this amount of Ag. However, elements which correlate with Cu usually will not correlate with Au or Ag as the source of copper is always different than that of gold and silver.

This can easily be checked by plotting the trace element of interest against each of the major components.

- ii. **The Negative Correlation:** when a plot of a trace element versus a major component shows a negative correlation then this indicates that the addition of this major element has a diluting affect on the trace element.
- iii. **The Nothing Correlation:** is represented by a rather unsatisfying fog of points on the graph. Either all the major components contain this trace element in varying amounts or they do not contain it at all

The graphs below show which elements correlate with the three major alloy components.

### 3.4.3 Correlations

#### a) The correlation of Te with Ag

For many of the coinages, increased Ag content correlates with an increase in Te (Fig 3.21) . Coins showing a difference to this trend are the Sch. 23 and two of the Southern Rainbow Cups with higher Te/Ag and with lower Te/Ag a subgroup of Sch 30/V and a coin from Sch. 18 and two from Sch. 16. This shows that different silver may have been used for these coins.

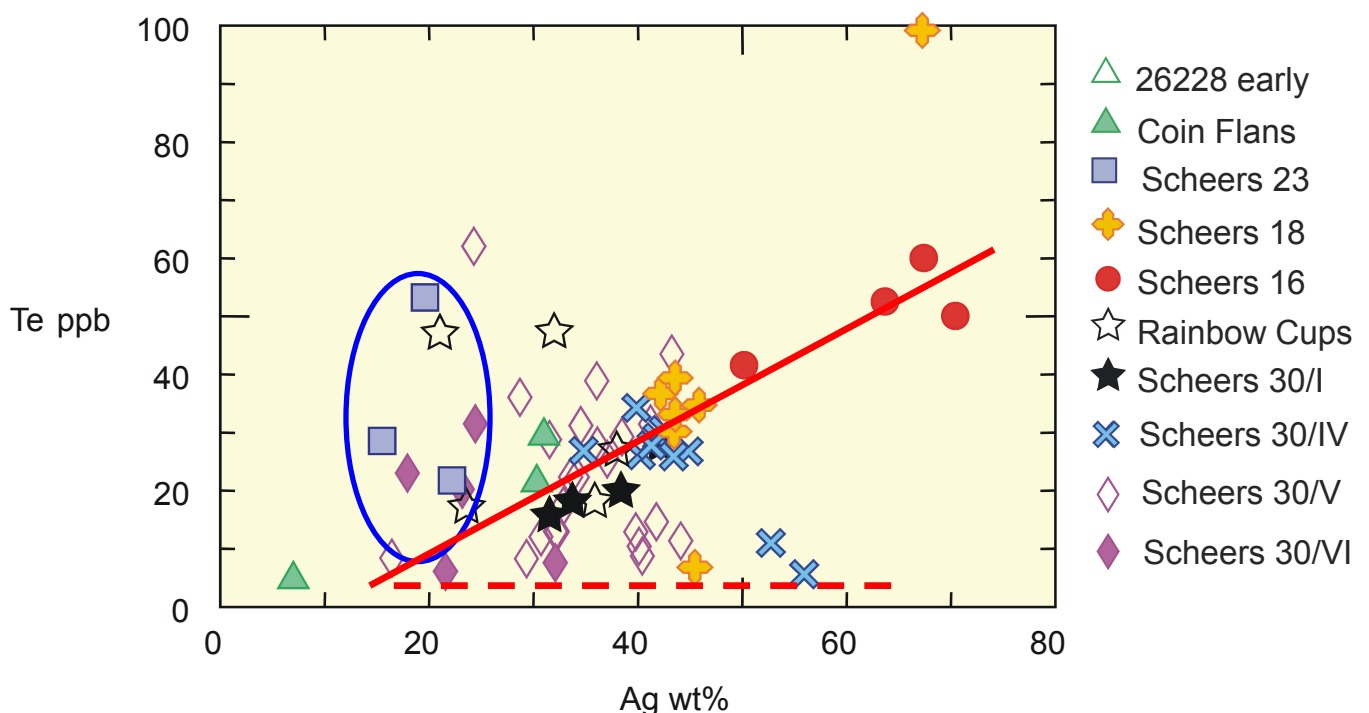


**Fig 3.21** :Different correlative trends between Ag and Te may represent different Ag/Te ratios of the silver sources used. The solid red line is a definite trend to which many of the coins belong, while the dotted line depicts a probable trend with lower Te/Ag and the ellipse highlights the Sch. 23 with higher Te/Ag ratios.



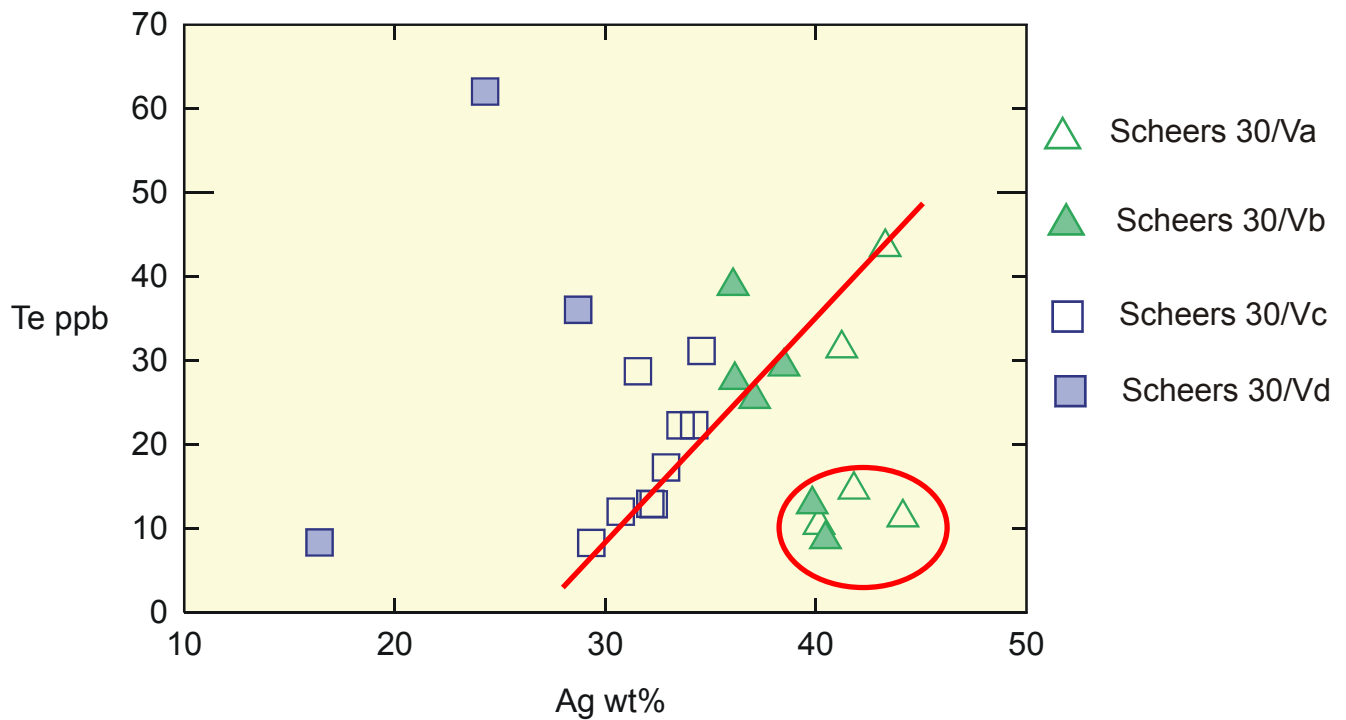


**Fig 3.22:** Takes a closer look at the Te/Ag ratios of coins from Sch. 30/V. The coins that lie along the positive trend most likely share a similar source of Ag. Those within the circle containing different Ag with lower Te/Ag ratios.

A close up look at the Sch. 30/V coins (Fig. 3.22) show a very consistent trend for the coins from subgroup Sch. 30/Vc, giving a strong indication that the same silver source has been used. Very different silver appears to have been used for the subgroup in the red circle. Three of the coins from this group belong to the alloy division Sch. 30/Va while the other two (filled triangles) are distinct as, although they have been put into group 30/Vb due to their Cu content, they have higher silver than the other coins in this subgroup. The coins from group 30/Vd appear to also have quite different silver sources and their differences will be further explored with consideration of the copper correlations.

Although, there are not really enough coins to characterise the silver source of the Sch 30/Vi coins (Fig. 3.23), a tentative trend can be drawn through coins 30449, Lux 1 and 20397 as they have similar alloy compositions and therefore probably more representative of the series. Coin 26227 (in red circle) is interesting as both its alloy composition, weight and Te/Ag ratio is the same as several coins from the Sch. 30/Vc subgroup. This suggests that this coin was made from an old Sch. 30/V coin which was merely remelted and restamped.

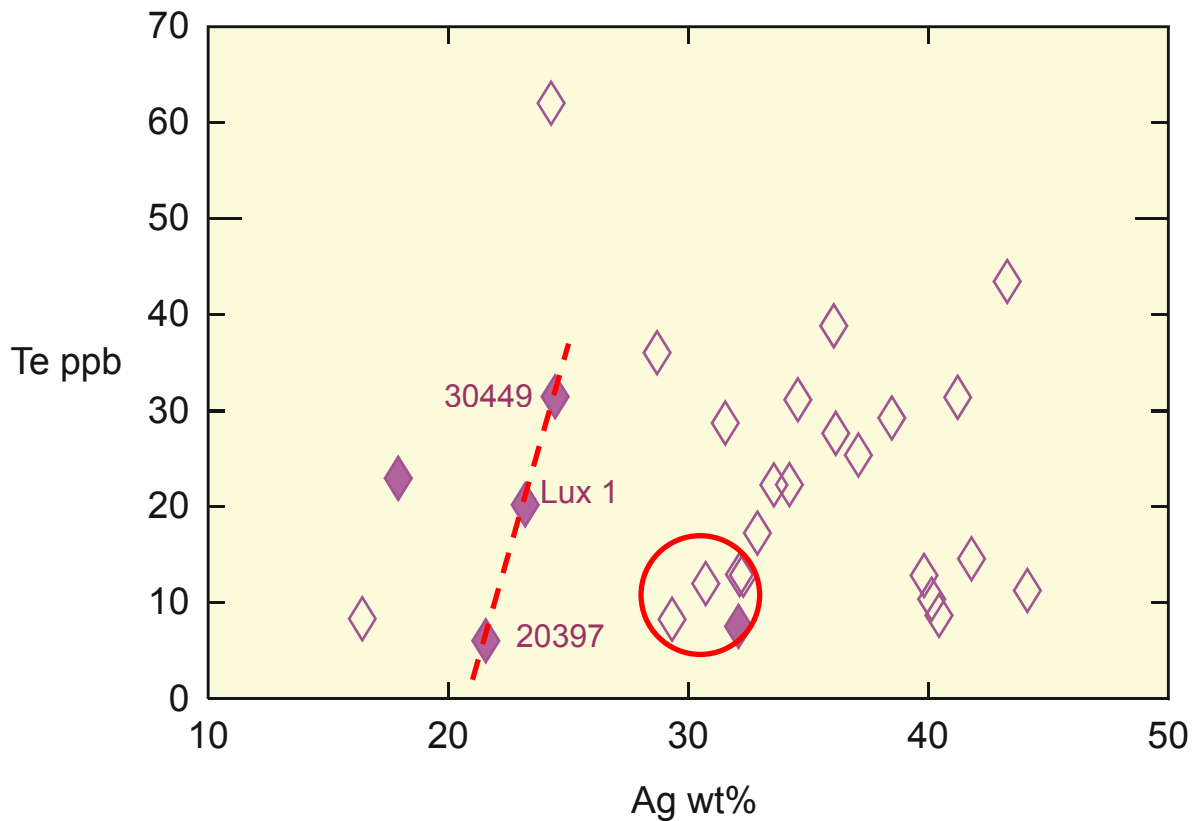


**Fig 3.23:** This plot highlights the difference in Te/Ag of the Sch. 30/VI from the Sch 30/V, the steeper gradient of the Sch 30/VI coins suggests that the silver used in their manufacture had more Te.

**b) The correlation of Sb and Ni with Cu**

Both Ni and Sb shows a steep and strong correlation with copper (Figures 3.24 and 3.25 respectively) for the later coinages Sch. 30/V and Sch. 30/VI. This is a significant change in the Ni/CU and Sb/Cu ratios of the copper that was added compared to the earlier coinages and represents a definite change in copper source. The difference of 21931 and 22008 is interesting as they have more copper without more Sb and Ni as with the other Series 30/V and 30/VI coins, they also contain a lot of Sn (Table 3.1) suggesting they were made with recycled bronze. A close up look at the last two coinages (Fig. 3.26) highlights again the difference of the two coins with recycled bronze and also that within the Sch. 30/V coins there may have been continued use of the older copper source with lower Sb for some of the coins (dark blue ellipse).

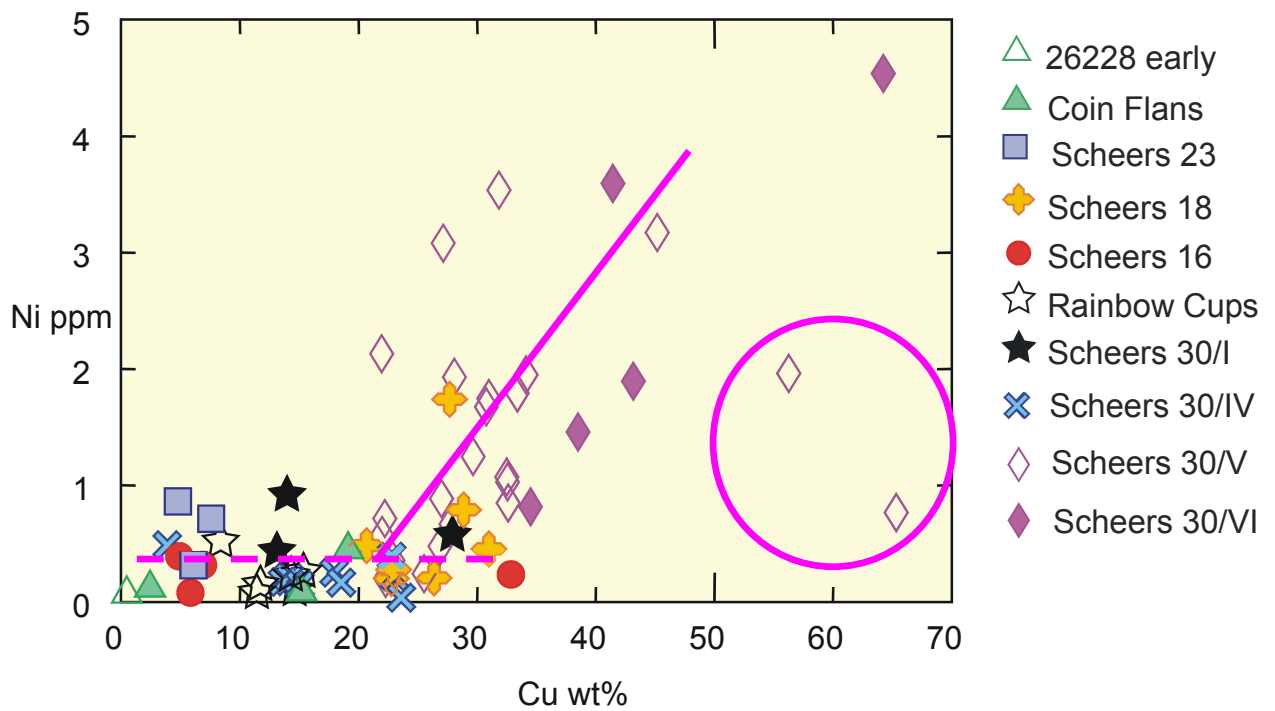


**Fig 3.24:** Ni shows a strong correlation with Cu (Solid purple line). The circle highlights the very different coins 21931 and 22088.

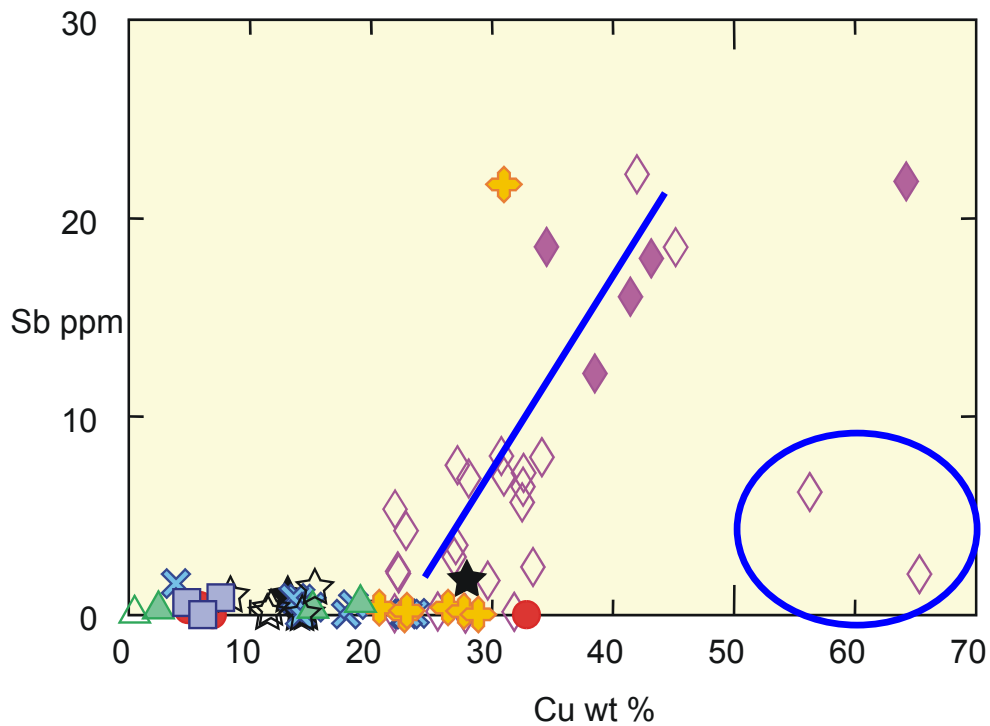


**Fig 3.25:** Sudden and steep increase of Sb in the Sch. 30/V and Sch 30/VI coinages (blue line) is the same as that observed for Ni. Coins 21931 and 22088 are once again highlighted by the circle.

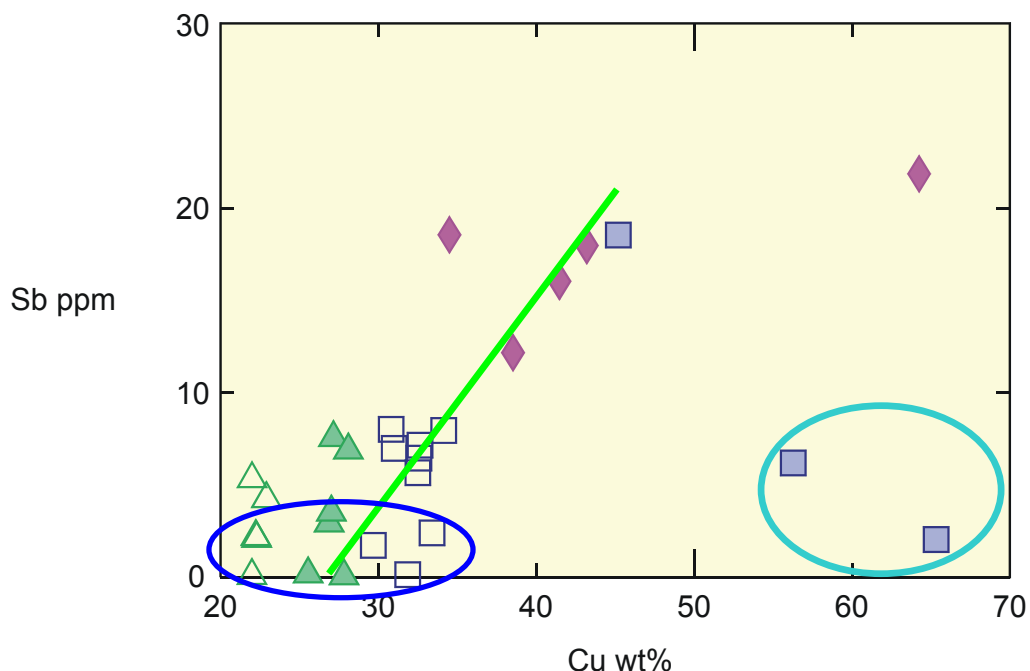


**Fig 3.26:** Takes a closer look at the Sch. 30/V and VI coinages. The green line shows the general trend with the dark blue circle showing those coins which may not belong to it. The light blue circle encompasses coins 21931 and 22088.

### c) The Pt and Au correlation

Of all the trace elements measured only Pt shows consistent correlation with Au. The Pt/Au ratios seem to follow two general trends (figures 3.27 and 3.28). One is shared by the very Pt rich coins from Sch. 23, Fö 116 and Fö117 and the Sch. 18 coins, while the other trend is followed by all the other coins. Focusing in on the later coinages (without the Pt rich Sch. 23), the two main trends are still evident and the Sch. 30/V and 30/VI coins may also be following a separate trend with higher Pt/Au ratios.

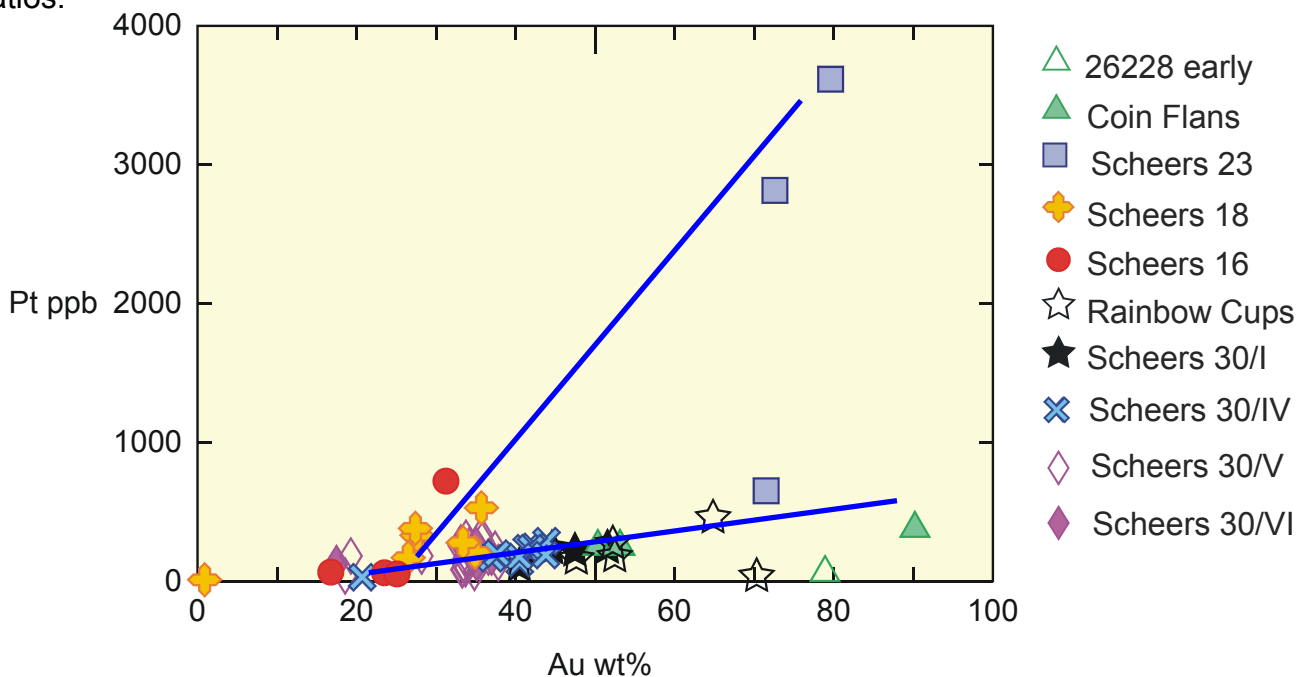


**FIG 3.27:** Au and Pt (1000ppb = 1ppm) show positive correlations (blue lines).

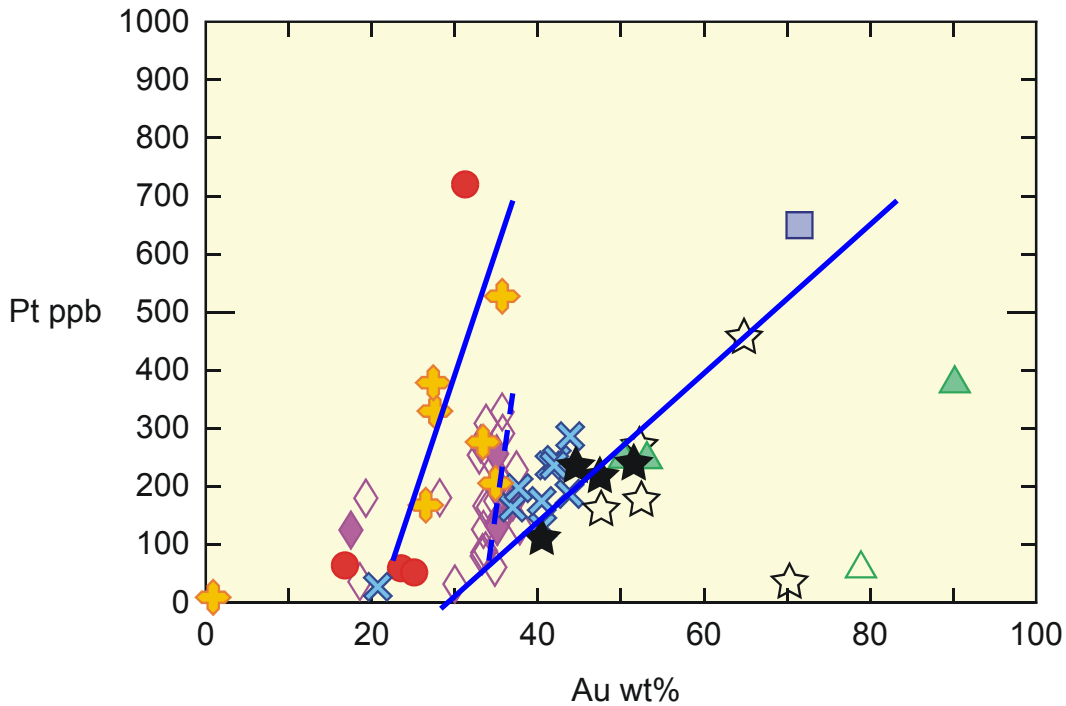


**Fig 3.28:** Takes a closer look at the coins without the two Pt rich Sch.23 coins (solid blue lines highlighting definite correlations with the dotted blue line showing a possible correlation for the Sch. 30/V coins).

Normalising the Pt to the Au composition allows the Pt concentrations to be compared without biasing the coins with high gold composition. That is to say that it should show the relative Pt contents of the gold that was added to the coins. Figure 3.29 highlights the differences between the Sch. 23, Sch. 18 and the later the coinages.

### Pt normalised to Au composition

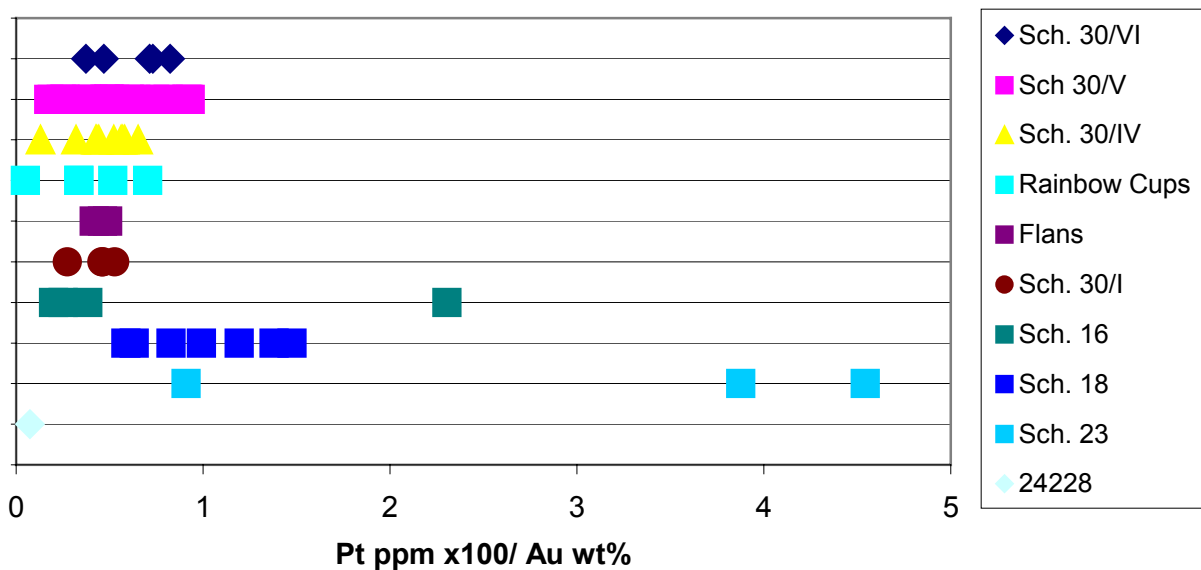


**Fig 3.29:** Here is a plot of the Pt concentration normalised to the gold composition of the coins.

### 3.4.4 Summary

By considering the trace element correlations with the major components, Au, Ag and Cu, an idea can be acquired as to the changes which occurred in the metal sources of the coins.

The correlation of Te with Ag shows a general trend, which most of the coinages follow. Only the Sch.23 and Southern Rainbow Cups show a marked difference with higher Te/Ag ratios. Also, a small group of Sch. 30/V coins appear to be made with different silver. The trend does not necessarily mean that the same source of Ag was used for all these coinages, as many silver sources may contain Te in similar amounts, however, when trends form, like in Fig 3.13, with the Sch 30/Vc coins, then it can be fairly certain that the same Ag was used and that the trend represents a direct correlation between the Te and the amount of Ag added. It also adds to the integrity of this subgroup which was created based on the alloy composition.

The Te/Ag ratio of the Sch. 23 and the Southern Rainbow Cups could occur either by the use of Ag with more Te or, because it is an almost vertical trend, contribution from the Au source used. This is somewhat confused for these earlier coins because most of the silver is probably originally introduced with the gold as electrum. However, for the Sch 16 , Sch. 18 and the eye staters , so much silver has been added that almost all of the Te has come with silver.

The positive correlations of Sb and Ni with Cu give a very good basis for indicating that the Sch 30/V and Sch/VI were made with different copper than the earlier coinages. The EPMA data from the silver coins (Table 3.3 and Wigg and Riederer, 1998) also show an increase in Sb for a subgroup of the Sch. 55 with a ring.

There are some coins from these series that do not show the same contribution of Sb and Cu and they are: 30V549, 30VG179, 20163 and 30V542 and may have been made with copper similar to what was used in the Sch. 30/IV coins.

Many of the coins from group 30/Vd are oddities with very high Cu and Sn , suggesting that recycled copper(bronze) was used in their production. This difference is also observed in the trace elements (Sb and Ni), which also show that 21931, 22008 were made from very different copper.

The Pt/Au correlation is the only tool we have for observing changes in gold apart from the indication of the utilisation of refined gold from the alloy compositions and debasement patterns (Section 3.2.11).

The high Pt for Sch 23 and also Sch 18 sets them aside containing obviously different gold from the later coinages. Changes in gold sources for these later coinages may have occurred but the differences between them are not detectable. The high Pt is accompanied by high Os and Ir, Table 3.5.

	Os ppm	Ir ppm	Pt ppm
Sch. 30/IV	0.36	0.01	0.19
Sch. 23	3.56	0.05	2.35

**Table 3.5:** Average Os , Ir and Pt concentrations (ppm) of the Sch. 23 and Sch. 30/IV coinages

### 3.5 Pb Isotopes

The lead isotopic data was acquired by both solution and laser ablation and these methods are discussed in section(2.5). The collected data is given in appendix 7 showing which method was used and the precision of each analysis. The precision (error) is always smaller than the symbols used in the plots below. For the bulk of the coins and in particular those from the museums in Brussels, Luxembourg, Trier and Frankfurt, only laser ablation analysis was possible and so only the  $^{207}\text{Pb}/^{206}\text{Pb}$  and the  $^{208}\text{Pb}/^{206}\text{Pb}$  ratios can be used as the abundance of isotope  $^{204}\text{Pb}$  is too low to provide accurate measurements by laser ablation.

#### 3.5.1 Results

From a plot of  $^{208}\text{Pb}/^{206}\text{Pb}$  vs.  $^{207}\text{Pb}/^{206}\text{Pb}$ , Fig 3.30, three general trends (groups) can be seen. A tentative one involving the Sch23 coins and coin Fö105 (Sch. 18), A second including the majority of the Sch. 18 and Sch.16 coins (with coin 26228 grouping with them). SFLAN3000 and a coin from Sch. 30/IV are intermediate between this group and the major trend which includes all the Eye staters and some of the Rainbow Cup staters (in particular the ones from Hessen). The Southern Rainbow Cups are somewhat lower down the trend and to the left of it.

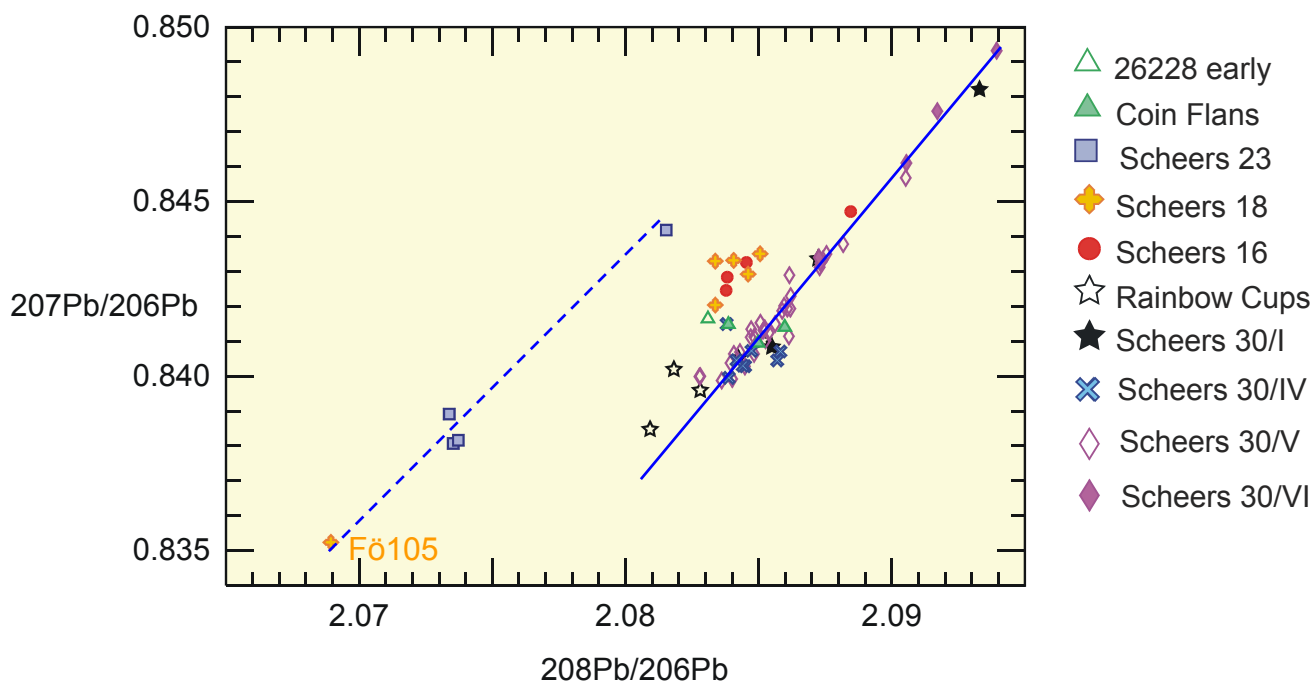


**Fig. 3.30:**  $^{208}\text{Pb}/^{206}\text{Pb}$  vs.  $^{207}\text{Pb}/^{206}\text{Pb}$  of the data acquired by both solution and laser MC-ICPMS.

The following interpretations can be made from this plot:

1. The Sch 23 coins lie on a different trend than the other coinages.

- Sch 18 and Sch16 also seem to have their own group somewhat different to the Sch. 23 and other coinages, except Fö105 a Sch. 18 coin which lies at the lower end of the Sch 23 trend.
- All the eye staters lie on the same trend with rainbow cups at the lower end.
- Coin 26228 appears to have a similar Pb isotopic signature to the Sch. 18 and 16 coinages.

Recalling the question of the coin Flan and its connection to the coinages figure 3.21 shows that its Pb isotopic signature also closely resembles that of coin SFLAN507 with which it shows strong compositional and weight similarities. Also Fö124 is shown here indicating a close connection between the Northern Rainbow Cups and the Sch. 30/I coins.

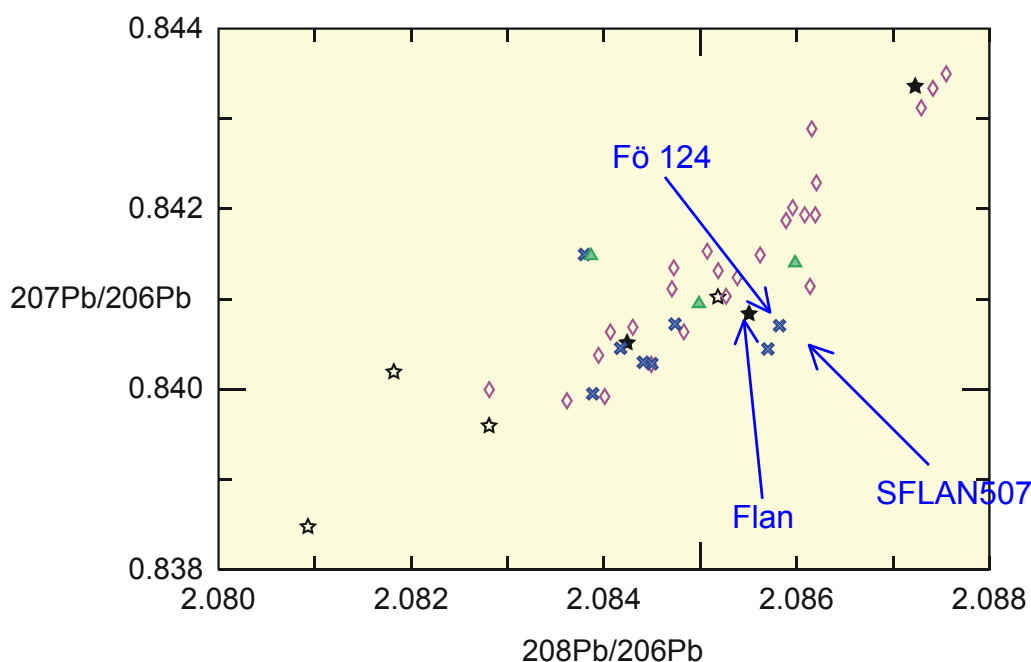


**Fig 3.31:** A close up of the Sch. 30/I, IV, V, the Rainbow Cups and flans showing the similarity between the FLAN and these coins. Coin Fö 124 (Northern Rainbow Cup) and SFLAN507 (Sch. 30/I coin) are highlighted.

### 3.5.2 Controls on mixing lines

To examine the controls on the Pb isotopic mixing line, defined by the eye staters, a plot of Cu content vs. the  $^{208}\text{Pb}/^{206}\text{Pb}$  (Fig 3.32) shows that the addition of copper is the prime factor, indicating a copper source with Pb isotopic ratios

Comparing the Pb signatures of the silver and copper alloys (Fig 3.33) reveals the silver coins Sch 54 forming a distinct group with lower  $^{207}\text{Pb}/^{206}\text{Pb}$  and  $^{208}\text{Pb}/^{206}\text{Pb}$  ratios than the eye staters. The later Sch 55 coins have similar isotopic signatures to the eye staters. Most of the copper alloy coins tend to high  $^{207}\text{Pb}/^{206}\text{Pb}$  and  $^{208}\text{Pb}/^{206}\text{Pb}$  ratios enhancing the interpretation that the mixing line is indicating a copper source further up to the right.

It is unclear what effect the lead from the gold sources can have on the signature. Theoretically it should have a considerable effect: the average Pb concentration for the gold samples was 34ppm compared with 21ppm for the gold coins. Possibly



some of the spread in the values, rather than a single line produced by a two component mixing, is the result of mixing with gold. A gold source maybe indicated by the offset of the Southern Rainbow Cups suggesting a gold source with lower  $^{207}\text{Pb}/^{206}\text{Pb}$  and  $^{208}\text{Pb}/^{206}\text{Pb}$  ratios. The trend observed for the eye staters is a mixing line between a copper source with higher Pb isotopic ratios and possibly a mixed silver and gold source at the other.

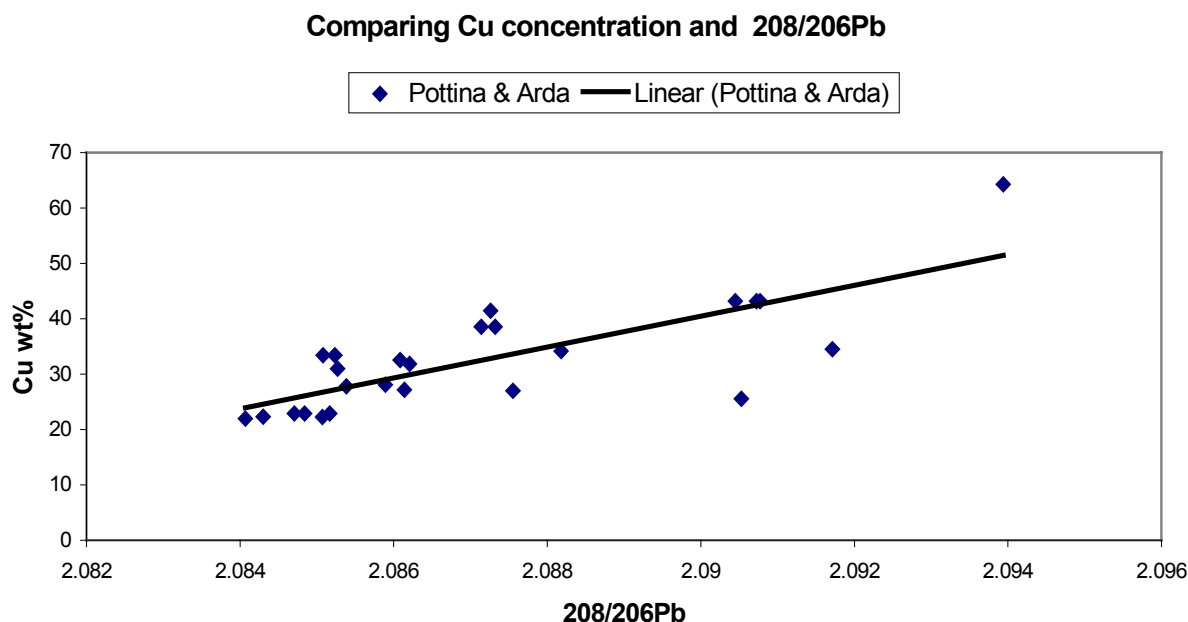


**Fig 3.32:** A plot of the  $^{208}\text{Pb}/^{206}\text{Pb}$  ratio with Cu wt% for the eye staters indicates that the higher lead ratios are pointing the way to a copper end member of the mixing line.

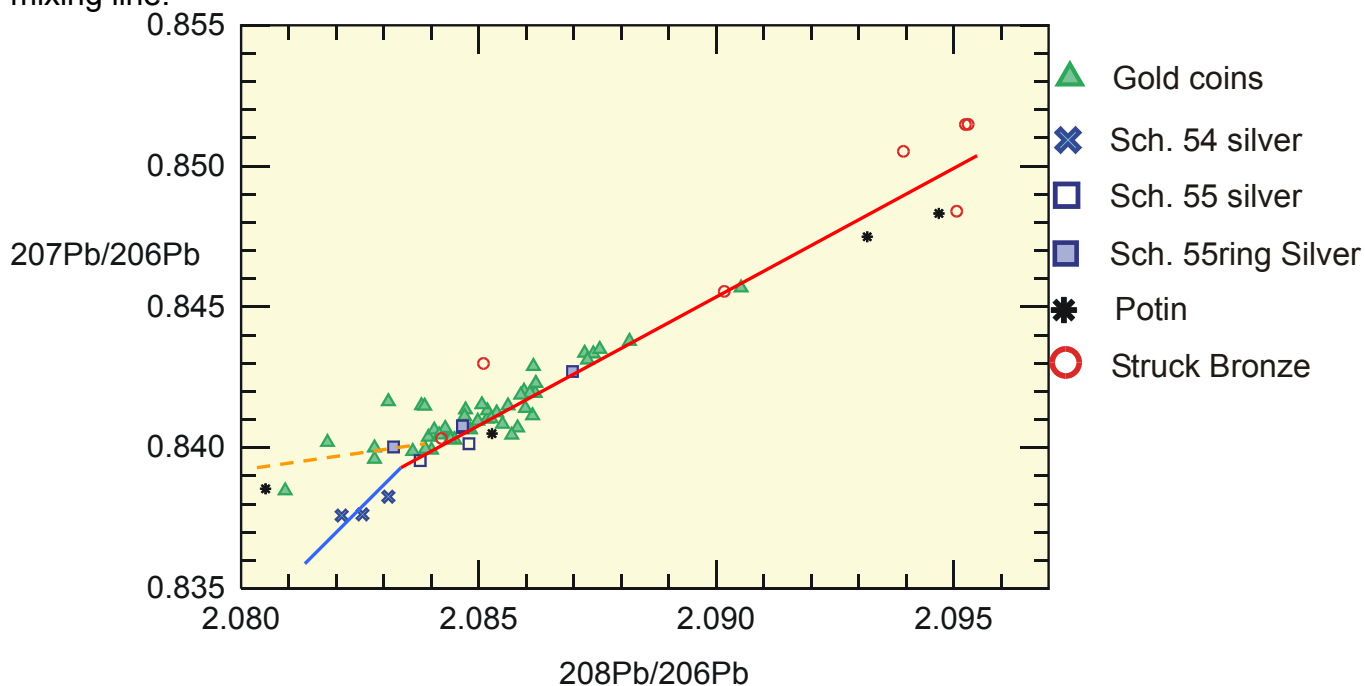


**Fig 3.33:** The silver and copper alloy coinages are included on this plot. The red line indicates the mixing line controlled by the addition of copper while the blue indicates the direction of a possible silver source and the tentative gold line following the southern rainbow cup coins (Fig 3.31) in the possible direction of a gold source.

### 3.5.3 Regional comparison

Comparison with the Pb-isotope database (compiled from; Stos-Gale et al 1995, Stos-Gale et al 1996, Rohl 1996, Gale et al 1997, Stos-Gale et al 1998, Large et al, 1983 and Wagner et al, 2002), Figure 3.34, shows that there may be a mixing between Tuscan and Spanish sources of metal (gold and silver together representing the lower end of the mixing line) with progressive addition of copper from Sardinia or Spain for the later coins. Possibly Sch. 23 has its source of metals in the Aegean or Cyprus and shows evidence of having derived metal from the local sources of the Rheinisches Schiefergebirge. However, only three coins from this series have been analysed and this early coinage requires a lot more Pb isotopic analyses before the mixing line can be definitely established and its controls understood.

Comparison of major gold producing areas (Fig. 3.35) shows that the Ardenne and the Limousin (Massif Central, France) are at the wrong end of the eye stater mixing line (copper) to be possible gold sources. Possible nearby gold producing regions at the other end include Alpine gold deposits and also lie in the direction indicated by the three Southern Rainbow Cup coins analysed. More analyses of the Rainbow cup coins may help to clarify the possible source of gold used in the Eye staters. Also more analyses of the Sch 23, 16 and 18 coins is needed.

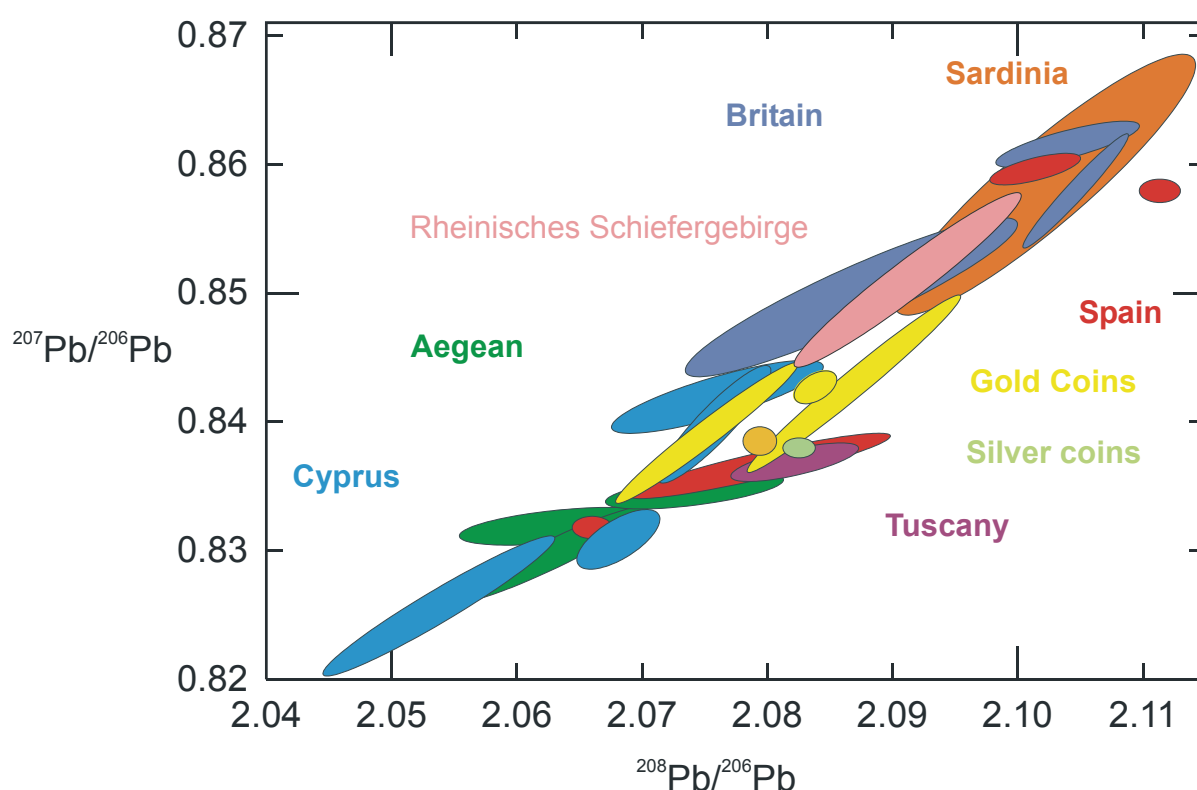


**Fig 3.34:** Pb-isotope data from the coins (yellow) on top of the Pb isotope dataset produced from regional analyses of copper sources over the last twenty years (see text for references). The slightly darker yellow spot at the lower end of the Eye stater mixing line indicates the position of the Southern Rainbow Cups.

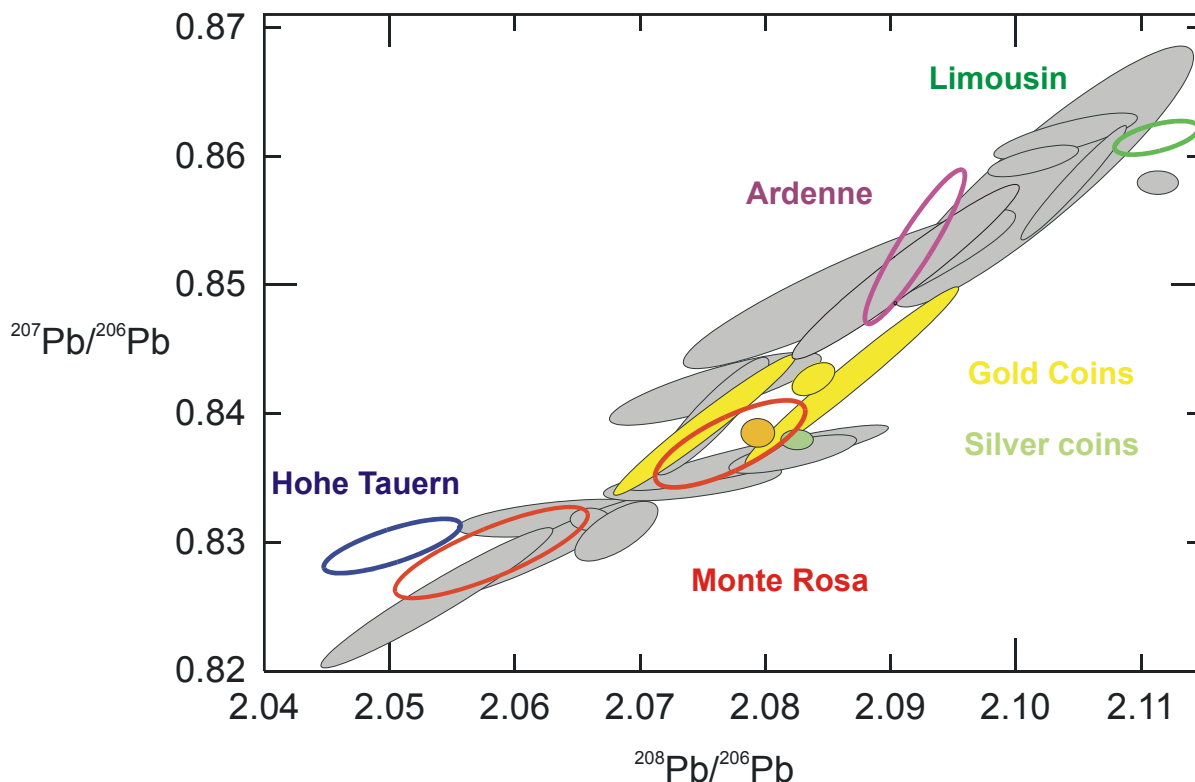


**Fig 3.35:** Shows the Pb isotopic signature of major gold producing regions (see Gold Chapter section 4.7 for details).

### 3.6 Cu Isotopes

A by-product of the chemistry to isolate the Pb from the coin drillings prior to solution analysis, is a Cu separate solution. This provided the opportunity to make some preliminary investigations of the applicability of the Cu isotopic system to the aims of the project. The methodology and a short history of the development of Cu isotopic analyses is given in Chapter 2. It is still unclear whether Cu isotopes will provide an extra tool for helping to provenance sources of copper, as variations within deposits can be quite broad. However, Fig 3.36 does show some consistent differences for the coinages analysed. The earlier coinages seem to have more negative  $\delta\text{Cu}65$  than the later coins. Of particular interest is the high  $\delta\text{Cu}65$  values recorded for the Sch. 30/V gold coins and the Sch 55 silver coins which have already shown a strong connection through their similar trace element and Pb isotopic signatures.

Previous Cu isotope studies (Gale et al, 1999, Zhu et al, 2000) of different minerals have shown that the difference in  $\delta\text{Cu}65$  values is related to different copper minerals and possibly the chemical fractionation of the copper isotopes during the formation of these minerals (section 2.6 for a more in-depth discussion). The differences seen here may therefore represent different types of copper ore. With reference to the figure of  $\delta\text{Cu}65$  analyses of different minerals (Fig.2.11. section 2.6) this may indicate an oxidised ore body for the copper in Sch. 30/V.

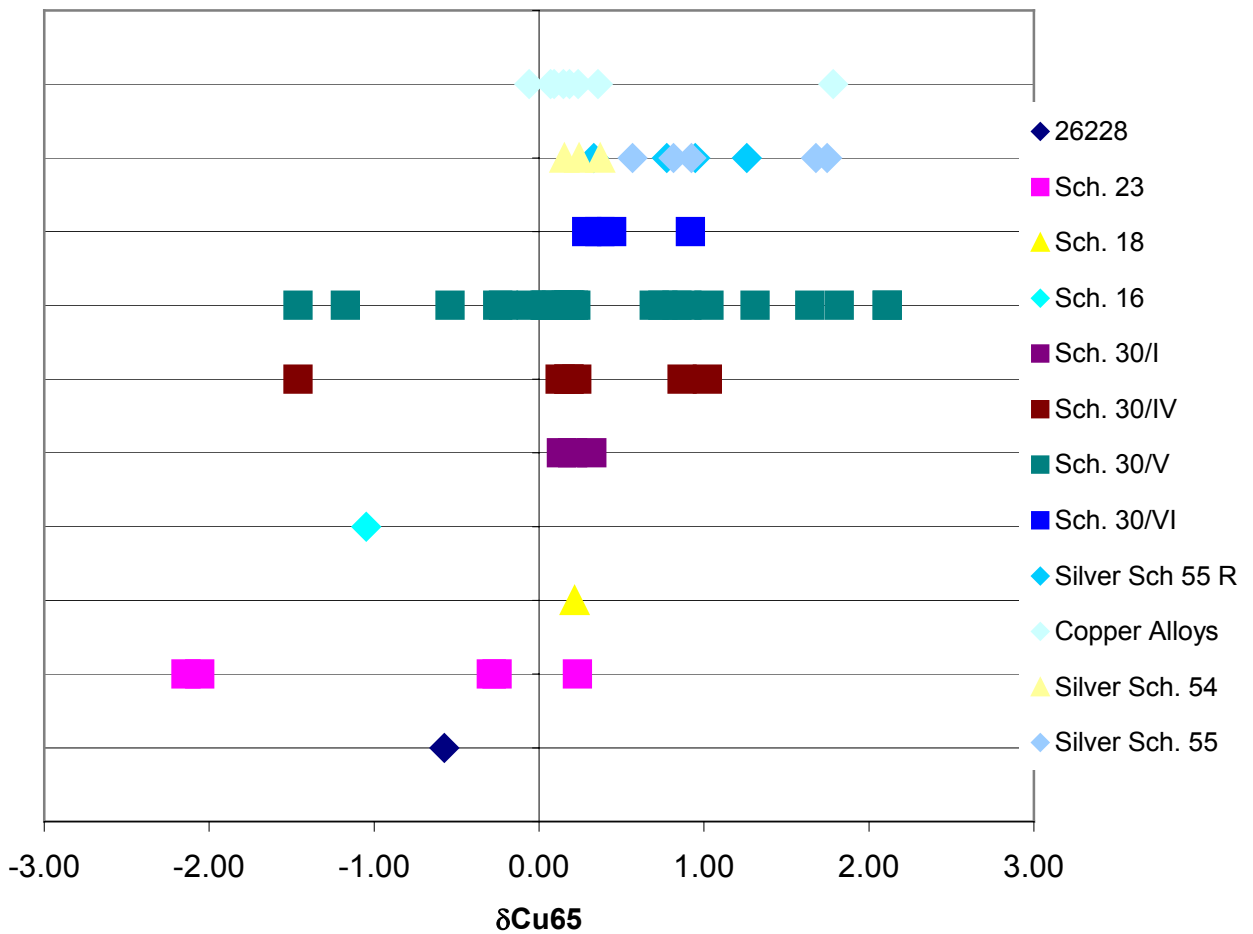


**Fig 3.36:** Results of the Cu isotope analyses are plotted horizontally and show that although the earlier coins are poorly represented, there is a trend to more positive  $\delta\text{Cu}^{65}$  values for the later coinages and in particular Sch. 30/V.

Tylecote (1977), after making a number of experiments on the refining of different types of copper ores, noted that oxide ores, which merely undergo a reducing process to acquire the metal, are more likely to preserve high levels of Sb than sulphide ores, which first require roasting to drive off the sulphur and most of the Sb would be removed with the sulphur. It is interesting to note that the coins Sch. 30/V and 30/VI with high Sb concentrations are also associated with positive  $\delta\text{Cu}^{65}$  values. Oxide ores could be the possible source of copper used to manufacture these alloys.

However, the presence of copper rich sulphide droplets in coin 30449 (Sch 30/VI) is evidence to the contrary, suggesting instead that sulphide ores were used. High Sb is also associated with sulphide ores containing antimony sulphide minerals such as fahlore.

### 3.7 Discussion

In the Middle Rhine/Moselle region there are three main successive gold coinages: the first Sch. 23 followed second by the “Armorican” types, Sch. 18 and 16 and finally the “Eye Staters” Sch. 30/I, IV-VI. This typological succession is mirrored in the changes observed in the coin alloys, trace elements and isotopic signatures. These groups are defined and summarised below.

#### Scheers 23

- i. The most gold rich of the coins studied with an average of: 75% Au, 19% Ag and 6%Cu. This composition could have been produced via copper addition to native unrefined gold (electrum).
- ii. They contain distinctive traces of PGE's (Pt, Os) and Te. Coins Fö 117 and Fö116 have very high Pt/Au ratios while the coin Robiano has a similar ratio to the later coinages.
- iii. Their Pb isotopic signatures form a trend which appears unrelated to the later coinages. However, as with the trace elements the isotopic signature of Robiano is very different from the other two and may or may not be isotopically associated with them. Therefore the tentative trend that is drawn between them may not be real.

#### The Armorican Types

##### Scheers 18

- i. The coinage can be divided into two relatively gold poor alloy groups;  
18a: 27% Au, 45% Ag and 28%Cu  
18b: 35% Au, 43% Ag and 22%Cu
- ii. Their Pt/Au ratios are also higher than the bulk of the coinages studied, although much less than the two coins from Sch. 23. their Te/Ag ratios place them on a trend intermediate between the “Eye” Staters and Sch. 16
- iii. Their Pb isotopic signatures place them in a group with the Sch. 16 coins, separate from the other coins studied. It does not seem to be connected to any other mixing line. Coin Fö 105 is an exception and may form one end of a mixing line with the Sch. 23 coins.

##### Scheers 16

- i. Forms one silver rich alloy group: 27% Au, 67% Ag and 6% Cu (with one odd copper rich coin)
- ii. With the highest silver content of the coinages studied they also have the highest concentration of tellurium forming the high end of a Te/Ag

trend which appears to incorporate many of the coins from the other coinages. The Pt/Au ratios of these coins are distinctly lower than the Sch. 18.

- iii. As mentioned above their Pb isotopic signatures place them in a group with the Sch. 18 coins.

## The “Eye Staters”

### **Scheers 30/I**

- i. Only three real coins from this prolific coinage have been analysed and their average composition is: 48% Au, 38% Ag and 14% Cu, with considerable variation between them and one plated coin, which has not been included in the average, has a composition resembling more the Sch. 30/V coins.
- ii. Their trace element signatures are unremarkable, they have Te/Ag and Pt/Au ratios consistent with the Sch. 16 and the succeeding Sch. 30/IV.
- iii. Their Pb isotopic signatures place them intimately associated with later eye stater coinages on a trend (mixing line) distinct from the earlier Sch. 23, 18 and 16 coinages.

### **Scheers 30/IV**

- i. Average alloy compositions of: 39% Au, 40% Ag and 21% Cu places this coinage on a possible debasement trend from natural gold compositions along with Sch 23 and Sch. 30/I.
- ii. With trace element ratios consistent with Sch. 30/I
- iii. Pb isotopic ratios are similar to Sch. 30/I

### **Scheers 30/V (POTTINA)**

- i. The alloy compositions are distinctively different from the previous two coinages with a steep increase in copper at the expense of silver while the gold composition remains relatively constant. Four subgroups are defined in terms of copper composition with the last group Vd being composed of coins with very high amounts of copper +/- tin with large variations from coin to coin.

Va: 35% Au, 42% Ag and 22% Cu

Vb: 36% Au, 36% Ag and 28% Cu

Vc: 32% Au, 32% Ag and 33% Cu

Vd: 30% Au, 30% Ag and 40% Cu (21931 and 22008 up to 60% Cu+Sn)

- ii. Most of the coins from this coinage show a distinctive steep rise in Sb and Ni, indicating an obvious change in copper source from the

previous coins. The Te/Ag ratios of the coins show a very good trend for the subgroup 30/Vc and some of the Vb and Va coins, strongly indicating that the same source of silver was used. There is also a group of coins with distinctively lower and consistent Te/Ag ratios pointing to another silver source for those coins.

- iii. The Pb isotope ratios are the same as for the previous Sch. 30 coinages, although showing the effects of increased mixing with a copper source represented by higher  $^{207}\text{Pb}/^{206}\text{Pb}$  and  $^{208}\text{Pb}/^{206}\text{Pb}$  ratios.
- iv. The steep rise in Sb is also seen in the Sch. 55 (with a ring) silver coinages and this is reflected in the copper isotopes as well, the  $\delta\text{Cu65}$  ratios of these coinages both trending to more positive values.

### **Scheers 30/VI (ARDA)**

- i. Average alloy composition is: 35% Au, 22% Ag and 43% Cu and continues the trend of increasing copper with stable gold content and less silver.
- ii. The steep Sb and Ni trend continues for these coins suggesting the copper source has remained the same. Te/Ag ratios are inconclusive as are the Pt/Au ratios.
- iii. The Pb isotope ratios are higher due to their higher Cu compositions and lie on the same mixing trend as the other eye stater coins.

### **Rainbow Cups**

Several Northern and Southern Rainbow Cup coins were studied to examine the links to neighbouring regions.

#### **Southern Rainbow Cups**

- i. Three typological groups are represented with three quite different alloy compositions, ranging from 52-70% Au, 32-21%Ag and 15-8% Cu. These compositions putting them on the possible debasement trend which includes the Sch. 23 and Sch 30/I-IV coins.
- ii. The Pt/Au and Te/Ag ratios of the two gold rich coins are very similar to the Sch. 23 coin Robiano, while the trace element signature of the other is more similar to the Northern Rainbow Cups.
- iii. The Pb isotopic ratios are different from the Sch 23 and Sch. 16-18 while being more similar to the Sch. 30 coinages. However they do not sit right on the trend with  $^{207}\text{Pb}/^{206}\text{Pb}$  ratios a little too low. Considering their higher Au compositions they may indicate the direction in which a possible gold source maybe found.

## Northern Rainbow Cups

- i. Again two quite different examples of this group of coins, with compositions of 48-52% Au, 38-35% Ag and 14-11% Cu. These compositions are very similar to the neighbouring and roughly contemporary Sch. 30/I coins.
- ii. Pt/Au and Te/Ag ratios are also similar to the Sch. 30/I coins.
- iii. Pb isotope ratios are also similar to the eye staters (Sch. 30 coinages).

## Flans

It can be quite certain that one of these objects the “Flan”, from the Martberg, really is one and that SFLAN1148 was very likely intended for minting (a “protoflan”), however the third, SFLAN3000, contains 10% more gold and is 0.3g heavier than the most gold rich coin studied here. It is also an odd shape (photo appendix). The first two are therefore of most interest and in particular the Flan which was found at the Martberg. By its composition, trace element content and Pb isotopic signature it is very similar to the Sch. 30/I and Northern Rainbow Cup coins with an almost identical weight to coin SFLAN507 (Sch. 30/I). Its presence within the Martberg Sanctuary is therefore an interesting mystery as the only example of these coinages found there was the plated 22011 from Sch. 30/I. Perhaps future investigations of the settlement site immediately adjacent to the sanctuary area on the Martberg plateau, will provide more information as to its presence there, and help clarify the question of whether there was a mint located at the Martberg.

The other protoflan, SFLAN1148 from the Wallendorf oppida also has a composition comparable to the Sch. 30/I and the Northern Rainbow Cup coins, however it is too light. 5.4g resembling more the Sch. 30/V coins.

## 3.8 Summary

Through the combined use of alloy, trace element and lead isotopic information it is possible to describe the changes in metal sources used in the manufacture of the coins through time.

Alloy compositional data has revealed that a debasement trend governed the production of the Sch. 23, Sch. 30/I and Sch.30/IV coins with a sharp change to increased copper contents with Sch. 30/V and Sch. 30/VI. Also that Sch. 16 and Sch. 18, the “Armorican” types, are not part of this trend.

The plotting of trace element ratios such as Pt/Au, Te/Ag, Sb/Cu and Ni/Cu on x,y graphs can show changes in metal sources. Gold sources have changed from the high Pt/Au contents of the Sch. 23 to the moderately high Pt/Au of the Sch. 18 to the Sch. 16 and eyestaters where further distinctive changes in gold source can not be detected. High Pt, Os, Ir and Ru in Scheers 23 coins may be related to the coinages previously studied from Manching where over a third of the coins



contained osmiridium inclusions. Such inclusions are the result of PGE inclusions which are incorporated in the gold separate while panning gold from rivers and were suggested as originating from Greek deposits. Upon melting all the Pt and Pd is dissolved in the gold while the immiscible Os, Ir and Ru remain as microscopic nuggets. Gondonneau (1996) has reported Pt concentrations up to 250ppm from analyses of Gaulish staters and 500 to 1000ppm for the original Greek Staters of Phillipus II (all these coins were extremely pure with over 99% Au). Hartmann's (1976) previous analysis of the Rainbow cup coins, both Northern and Southern also associated high Pt concentrations as occurring through the addition of alluvial gold, however he indicated the Rhine as a possible source due the presence of Pt bearing minerals in the river.

Analyses of placer and lode gold deposits made during this study (Chapter 4.0) has shown that most samples contain sufficient Pt to provide the concentrations seen in most of the coins here, even for the Fö 116 and Fö117. However, the presence of high Os, Ir and Ru also in these two coins does suggest that microscopic inclusions may have been present. Whether this represents the Rhine or the Aegean is unclear. The Pb isotopic data could be interpreted as indicating an Aegean source of metal, also although the presence of Pt minerals such as sperrylit have been documented from the Rhine, no inclusions of these minerals were noted in the small samples studied here.

As far as a more definite indication of gold source using the other trace elements is concerned, this is not possible as the addition of silver and copper has disturbed the gold signature too much and only Pt and perhaps Pd can be clearly seen to correlate to gold.

Examination of the Te/Ag ratios has shown that there may have been a fairly consistent source of Silver especially for some coinages and subgroups such as Sch. 30/Vc.

The change in debasement trend seen in the alloy compositions from Sch. 30/IV to Sch. 30/V is reinforced with a sudden change in copper source with elevated Sb and Ni which persists into Sch. 30/IV. From the analyses of the Silver coinages made by EPMA and those of Wigg and Riederer (1998) two groups of Scheers 55 with a ring one very similar to the Sch 55 (no ring) and another which shows an increase in Cu and Sb. This increase is also steep indicating a change of copper source and the place in the numismatic chronology proposed by Wigg and Riederer() originally places this coinage as appearing at the same time as Sch. 30/V (Pottina). The trace element data therefore allows a more concrete connection to be made between the silver and gold coinages. It should be noted that the change from Potin to Struck Bronze is not accompanied by steep rise in Sb. However, these coins have only been analysed by electron microprobe and the method of analysis may not be representative of the coinage (see section 2.7.2)

The Pb isotopic data provides corroborating evidence to backup the observations provided by the alloy and trace element data. However, it does give rise to one major discrepancy and that is: why do we see a change in copper source in the trace elements during the Sch. 30 coinages while the Pb isotopic mixing line remains unchanged? Perhaps the new copper source is located within the same

region thereby acquiring its metals from similar country rocks. Or, if the evidence of the high Sb and positive  $\delta\text{Cu}65$  is to be considered then perhaps there was a move to a previously undiscovered oxide ore within the same deposit.

### **3.9 Recommendations for future work**

Pb isotopic studies provide the best method for identifying possible source regions and the use of Laser Ablation should make a large range of coins available for analyse. Trace element analyses provide information on deposit changes within regions defined by the Pb isotopes. Coinages of particular interest to the local story would be Sch 30/I, Sch 23 and the Rainbow Cups. For the Sch 16 and 18 coins a comparative study with other Armorican types could help explain the remarkable composition of these coins.

A more comprehensive Pb isotopic database focussed on a wider range of gold deposits would be needed.

## **4.0 Geochemistry of Gold Sources**

### **4.1 Introduction**

Studies of gold mines thought to be of Celtic origin have been made in France (Cauuet, 1999a, 1999b) and a preliminary study of ancient gold mining activity has been made in Belgium (Dr. Veronique Hurt pers comm.). However, to a large extent hard rock gold mines of Celtic origin have not been studied or identified in Western Europe. Therefore, alluvial gold sources, also known as “Placer Deposits”, were considered to be appropriate for this study as samples were easier to attain and they were an obvious source of gold for any ancient people.

#### **Aims**

1. To determine if it is possible to distinguish between gold deposits and in particular “Placer” gold deposits based on their trace element and isotopic signatures.
2. To see if it is possible to use such data in finding correlations between gold sources and Celtic gold coinages.

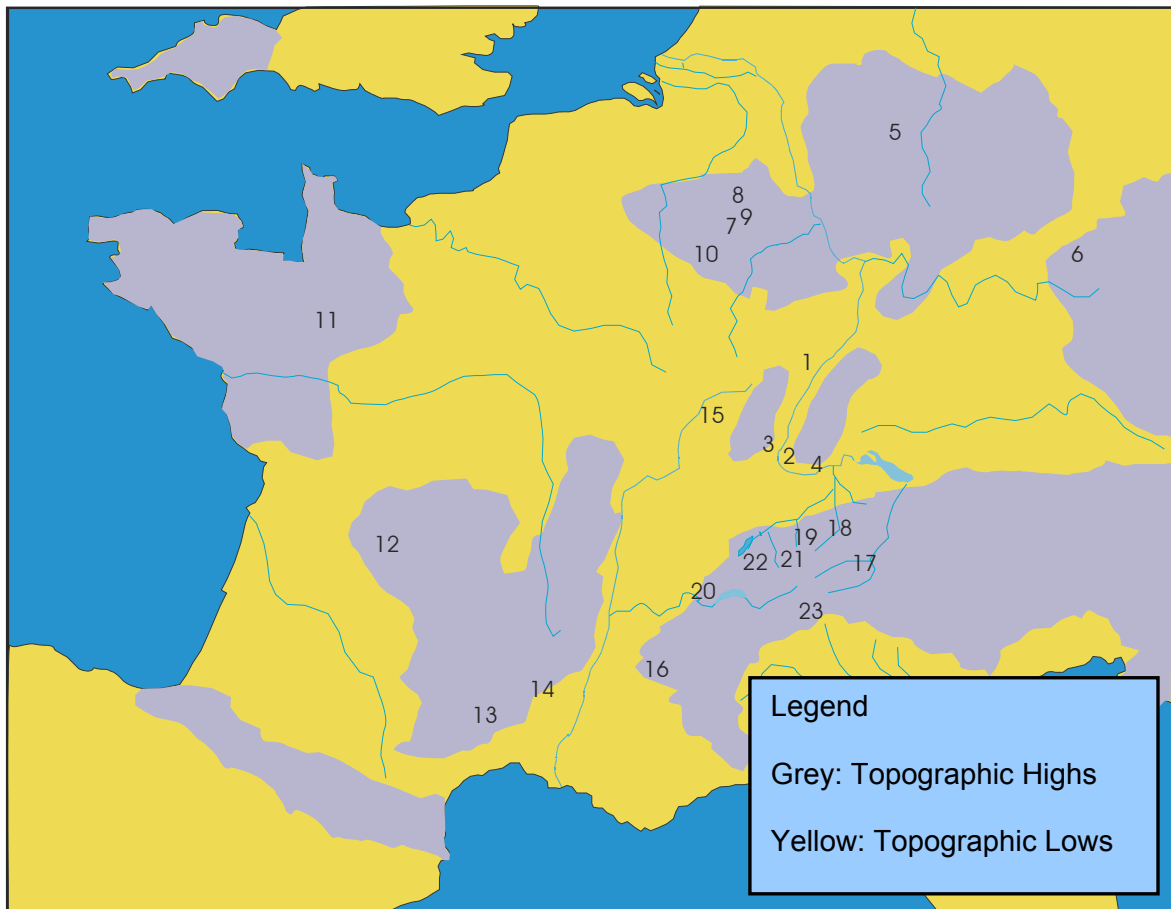
Gold deposits which are found in or near the study area include the placer deposits of the Rhine River valley, those of the Rheinisches Scheifergebirge and in particular the placer and hard rock deposits of the Belgian Ardenne. Gold samples were acquired mostly from private collectors and associations concerned with gold prospecting and washing in Europe. Most of the samples come from the areas mentioned above but there are also a number of samples from Eastern Germany, Italy, Switzerland, France and the British Isles (Map 4.1).

The different types of deposit are described with a more in-depth description of placer gold deposits as they form the bulk of the samples analysed. This introduction is followed by a brief description of the sample localities and the characterisation of each sample by its trace element and isotopic signature.

### **4.2 Gold Deposits Types and Classification**

The term gold deposit can be divided into two basic groups:

- I) Primary deposits; those concentrations of gold which are found deposited within rock formations, usually as a result of igneous and hydrothermal activity. The chemistry of gold means that it is most commonly associated with quartz veins and/or associated with sulphide mineralisation. As hydrothermal fluids are required to carry and deposit the metal, this means that this occurs more in metamorphic orogenic belts (e.g., the Alpine, Variscan or Caledonian orogenies in Europe) or around convergent margins associated with subduction (epithermal and porphyry deposits, e.g.; Pacific island arcs, Andes, etc).
- II) Secondary deposits of gold more commonly known as “Placer Deposits” are produced via the weathering of the primary deposits to concentrate gold within rivers, streams and glacial till. Placer deposits can be many times richer than the adjacent primary mineralisations from which they are



**Map 4.1:** Gold Deposit Locations.

Germany

- |    |      |              |
|----|------|--------------|
| 1. | M-14 | Karlsruhe    |
| 2. | M-12 | Istein       |
| 3. | M-18 | Rosenau      |
| 4. | M-8  | Rheinfeldern |
| 5. | M-7  | Eder         |
| 6. | M-17 | Schwarza     |

France

- |     |      |                  |
|-----|------|------------------|
| 11. | Br-2 | Kergal           |
| 12. | Br-1 | Limousin         |
| 13. | Br-3 | Roche-gude       |
| 14. | Br-5 | Lézan            |
| 15. | M-11 | Saone River      |
| 16. | M-4  | Iserre, Grenoble |

Belgium (Ardenne)

- |     |      |                  |
|-----|------|------------------|
| 7.  | Br-4 | Baraque Fraiture |
| 8.  | Br-5 | Recht            |
| 9.  | Br-7 | Amel             |
| 10. | Br-8 | Suxy             |

Switzerland

- |     |               |                            |
|-----|---------------|----------------------------|
| 17. | M-1           | Rein del Medel             |
| 18. | M-3           | Emme                       |
| 19. | M-10          | Luther                     |
| 20. | M-13          | Allondon                   |
| 21. | Grf28 & 34    | Grosse Fontanne            |
| 22. | Rot41         | Rotache                    |
| 23. | Cam20, 21, 22 | Camedo, Centovalli, Ticino |

derived as the weathering and fluvial processes effectively scavenge the gold from the surrounding catchments, concentrating it in the river bed.

Gold samples from placer deposits form the bulk of the samples analysed and so they are described in more detail highlighting the terminology which was used to describe the samples and the processes which cause physical and chemical alteration of the gold particles during transport.

### **4.3 Placer gold; characteristics and classification**

There are a number ways to characterise a placer gold sample. These include;

- i. The morphology of the gold grains.
- ii. The presence or absence of a pure gold rim on the grains.
- iii. The mineral inclusions present in the grains.
- iv. The composition and trace element signatures of the grains.

Of most interest to this study are the compositions and trace element signatures of the grains but these are affected by the presence of mineral inclusions and by transport processes, which produce morphological changes and cause the development of high purity gold rims. Therefore each of these aspects are described below and used to classify the samples.

#### **4.3.1 Gold Morphology and Classification**

Because gold is malleable and ductile, the complex and angular shapes that the gold particles inherit from their lode source are lost during fluvial transport. It is well accepted that the shape of placer gold particles and in particular their degree of flatness is related to the distance of transport (Knight, 1999, Youngson and Craw, 1999). With an adequate number of particles at a sample site, there is a semi-quantitative relationship between average shape (flatness and roundness) average rim characteristics (thickness and rim percentage) and distance of transport from the lode source (Knight et al 1999).








The morphology of a gold particle can be described by five general parameters;

- i. The degree to which the particle is flattened (flatness).
- ii. The degree to which the particle is rounded (roundness).
- iii. The outline shape of the particle as it lies on its preferred side (outline).
- iv. The thickness of the particle as determined from its cross-section.
- v. Its surface texture.

Knight et al (1999) and Youngson and Craw (1999) assigned numerical values to these descriptors and then used them to provide a semi-quantitative context in which to show the progressive modification of gold particles with distance.

This is not the aim of this study as no specific primary sources are known for the alluvial samples and so the classification system will be used purely to describe the gold and is sufficient to show whether the gold particles in a sample are

physically consistent and if they are derived from primary sources which are nearby or far away. The descriptors are shown in Figure 4.1 and the samples are presented and described in Table 4.1.

Roundness	Angular 		Irregular 		Rounded 	
Outline	Equant 	Elongate 	Complex 	Branched 		
Thickness	Thick 1mm		Intermediate 0.35mm		Thin 0.2mm	
Surface Texture	Matte		Mirror-like	Scratched		Pitted

**Fig: 4.1** Gold descriptors from Knight et al (1999), used in this study to describe the placer gold samples presented in Table 4.1.

### 4.3.2 Gold Compositions.

The Au and Ag composition of large numbers of gold particles from individual sample sites has been used in several studies to show that gold in these placers is derived from more than one source (Knight et al 1999, Chapman et al 2002). In general it seems that the Au-Ag composition of individual mineralising events should be approximately the same, although it is quite possible that more than one gold mineralising event could be represented within a primary deposit.

The Au, Ag, Cu, Hg and Pb composition of the grains were measured by electron microprobe (see section). A table of results can be found in appendix 4.

Most of the samples are composed of between 10 and 30 grains or flitters, which can display a broad range of Au-Ag compositions. Almost all of them contain around 1%Hg and Pb and Cu are usually present in the sub 0.5wt% range, except where inclusions of chalcopyrite or galena are present.

### 4.3.3 Gold Rimming

#### a) Previous Studies

Most placer gold particles develop a rim of nearly pure gold during transport, (Figures 4.2 a & b). Groen et al (1990) have discussed the various processes whereby the rims form. These include:

- 1) Preferential dissolution of silver, or



**Table 4.1:** Lists all the gold samples featured in this study. The physical characteristics are described with reference to Figure 4.1 along with the inclusions observed during reflected light microscopy and EPMA analysis

Name	Locality	Roundness	Outline	Thickness	Size(mm)	Rimming	Inclusions
<b>M-1</b>	Rein del Medel	Angular to irregular, smaller grains more rounded	Complex	Thick, prismatic	1-1.5 & 1-4	Very thin <5µm	Quartz
<b>M-3</b>	Emme	larger irregular, smaller angular	equant to elongated and complex	Intermediate	0.2-1.0	No	Quartz
<b>M-4</b>	Isere	Irregular (folding)		Intermediate	1.0-2.0	Yes	Feldspar
<b>M-5</b>	Ochills, Scotland	Mostly Irregular one rounded	equant and some elongate	Intermediate, one thick prismatic	1.0-3.0	yes	Quartz, Cu-rich phases
<b>M-7</b>	Eder, Hessen	grains & flitters, rounded to irregular	equant, elongate and complex	Thin	0.05 - 0.2	Yes	
<b>M-8</b>	Rheinfelden, Baden-Württemberg	mostly rounded flitters	equant	Thin	0.5-1.5	Yes	Quartz
<b>M-9</b>	Rio Elvo, Piemont, Italy	rounded and folded flitters	equant to complex	intermediate	2.0 -4.0	Yes	Quartz
<b>M-10</b>	Luther, Napfgebiet, Switzerland	Rounded to irregular flitters	equant to complex	thin to intermediate	0.5 -1.0	No	
<b>M-11</b>	Saone, France	Micrograins & flitters, irregular & Folded	equant & complex	very thin	0.1 - 0.2	Yes	Quartz, rutile
<b>M-12</b>	Altrhein, Istein	Nicely rounded flitters	equant & complex	thin	1.0 -3.0m	Yes	
<b>M-13</b>	Allondon, Genf, Switzerland	large rounded Flitters and smaller irregular flitters & grains	Large equant and small elongate & complex	thin	0.5-1 & 1-2	Yes	
<b>M-14</b>	Altrhein, Karlsruhe	small generally rounded flitters	elongate and complex	very thin	0.05-0.2	Yes	Fe-oxides
<b>M-17</b>	Schwarza, Thüringen					No	Feldspar
<b>M-18</b>	Altrhein , Rosenau	Irregular	Equant	Intermediate	1-2mm	No	



<b>Br-1</b>	Laurieras, Limousin, Quartz Reef	gold crystals			1-3	No	Pyrite, arsenopyrite, sphalerite
<b>Br-2</b>	Kergal, Bretagne	Rounded flitters and grains	elongate and complex	thin	0.1to 1.0	yes (only on some)	
<b>Br-3</b>	Céze, Gard (RocheGude)	rounded flitters	equant and complex	thin	1.0 to 2.0	Yes	pyrite & chalcopyrite
<b>Br-4</b>	Massotais, Baraque Fraiture	gold crystals			0.2 to 1.0		Quartz, telluride and pyrite
<b>Br-5</b>	Gardon, Gard (Lézan)	rounded flitters	equant and complex	thin	0.3 to 1.5	yes	Galena with quartz & rutile
<b>Br-6</b>	Ru De Poteau, Recht	irregular to rounded	complex and some slightly branched	intermediate to thin	0.2 to 1.0	no	Quartz, Fe-oxides
<b>Br-7</b>	Schinderbach, Amel	irregular grains	elongate and complex	intermediate to thin	0.1 to 1.0	no	Quartz, rutile
<b>Br-8</b>	Side Creek, Suxy	Angular to irregular	complex an branched	thin to intermediate	0.1 to 1.0	no	Galena
<b>Br-9</b>	Kildonan Burn, Kildonan	Rounded to irregular flitters and grains	equant, complex and elongate	thin to intermediate	0.3 to 1.5	yes	Quartz, feldspar, rutile, galena
<b>Grf28</b>	Grosse Fontanne, Napf area	Rounded and irregular grains	Equant	Intermediate	0.3 to 1.0		
<b>Grf34</b>	Grosse Fontanne, Napf are	Irregular	Equant and complex	Intermediate	1 to 1.5mm	Yes	Quartz
<b>Rat31</b>	Rotache river, Near Thun	Rounded	Equant	Thick	~2.0mm	Yes	
<b>Cam20</b>	Camedo	Irregular	Equant	Intermediate	0.5mm		Quartz, Fe-Ox, galena, sphalerite
<b>Cam21</b>	Centovalli	Rounded	Equant	Intermediate	0.5mm	Yes	
<b>Cam22</b>	Ticino	Angular	Complex	Intermediate to thin	0.2 to 0.5mm	Yes	

2) Precipitation of gold on the surface via cementation and or electro refining processes.

The development (thickness) of these rims may also be related to the distance of transport.

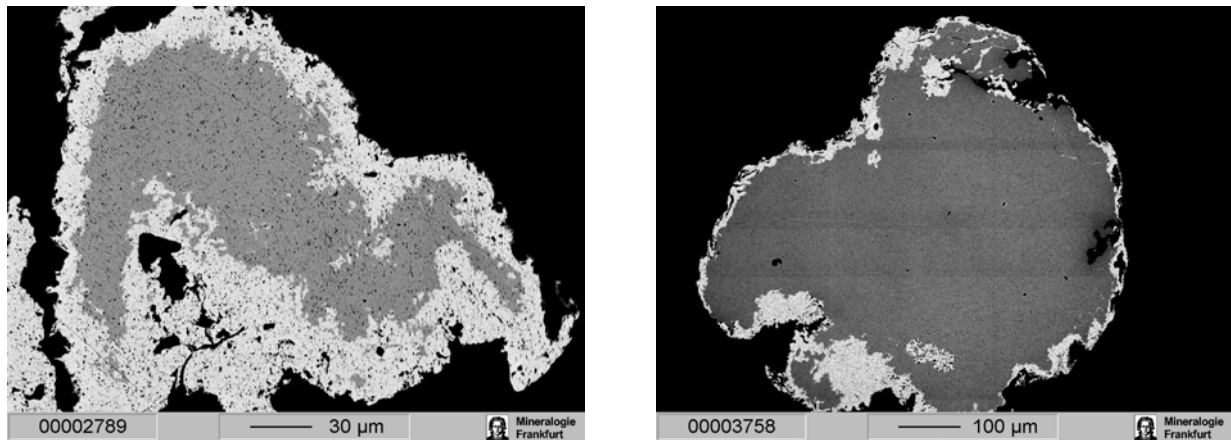
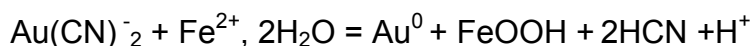


**Fig. 4.2:** a) sample M14, b) sample Br9, both showing typical rimming features.

Their view is that selective leaching of silver from the margin of gold grains seems to be impossible as there is no means by which the solutions can physically extract the silver from more than the outer few angstroms of the grain. A process whereby gold is precipitated on the surface is therefore preferred. However, Knight et al (1999), prefer the preferential removal of Ag, Hg and Cu to form the pure gold rims of samples from the Klondike area of Northern Canada and suggest that hammering, folding and other processes which cause physical deformation of the gold during transport could provide a means to expose more of the gold/electrum cores to the leaching processes.

The cementation model proposed by Groen et al (1990), is cited as occurring via reactions involving the following dissolved species; CN<sup>-</sup>, OH<sup>-</sup>, NH<sub>3</sub><sup>-</sup>, Cl<sup>-</sup>, I<sup>-</sup>, Br<sup>-</sup>, HS<sup>-</sup> which are generally present in sufficient quantities in surficial waters to make such processes viable. Of particular note is a precipitation mechanism involving Fe<sup>2+</sup> as a reducing agent via the following reaction:



The reaction causing the simultaneous precipitation of native gold and ferric hydroxide, the presence of iron hydroxide as coverings on placer grains and inclusions within the surface are sighted as evidence for such a process.

Electro refining involves the dissolution of the Au-Ag alloy leaving the Ag in solution while the Au plates back on. The driving force for this reaction being the result of the electromotive force between two dissimilar metals in solution whose Eh is higher than that in which the starting alloy is stable. Basically, once in solution the more easily oxidised Ag is washed away while the more easily reduced Au precipitates back on to the nugget surface.

#### **b) Observations from this study**

Several qualitative observations which are pertinent to this discussion were made during this study.

- 1) Gold rimming seems to be more complete and thicker on gold grains with higher Ag contents.

- 2) Comparative analyses of common trace elements (Cu, Pb, Hg, Bi and Sb) shows that the pure gold rims are often enriched in these traces with respect to the cores (Fig 4.3).

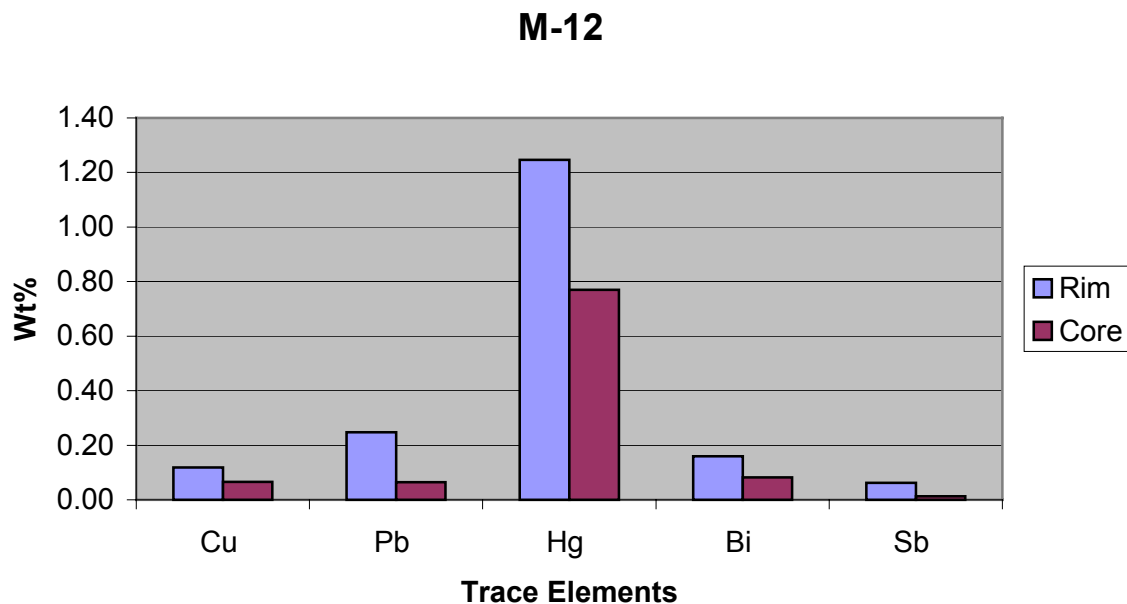


**Figure 4.3:** Shows analyses made on the rim and the core of sample M-12 by EPMA. All these trace elements show an enrichment in the rim.

These two observations suggest that selective leaching of Ag has a large part to play as it is the more Ag rich grains which are most affected. Conversely it seems some sort cementation or electro refining mechanism is also at work leading to the enrichment of trace metals in the rims.

It is unclear as yet why Ag would be removed while these elements are enriched. One possibility is that porosity created during dissolution of the Ag may later provide sites for the redeposit ion of these more common elements after some change in the chemical regime has occurred during transport.

Considering the observations made here, it is suggested that the study of gold rimming would benefit from a quantitative study of the correlation between Ag compositions and the extent gold rimming.

It is important to note here that chemical modification of the gold grains during transport is a common feature, and that this may affect the trace element and isotopic signatures of the gold.

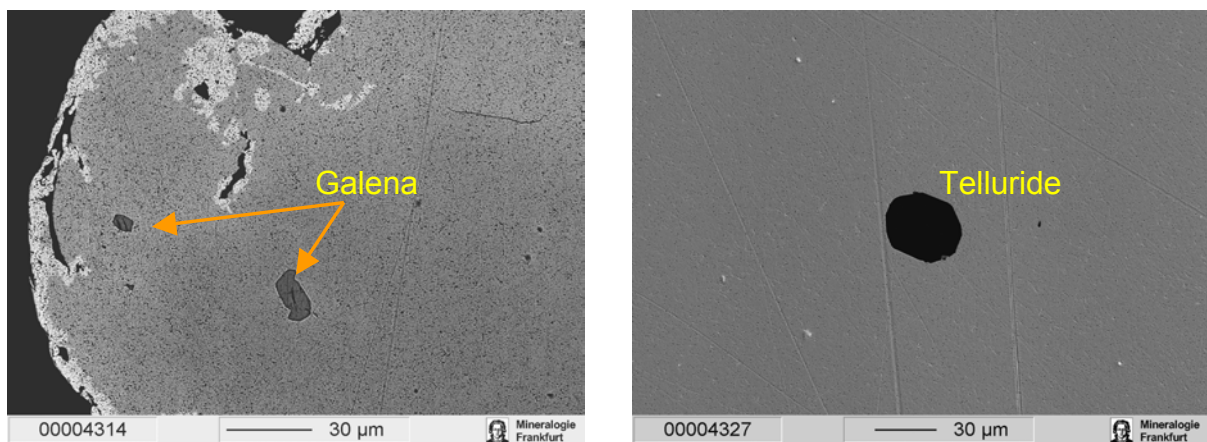
#### 4.3.4 Inclusions

Chapman et al (2002) have developed techniques of characterising gold particles by their micro chemical signatures, using the inclusions found within gold grains to connect the gold grains to particular types of gold mineralisation styles. As mineral inclusions represent high concentrations of particular elements, their presence will tend dominate the trace element signatures acquired by Laser-Ablation ICPMS

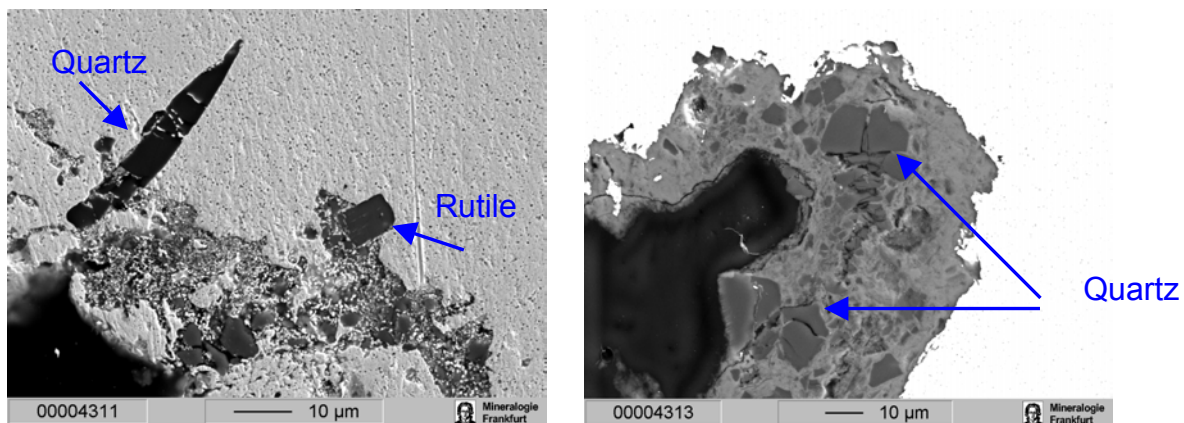
There are two main groups of inclusions;

- 1) Primary inclusions, those associated with the primary mineralisation of the gold and usually found well within the gold grain (sulphides, quartz, telluride's, sulphosalt's etc), although some such as quartz may still be present on the edges.
- 2) Secondary inclusions are usually present on the edge of the grains representing a range of minerals which are resistant to weathering or which are products of weathering, these include, quartz, rutile, feldspars, iron oxides and hydroxides.

Some examples of primary inclusions can be seen in Figures 4.4 a,b,c and d.



**Figures 4.4:** Are both BSE images made on the Electron Microprobe **a)** Is a nugget from sample Br-5 which contains at least two inclusions of Galena. **b)** shows a tellurium rich crystal imbedded in a gold grain from sample Br-6.



**c)** Another gold nugget from Br-5 showing rutile and quartz embedded in the edge of the gold grain (backscattered image). **d)** Is a compositional picture of a grain from Br-6. The white area is the edge of the gold grain which partially surrounds a grey mass of iron-oxyhydroxides with grains of quartz embedded in it. The shape of the cavity with its almost 90° cubic corners probably represents the hole left behind by pyrite which has since oxidised to the iron-oxyhydroxides.

Inclusions have a major effect on the trace element signatures which are acquired by laser ablation analysis. The presence of rutile in the edge of many placer gold grains hinted at the possibility of tracing the placer origin of ancient gold by its titanium content as both the lode gold samples (Br-1 and Br-4) contain no Ti. However, qualitative analysis of the Celtic gold, copper and silver coins has shown that they all have high Ti, which is probably a result of refining copper by adding silica in the form of sand (sand contains significant traces of rutile).

One important consideration which has been brought up every time the coins of the region were studied is whether the gold comes from the Aegean or the Rhine based on the presence of PGE inclusions. Gebhard et al (1999), believe this indicates an Aegean origin while others, considering the PGE minerals occasionally found in the Rhine, would suggest the Rhine gold, Hartmann (1976).

However, No PGE nuggets or minerals were noted embedded in these nuggets, although it must be noted that the sample sizes studied were small.

#### **4.4 Trace Elements**

Past studies dealing with the trace element fingerprinting of gold have avoided quantitative measurements due to the inherent difficulties of standardisation (see section 2.4). Distinguishing between deposits has depended on the presence or absence of various elements and element associations. Taylor et al (1995), have also compared the intensities measured by plotting them on tri-plots showing that deposits can be characterised in this way. This study has taken the next step by producing quantitative data (as described in section 2.4) and applying it to the characterisation of placer gold samples.

The following discussion examines the data, selecting those elements which show the least variation within samples and using them to characterise the deposits. The least variable elements representing those which are relatively unaffected by the transport alteration processes described above. Examples from the dataset are shown with the bulk of the data summarised by country later in the chapter.

Two methods of visualising the data are compared.

- I) Ternary (Tri-plots) of the least variable elements
- II) Bar graphs of the complete suite of trace elements.

The first method compares the relative abundances of the elements plotted while the second allows distinctions to be made based upon the presence or absence of different element associations.

##### **4.4.1 Selecting elements unaffected by transport effects**

An idea about which elements will be the most useful for characterising placer deposits can be gained by examining the variation of the trace elements from analyses of gold grains in one sample. The variation can be expressed as %RSD calculated for each element from the average and standard deviation of ten

analyses. Figure 4.5 shows a plot of %RSD for each element from analyses of ten gold grains from sample M-1. The elements with low variation include the PGE's; Pd, Pt and Ir, Ag, Co, Sn, Te and Pb also show low enough variation to be used for characterising the deposit. It should be noted that the elements with extremely high %RSD's are ones which are present in very low amounts. For other samples Cu, Sb, W, Ni and Fe also have low %RSD's.

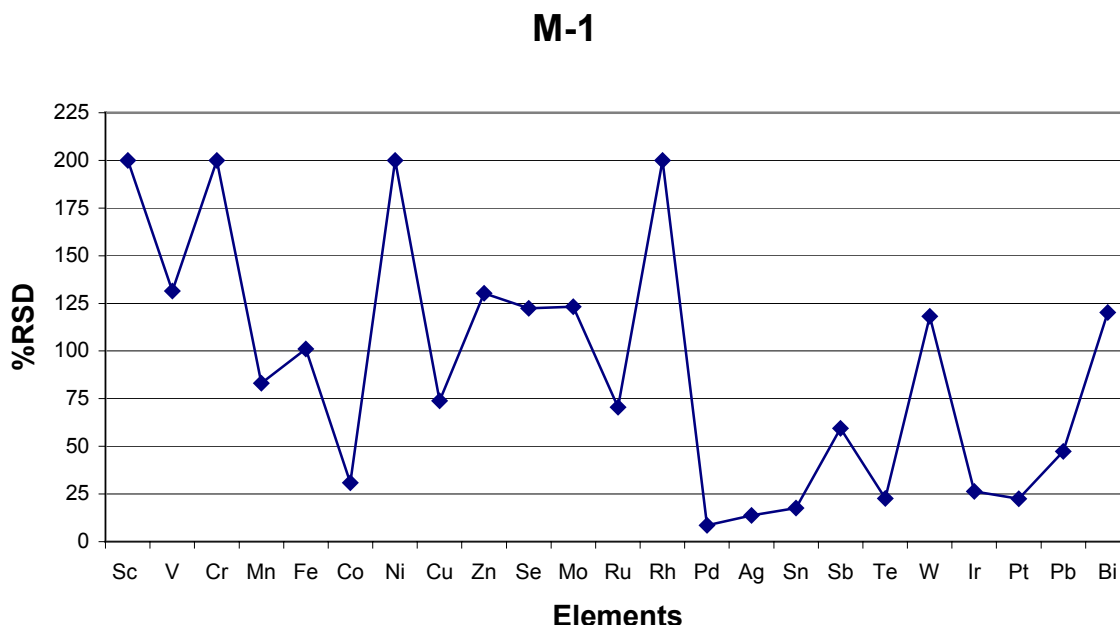


**Fig. 4.5:** The %RSD for each element measured from ten analyses made by LA-ICPMS on ten gold grains from sample M-1.

The elements with the lowest variation are those which are most unaffected by the transport related processes described in the previous sections. Obviously the PGE's can be relied upon to provide consistent signatures of the different gold groups, due to their refractory nature. The usefulness of the other elements seems to depend on their concentrations. The higher the original concentration of the element the less overall affect is produced by alteration processes, whereas the elements with low concentrations could be almost totally removed or become relatively enriched during transport.

#### 4.4.2 Visualising the data

To investigate the usefulness of some of the elements chosen for their low variation between gold grains, a series of tri-plots were made. The data presented represents the analysis of up to ten grains from each sample which have been grouped together into "subgroups" with reference to their Ag compositions. Each subgroup is then averaged together. An example from the Belgian deposits is shown in Fig 4.6 which is a ternary plot of Cu, Pt and Pb. It shows that samples Br-4, Br-6 and Br-7 can be characterised using these elements while the analyses of Br-8 show that it is the most heterogeneous sample. The silver composition of this sample shows three distinct subgroups (Appendix 2; Br-8) and an overall visual examination of the presence or absence of the other trace elements (Fig 4.7) also shows these three subgroups.

Group Br8-1 can be characterised as containing no V, Cr, Ni, Zn, Ga, Mo, Rh or W while Br8-2 contains all the elements (except with lower Ru and Pd) while Br8-3 is typified by its lack of the lighter elements Sc, Ti, V, Cr, Mn and Fe.

On the tri-plot sample Br-7 is shown to form a loose group of three subgroups (including two very similar subgroups) while the fourth contains more copper. Visual comparisons of their entire trace element pattern (Fig 4.8) reveals that groups Br7-1 and Br7-2 look very similar. Br7-3 looks similar to the first two but it lacks Cr, Ga, Mo and Ni. Br7-4 is the most different with no Ti, V, Cr, Mn, Fe, Ni, Ga, Mo, Rh and W.

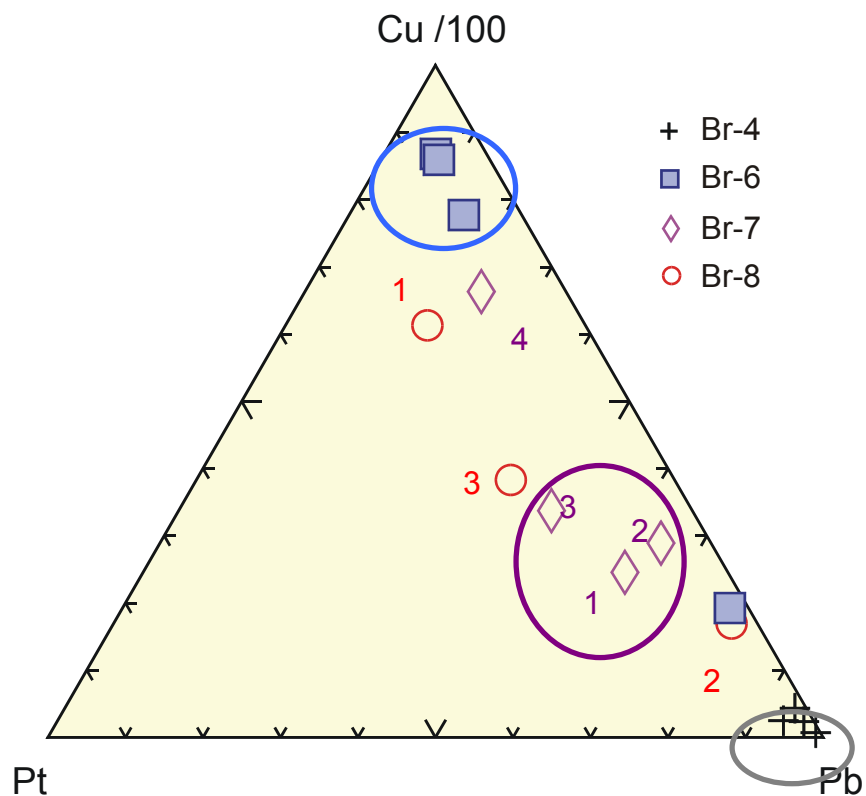
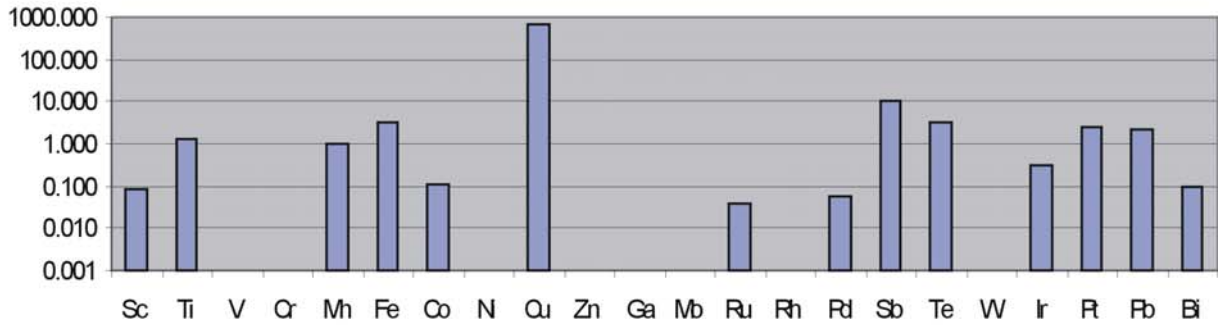
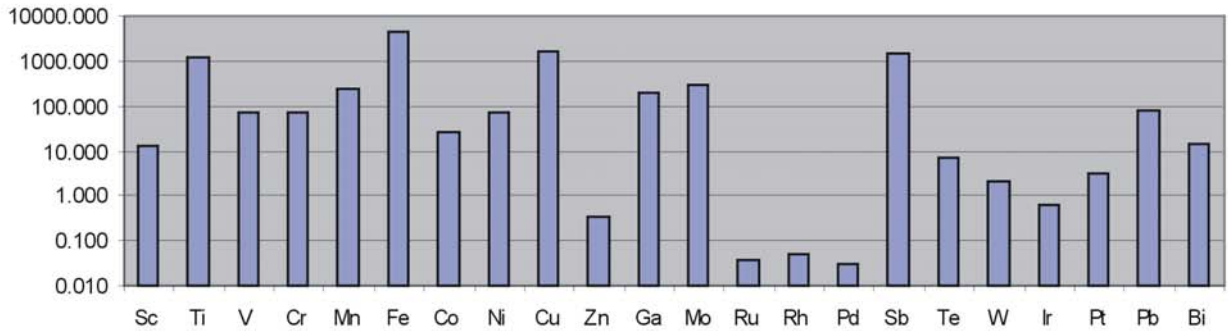


**Fig. 4.6:** On this tri-plot of Cu, Pt and Pb the Cu concentrations have been divided by 100 so that they do not dominate the plot. The numbered points relate to the subgroups of Br-7 and Br-8 and are discussed in the text with reference to the following two figures.

**Br8-1**



**Br8-2**



**Br8-3**

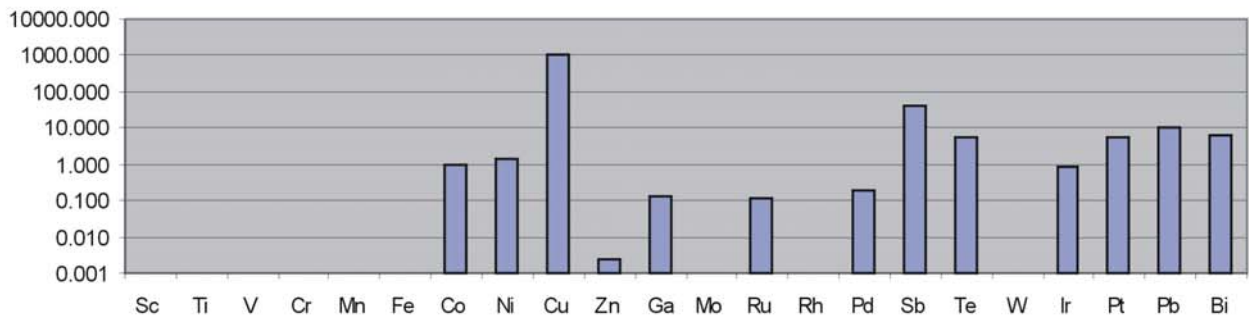
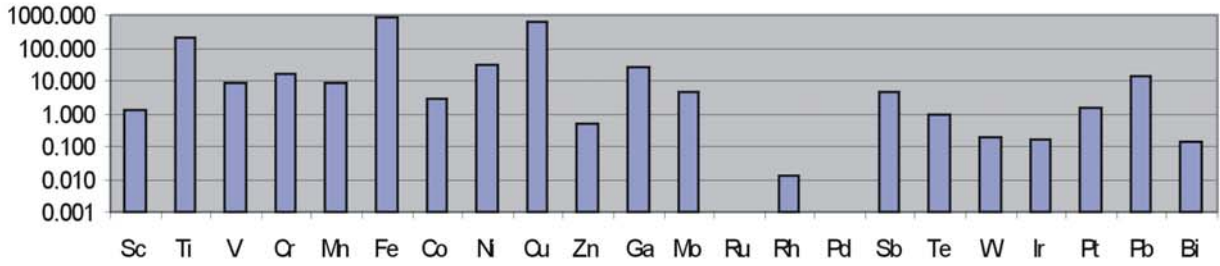


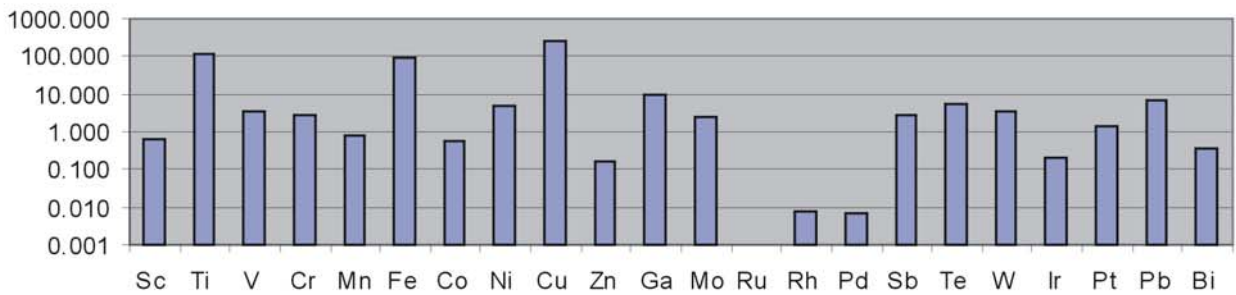
**Fig 4.7:** The concentrations of all the trace elements measured are shown here on a log ppm scale. The data represents five analyses which have been grouped depending on their Ag compositions and then each group has been averaged together. A simple visual comparison of the patterns reveals obvious differences between the groups



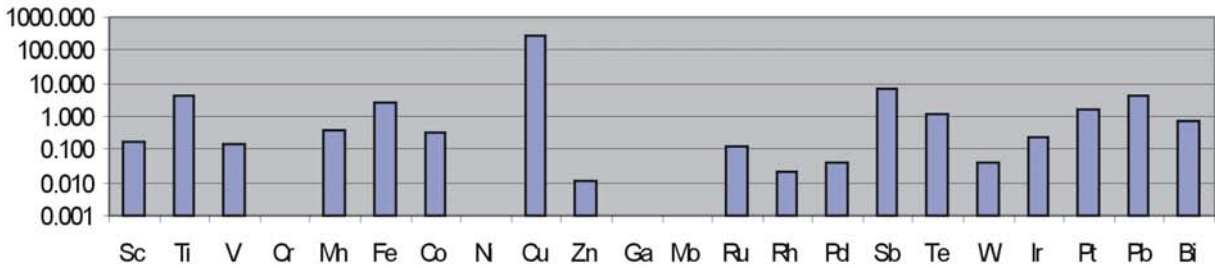
Br7-1



Br7-2



Br7-3



Br7-4

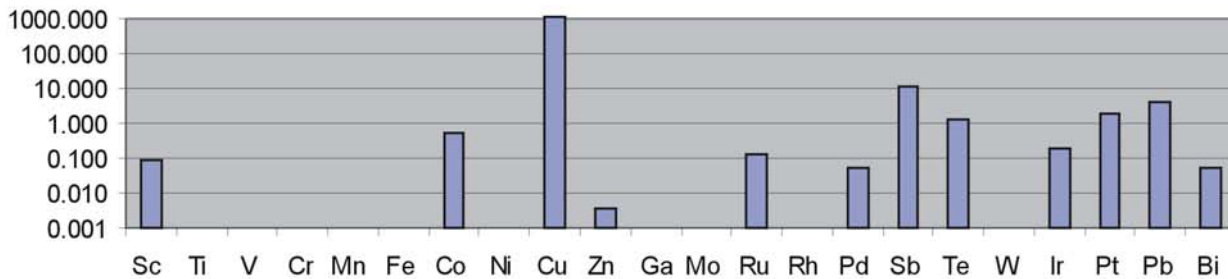


**Fig 4.8:** As with the previous figure, the trace element concentrations are shown here on a log ppm scale. A visual comparison of the patterns shows that Br7-1 and Br7-2 are very similar while the other two are different.

### 4.4.3 Summary

Comparing tri-plots, of the least variable elements (in terms of %RSD for most samples), with the visual examination of the entire trace element patterns, plotted as a bar graph of trace element concentrations (log ppm), shows that both ways of visualising the data are in good agreement and can complement each other to reveal groups within samples. Whenever there is a significant change in the less variable elements then this is usually accompanied by changes in the overall trace element pattern,. The subgroups that are revealed should relate to different primary sources.

With respect to the ability of such data to answer questions of provenance, for archaeological artefacts, tri-plots of the more highly concentrated and refractory elements should provide indications of the most likely source deposit despite the transport alteration processes which may affect many of the other trace elements. Samples Br-4 (quartz vein sample), Br-6 and Br-7 show consistent overall groupings. However, there is no consistent signature associated with sample Br-8, and whether this is due to transport related alteration, or mixed primary sources, is unclear.

As many of the most useful elements, for characterising gold deposits, are also provided by the Ag and Cu added to the Celtic gold coins, no matches of gold deposits to gold coins can be made with the data presented here. To be able to make confident matches between gold artefacts and gold deposits, the artefacts will need to be as unalloyed as possible. Also, such studies should be restricted to questions of very localised production. The more deposits, which are considered as possible sources, increases the problems of overlapping fields and distinguishing between individual deposits becomes impossible.

The following section will now use a variety of tri- and x,y plots of trace element concentrations, to summarise the characterisation of all the samples studied.

## 4.5 Gold Sample Localities: Description and background Information

The localities investigated are shown on Map 4.1. The samples are summarised by country and each sample is described in more detail in Appendix 2. Bar graphs of their trace element patterns and the complete dataset can also be found in Appendix 2 and 6.

### 4.5.1 Germany

Germany is shown in two parts, the first are the gold deposits from the Rhine and the second are the two other gold deposits studied from Germany.

#### a) The Rheingold

The following locations have provided gold samples from the Rhine river. Those localities described as “Altrhein” mean that the gold was collected from oxbow lakes and other such features of where the Rhine River used to flow but which have been left behind and isolated from the main flow as it has migrated across the valley. Samples include:

<b>Rheinfelden:</b>	<b>Southern Oberrhein (M-8)</b>
<b>Altrhein, Istein:</b>	<b>Southern Oberrhein (M-12)</b>
<b>Altrhein, Rosenau:</b>	<b>Southern Oberrhein (M-18)</b>
<b>Altrhein, Karlsruhe:</b>	<b>Middle Oberrhein (M-14)</b>

A lot has been written about the *Rheingold* and where it comes from. A small part could come from the Schwarzwald and the Vogesen, but probably most of it comes from the Alps and the Molasse zone. Kirchheimer (1965), suggests that the quarrying of quartz gravel in the mountains has had a lot to do with enriching the gold deposits of the lower Rhine in the last few centuries.

There are no nuggets in the *Rheingold*, only gold flitters, which shows that the *Rheingold* has been transported a long way. Its source was investigated through the study of the heavy mineral concentrates associated with the gold from the *Neiderterrasse* of the *Badischen Oberrheintals* but no definite source could be identified (Ramdohr, 1965) and no proof of a purely Alpine source was found. It was suggested that the *Rheingold* could have come from the glacial erosion of the Alps and Molasse Zone and so a lot of mixing of gold sources would be expected. However, the specific composition of gold found in the Ills and Birs (with high silver contents) suggests the contrary, that mixing of gold has not occurred and that large scale glacial erosion and mixing of gold sources is not evident (Ramdohr (1965), Kirchheimer, (1965). The reduction in size of the gold flitters to the North of the Rhine and the same size of the flitters in each place along the Rhine indicates that all the gold in the Rhine had a common source to the south.

Cu, Pb, Sb and Pt were chosen to characterise the Rhinegold deposits. The following figures (Fig 4.9 & Fig 4.10) show obvious differences between the samples. M-8 is characterised by high Pb and Sb with interesting correlations produced with Pb vs. Cu and Pb vs. Sb. The analyses of different grains from this sample lie along correlation lines with highly variable element concentrations but with very consistent Pb/Cu, Pb/Sb ratios. M-18 shows high concentrations of Cu and Sb, which are also variable but do not have a constant ratio. M-14 and M-12 both have relatively low amounts of these elements.

The triplot in figure 4.11 of Pt, Cu and Pb shows the distinct signature of M-8 with those of the others tending to group together due to their lower Pb contents.

With respect to the geological questions of the provenance of gold in the Rhine, it is interesting to note that M-8, in particular, and to a lesser extent samples M-18 and M-12, have consistent trace element signatures that allow one deposit to be distinguished from another, reinforcing the conclusion that no major mixing of gold sources by glacial erosion has occurred. However, this conclusion was first made on the basis of consistent Ag compositions of gold samples from the Ills and Birs and in sharp contrast to this are the analyses made here which show that the samples have highly variable Ag compositions (see Appendix 2). Why M-8, in particular has such a consistent trace element signature with Ag compositions ranging from 4% to 16% can only be guessed at. Perhaps this sample represents different mineralising events from the same deposit or different degrees of transport related alteration of gold from the same deposit.

M-14 (Karlsruhe) has the most variable trace element signature, and the smallest and thinnest grains (0.05-0.2mm), consistent with it having been transported a long way.

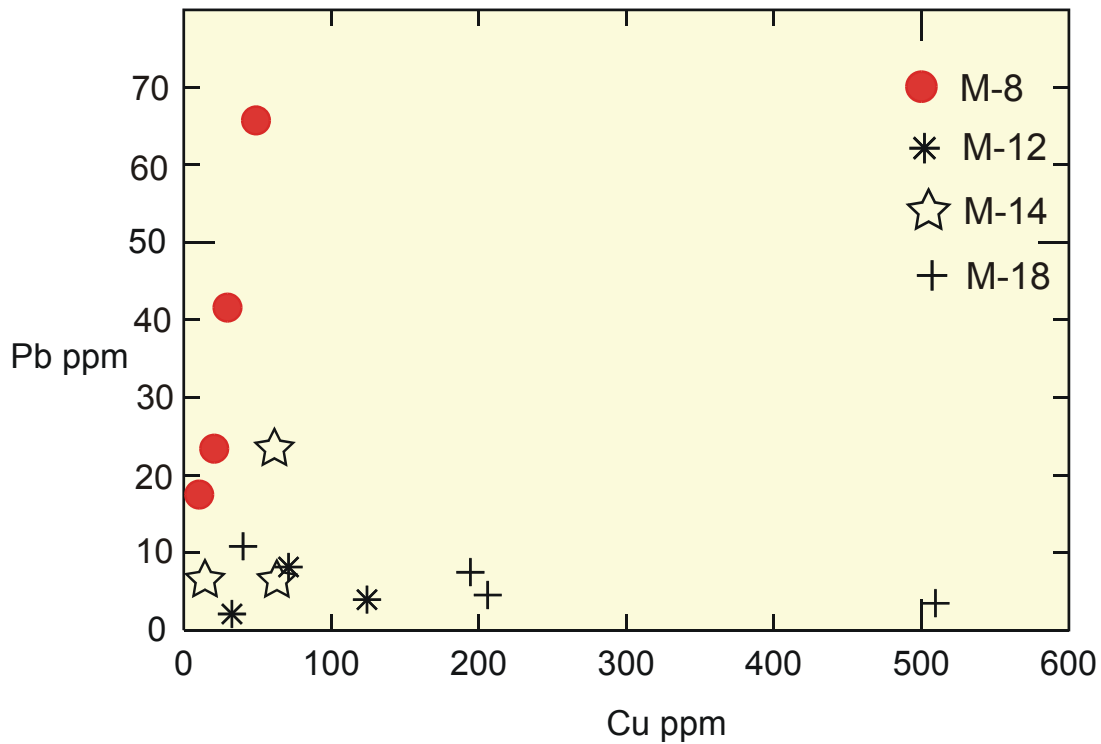


**Fig 4.9:** Cu vs. Pb (ppm) displays distinct differences in the Pb/Cu ratios of the samples. The groups from sample M-8 show a positive correlation with a consistent Pb/Cu ratio while Pb appears negatively correlated to Cu in sample M-18.

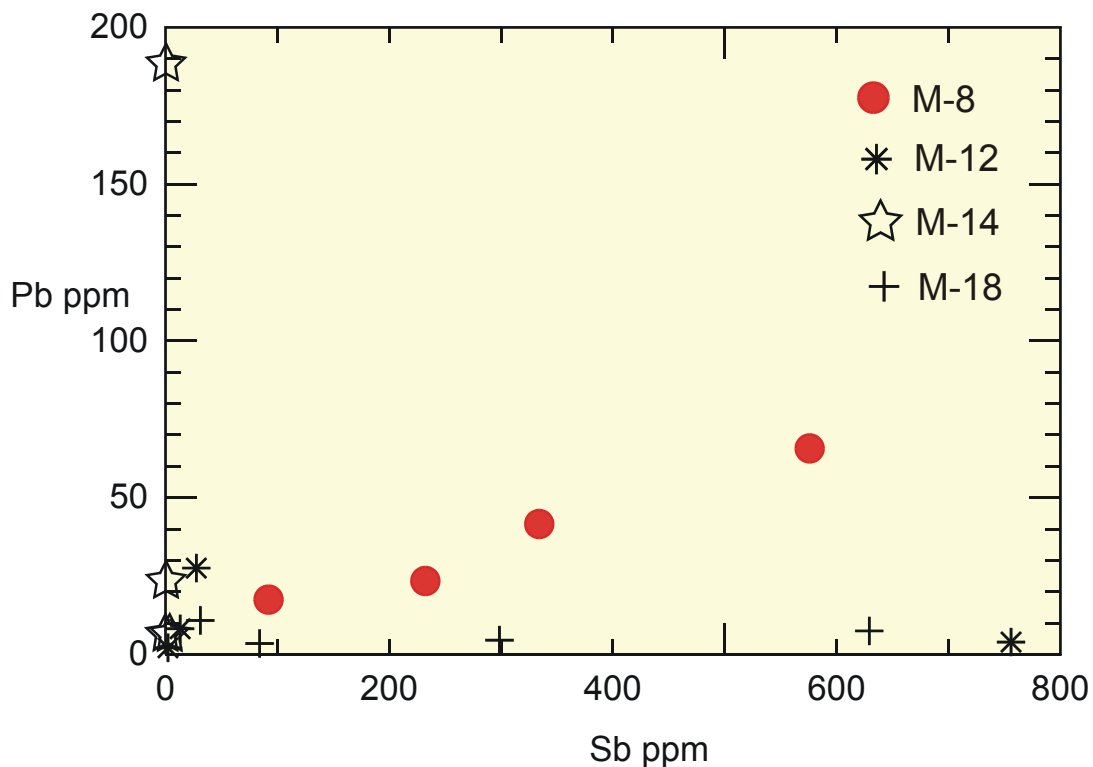


**Fig 4.10:** Sb vs. Pb (ppm) shows some major differences between the samples. Again M-8 shows a positive correlation with a consistent Pb/Sb ratio.

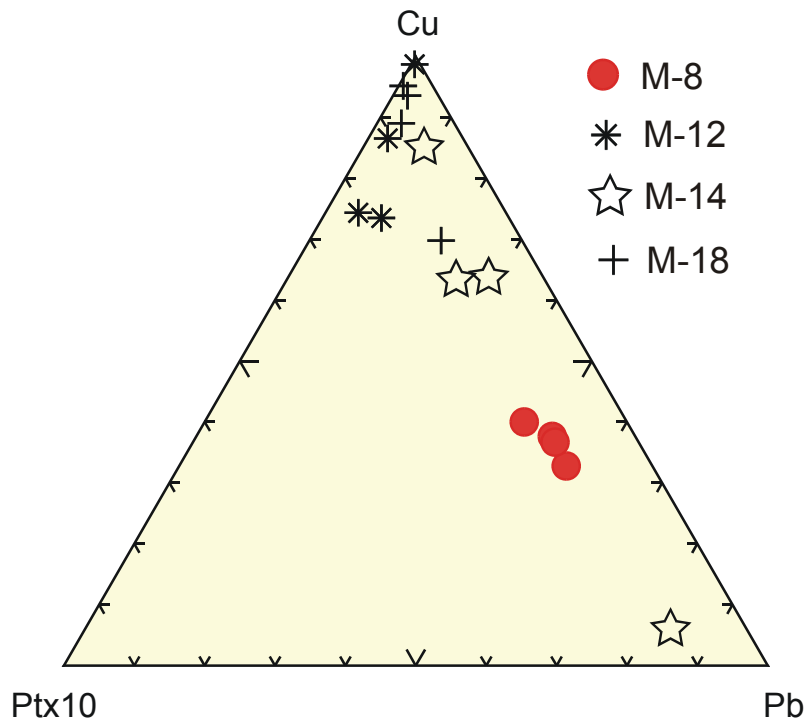


**Fig 4.11:** Pt, Cu and Pb (ppm) with Pt multiplied by ten. The M-8 analyses appear particularly well constrained by Cu and Pb

Microscopic Pt minerals such as sperrylith and platinum crystals have been found in the Rhine (Störk, 2000). Hartmann (1976) reported a platinum content of approximately 0.1% in a sample of gold melted from a panned concentrate from the River Rhine. No platinum minerals were found embedded in any of the grains studied here, although the sample sizes are relatively small. The average Pt concentrations measured in the gold samples (Fig. 4.12) is not exceptional and is similar to other gold deposits studied in this project.

#### Average Pt concentration of Rhine samples

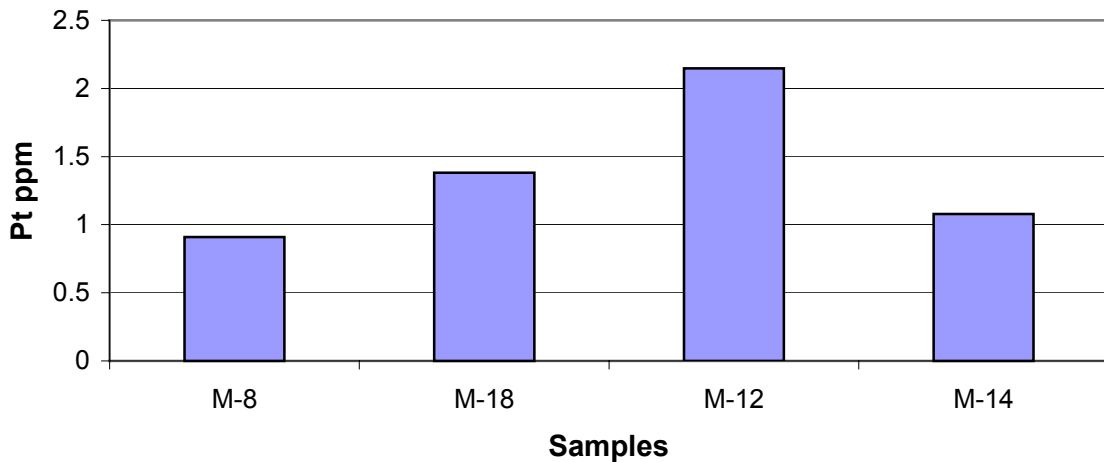


**Fig 4.12:** The average Pt concentrations of the Rhine gold samples are generally less than 2 ppm. One grain from M-12 contained 4.3 ppm Pt.

**b) Eder, Hessen (M-7)**

The origin of the alluvial gold found in the Eder is not definitely known only that it must be derived from the surrounding Rheinisches Schiefergebirge. A small operation has applied modern placer mining techniques to recover gold from the river in the last few decades, although with limited success (Prof T. Kirnbauer pers. Comm.).

The Tri-plot in Fig 4.13 shows the relative concentrations of Cu, Pt and Sb for samples M-7 and M-17. M-7 has higher amounts of Pt and is relatively variable. The actual Pt concentrations are shown in Figure 4.14.

**c) Schwarza, Thüringen (M-17)**

The primary gold deposits in this area have never been investigated in detail. Those placer deposits, which have been investigated, occur in close association with Palaeozoic volcanics of basaltic composition (Lehrberger, 1995).

This sample can be divided into three subgroups based on the Ag compositions of the grains (appendix M-17), one with 1-10% Ag, another with 20-30% Ag and finally one with 45-50% Ag. The trace element subgroup with very high Sb, Fig 4.13, is associated with the two groups with Ag contents over 20%.

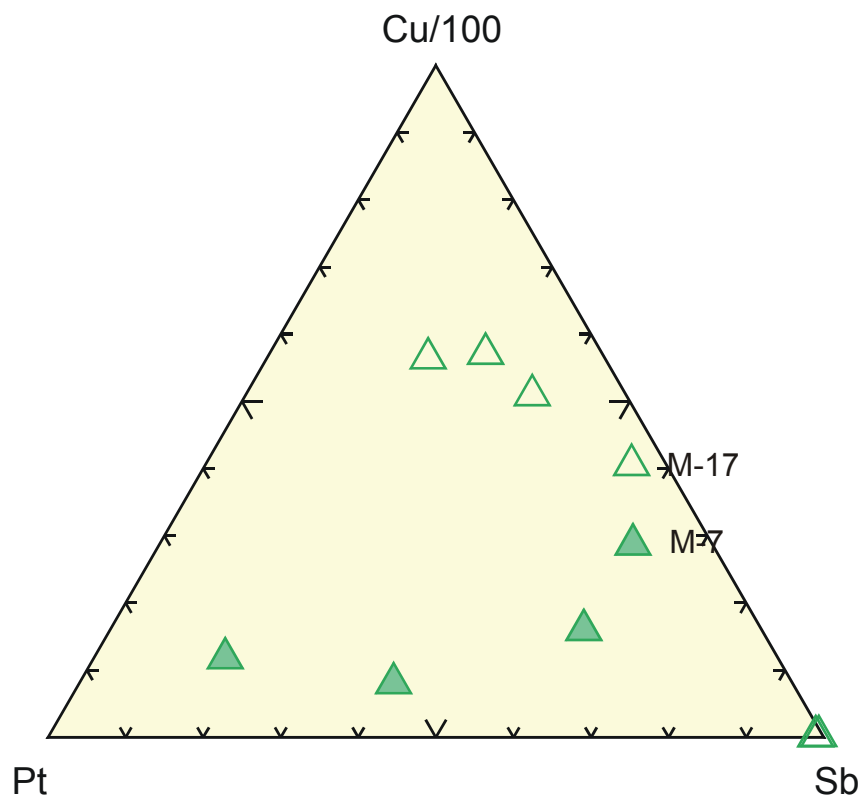


**Fig 4.13:** The relative Cu/100, Pt and Sb concentration of samples M-17 and M-7.

### Average Pt concentrations

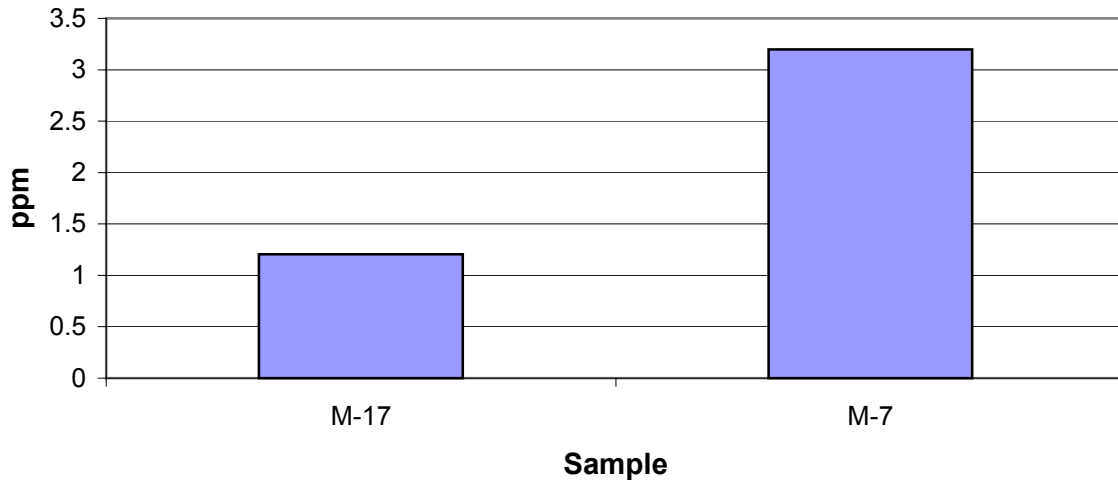


**Fig 4.14:** The average Pt concentration of the Eder sample (M-7) is almost three times higher than that of the Thüringen sample and two times higher than the Rhinegold samples (Fig. 4.12).

#### 4.5.2 Switzerland

Alluvial gold is known from different localities in Quaternary and Tertiary sediments of the Molasse basin. The Allondon river near Geneva contains placer gold due to secondary concentrations of particles already contained in morainic material. During the latest glaciation this material was transported westward and northward from primary sources in the Alps (Jaffé, 1989). One sample from this area is represented (M-13).

Placer deposits also occur in the Tertiary Molasse conglomerates which formed through erosion and resedimentation of the Alpine range. Small placers in the Napf region occur where local streams and rivers intersect the Napf conglomerate. Samples from this area include M-3, M-10, Grf28, Grf34 and Rat31.

The three samples from the Camedo area (Cam20, Cam21 and Cam22) may represent gold that is partially derived from the ultramafic Ivrea complex (Dr. B. Hofmann pers Comm.)

<b>Rein Del medel:</b>	<b>(M-1)</b>
<b>Emme, Napfgebiet :</b>	<b>(M-3)</b>
<b>Luther, Napfgebiet :</b>	<b>(M-10)</b>
<b>Allondon, Genf :</b>	<b>(M-13)</b>
<b>Grosse Fontanne River, Napfgebiet:</b>	<b>(Grf28 , Grf34)</b>
<b>Ratoche River:</b>	<b>(Rat31)</b>
<b>Camedo, Centovalli, Ticino:</b>	<b>(Cam20, Cam21, Cam22).</b>

The elements used to characterise these deposits include Sb, Cu, Pb, Te and Pt (Figures: 4.15 and 4.16). The samples from Ratoche and Comedo only consist of several grains and so are not truly representative of the deposits.

M-1: Very consistent signature for all grains with the same Cu, Pt and Pb concentrations and high Sb compared to other samples.

M-3: Pb and Sb provide a consistent signature, one subgroup shows higher copper.

M-10: There is one main group consisting of three subgroups (with higher Pt) and two which are more variable.

M-13: One main group with two subgroups, which have higher Sb and Cu than the others.

Grf28: Is relatively variable but has much higher Pb than Sb or Te.

Grf34: Is quite different from Grf28 with higher Cu and less Pb .

Rat31: Has high Cu .

Cam20: Has higher Pb than most of the other samples but is otherwise quite variable.

Cam21: Is also variable

Cam22: Has a very consistent Cu, Pt and Pb signature

The Pt concentrations of the samples (Fig 4.17) reveals that Cam20 contains over 18ppm Pt compared to less than 5ppm for the others. This is perhaps an indication of its ultramafic source as suggested above.

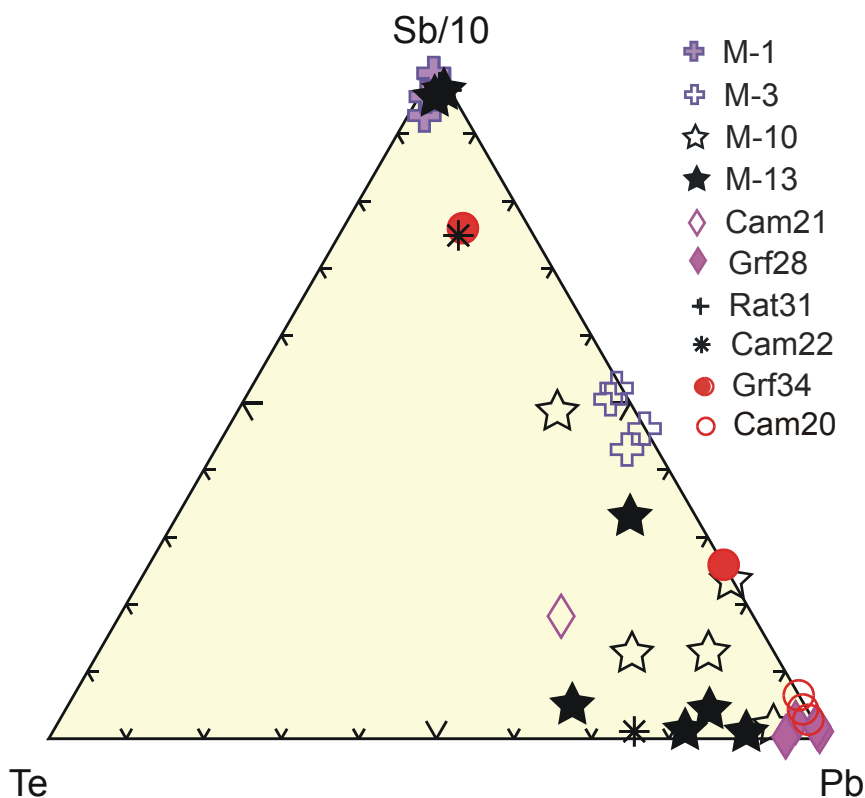


**Fig 4.15:** Sb, Pb and Te tri-plot, high Sb is often associated with low Pb.



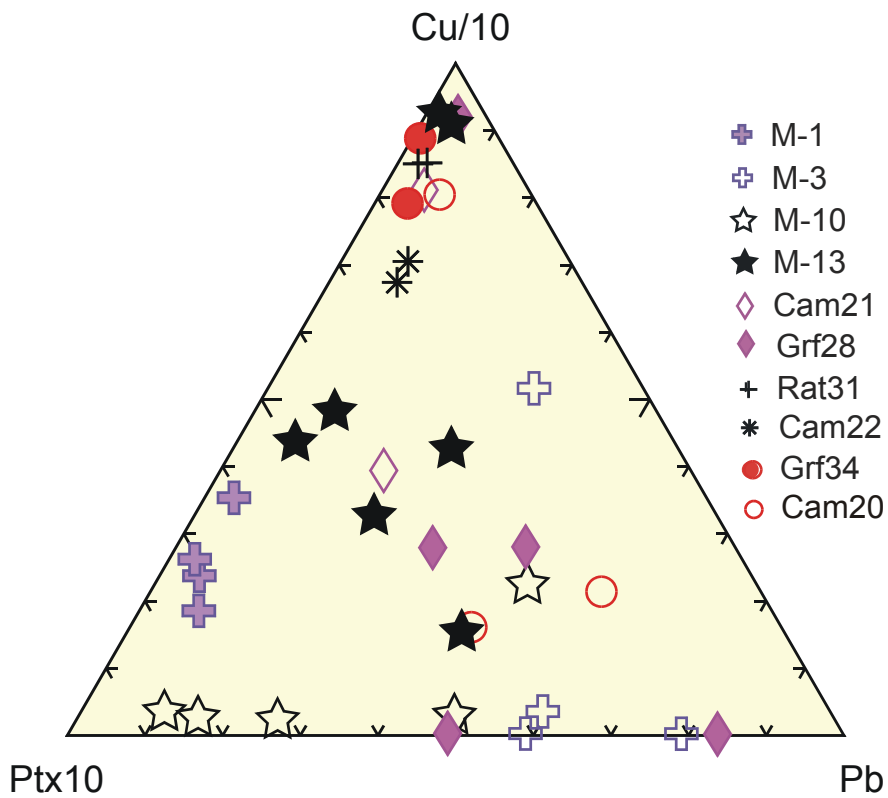


**Fig 4.16:** Cu/10, Ptx10 and Pb Tri-plot.

Pt concentration of Alpine deposits

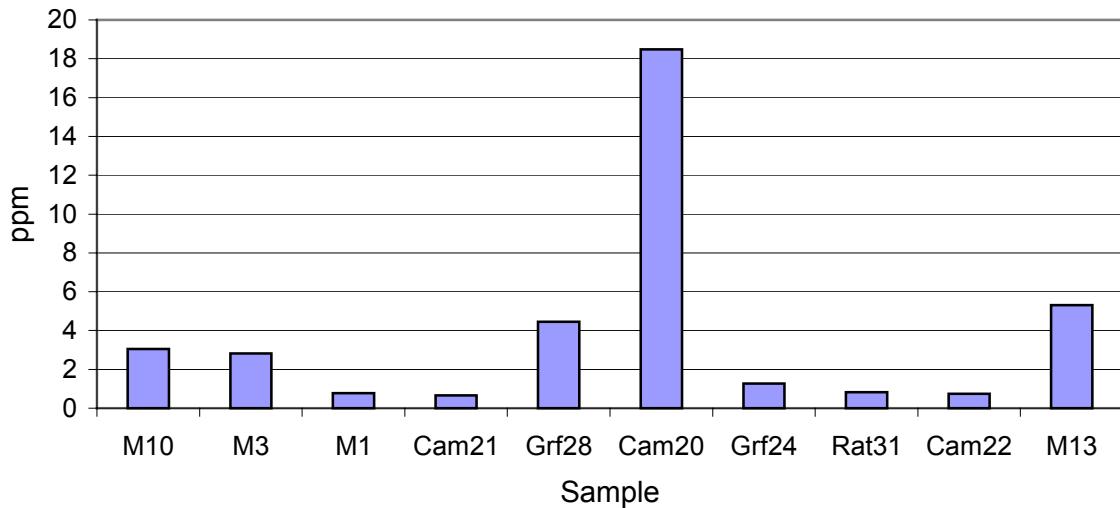


**Fig 4.17:** While most of the samples contain less than 5ppm Pt, Cam20 is outstanding with 18.5ppm Pt.

### 4.5.3 France

The central Limousin , Saint –Yreix district has the greatest number of gold mineralisations of the French hercynian basement and has been known since Gallo-Roman times (“Gallia Aurifera”). Only Le Bourniex and Laurieras are in operation now. Gold is associated with galena and sulphosalt’s which postdates pyrite and arsenopyrite, impregnations in brecciated quartz lenses are typical (Touray et al 1989). Little is known about the other deposits, which are all placer deposits, except their broad regional associations.

<b>Laurieras Limousin</b>	<b>French Massif Central</b>	<b>Br-1)</b>
Celtic mine Quartz reef, Arsenopyrite, pyrite, antimony, Galena		
<b>Iserre river, Grenoble</b>	<b>Flows from the Alps</b>	<b>(M-4)</b>
<b>Saone river</b>	<b>Flows from the Vogesen</b>	<b>(M-11)</b>
<b>Kergal -Bretagne</b>	<b>Armorican Massif</b>	<b>(Br-2)</b>
<b>Gardon Lézan -Gard</b>	<b>Flows from French Massif Central</b>	<b>(Br-5)</b>
<b>Céze, Gard (RocheGude)</b>	<b>Flows from French Massif Central</b>	<b>(Br-3)</b>

These samples can be characterised on triplots of W, Ir and Pb (Fig 4.18) and Pt, Cu and Pb (Fig 4.19). Not surprisingly Br-1 forms a very consistent group, as it is a lode gold sample. One grain shows a higher Cu concentration and this probably reflects the ablation of one of the sphalerite inclusions (containing 0.5% Cu, appendix Br-1) . Of note is the total lack of Ti compared to the others (see trace element patterns in the appendices) as the presence of Ti in ancient gold artefacts could potentially be used to distinguish between placer and hard rock sources. The higher W content of Br-3 and Br-5 is interesting as they both come from rivers flowing out of the southern end of the Massif Central. Sample M-4 contains two subgroups with almost identical trace element signatures despite a 7% difference in Ag content between them, with a third very different subgroup. Sample M-11 is very well constrained by Cu, Pb, Ir and W.

A correlation between Pt and Cu (Figure 4.20) is a common feature of all the gold samples and will be discussed further in the summary. It is interesting to show the variation in the Pt concentrations of the samples which are presented as averages in Figure 4.21 and shows that sample M-4 has by far the highest Pt concentration with an average of 42ppm Pt.

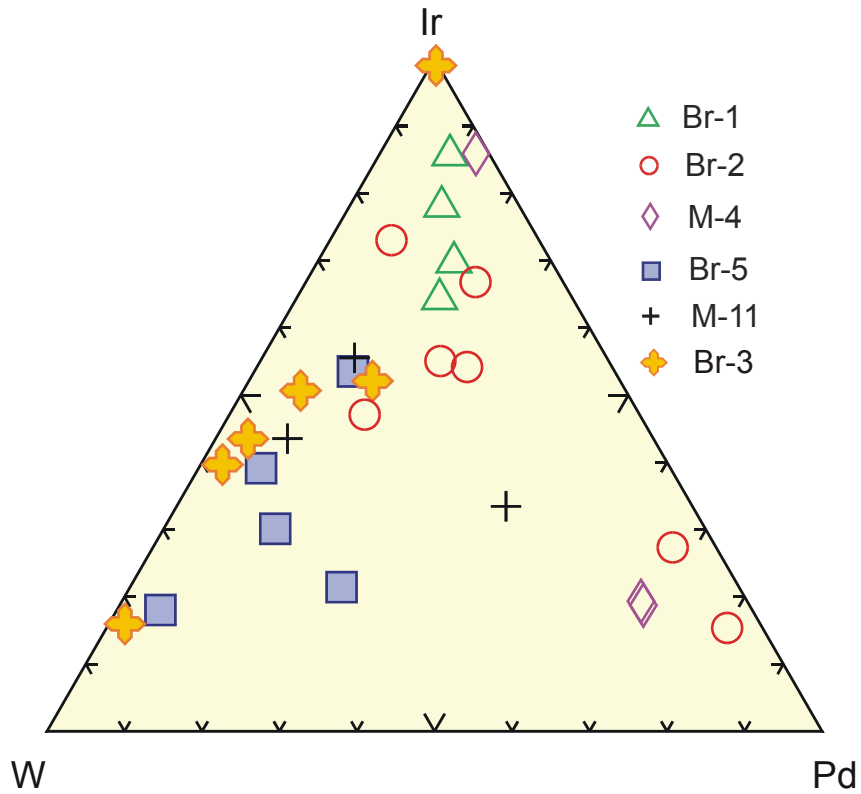


**Fig 4.18:** Tri-plot of W, Ir and Pd.

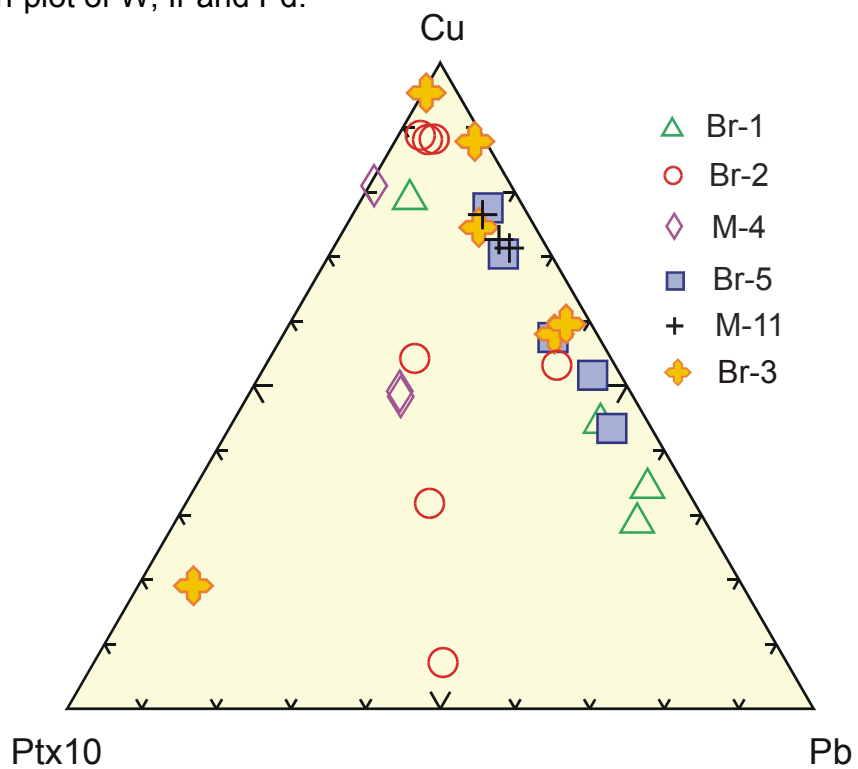


**Fig. 4.19:** Tri-plot of Pt, Cu & Pb. Some subgroups from Br-2 and M-4 show higher Pt than the others.

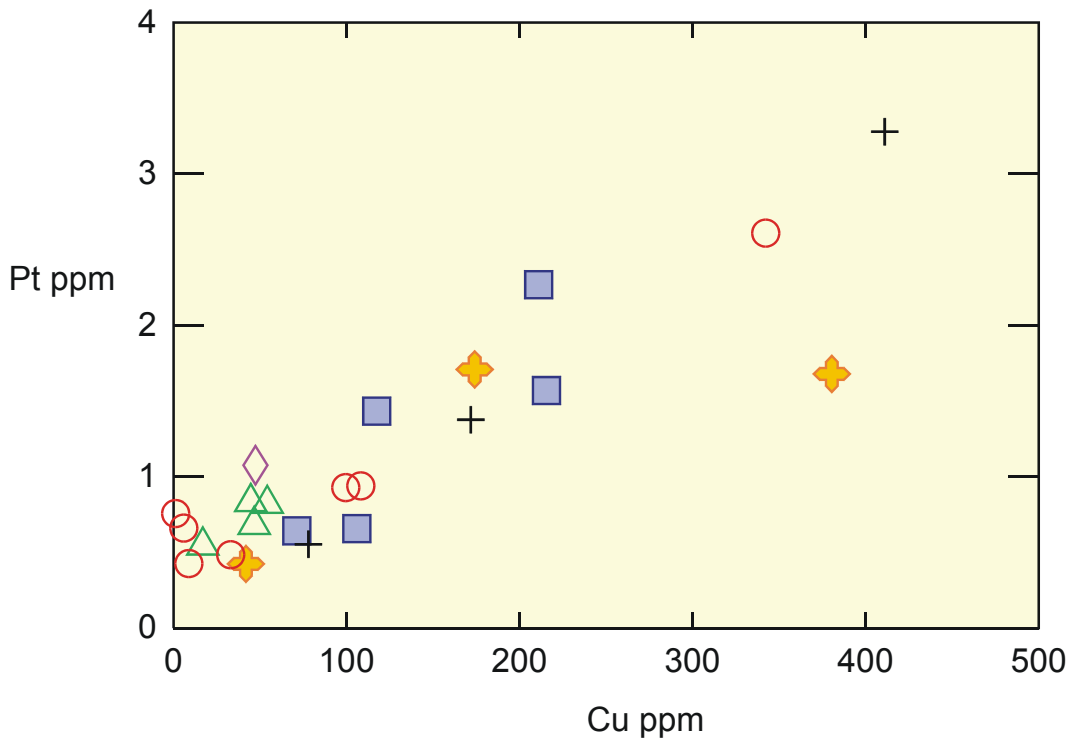


**Fig 4.20:** Pt vs. Cu shows an interesting correlation (subgroups M4.1 and M4-3 are not plotted due to their extremely high Pt/Cu content, 100/1500 and 25/400 respectively).

#### Pt Concentrations of French Deposits

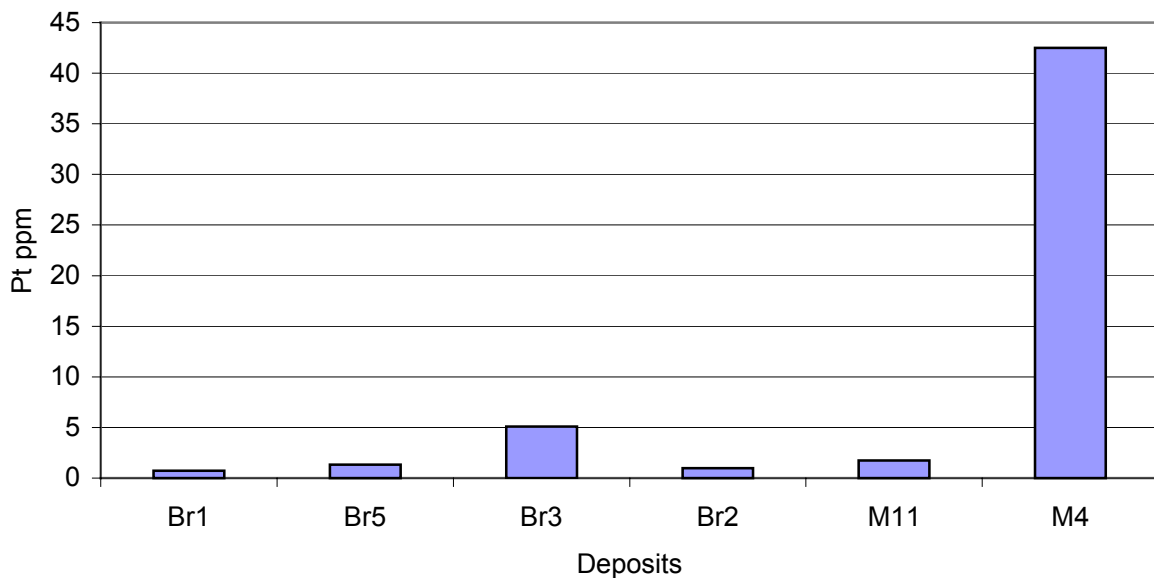


**Fig. 4.21:** The Pt concentrations for most of the deposits are under 5 ppm. Sample M-4 is highly distinctive with an average Pt concentration of 43ppm.

#### 4.5.4 Belgium

Gold has been found during alluvial prospect ion surveys and panning in the Ardenne, and in particular the areas known as the Massifs de Rocroi, de Serpont and de Stavelot (Hanssen,1979, Nonnon, 1984, Dejonghe, 2000) with an average gold fineness of 980.

<b>Ru De Poteau –Recht</b>	<b>(Br-6)</b>
<b>Schinderbach –Amel</b>	<b>(Br-7)</b>
<b>Massotais -Les Tailles (Baraque Fraiture)</b>	<b>(Br4)</b>
Reef gold from a Roman Mine dated to +/- 450BC	
<b>Vague Des Gommets ( Rau Du Moulin) –Suxy</b>	<b>(Br8)</b>

The trace element signatures of these deposits have already been discussed in section: 4.4.2, and are well characterised by Pt and Cu, Fig 4.22.

The Belgian deposits contain on average 3.5 ppm Pt with one group of grains from Br-6 containing over 15 ppm Pt.

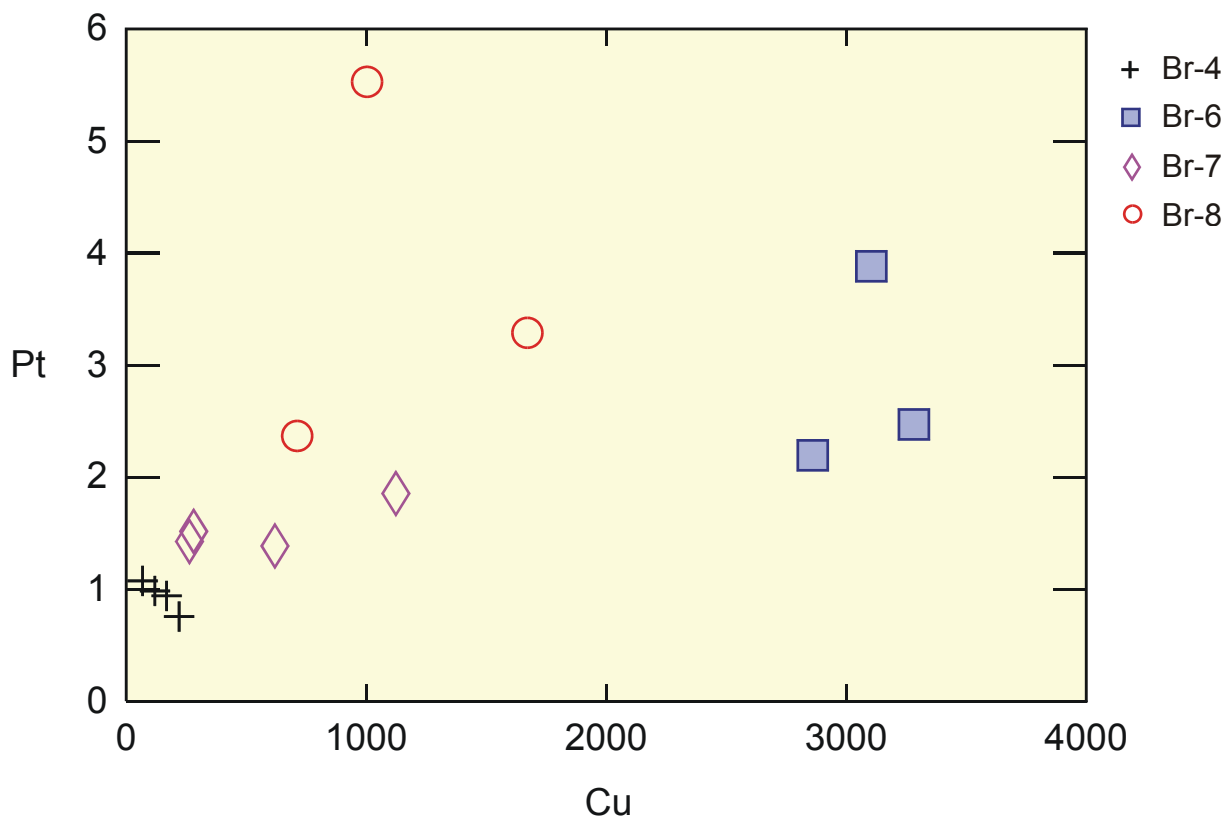


**Fig. 4.22:** Cu vs. Pt (ppm). One subgroup of Br-6 contains ~15ppm Pt and is not shown here.

#### 4.5.5 Other areas including: Scotland and Italy

Rio Elvo, Piemont, Italy (M-9)  
Ochills, Scotland (M-5)  
Kildonan Burn, Scotland (Br 9)

Of these three samples Br-9 is highly distinctive with higher W than the others (Fig 4.23). M-5 Consists of two groups, one with higher Sb and a very different total trace element pattern (appendix M-5).

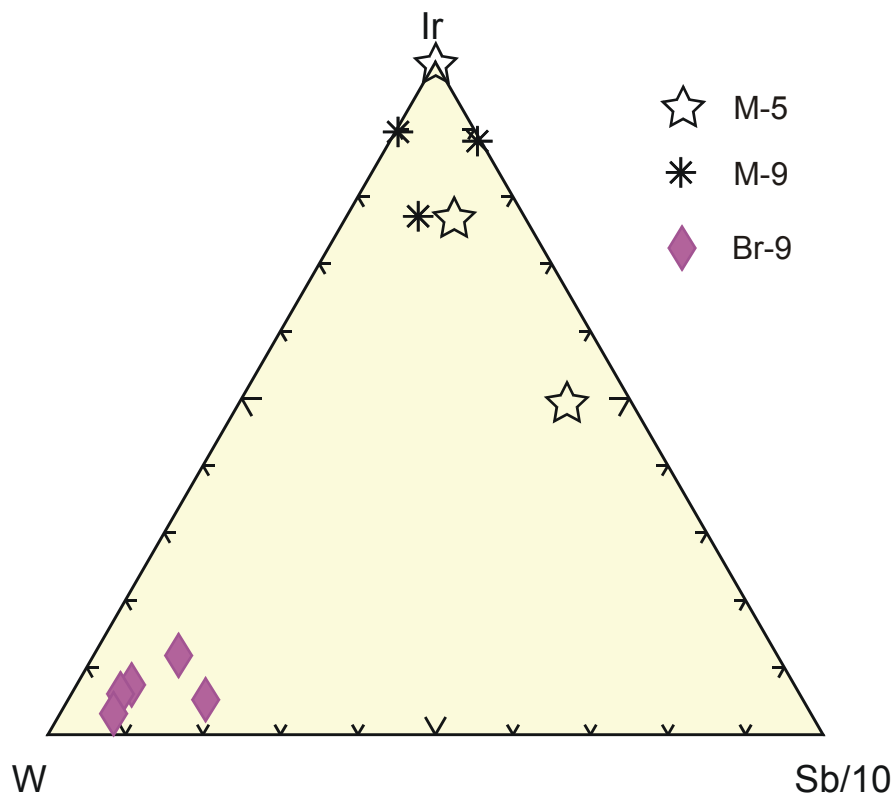


**Fig 4.23.:** The higher W content of sample Br-9 gives it a consistent and distinctive signature.

#### 4.6 Discussion

The central idea of trace element fingerprinting is based on the ability to distinguish one deposit from another. It can be seen that for hard rock samples, Br-1 and Br-4, this is not a problem. However, for samples from placer deposits this becomes more difficult as transport related alteration processes can alter the trace element signatures.

The most important observation from this study is that obvious differences in the entire suite of trace elements; where one group can be distinguished from another by the presence or absence of various trace elements, are also reflected by those elements such as the PGE's, Cu, Pb and Sb. These elements are either highly refractory or present in high enough concentrations to be relatively unaffected by

transport alteration processes. The two methods of visualising the data can therefore be used to characterise each sample and its subgroups.

With respect to the archaeological objectives of this study, the tri-plots shown above can be used to distinguish one deposit from another. Where overlap of deposits occurs two or more different plots should help to distinguish between deposits.

There are some interesting observations which obviously relate to the physical and chemical conditions which existed during precipitation of the primary sources and may also represent the predominance of particular source rocks for the metals. For instance plots of Cu vs. Pt (Fig 4.24a) show a consistent positive correlated trend, while Ag vs. Cu shows a negative trend (Fig 4.24b). It is well accepted that the Ag composition of native gold (electrum) is controlled by,  $a_{H_2S}$ ,  $p_h$ ,  $a_{Cl^-}$  and in particular the temperature of precipitation (Barton, 1980) with higher Ag contents at lower temperatures. It has also been previously observed that the Ag content of electrum in Cu-rich deposits is usually lower than in Cu-poor deposits associated with epithermal and hypo/mesothermal Au vein type mineralisation (Shikazono and Shimizu, 1988). It therefore seems likely that Pt favours conditions similar to Cu during the precipitation of Au.

Considering the plot of Ir, W and Pd (Fig 4.18) the groupings may represent different source rocks, the more mafic source rocks (with higher Ir, Pd and Pt) and more acidic (granitic) source rocks with higher W. Such considerations could be useful during gold deposit exploration as then particular rock associations could be targeted. The idea of linking placer gold grains to different types of gold deposits has already been proposed from inclusion studies (Chapman et al, 2002) which require very large suites of samples and a lot of time. Quantitative trace element studies of smaller sample sizes by laser ablation could make such efforts more routine.

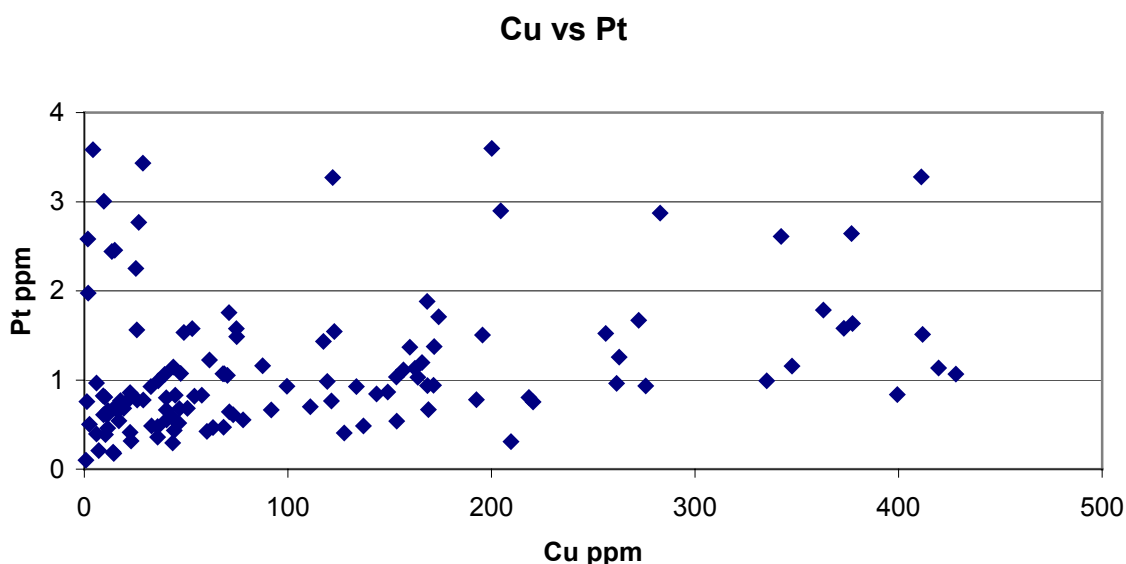


**Fig. 4.24a:** The concentrations of Cu and Pt for all the gold grains are presented here and show a positive trend between Cu and Pt.

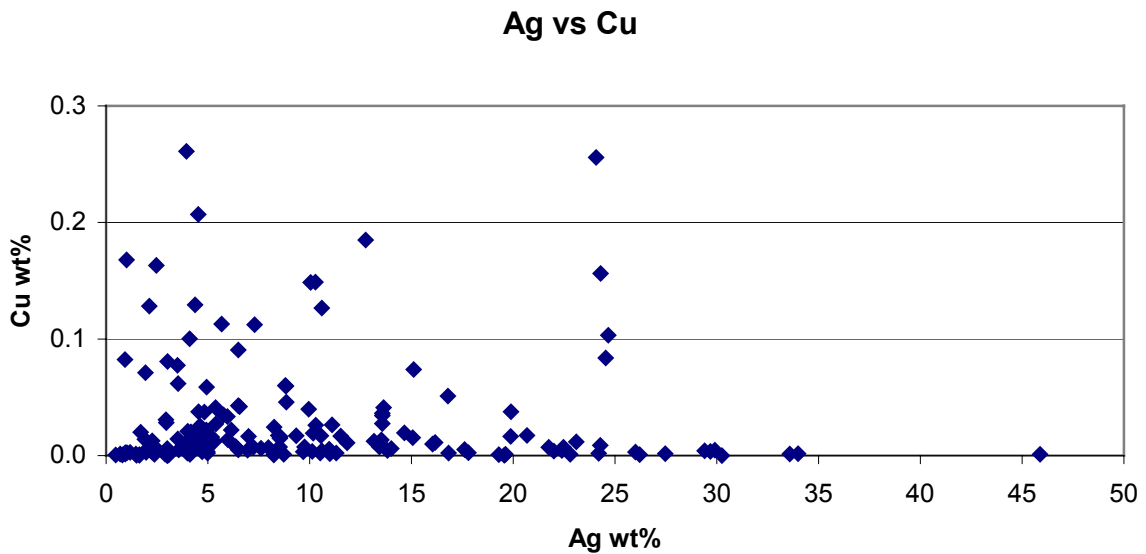


**Fig. 4.24b:** The concentrations of Ag and Cu for all the gold grains are presented here and show a negative trend between Ag and Cu.

## 4.7 Pb Isotopes

### 4.7.1 Results

A few grains from each sample were dissolved to provide lead for isotopic analysis by solution MC-ICPMS. The results are listed in Appendix 7 and shown on the following plots of Pb isotopic ratios (Figures 4.25 and 4.26) along with data from regional gold producing areas represented in the literature (Empty blue X's: Touray et al, 1989, Filled blue X's: Curti, 1987, Purple Crosses: Horner et al, 1997).

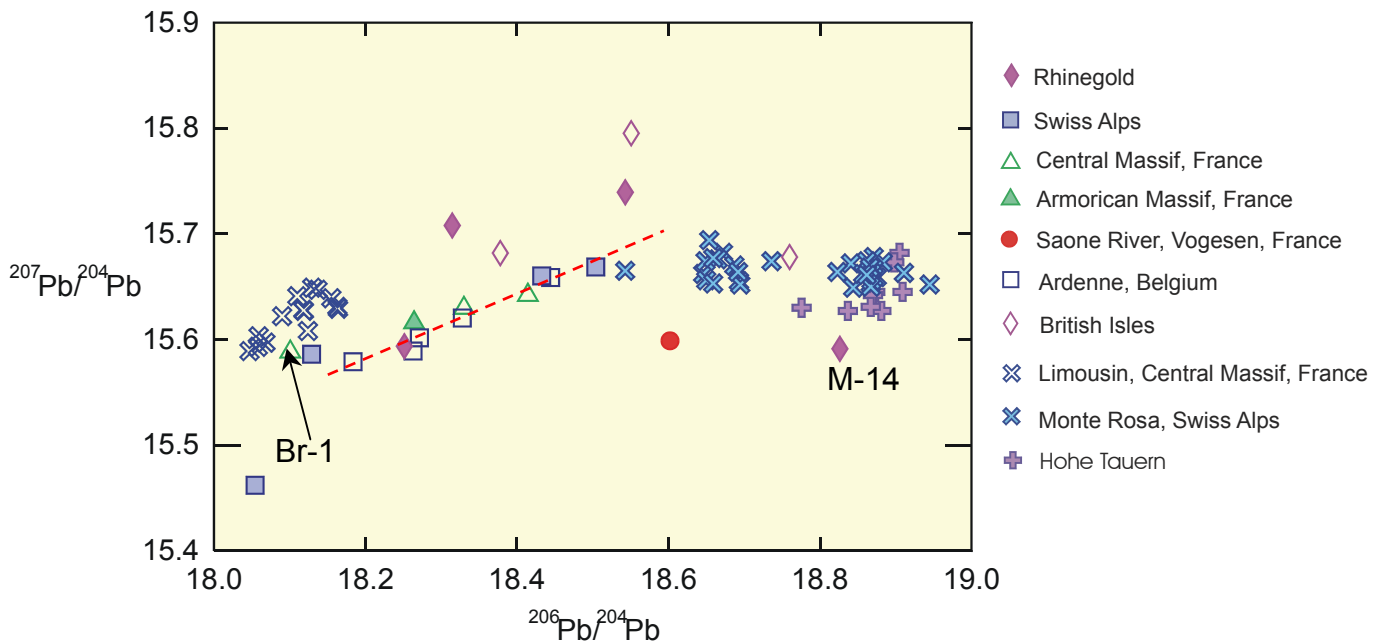


**Fig 4.25:**  $^{206}\text{Pb}/^{204}\text{Pb}$  vs.  $^{207}\text{Pb}/^{204}\text{Pb}$  ratios. The dotted red line represents the mixing line on which all the samples from the Ardenne sit. Both the filled and empty blue X's, and the purple crosses represent literature data (see above)



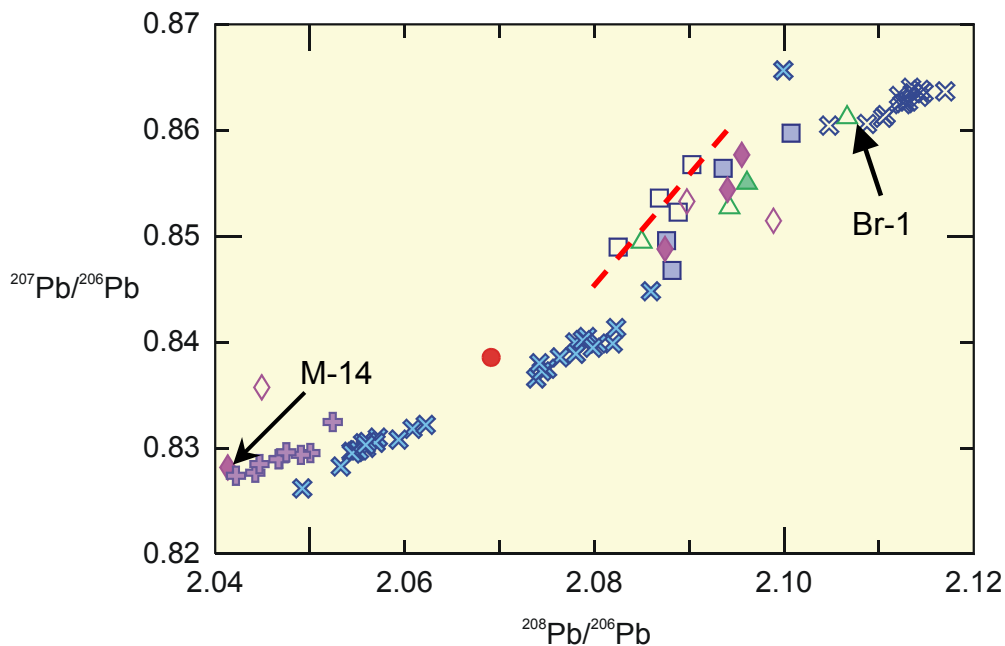


**Fig. 4.26:**  $^{207}\text{Pb}/^{206}\text{Pb}$  and  $^{208}\text{Pb}/^{206}\text{Pb}$  ratios showing the trend of the Ardenne samples and highlighting the distinct difference between M-14 (Middle Oberrhein) and the Southern Oberrhein samples.

Firstly, it is peculiar that many of the samples from the Alps, the American massif, Ardenne and the Massif Central all seem to group together despite their diverse geological contexts. Although, the result for sample Br-1 (sampled from a gold bearing quartz vein) is exactly where it should be with the cloud of data points representing analyses from gold deposits in the Limousin region. Perhaps the need to dissolve more than one gold grain to acquire sufficient Pb for analysis has somehow homogenised the Pb isotope signatures. Further work is recommended utilising the laser ablation method used for the coins on individual gold grains to see if any more diversity can be detected and also to provide a better characterisation of the gold samples and gold producing regions.

The results from the Ardenne are highlighted as they form a consistent group in both isotope ratio plots and are not represented in the literature.

The Rhine gold appears to have very diverse  $^{207}\text{Pb}/^{204}\text{Pb}$  and  $^{206}\text{Pb}/^{204}\text{Pb}$  ratios while conversely displaying fairly uniform  $^{207}\text{Pb}/^{206}\text{Pb}$ ,  $^{208}\text{Pb}/^{206}\text{Pb}$  ratios. This does not include sample M-14 (Middle Oberrhein), which is very different from the Southern Oberrhein samples in both plots.

Superimposing the gold coin data onto the plot of  $^{208}\text{Pb}/^{206}\text{Pb}$  vs.  $^{207}\text{Pb}/^{206}\text{Pb}$  (Fig. 4.27) shows that most of the gold deposits are at the wrong end of the coin mixing line which is defined by the addition of Mediterranean copper with higher  $^{207}\text{Pb}/^{206}\text{Pb}$ ,  $^{208}\text{Pb}/^{206}\text{Pb}$  ratios. The literature data from Monte Rosa in Switzerland and the analysis of M-11 (Saone river France) are closely associated with the lower end of the coin mixing line. However, considering the extreme overlap of the data acquired during this study and the many gold deposits which are unrepresented here, no conclusions can be drawn about gold sources.

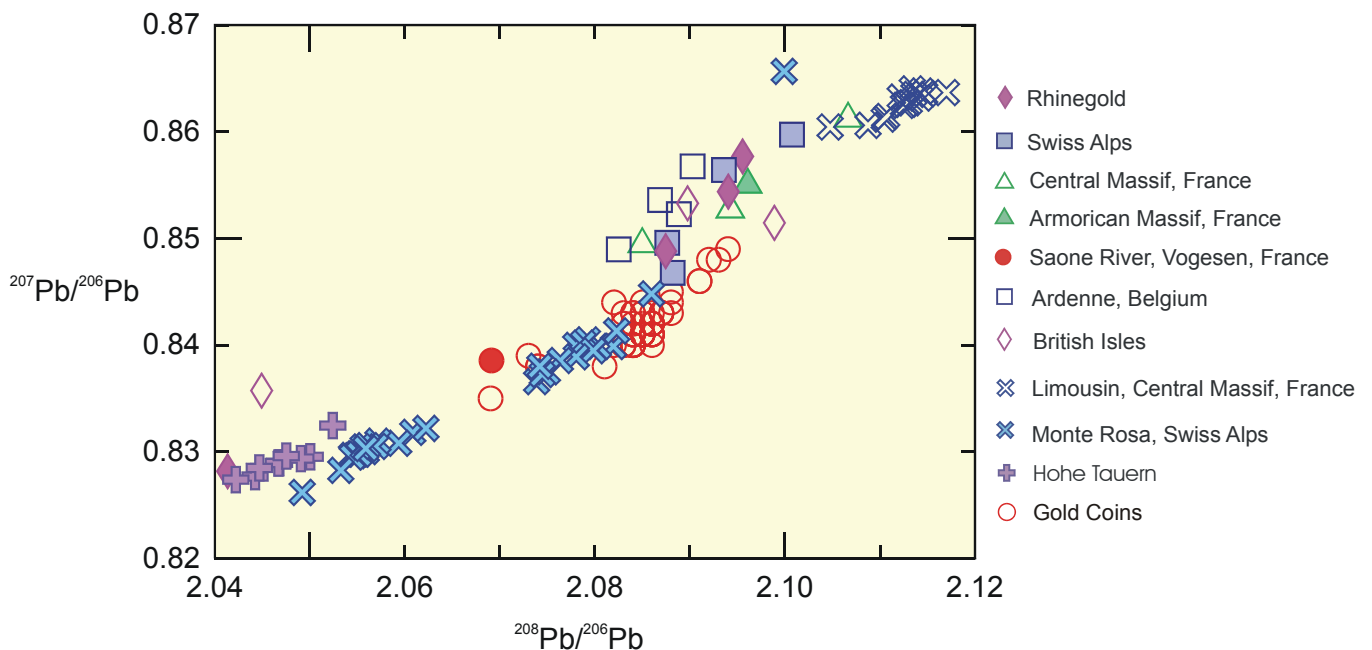


**Fig 4.27:** Pb-isotopic ratios from the gold coins have been added to the gold deposit data.

#### 4.7.2 Conclusions

The Pb isotopic analyses made by solution MC-ICPMS are not sufficient to truly characterise any particular region. The laser sampling method should now be applied to the gold samples, to make at least 10 analyses from each sample, which would allow a better characterisation of each deposit and area. It would also provide a much better idea as to the provenance of the gold in the Rhine. Especially as analyses here of M-14 (Karlsruhe) hints that contributions from the Vogesen and/or the Schwarzwald are probably responsible for its distinct Pb isotopic signature from the Southern Oberrhein samples.

The Limousin area is already well characterised from previous studies of the mineralisation there and the analysis, made during this project directly on lead derived from the gold grains, agrees with them very well. The Ardenne also seems to have a consistent Pb isotopic signature, but the other areas all require further analysis.

The concentration of lead in natural gold samples and ancient gold coins is similar (section 3.5) and suggests that the identification of gold sources should be possible using Pb isotopes. However, remelting experiments of Taylor et al (1995), have shown that up to 50% of Pb can be lost during melting due to the volatility of Pb at the melting point of gold. Therefore, the analysis of more pure gold artefacts is required for gold sources to have a chance of being positively identified.

#### 4.8 Gold; Summary and Conclusions

To be able to use the trace element and isotopic signatures of gold sources to match them to ancient artefacts, the following must be considered.

- 1) Any additions to the gold alloy will disturb most of the elements which typified the deposit, especially as some of the main ones such as Ag, Cu, Pb and Sb are the major impurities of such additions. Therefore only unalloyed artefacts should be used.
- 2) Such studies would be most effective when they are constrained to studying local production (artefacts) and a limited number of local deposits. Especially when considering placer deposits and the large overlap in geochemical signatures which can occur.
- 3) Elements of a highly refractory nature or with high concentrations have been shown to be useful in characterising gold deposits and even placer gold deposits. These include the PGE's (especially Pt), and Cu, Sb, and Pb. PGE's because they are noble and inert enough so as to remain relatively unaltered and the others as they are usually present in high enough levels that subsequent transport related alteration does not disturb their ability to constrain the grouping of the analyses of grains from placer deposits.
- 4) Particular trace element assemblages may indicate the different source rocks which provided the gold for the primary mineralisations, and may reflect the physio-chemical conditions which existed during precipitation of the gold.
- 5) Pt concentrations for most deposits are fairly uniform, with concentrations ranging from 2-5ppm Pt, A few deposits show more distinguishing Pt contents and these include: M-4 (43ppm), Cam20 (18.5) and one grain from Br-6 (15ppm). Any of these deposits could provide more than enough Pt for the Sch. 23 gold coins.
- 6) Pb isotopic ratios have an important part to play in characterising gold locations as it provides a very powerful extra tool for helping to distinguish between deposits. However, this will require more analyses of gold artefacts, which have not been extensively alloyed with Ag or Cu, and potential gold sources.

## References

Allen, D.F., 1980, *The Coins of the Ancient Celts*, Edinburgh.

Barton, M.D., 1980, The Ag-Au-S system, *Economic Geology*, 75, 303-316.

Bayley, J., Eckstein, K., 1997: 'Silver refining - production, recycling assaying'. In *Archaeological Science*, Sinclair, A., Slater E., and Gowlett J., eds., *Oxbow Monograph Series 64* 107-111.

Chapman, R., Leake, B., Styles, M., 2002, Microchemical Characterization of Alluvial Gold Grains as an Exploration Tool, *Gold Bulletin*, 35, 2, 53-65.

Charles, J.A., Slater, E.A., 1970, Archaeological classification by metal analysis, *Antiquity* 44, 207-213

Cauuet, B., 1999a, L'exploitation de l'or en Gaule à l'Age du Fer, In: *L'or dans l'Antiquité. De la mine à l'objet*, Cauuet, B. ed., *Aquitania suppl. 9* (Toulouse), 31-86.

Cauuet, B., 1999b, Keltischer Goldbergbau im Limousin (Frankreich), *Der Anschnitt*, 51, H: 2-3, s. 58-71.

Colbert de Beaulieu, J.B., 1973, *Traité de numismatique Celtique I. Méthodologie des ensembles* (Paris).

Cowell, M.R., 1998, An analytical survey of the British Celtic gold coinage, In: *Metallurgy in Numismatics*,: Oddy, A., Cowell, M., eds., *Royal Numismatic Society, Special Publication No. 30*, London.

Craddock, P.T., 1995, *Early Metal Mining and Production*, Edinburgh.

Creighton, J., 2000, *Coins and Power in Late Iron Age Britain*, Cambridge.

Cunliffe, B., 1988, *Greeks, Romans and Barbarians; Spheres of Interaction.*, B.T.Batsford Ltd, London.

Curti, E., 1987, Lead and Oxygen Isotope Evidence for the Origin of the Monte Rosa Gold Lode Deposits (Western Alps, Italy): A Comparison with Achaean Lode Deposits, *Economic Geology*, 82, 2115-2140.

Dejonghe, L., 2000, L'or des Ardennes, *Athena*, 164, 69-71.

Dunstan, L.P., Gramlich, J.W., Barnes, I.L., Purdy, W.C., 1980, *J. Res. Natl. Bur. Stand.*, 85, 1, 1-10

Gale, N.H., Stos-Gale, Z.A., 1981, Cycladic lead and silver metallurgy, *Annu. Brit. Sch. Athens*, 76, 169-224.

Gale, N.H., Stos-Gale, Z.A., Maliotis, G., Annetts, N., 1997, Lead isotope data from the Isotracer Laboratory Oxford: Archaeometry data base 4, ores from Cyprus, *Archaeometry*, 39, 1, 237-246.

Gale, N.H., Woodhead, A.P., Stos-Gale, Z.A., Walder, A., Bowen, I., 1999, Natural variations detected in the isotopic composition of copper: possible applications to archaeology and geochemistry, *Int. J. of Mass Spec.*, 184, 1-9.

Gebhard, R., Lehrberger, G., Morteani, G., Raub, Ch., Steffgen, U., Wagner, U., 1999, Production techniques of Celtic gold coins in Central Europe, In: *L'or dans l'Antiquité. De la mine à l'objet*, Cauuet, B. ed, Aquitania suppl. 9 (Toulouse), 217-233.

Gondonneau, A., Guerra, M.F., Barrandon, J.-N., 1996, Sur Les Traces De L'or Monnayé : Recherche De Provenances Par LA-ICP-MS, *Rev. d'Archéométrie*, 20, 23-32.

Gratuze, B., Giovagnoli, A., Barrandon, J.N., Telouk, Ph. et Imbert, J.L., 1993, Apport de la méthode ICP-MS coulée à l'ablation laser pour la caractérisation des archéomatériaux, *Rev. d'Archéométrie*, 17, 89-104.

Gratuze, B., Barrandon, J.-N., 1999, Apports des analyses dans l'étude de creusets liés à la métallurgie de l'or: étude d'un creuset et de quatre fragments de creusets provenant du site de Cros Gallet (Le Chalard, Haute-Vienne), In: *L'or dans l'Antiquité. De la mine à l'objet*, Cauuet, B. ed, Aquitania suppl. 9 (Toulouse), 205-212.

Grigorova, B., Anderson, S., de Bruyn, J., Smith, W., Stülpner, K., Barzev, A., 1998a, The AARL gold fingerprinting technology, *Gold Bulletin*, 31, 1, 26-29.

Grigorova, B., Smith, W., Stülpner, K., Tumilty, J.A., Miller, D., 1998b, Fingerprinting of gold artefacts from Mapungabwe, Bosutswe and Thulamela, *Gold Bulletin*, 31, 3, 99-102.

Groen, J.C., Craig, J.R., Rimstidt, D., 1990, Gold-rich rim formation on electrum grains in placers, *Canadian Mineralogist*, 28, 207-227.

Guerra, M.F., Sarthre, C.-O., Gondonneau, A., Barrandon, J.-N., 1999, Precious Metals and Provenance Enquiries using LA-ICP-MS, *J. of Arch. Sci.*, 26, 1101-1110.

Hanssen, E., Viaene, W., 1979, Données mineralogiques sur les paillettes d'or de la Bordure S. et S.E. du Massif de Stavelot, *Bulletin de la Société Belge de Géologie*, 38, 225-235.

Hartmann, A., 1976, Ergebnisse spektralanalytischer Untersuchungen an keltischen Goldmünzen aus Hessen und Süddeutschland, *Germania*, 54, 102-134.

Haselgrove, C., 1999, The development of Iron Age coinage in Belgic Gaul, *Numismatic Chronicle*, 159, 111-168.

Haselgrove, C., 1984, Warfare and its aftermath as reflected in the precious metal coinage of Belgic Gaul, *Oxford J. Archaeol.* 3, 81-105.

Heinrichs, J., (in print): Ubische Quinare im Lippegebiet. Ein Modell, In: Die Kelten und Rom. Neue numismatische Forschungen. Metzler, J. and Wigg, D.G eds.

Horn, I., Günther, D., 2002, The influence of ablation carrier gasses Ar, He and Ne on the particle size distribution and transport efficiencies of laser ablation-induced aerosols: implications for LA-ICP-MS, *App. Surface Sci.*, 207, 144-157.

Horner, J., Neubauer, F., Paar, W.H., Hansmann, W., Koeppel, V., Robl, K., 1997, Structure, mineralogy, and Pb isotopic composition of the As-Au-Ag deposit Rotgülden, Eastern Alps (Austria): significance for formation of epigenetic ore deposits within metamorphic domes, *Mineralium Deposita*, 32, 555-586.

Jackson, S.E., Günther, D., 2003, The nature and sources of laser induced isotopic fractionation in laser ablation-multicollector-inductively coupled plasma-mass spectrometry, *J.Anal. At. Spectrm.*, 18, 205-212

Jackson, S.E., Graham, S., Günther, D., 2003, In-situ Determination of High Precision Isotope Ratios by Laser Ablation-Multicollector-Inductively Coupled Plasma Mass Spectrometry (LA-MC-ICP-MS): Application to Cu and Fe Isotopes in Ore Minerals, In: 5<sup>th</sup> International Symposium on Applied Isotope Geochemistry, Heron Island, Queensland, Australia, Batts, B.D., Batts, J.E., eds., 101-103.

Jaffé, F.C., 1989, Gold in Switzerland, *Economic Geology*, 84, 1444-1451.

Jeffries, T.E., Jackson, S.E., Longriech, H.P., 1998: Application of a frequency quintupled Nd-YAG source ( $\lambda = 213 \text{ nm}$ ) for laser ablation inductively coupled plasma mass spectrometric analysis of minerals, *Journal of Analytical Atomic Spectrometry*, 13, 935-940.

Kirchheimer, F., 1965, Über das Rheingold, *Jh. geol. Landesamt Baden-Württemberg*, 7, 55-85

Kogan, V.V., Hinds, M.W., et Ra-Mendik, G.I., 1994, The direct determination of trace metals in gold and silver materials by laser ablation inductively coupled plasma mass spectrometry without matrix matched standards, *Spectrochimica Acta*, 49B, 4, 333-343

Klein, S., Lahaye, Y., Brey, G., von Kaenel, H.-M., (In Press), Blei- und kupferisotopenanalysen an kupfermünzen der römischen kaiserzeit., *Archaeometry*.

Knight, J.B., Morison, S.R., Mortensen, J.K., 1999, The Relationship between Placer Gold Particle Shape, Rimming, and Distance of Fluvial Transport as Exemplified by Gold from the Klondike District, Yukon Territory, Canada, *economic Geology*, 94, 5, 635-648.

Kogan, V.V., Hinds, M.W., Ra-Mendik, G.I., 1994, The direct determination of trace metals in gold and silver materials by laser ablation inductively coupled plasma mass spectrometry without matrix matched standards, *Spectrochimica Acta*, 49B, 4, 333-343

Large, D., Schaeffer, R., Höhndorf, A., 1983, Lead Isotope Data from Selected Galena Occurrences in the North Eifel and North Sauerland, Germany, *Mineral. Deposita*, 18, 235-243

Lehrberger, G., 1995, The gold deposits of Europe: an overview of the possible metal sources for prehistoric gold objects, In: *Prehistoric Gold in Europe*, Morteani, J. and Northover, J.P. eds, 115-144.

Lehrberger, G., Raub, Ch., 1995, A look into the interior of Celtic gold coins, In *Prehistoric Gold in Europe*, Morteani, G. and Northover, J.P., eds, 115-144.

Longreich, H.P., Fryer, B.J., Strong, D.F., 1987, Determination of lead isotope ratios by inductively coupled plasma-mass spectrometry (ICP-MS), *Spectrochimica Acta*, 42B, 1, 39-48

Loscheider, R., 1998: Untersuchungen zum Spätlatènezeitlichen Münzwesen des Trevererlandes, *Archaeologia Mosellana* 3 (Luxembourg), 69-225.

Maréchal, C.N., Télouk, P., Albarède, F., 1999, Precise analysis of copper and zinc isotopic compositions by plasma-source mass spectrometry, *Chemical Geology*, 156, 251-273.

Maréchal, C.N., Albarède, F., 2002, Ion-exchange fractionation of copper and zinc isotopes, *Geochim. et Cosmochim. Acta*, 66, 9, 1499-1509.

Mckerrell, H., Tylecote, R.F., 1972, The working of copper-arsenic alloys in the Early Bronze Age and the effect on the determination of provenance, *Proceedings of the Prehistoric Society*, 38, 209-218

Metzler, J., 1995, *Das treverische Oppidum auf dem Titelberg, Luxembourg.*

Nash, D., 1981, Coinage and state development in central Gaul, in *Coinage and Society in Britain and Gaul: Some Current Problems*, B. Cunliffe ed. Council For British Arch, No 38, 10-17.

Nash, D., 1987, *Coinage in the Celtic World*, London.

Nieto, S., Barrandon, J.-N., 2002, Le monnayage en or arverne: essai de chronologie relative à partir des données typologiques et analytiques, *Revue Numismatique*, 37-91.

Nonnon, M., 1984, Découverte de monazite grise et nodules d'or alluvionnaire dans le Massif de la Croix-Scaille, *Bulletin de la Société Belge de Géologie*, 93, 307-314.

Northover, J.P., 1992, Materials issues in the Celtic coinage, In: *Celtic Coinage: Britain and Beyond – The Eleventh Oxford Symposium on Coinage and Monetary History*, Mays, M., ed, 235-299.

Outridge, P.M., Doherty, W., Gregoire, D.C., 1998, Determination of trace elemental signatures in placer gold by laser ablation-inductively coupled plasma-mass spectrometry as a potential aid for gold exploration, *Journal of Geochemical Exploration*, 60, 229-240.

Pernicka, E., Bachmann, H.-G., 1983, Silbergewinnung in Laurion (III), *Erzmetall*, 36, 12, 592-597.

Pernicka, E., Begemann, F., Schmitt-Strecker, S., Grimanis, A.P., 1990, On the composition and provenance of metal artefacts from Poliochni on Lemnos, *Oxford Journal of Archaeology*, 9, 3, 263-98.

Pernicka, E., Begemann, F., Schmitt-Strecker, S., Todorova, H., Kuleff, I., 1997, Prehistoric copper in Bulgaria, *Zeitschrift für Archäologie Eurasiens*, 3, 41-180.

Pickhardt, C., Becker, J.S., Dietze, H.-J., 2000, A new strategy of solution calibration in laser ablation inductively coupled plasma mass spectrometry for multielement trace analysis of geological samples, *Fresenius J Anal Chem*, 368, 173-181.

Ramdohr, P., 1965, Rheingold als Seifenmineral, *Jh. geol. Landesamt Baden-Württemberg*, 7, 878-95.

Rohl, B.M., 1996, Lead isotope data from the Isotrace Laboratory, Oxford: *Archaeometry data base 2, galena from Britain and Ireland*, 38, 1, 165-180.

Russell, W.A., Papanastassiou, D.A., Tombrello, T.A., 1978, Ca isotope fractionation on the Earth and other solar system materials, *Geochimica et Cosmochimica Acta*, 42, 1075-1090.

Scheers, S., 1977, *Traité de numismatique Celtique II. La Gaule Belgique* (Paris).

Schulze-Forster, J., (in print): Der Dünsberg und die jüngsten keltischen Münzen in Hessen, In: *Die Kelten und Rom. Neue numismatische Forschungen*, Metzler, J. and Wigg, D.G. eds.

Scott, D.A., 1991, *Metallography and Microstructure of Ancient and Historic Metals*, The J. Paul Getty Trust, Los Angeles.

Shikazono, N., Shimizu, M., 1988, *Electrum: Chemical Composition, Mode of Occurrence, and Depositional Environment*, The Uni. Museum-The Uni. Of Tokyo Bulletin, 32, Tokyo.

Störk, W., 2000, *Das Rheingold – zwischen Mystik und Wissenschaft*, Sonderdruck aus *Markgräflerland* Band II, 65-111.

Stos-Gale Z.A., Gale, N.H., 1992, New light on the provenience of the copper oxide ingots found on Sardinia in the Mediterranean: In: *A Footprint in the Sea*, Tykot, R.H., & Andrews, T.K., eds., Sheffield Academic Press, Sheffield, 317-345.

Stos-Gale, Z.A., Gale, N.H., 1995, Lead isotope data from the Isotrace Laboratory, Oxford: *Archaeometry data base 1, ores from the western Mediterranean*, *Archaeometry*, 37, 2, 407-417.



Stos-Gale, Z.A., Gale, N.H., Annetts, N., 1996, Lead isotope data from the Isotrace Laboratory Oxford: Archaeometry data base 3, ores from the Aegean, part 1, 38, 2, 381-390.

Stos-Gale, Z.A., Gale, N.H., Maliotis, G., Annetts, N., 1997, Lead isotope characteristics of the Cyprus copper ore deposits applied to provenance studies of copper oxide ingots, *Archaeometry*, 39,1, 83-123.

Stos-Gale, Z.A., Gale, N.H., Annetts, N., Todorov, T., Lilov, P., Raduncheva, A., Panayotov, I., 1998, Lead isotope data from the Isotrace Laboratory, Oxford: Archaeometry data base 5, ores from Bulgaria., *Archaeometry*, 40, 1, 217-226.

Taylor, J.J., Watling, R.J., Shell, C.A., Ixer, R.A., Chapman, R.J., Warner, R.B., Cahill, M., 1995, From Gold Ores to Artefacts in the British Isles: a Preliminary Study of a new LA-ICP-MS Analytical Approach, In: *Archaeological Science*, Sinclair, A., Slater E., and Gowlett J., eds., *Oxbow Monograph Series 64* 107-111.

Touray, J-C., Marcoux, E., Hubert, P., Proust, D., 1989, Hydrothermal processes and Ore-forming Fluids in the Le Bourneix Gold Deposit, Central France., *Economic Geology*, 84., 1328-1339.

Tylecote, R.F., Ghaznavi, H.A., Boydell, P.J., 1977, Partitioning of trace elements between the ores, fluxes, slags and Metal during the smelting of copper, *J. of Arch Sci.*, 4, 305-333

Wagner, T., Schneider, J., 2002, Lead isotope systematics of vein-type antimony mineralization, Rheinisches Schiefergebirge, Germany: a case history of complex reaction and remobilisation processes, *Mineralium Deposita*, 37, 185-197.

Walder, A.J., Furuta, N., 1993, High-Precision Lead Isotope Ratio Measurement by Inductively Coupled Plasma Multiple Collector Mass Spectrometry, *Analytical Sciences*, 9, 675-680

Watling, R.J., Herbert, H.K., Delev, D., Abell, I.D., 1994, Gold fingerprinting by laser ablation inductively coupled mass spectrometry, *Spectrochimica Acta*, 49B, 205-291.

Wickens, J.M., 1996, The Production of Ancient Coins, Webpage: <http://www.lawrence.edu/dept/art/buerger/essays/production.html>, Lawrence Uni., Appleton, Wisconsin.

Wigg, D.G., Riederer, J., 1998, Die Chronologie der keltischen Münzprägung am Mittelrhein, In: *Stephanos numismatikos. Edith Schönert-Geiss zum 65. Geburtstag*, Peter, U., ed., Berlin, 661-674.

Wigg, D.G., 2000, The Martberg on the Lower Mosel and the development of the coin-using economy in North Gaul in the late Latène and early Roman period, In: *XII. Internationaler Numismatischer Kongress Berlin 1997. Akten – Proceedings – Actes*, Kluge, B. and Weisser, B., eds., Berlin, 447-452.

Youngson, J.H., Craw, D., 1999, Variation in Placer Style, Gold Morphology, and Gold Particle Behaviour Down Gravel Bed-Load Rivers: An Example from the Shotover/Arrow-Kawarau-Clutha River System, Otago, New Zealand., *Economic Geology*, 94, 615-634.

Zhu, X.K., O'Nions, R.K., Guo, Y., Belshaw, N.S., Rickard, D., 2000, Determination of natural Cu-isotope variation by plasma-source mass spectrometry: implications for use as geochemical tracers, *Chemical Geology*, 163, 139-149.

## **Appendices**

The main function of these appendices is to provide a database of all the samples that were studied, to be used for future investigations of Celtic gold coinages and European gold deposits.

### **Appendix 1: Coin Catalogue**

Photos of each gold coin are provided together with their classification and the collection where they are kept. The coins were provided by the following institutions and individuals;

Dr. David Wigg-Wolf  
Fundmünzen der Antike  
Johann Wolfgang Goethe-Universität  
(Includes the coins excavated from the Martberg, Sanctuary site)

Gino Languini  
Wallendorf

Johan van Heesch  
Cabinet des Medailles, Biblioteque Royale  
Brussels, Belgium

Dr. K.-J. Gilles  
Rheinisches Landesmuseum  
Trier

Francois Reinert, M.A.  
Musée National d'Histoire et d'Art  
Luxemburg

S. Berger  
Historisches Museum, Frankfurt

### **Appendix 2: Gold Samples**

Each gold sample studied is described. Photos of the gold grains allow the morphological characteristics of the samples to be easily observed and are accompanied by EPMA photos of rimming and inclusions which are typical of each

sample. A histogram of the Ag compositions of the gold grains gives an indication of the number of subgroups which maybe present. Finally the trace element results of each grain have been grouped depending on their Ag compositions, averaged together and plotted on a bar graph of Element Vs Log ppm to show the trace element characteristics of the subgroups present in each sample. The gold samples were provided by;

Werner Störk  
AG Minifossi

Bruno van Eerdenbrugh  
Belgium

Dr. Beda Hofmann  
Naturisches Museum Bern  
Switzerland

### **Appendix 3: Averaged EPMA results of the coin alloy measurements.**

Each coin was analysed ten times and averaged according to the method described in section 2.3. Includes 1 sigma standard deviation.

### **Appendix 4: EPMA results of gold samples**

Most of the grains from each sample were analysed twice and the results averaged together. The results in green represent inclusions, mostly sulphides.

### **Appendix 5: Trace element data; gold coins**

Provided by the LA-ICPMS analysis.

### **Appendix 6: Trace element data; gold samples**

Provided by the LA-ICPMS analysis.

### **Appendix 7: Pb isotope data**

Acquired by solution and Laser Ablation MC-ICPMS, for the gold, silver and copper coins and the gold samples.

### **Appendix 8: Cu isotope data**

Acquired by solution and Laser Ablation MC-ICPMS, for the gold, silver and copper coins and the gold samples.

# Chris Bendall

## Personal Details

**Date of Birth:** 12<sup>th</sup> of December 1973

**Nationality:** Australian – English

**Address:** Am Tiergarten 48, 60316, Frankfurt am Main

**Ph:** (069) 9494 3838 (Home), 798 22547 (Work)

**E-mail:** [Bendall@em.uni-frankfurt.de](mailto:Bendall@em.uni-frankfurt.de)

## Education

### 1996 Bachelor of Science – Honours Degree

Metalliferous and Economic Geology – Class 2A  
James Cook University of North Queensland, Australia

### 1992- Bachelor of Science Degree

1995 Geology and Archaeology  
James Cook University of North Queensland, Australia

### 1990- Senior Certificate – Good

1991 Pimilico State High School, Queensland, Australia

## Work Experience

### 2001- Position: Wissenschaftlicher Mitarbeiter BAT2II half

2003 **Employer:** Institut für Mineralogie, Uni-Frankfurt  
**Responsibilities:** Metallogenic research of Archaeological artefacts,

### 2000- Position: Stipendiat

2001 **Employer:** Graduiertenkolleg Archäologische Analytik, Uni-Frankfurt  
**Responsibilities:** Metallogenic research of Archaeological artefacts,

### 1998- Position: English Teacher in Prague

2000 **Employer:** LinguaErb  
**Responsibilities:** Teaching General and Business English to all levels of students

### 1997 Position: Exploration Field Geologist in Vanuatu

**Employer:** Terrasearch Pty Ltd  
**Responsibilities:** Day to day management of field operations

## Scientific References

Bendall, C., 1996 'Comparative study of an Ancient VHMS Deposit and a Modern Seafloor Sulphide Deposit.', Hons. Thesis. James Cook University.

Identification No.	Classification	Collection
Robiano	Sch. 23	Cabinet des Medailles, Brussels
NB:		



Identification No.	Classification	Collection
Fö 116	Sch. 23	Historisches Museum, Frankfurt
NB:		



Identification No.	Classification	Collection
Fö 117	Sch. 23	Historisches Museum, Frankfurt
NB:		



Identification No.	Classification	Collection
Stw4	Sch. 18	Rheinisches Landesmuseum, Trier
NB:		



Identification No.	Classification	Collection
2950	Sch. 18	Rheinisches Landesmuseum, Trier
NB:		



Identification No.	Classification	Collection
3321	Sch. 18	Rheinisches Landesmuseum, Trier
NB:		



Identification No.	Classification	Collection
FUG121	Sch. 18	Cabinet des Medailles, Brussels
NB:		



Identification No.	Classification	Collection
FU G122	Sch. 18	Cabinet des Medailles, Brussels
NB:		



Identification No.	Classification	Collection
Fö 105	Sch. 18	Historisches Museum, Frankfurt
NB:		





Identification No.	Classification	Collection
87150	Sch. 18	Rheinisches Landesmuseum, Trier
NB: This coin contains less than 1% Au with 67% Ag and 31% Cu		



Identification No.	Classification	Collection
9800	Sch. 16	Rheinisches Landesmuseum, Trier
NB:		



Identification No.	Classification	Collection
Stw4a	Sch. 16	Rheinisches Landesmuseum, Trier
NB:		



Identification No.	Classification	Collection
FUG 93	Sch. 16	Cabinet des Medailles, Brussels
NB:		



Identification No.	Classification	Collection
FUG 77	Sch. 16	Cabinet des Medailles, Brussels
NB:		



Identification No.	Classification	Collection
Fö 124	Rainbow cup	Historisches Museum, Frankfurt
NB: Northern Rainbow Cup, Hessen		



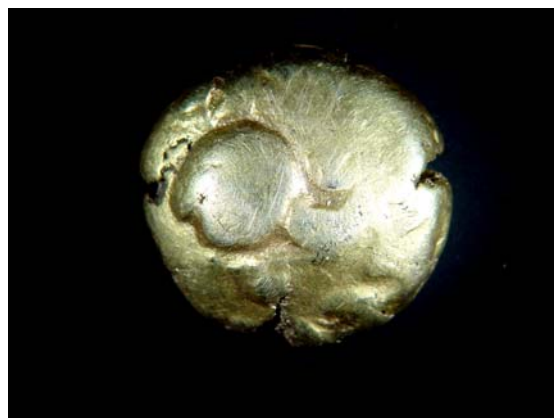
Identification No.	Classification	Collection
6124	Rainbow Cup	Rheinisches Landesmuseum, Trier
NB: Southern Rainbow Cup, Bavarian IIc		



Identification No.	Classification	Collection
8543	Rainbow Cup	Rheinisches Landesmuseum, Trier
NB: Southern Rainbow Cup, Bavarian IIe		



Identification No.	Classification	Collection
SFLAN1045	Rainbow Cup	Languini- Wallendorf
NB: Southern Rainbow Cup, Bavarian IIIa		



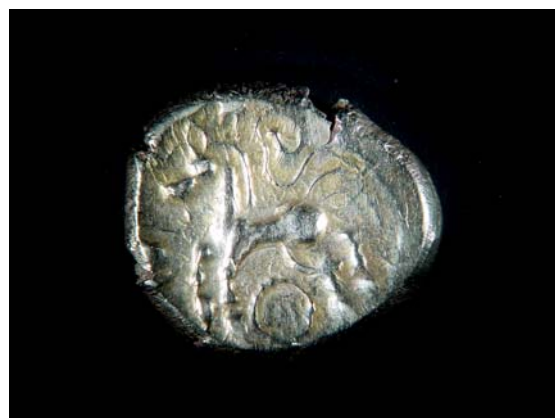
Identification No.	Classification	Collection
Regen	Rainbow Cup	Marburg
NB: Northern Rainbow Cup, Hessen		



Identification No.	Classification	Collection
SFLAN507	Sch. 30/I	Languini- Wallendorf
NB:		



Identification No.	Classification	Collection
Lt8799	Sch. 30/I	Cabinet des Medailles, Brussels
NB:		



Identification No.	Classification	Collection
Lux 7	Sch. 30/I	Musée Nat. d'Hist. et d'Art, Lux
NB:		



Identification No.	Classification	Collection
22011	Sch. 30/I	FdA Uni-Frankfurt
NB:		



Identification No.	Classification	Collection
22807	Sch. 30/IV	FdA Uni-Frankfurt
NB:		



Identification No.	Classification	Collection
30IV575	Sch. 30/IV	Cabinet des Medailles, Brussels
NB:		



Identification No.	Classification	Collection
30IV582	Sch. 30/IV	Cabinet des Medailles, Brussels
NB:		



Identification No.	Classification	Collection
30IV586 c. Bamps	Sch. 30/IV	Cabinet des Medailles, Brussels
NB:		



Identification No.	Classification	Collection
30IVG176	Sch. 30/IV	Cabinet des Medailles, Brussels
NB:		



Identification No.	Classification	Collection
30IV329	Sch. 30/IV	Languini- Wallendorf
NB:		



Identification No.	Classification	Collection
87149	Sch. 30/IV	Rheinisches Landesmuseum, Trier
NB:		



Identification No.	Classification	Collection
32243	Sch. 30/IV	FdA Uni-Frankfurt
NB: Very silver rich coin.		



Identification No.	Classification	Collection
31433	Sch. 30/IV	FdA Uni-Frankfurt
NB: Gold plated copper core, very low Cu content of plating, broken edges		



Identification No.	Classification	Collection
22007	Sch. 30/Va	FdA Uni-Frankfurt
NB:		





Identification No.	Classification	Collection
Lux 5	Sch. 30/Vc	Musée Nat. d'Hist. et d'Art, Lux
NB:		



Identification No.	Classification	Collection
30V542	Sch. 30/Va	Cabinet des Medailles, Brussels
NB:		



Identification No.	Classification	Collection
30V549	Sch. 30/Vc	Cabinet des Medailles, Brussels
NB:		



Identification No.	Classification	Collection
Lux 2	Sch. 30/Vc	Musée Nat. d'Hist. et d'Art, Lux
NB:		



Identification No.	Classification	Collection
Lux 3	Sch. 30/Vb	Musée Nat. d'Hist. et d'Art, Lux
NB:		



Identification No.	Classification	Collection
Lux 4	Sch. 30/Vb	Musée Nat. d'Hist. et d'Art, Lux
NB:		



Identification No.	Classification	Collection
6179	Sch. 30/Vb	Rheinisches Landesmuseum, Trier
NB:		



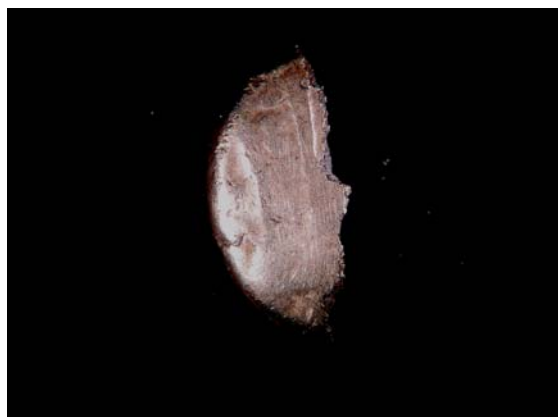
Identification No.	Classification	Collection
8544	Sch. 30/Vd	Rheinisches Landesmuseum, Trier
NB: Plated		



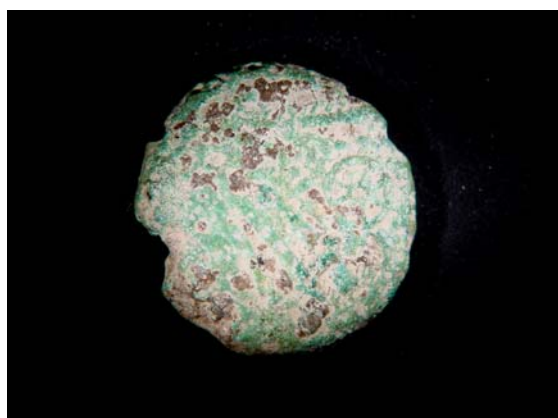
Identification No.	Classification	Collection
12325	Sch. 30/Vc	Rheinisches Landesmuseum, Trier
NB:		



Identification No.	Classification	Collection
20409	Sch. 30/Vc	FdA Uni-Frankfurt
NB:		



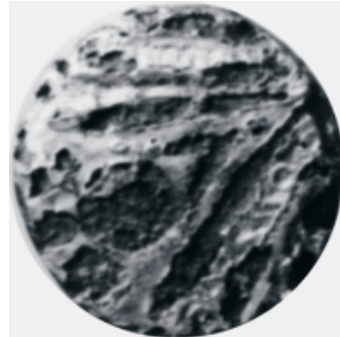
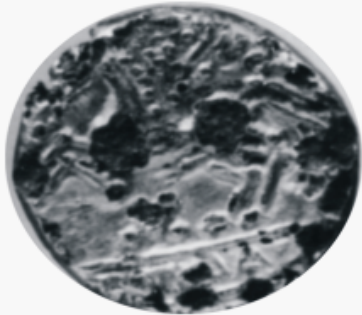
Identification No.	Classification	Collection
21932	Sch. 30/Vd	FdA Uni-Frankfurt
NB:		



Identification No.	Classification	Collection
22006	Sch. 30/Vc	FdA Uni-Frankfurt
NB:		



Identification No.	Classification	Collection
19698	Sch. 30/Vd	FdA Uni-Frankfurt
NB: Gold plated copper core		



Identification No.	Classification	Collection
22009	Sch. 30/Vb	FdA Uni-Frankfurt
NB:		



Identification No.	Classification	Collection
21931	Sch. 30/Vd	FdA Uni-Frankfurt
NB:		



Identification No.	Classification	Collection
22010	Sch. 30/Vc	FdA Uni-Frankfurt
NB:		



Identification No.	Classification	Collection
22113	Sch. 30/Vc	FdA Uni-Frankfurt
NB:		



Identification No.	Classification	Collection
26827	Sch. 30/Vc	FdA Uni-Frankfurt
NB:		



Identification No.	Classification	Collection
28323	Sch. 30/Va	FdA Uni-Frankfurt
NB:		



Identification No.	Classification	Collection
Fö 106	Sch. 30/Va	Historisches Museum, Frankfurt
NB:		



Identification No.	Classification	Collection
22008	Sch. 30/Vd	FdA Uni-Frankfurt
NB:		



Identification No.	Classification	Collection
30VG179	Sch. 30/Vb	Cabinet des Medailles, Brussels
NB:		



Identification No.	Classification	Collection
20163	Sch. 30/Vb	FdA Uni-Frankfurt
NB:		



Identification No.	Classification	Collection
Lux 6	Sch. 30/VI	Musée Nat. d'Hist. et d'Art, Lux
NB:		





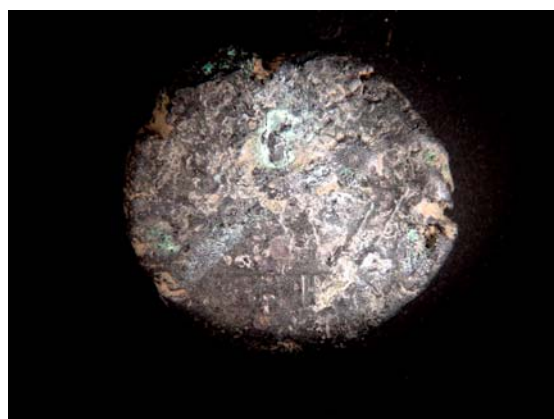
Identification No.	Classification	Collection
Lux1	Sch. 30/VI	Musée Nat. d'Hist. et d'Art, Lux
NB:		



Identification No.	Classification	Collection
SFLAN1451	Sch. 30/VI	Languini- Wallendorf
NB: Bronze		



Identification No.	Classification	Collection
SFLAN617	Sch. 30/VI	Languini- Wallendorf
NB: Brass		



Identification No.	Classification	Collection
20397	Sch. 30/VI	FdA Uni-Frankfurt
NB:		



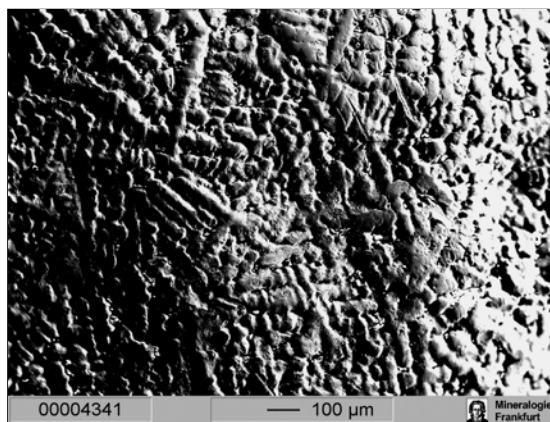
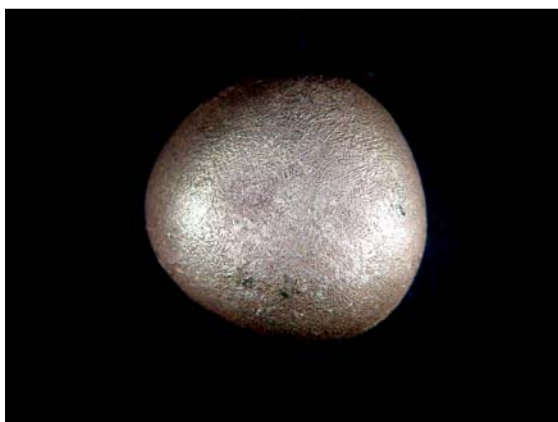
Identification No.	Classification	Collection
30449	Sch. 30/VI	FdA Uni-Frankfurt
NB:		



Identification No.	Classification	Collection
26227	Sch. 30/VI	FdA Uni-Frankfurt
NB:		



Identification No.	Classification	Collection
SFLAN1148	Proto-Flan	Languini- Wallendorf
NB: Second photo is a backscattered image (EPMA) showing the dendritic crystals		

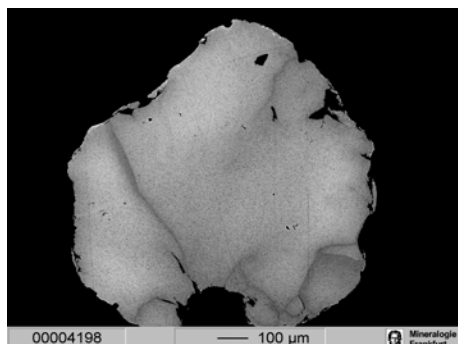
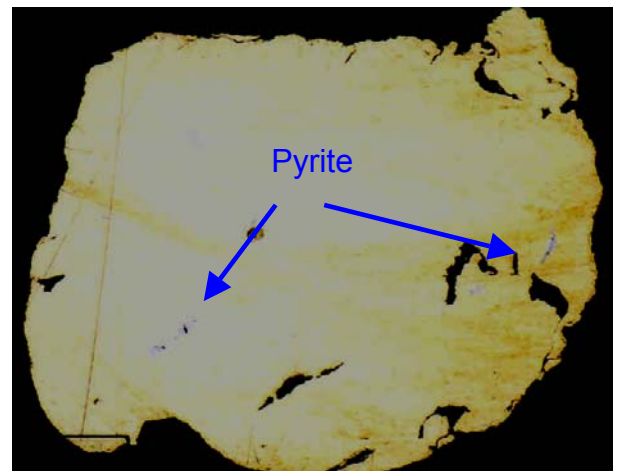
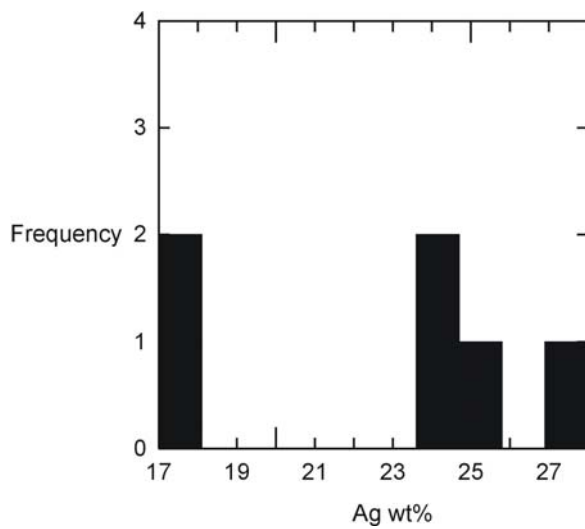


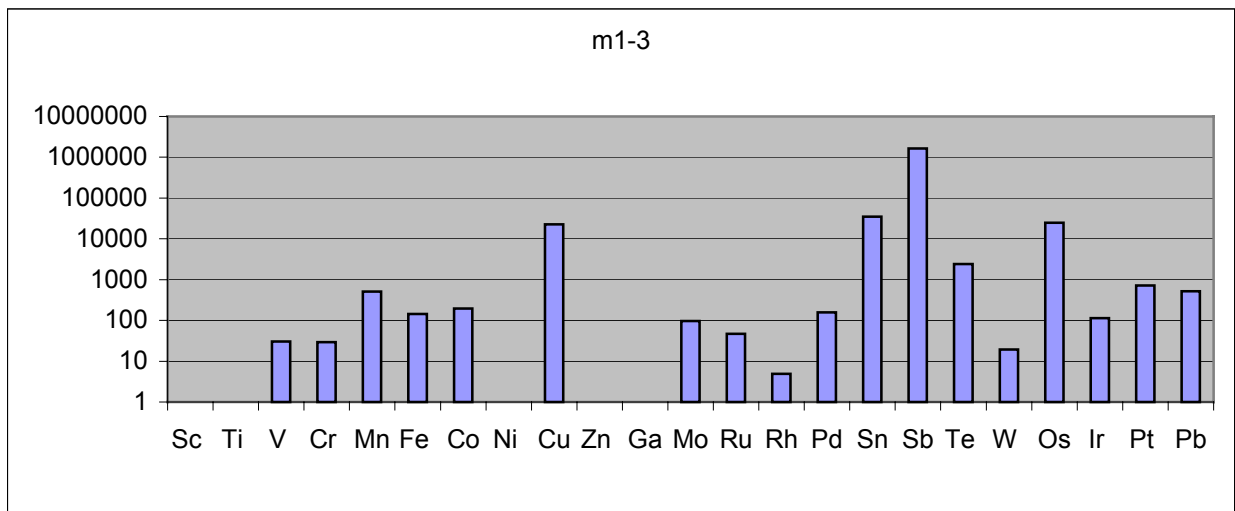
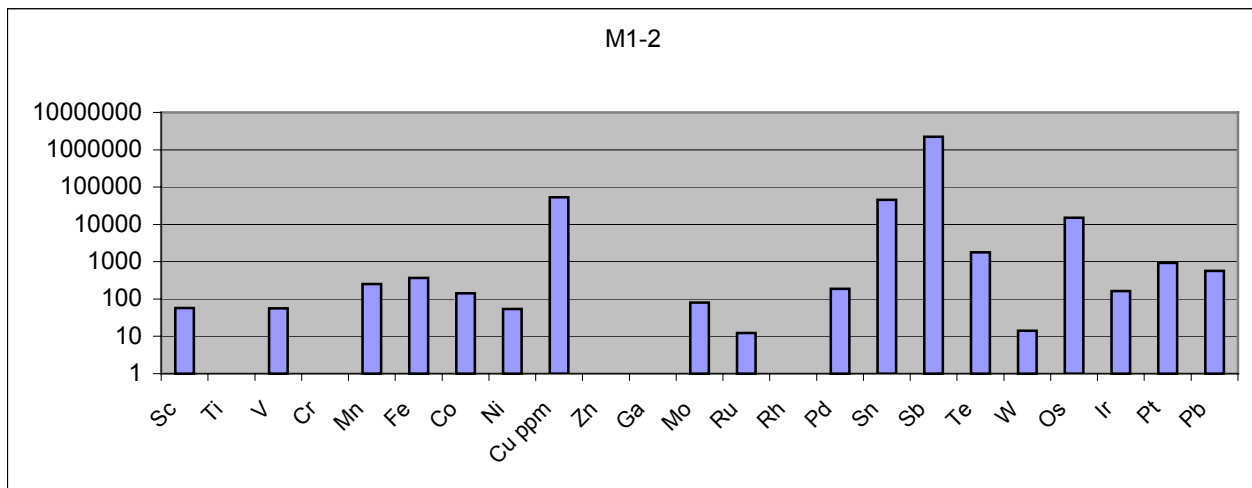
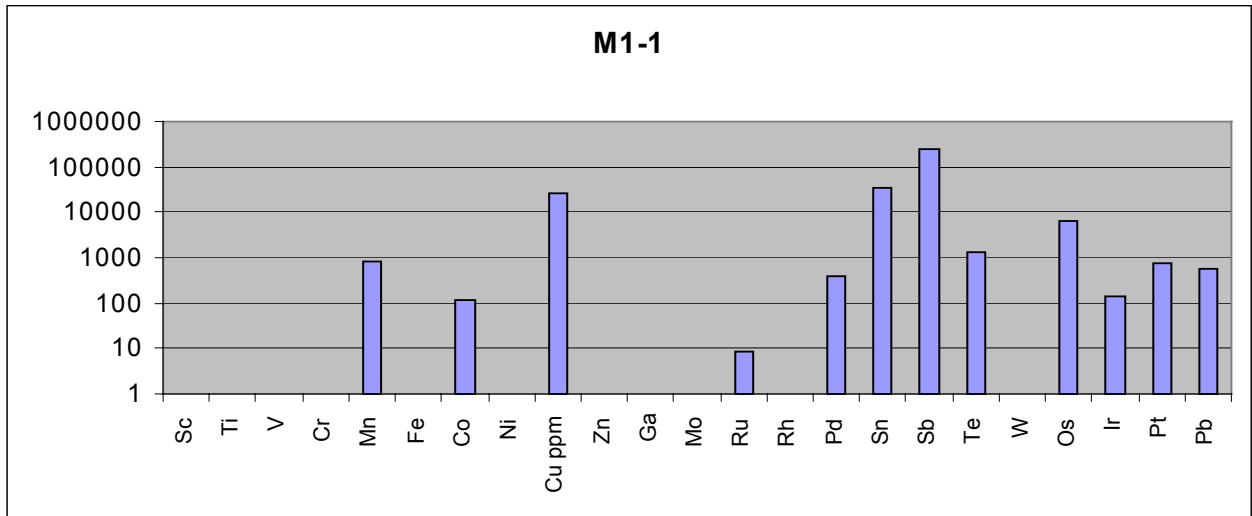
Identification No.	Classification	Collection
SFLAN3000	Proto-Flan	Languini- Wallendorf
NB:		



### M-1: Rein Del medel

The complex, angular and prismatic shapes of these grains along with the quartz present crusted on the outside of two of the larger grains and the very thin pure gold rims (<5 $\mu$ m) all point to limited transport of these grains. Although their Ag composition varies from 17 to 27%, their trace element signatures are very consistent.

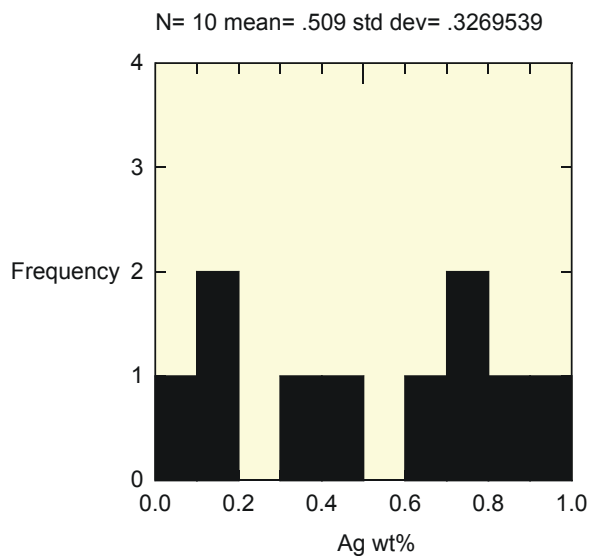
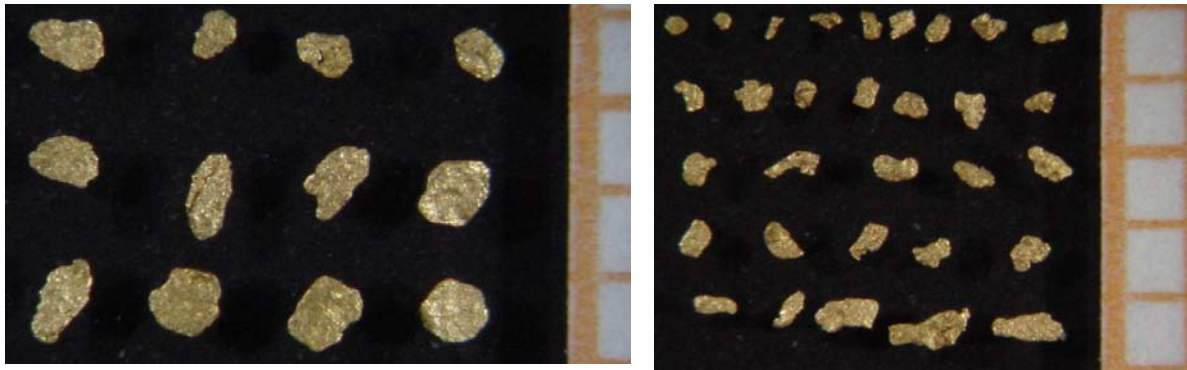




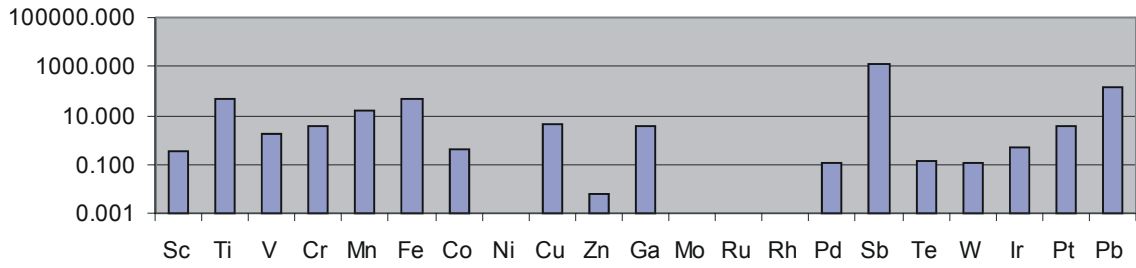
### M-3: Emme, Napfgebiet

There are two morphological groups, one with larger, ~1mm flitters which are irregular and equant and another consisting of smaller grains (>0.5mm) with angular, elongate and complex shapes. All the grains are consistently pure with over 99% Au.

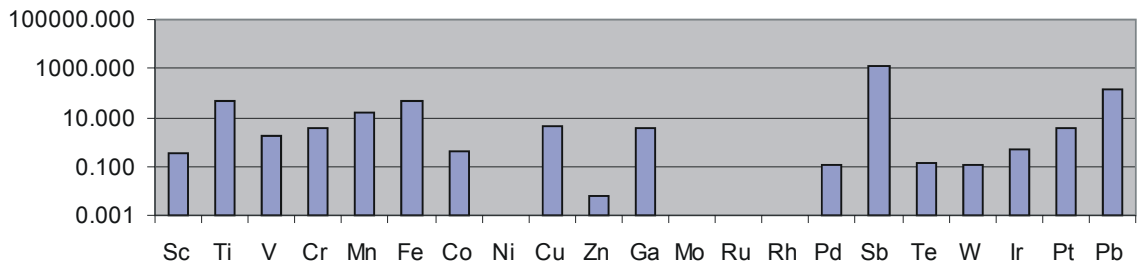
Pb and Sb provide a consistent signature, one subgroup shows higher copper.



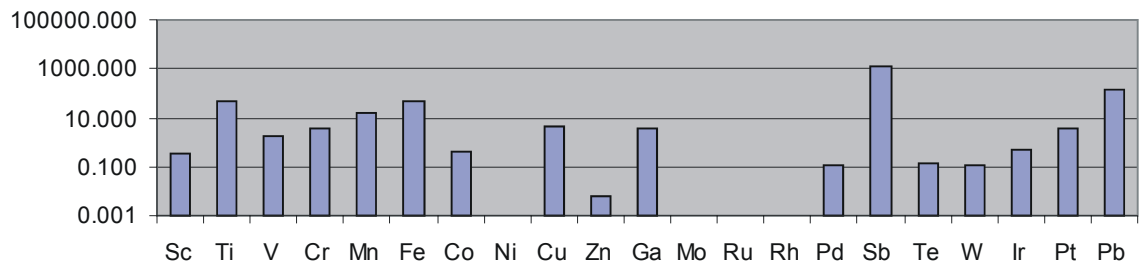
M3-1



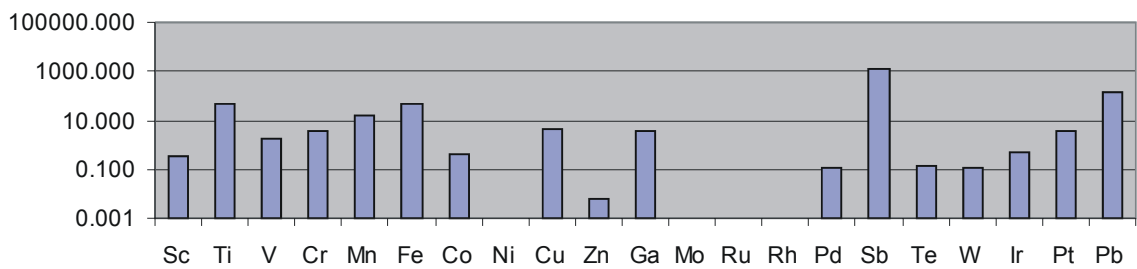
M3-1



M3-1



M3-1



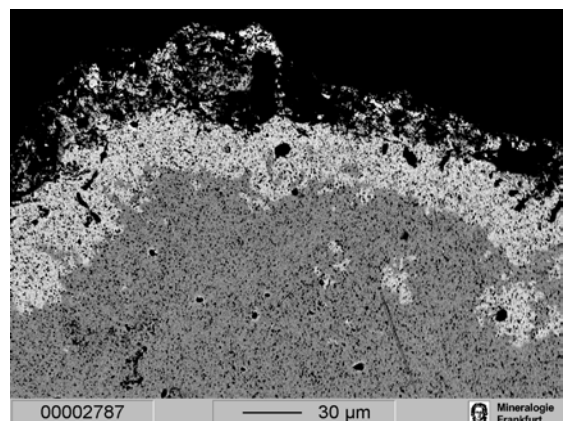
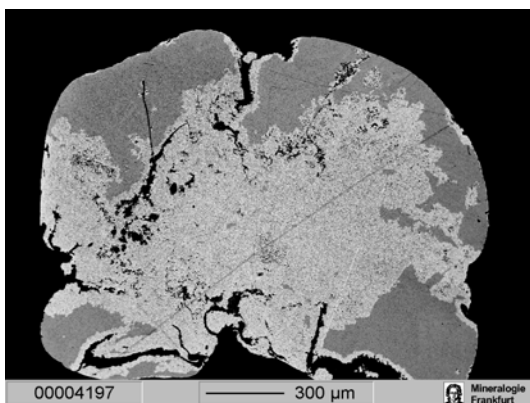
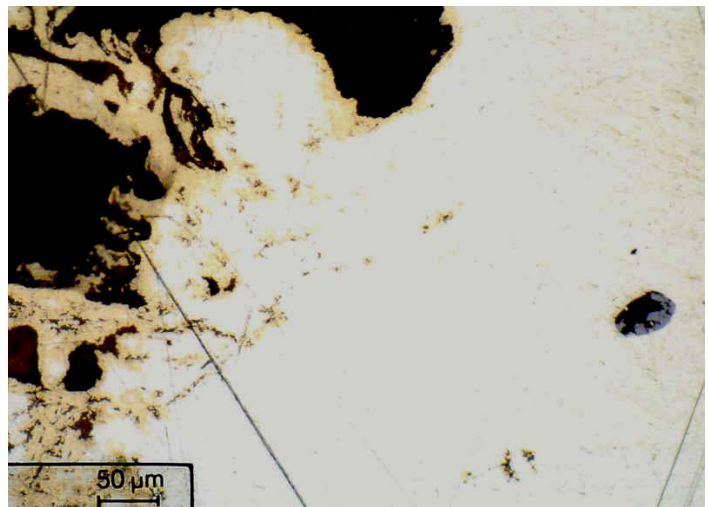
#### M-4: Isere, Grenoble; Flows from the Alps

Two grains, which were analysed by EPMA, gave Ag and Au compositions of

1) 33.15 Ag wt% 66.41 Au wt% 2 24.36 Ag wt% and 75.25 Au wt%

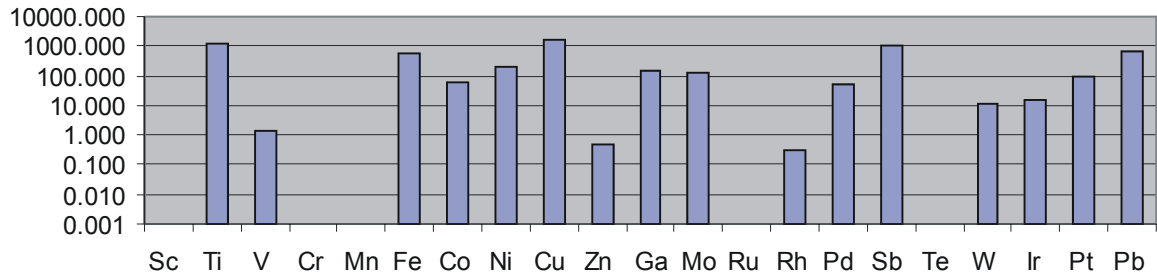
The second photo shows the typical white colour of high silver gold (electrum) under the microscope. The pure gold rim can be easily seen with thickness up to 20µm.

Interestingly, although subgroups M4-1 and M4-3 show a large difference in Ag content, 24% and 33% respectively. They have almost identical trace element signatures, which can be seen on the triplots, and the trace element patterns below. Subgroup M4-2 is noticeably different.

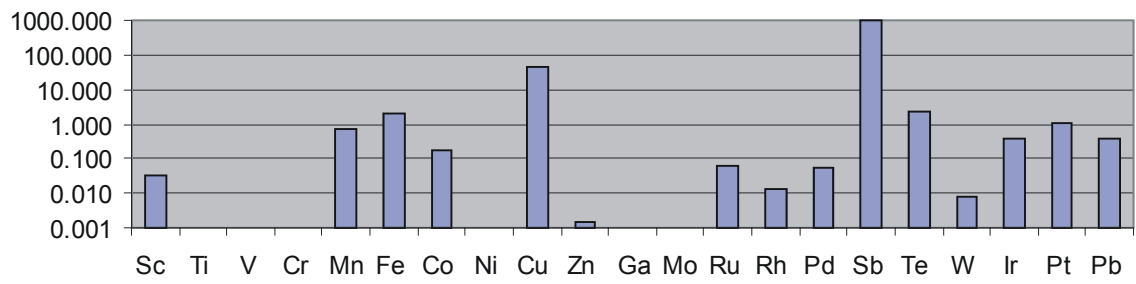




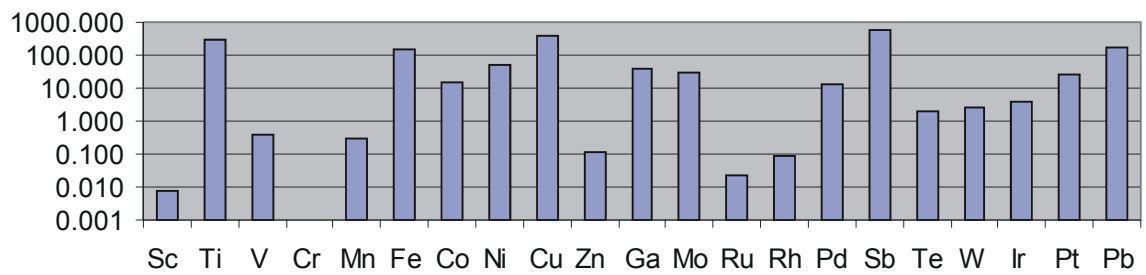
M4-1 24% Ag



M4-2 30% Ag



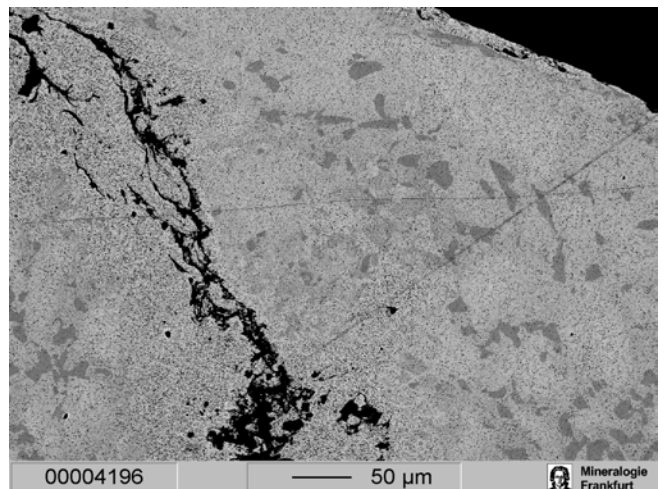
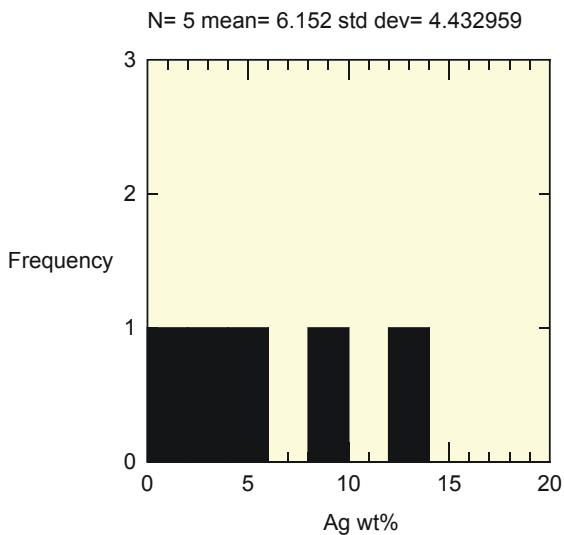
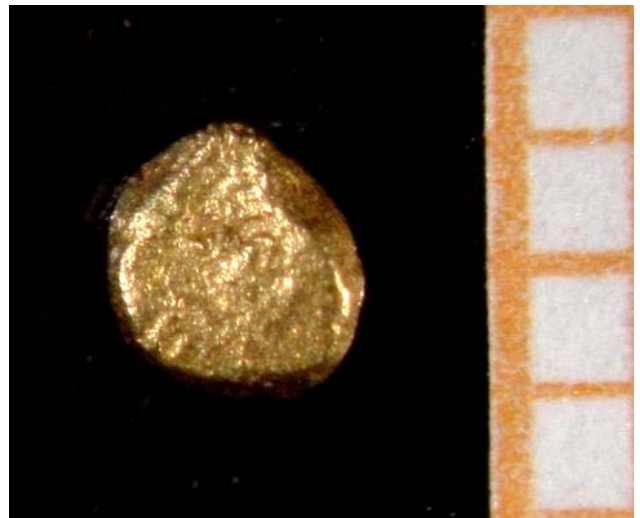
M4-3 33%Ag



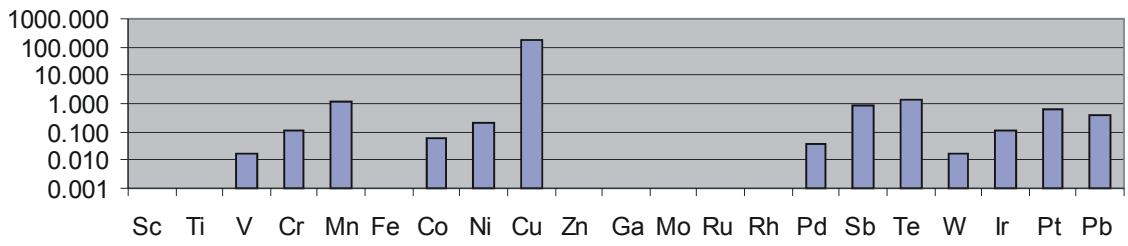
### M-5: Ochills, Scotland

Most of the grains are irregular flitters equant to elongate in outline, 1-3.0mm in size and of intermediate thickness. However, one of them appears more massive and spherical with flat faces that give it a prismatic appearance. Dark patches in the EPMA photo represent patches of a Cu-rich phase.

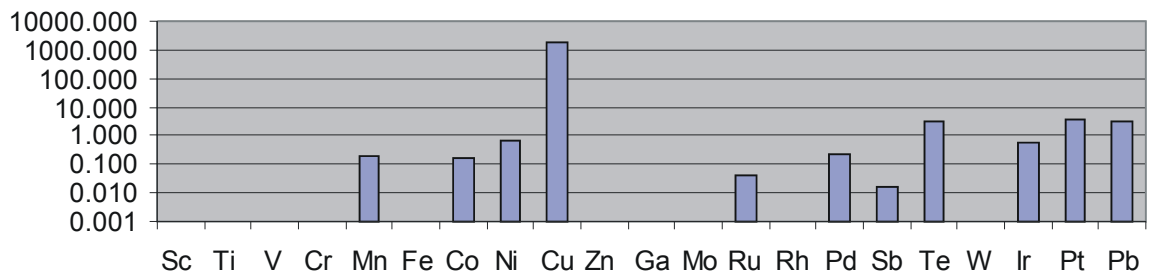
Trace elements appear fairly diverse, there maybe two groups.



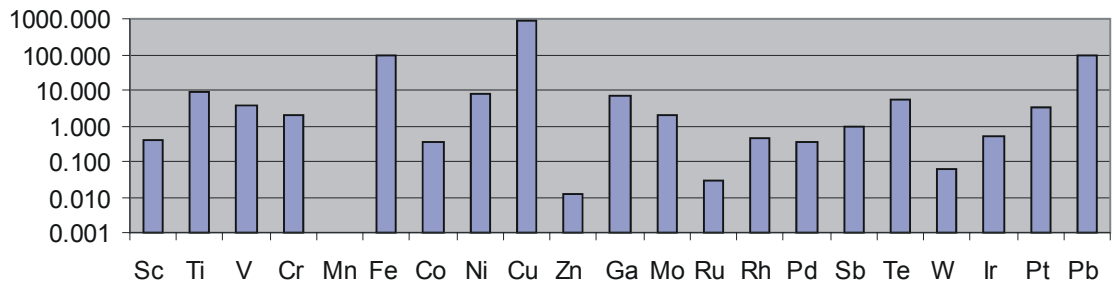
M5-1



M5-3



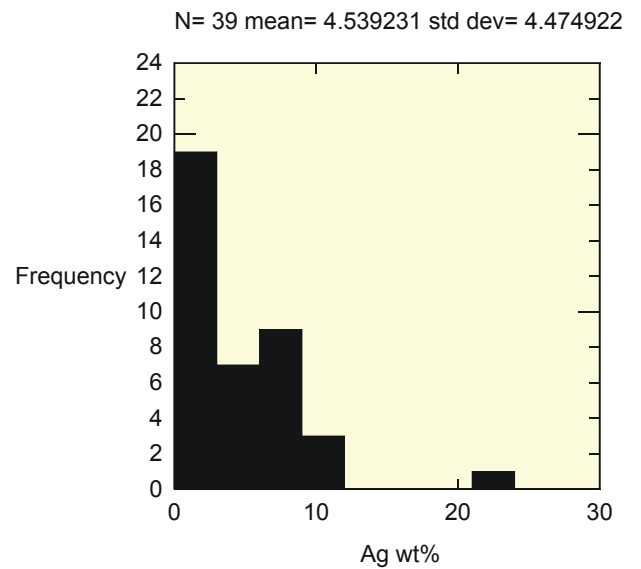
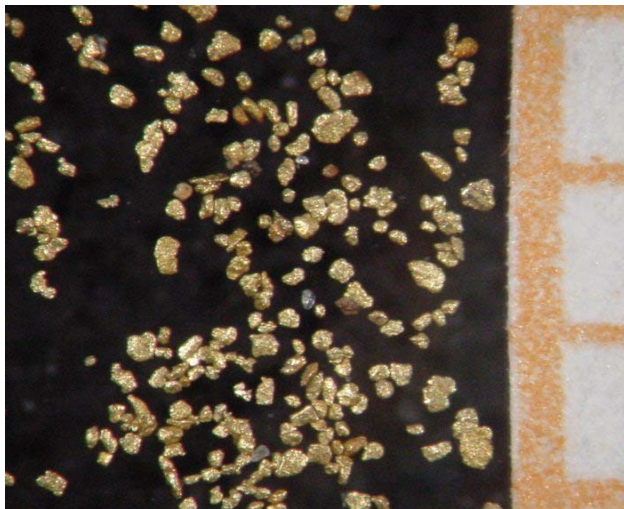
M5-2



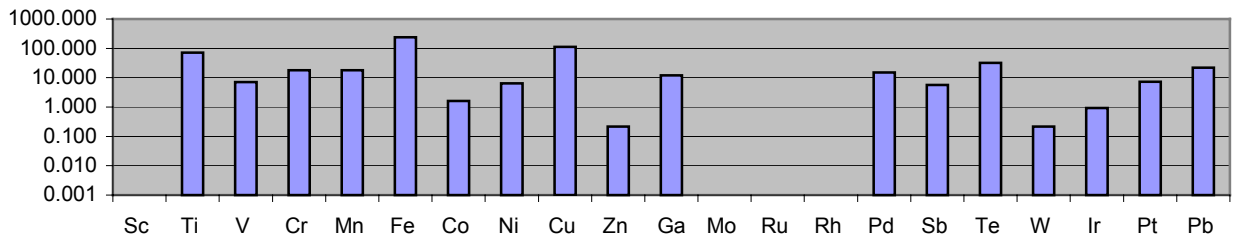
## M-7: Eder, Hessen

The gold is very small, < 0.2mm, mostly micronuggets, grains. Fairly consistent Ag content, mostly less than 10% Ag.

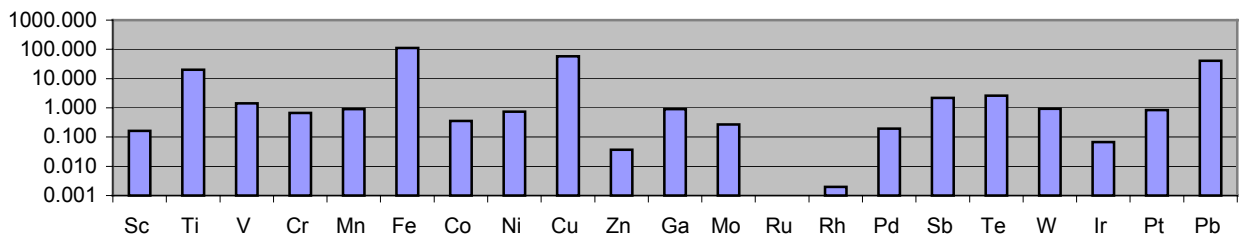
The Tri-plot (section 4.5.1 b) shows the relative concentrations of Cu, Pt and Sb for samples M-7 and M-17. M-7 has higher amounts of Pt and is relatively variable.



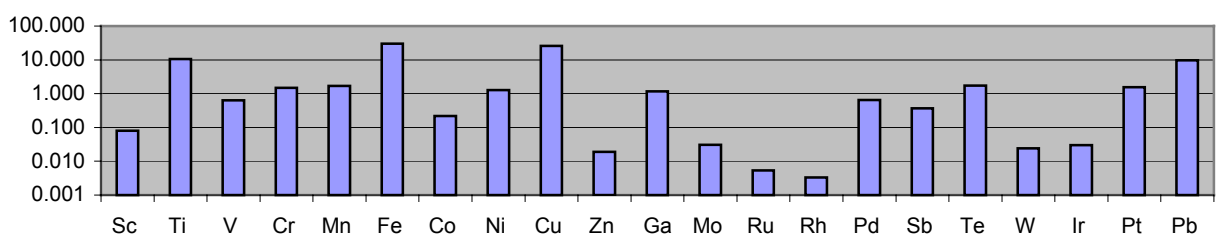
M7-1



M7-2



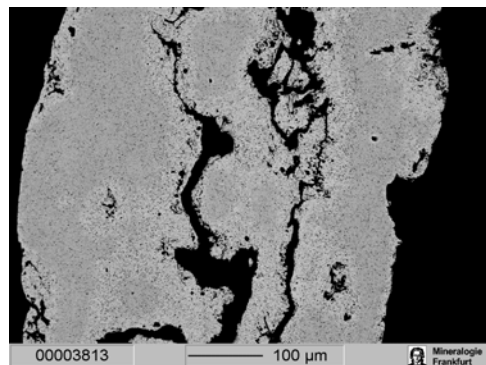
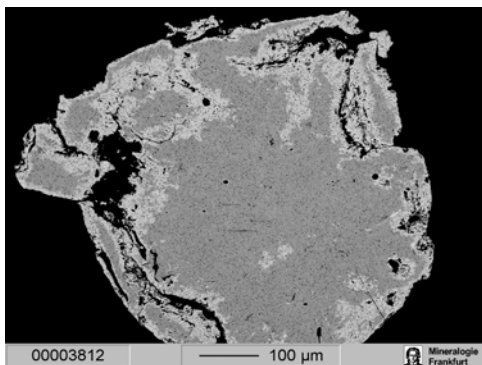
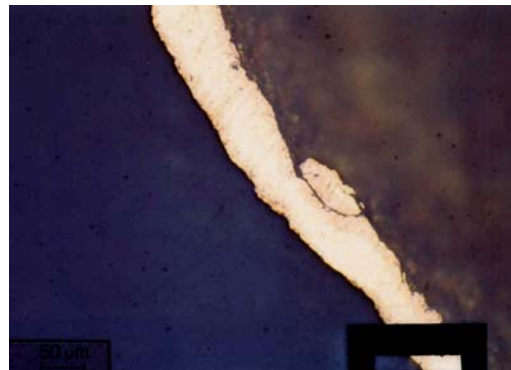
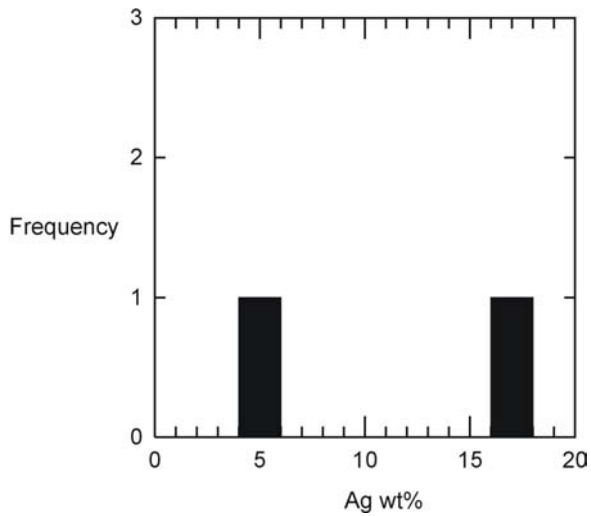
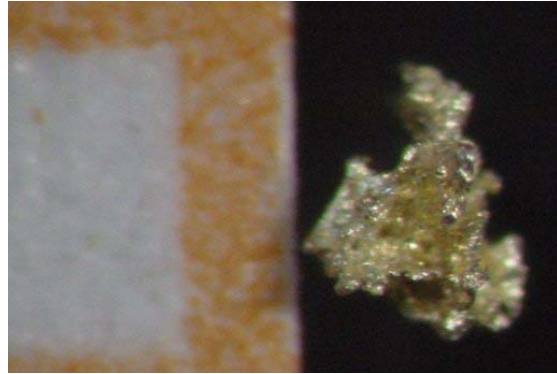
M7-3

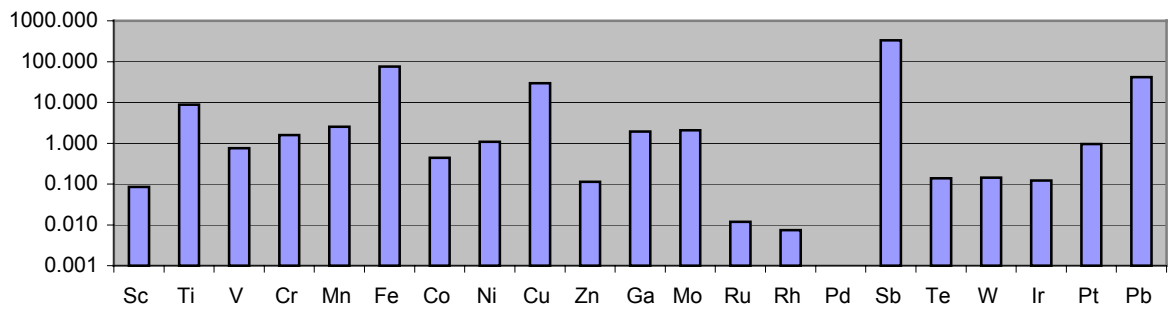
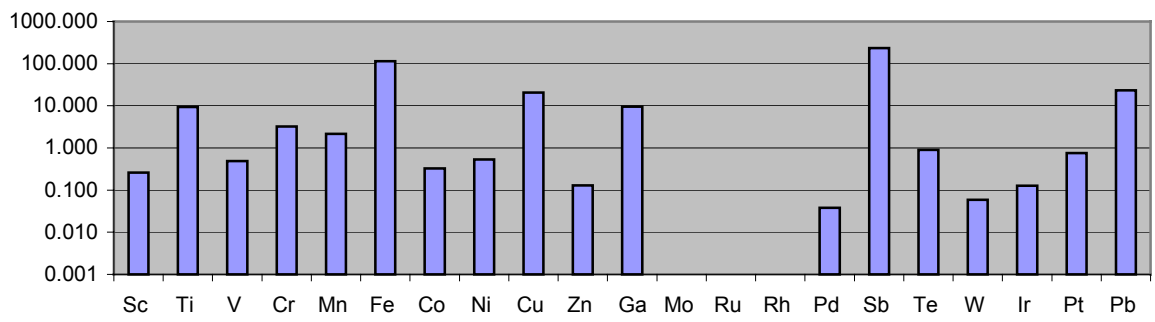


## M-8: Rheinfelden

Almost entirely well rounded equant thin flitters 0.5 to 1.5mm in size. There is one peculiar grain, which appears to have come straight out of the rock.

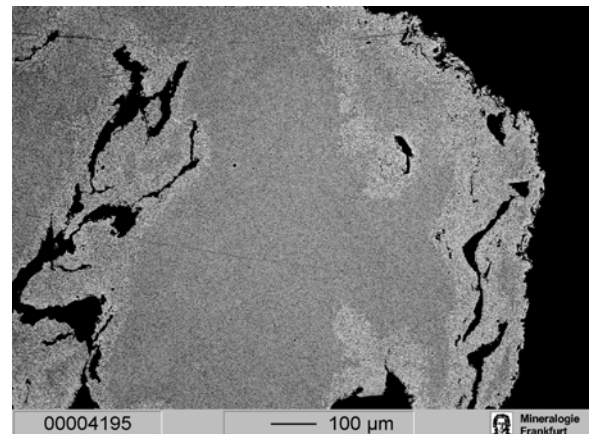
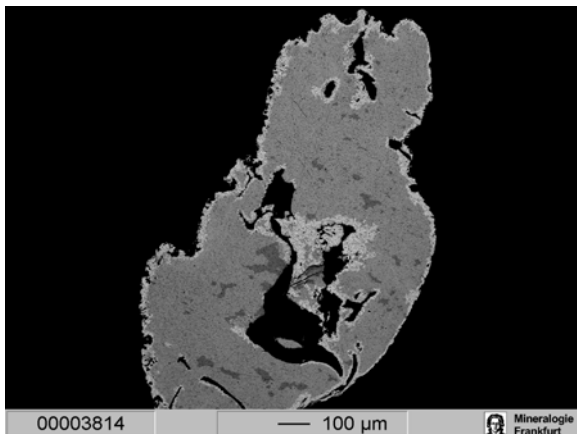
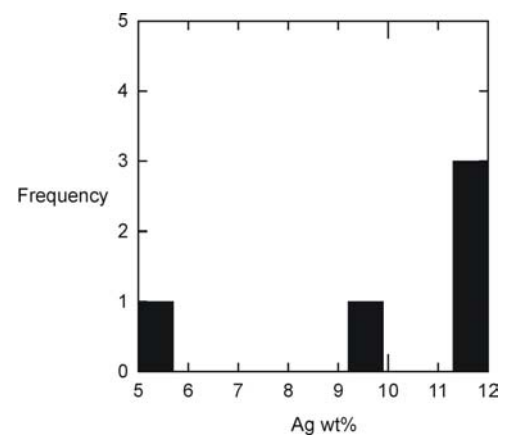
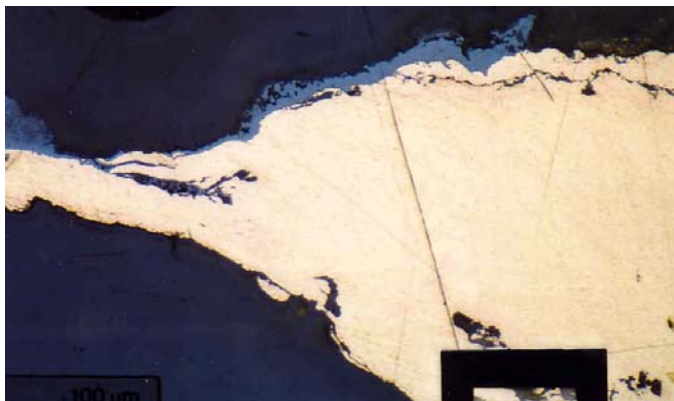
M-8 is characterised by high Pb and Sb with interesting correlations produced with Pb vs Cu and Pb vs Sb. The analyses of different grains from this sample lie along correlation lines with highly variable element concentrations but with very consistent Pb/Cu, Pb/Sb ratios.



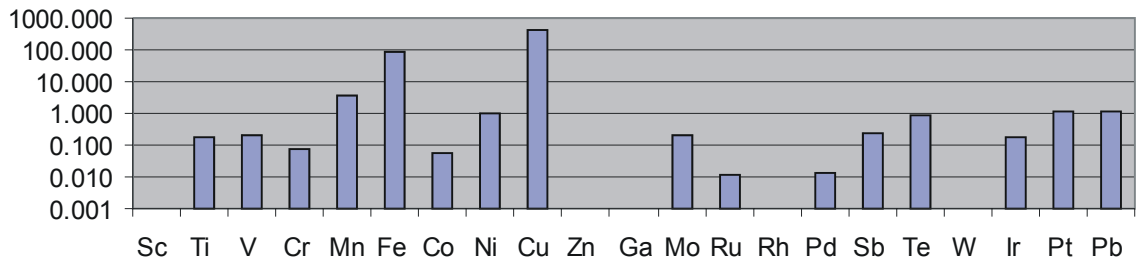


### M-9: Rio Elvo, Piemont, Italy

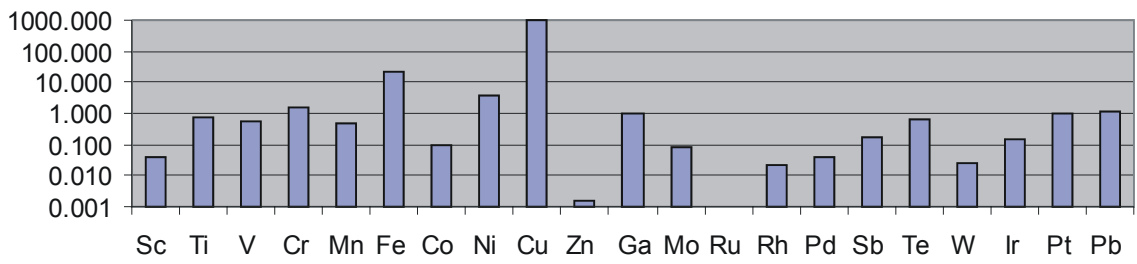
Mostly flitters of intermediate thickness, rounded and equant with complex shapes of 1.5 to 4mm in size, Many of them are folded while one spherical grain, which has an almost complex outline, is 3mm in diameter. Three Ag groups. Perhaps two trace element groups.



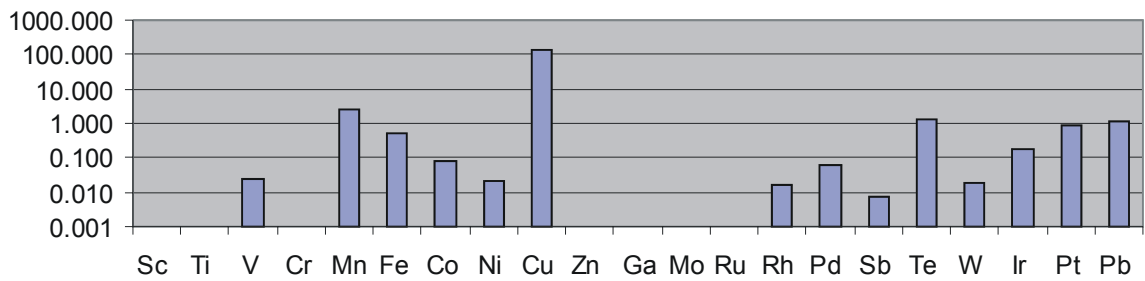
M9-1



M9-2



M9-3

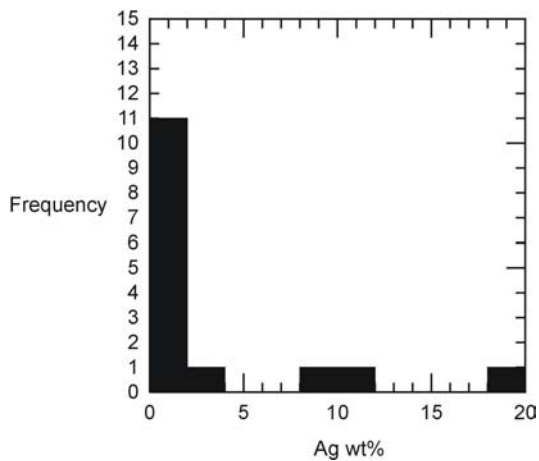
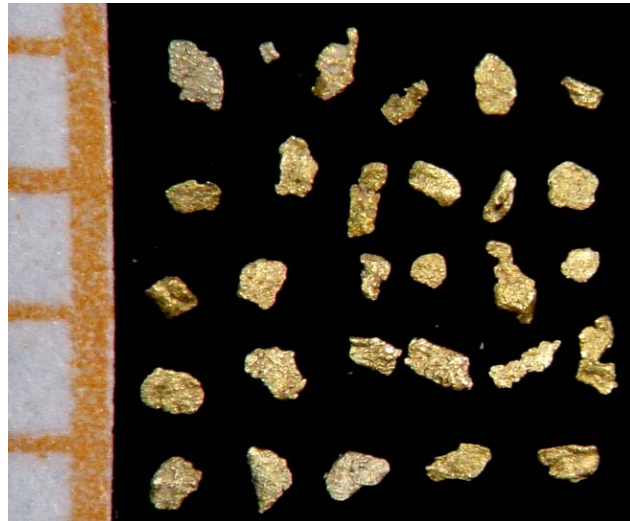




### M-10: Luther, Napfgebiet

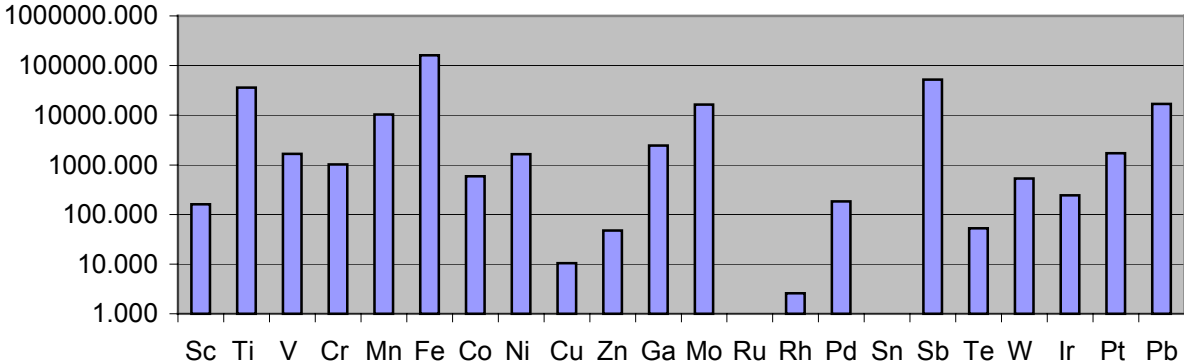
Rounded and irregular grains displaying equant to complex shapes of thin to intermediate thickness and 0.5 to 1. mm in size. Many of the grains are fairly pure with over 98% Au, although there are several grains with up to 20% Ag. Therefore rimming is not evident.

The Triplot shows two groups. There is one main group consisting of three subgroups (with higher Pt) and a second more variable group. This is not evident from the trace element patterns below.

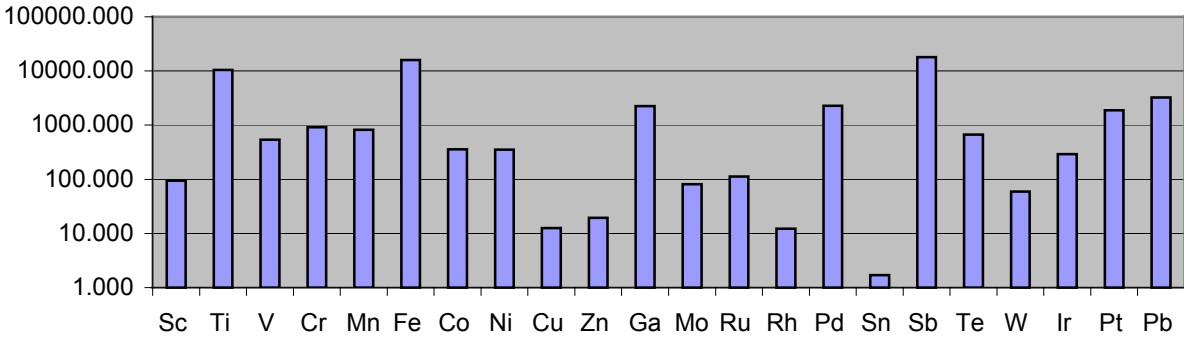


**NB: All these values are in ppb except Cu, which is in ppm.**

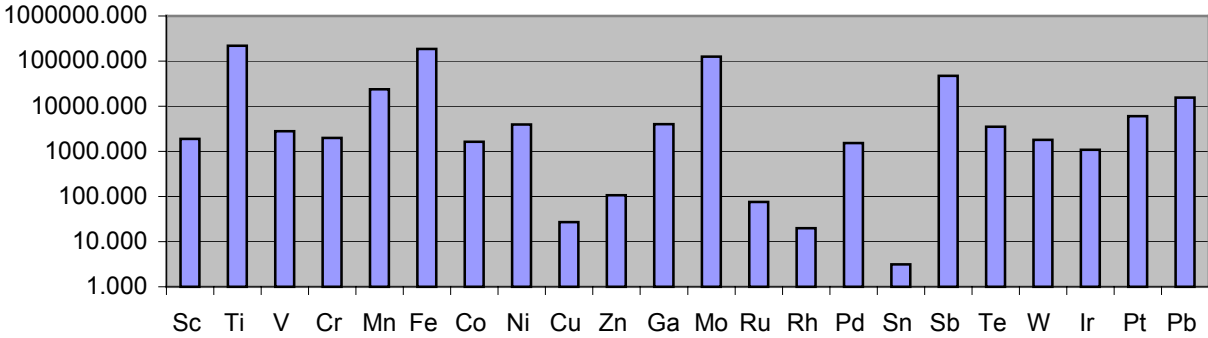
M10-1



M10-2



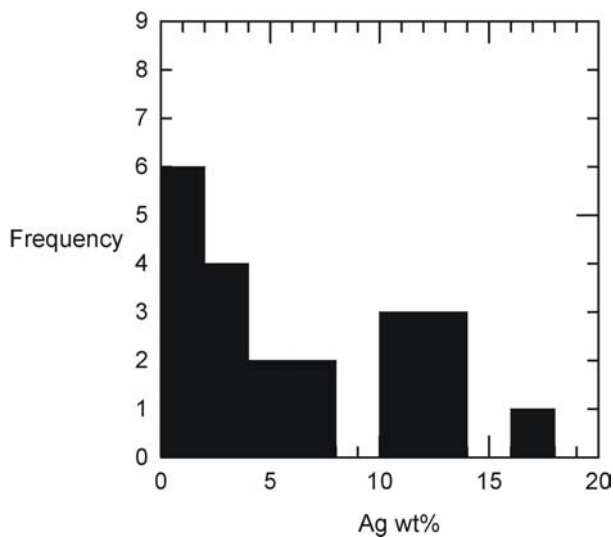
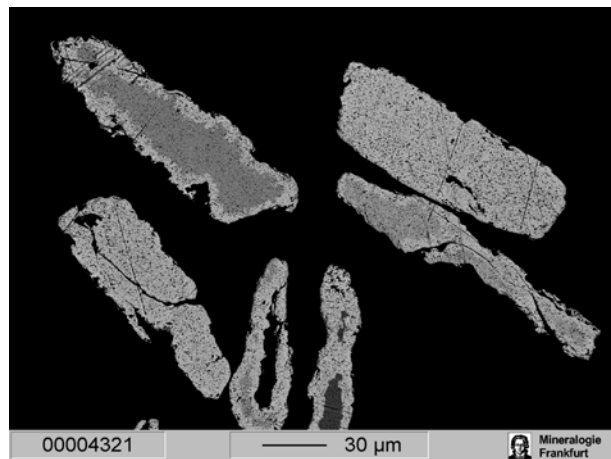
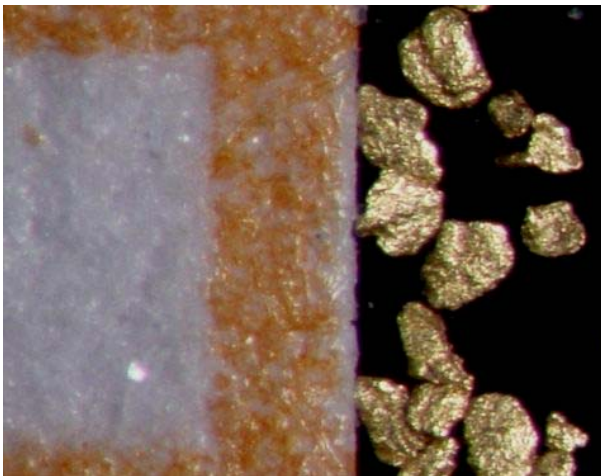
M10-3



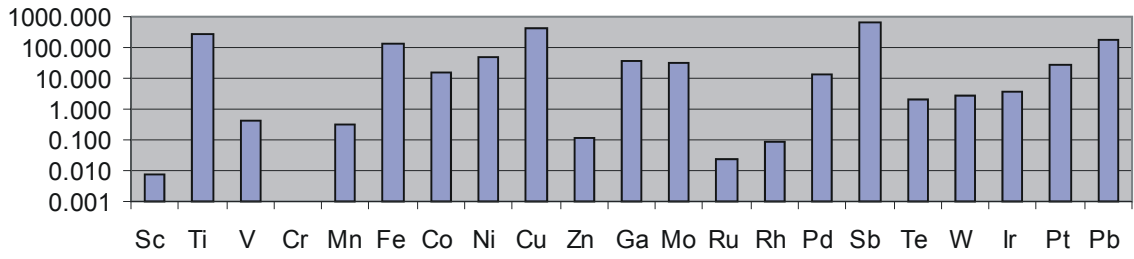
### M-11: Saone River; Flows from the Vogesen

These grains and flitters are very small, averaging not more than 0.2mm in size and very thin in cross-section. Rimming is well developed in most grains with some grains appearing to be completely altered to higher fineness, although this could also be the effect of insufficient polishing which has failed to expose the more Ag rich cores. Folding is a common feature of the flitters.

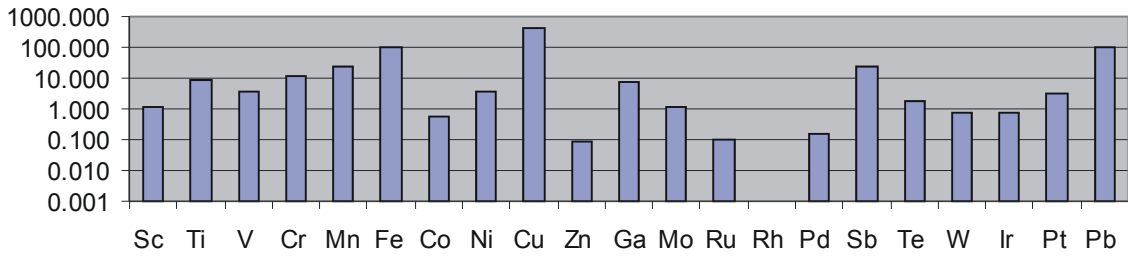
Despite the large range in Ag compositions. The trace element signatures are very consistent, showing clear groups especially with respect to W, Ir, Cu and Pb. The trace element patterns below are also very similar



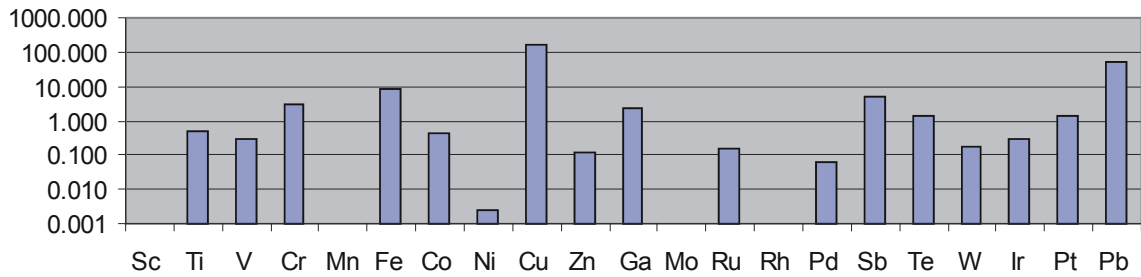
M11-1 6% Ag



M11-2 14% Ag

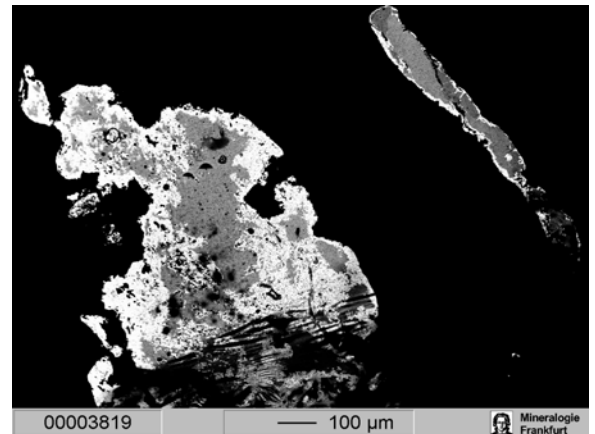
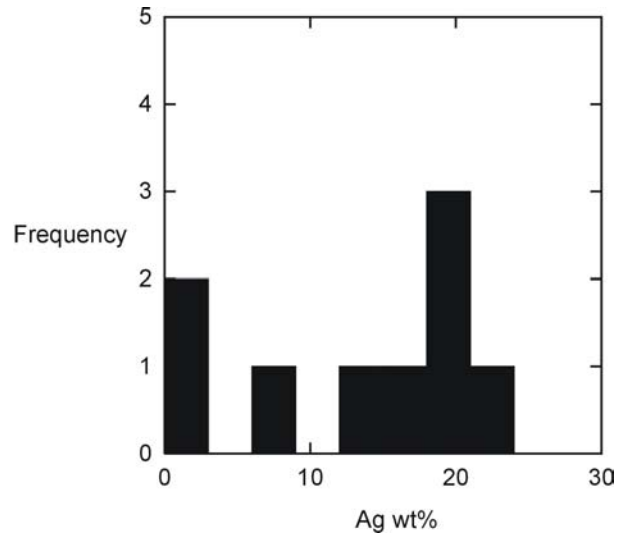


M11-3 20% Ag

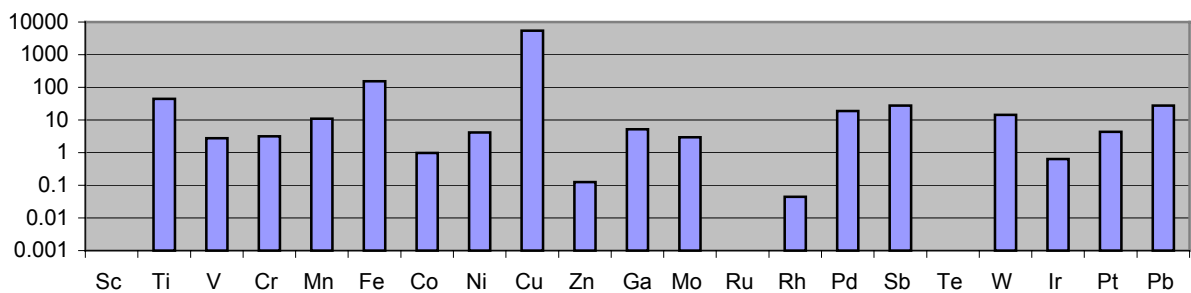


## M-12: Altrhein, Istein

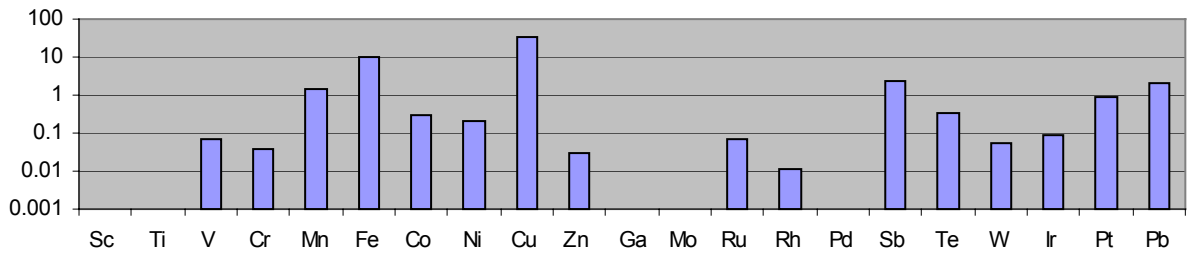
These flitters are well-rounded thin flitters with mostly equant and complex shapes and display a high degree of rimming. Most of the grains have between 15 and 20% Ag and their trace element signatures can be distinguished by the low Pb, Sb and Pt compared to the neighbouring Rhine gold samples.



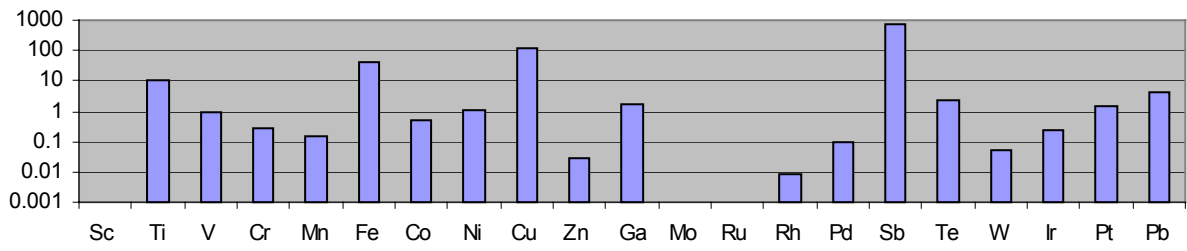
### M12-1



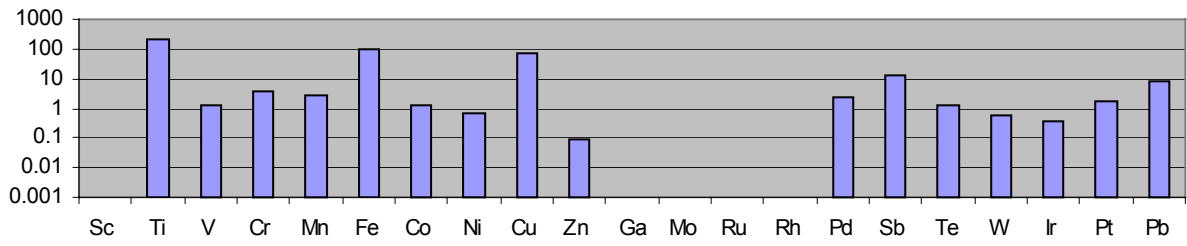
**M12-2**



**M12-3**



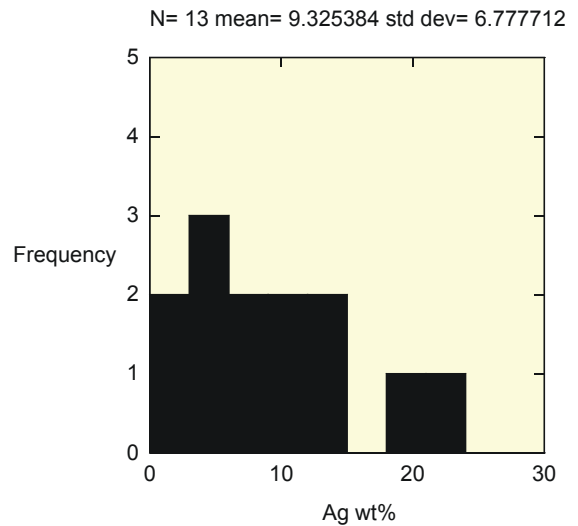
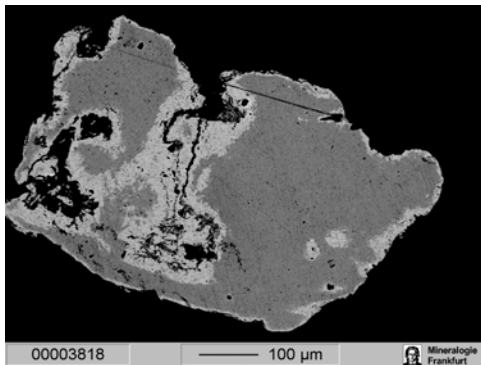
**M12-4**



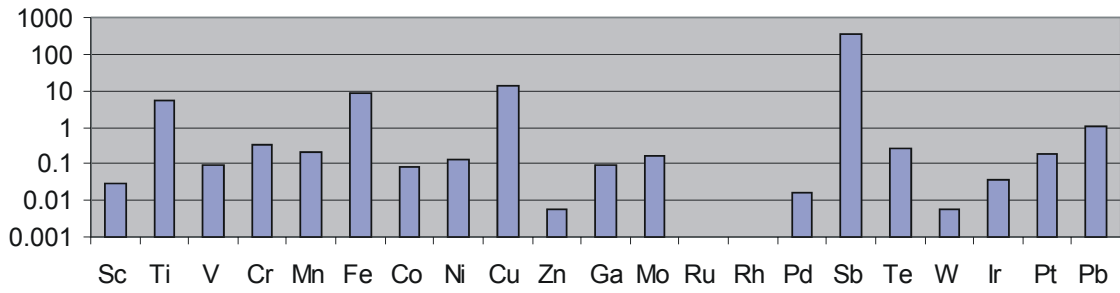
### M13: Allondon, Genf

This sample contains large rounded and equant flitters (0.5 to 1.5mm) and smaller irregular, elongate and complex flitters and grains (> 1.0mm). Most of the grains show well developed rimming. There is a large range of Ag compositions with most grains having between 1 and 10% Ag while a small subgroup contains ~20% Ag.

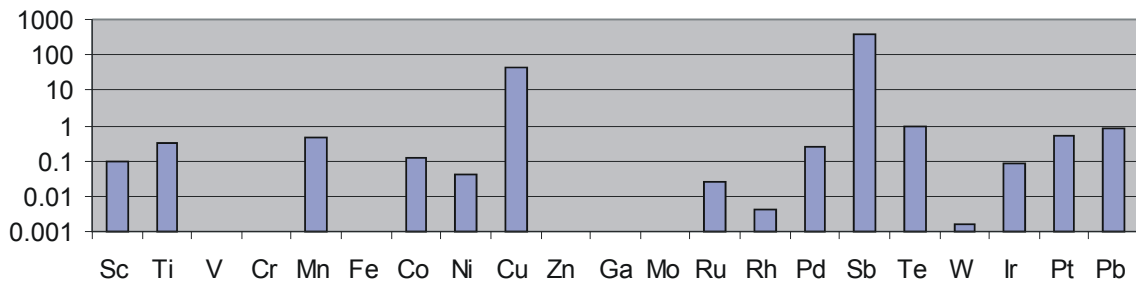
There is one main group and a smaller subgroup, which has higher Sb and Cu than the others (M13-1 and M13-2).



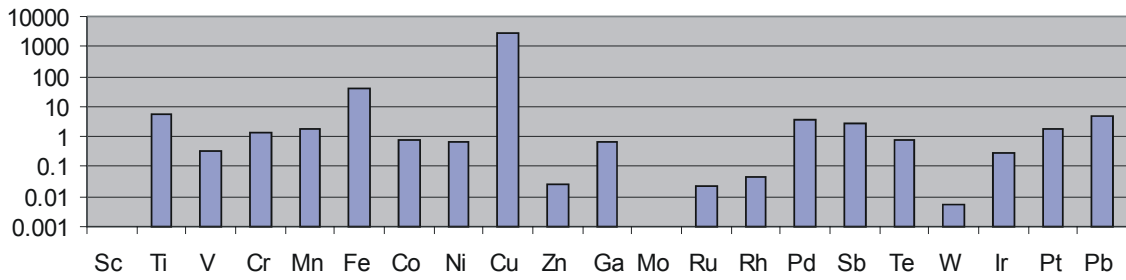
M13-1



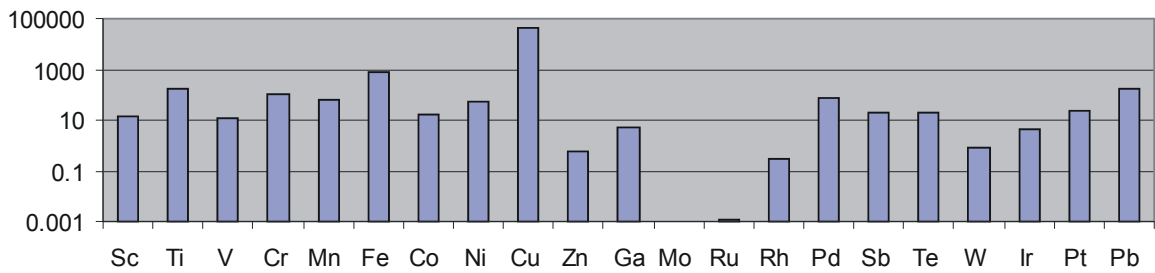
M13-2



M13-3

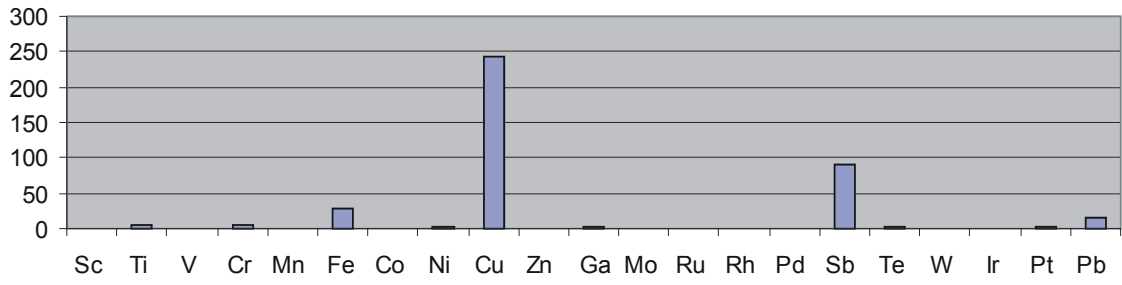


M13-4

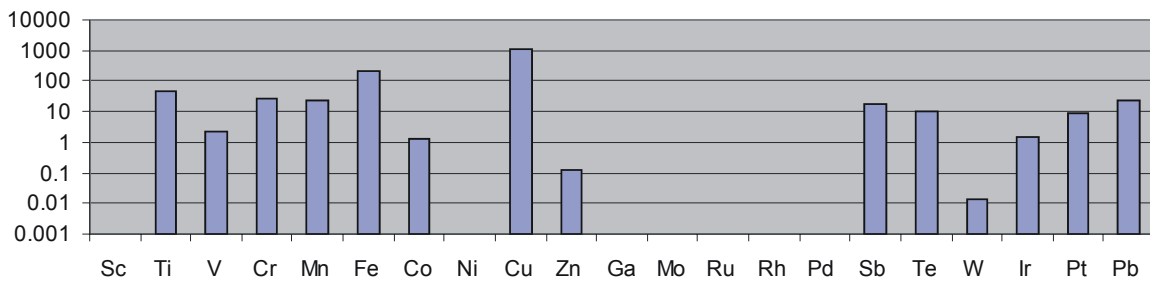




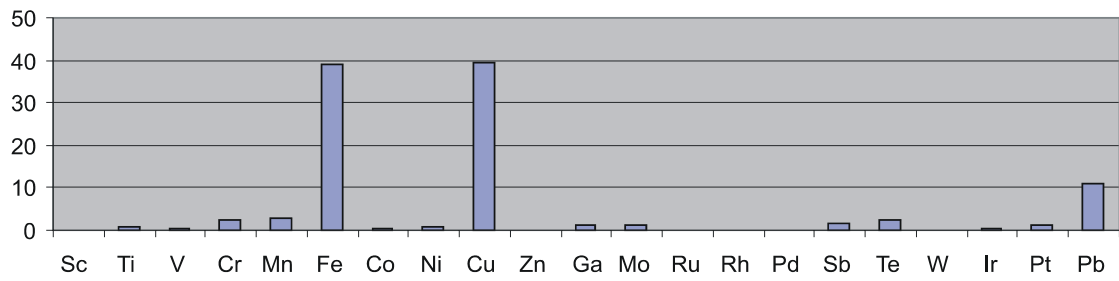
M13-5



M13-7

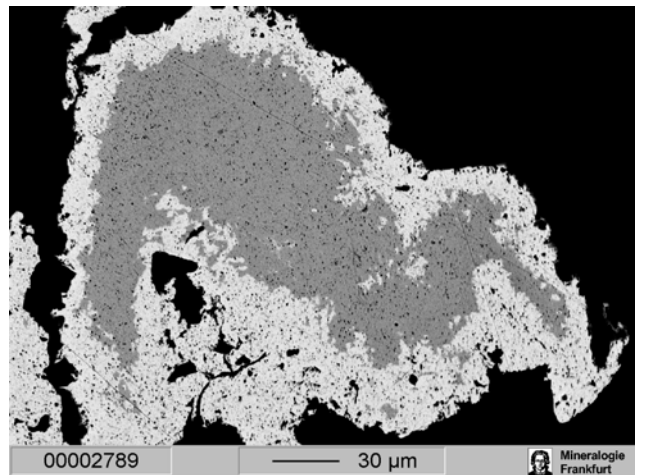
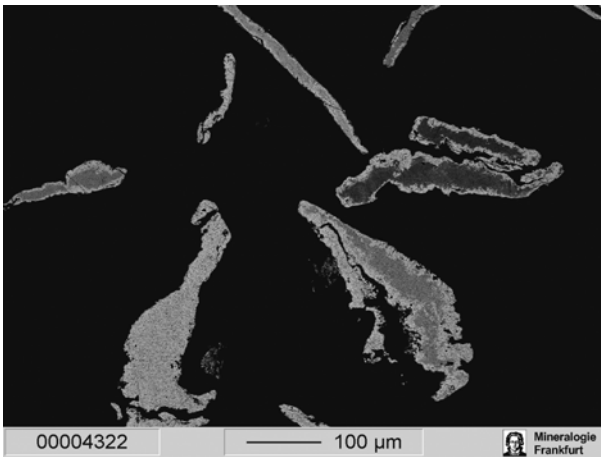
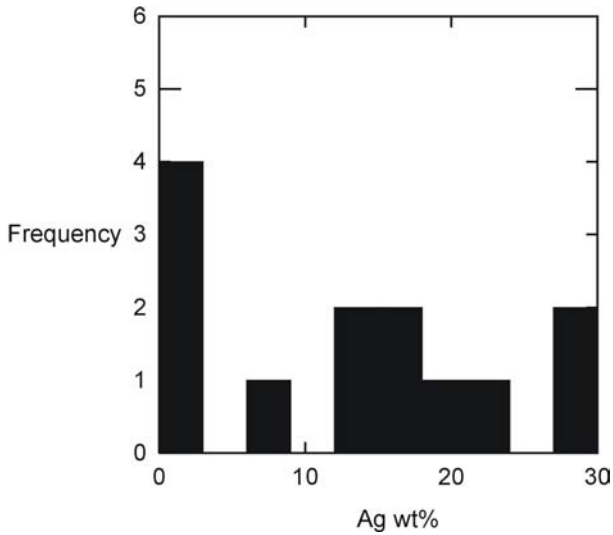


M13-6

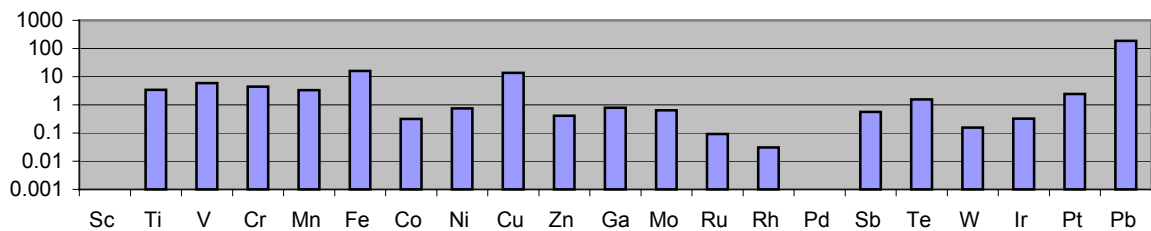


**M-14: Altrhein, Karlsruhe**

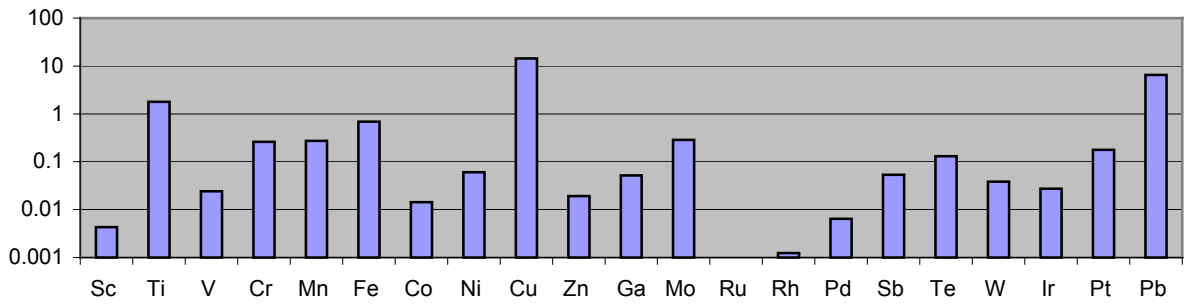
The very small size and extreme thinness of these flitters is consistent with them having travelled a long way down the Rhine. They are rounded and elongate with some folding and well developed rimming. They also show a large variation in Ag compositions and trace element concentrations suggesting a large degree of mixing. It is worth noting that the Pb isotope signature is very different from any of the other Rhine samples. Of all the Rhine samples studied here this is the only one, which could have gained a contribution of gold from the Schwarzwald or the Vogesen.



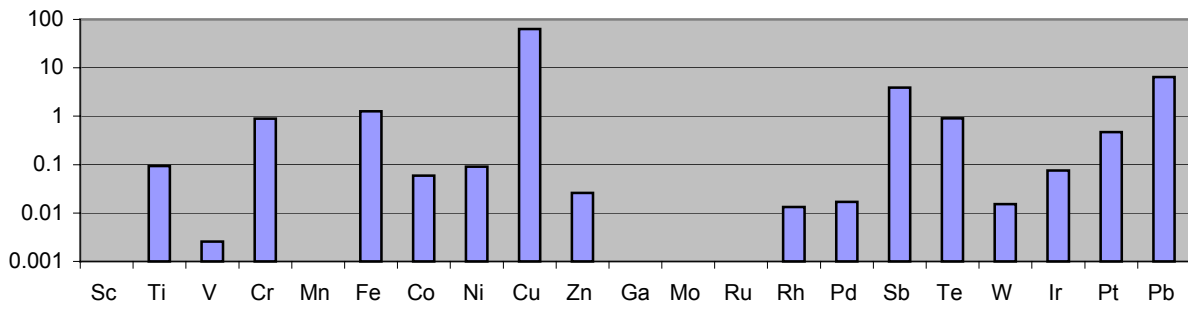
**M14-1**



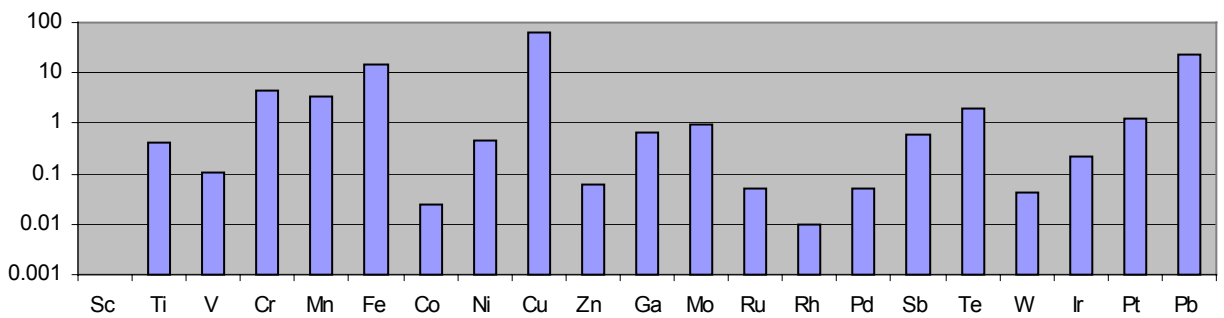
**M14-2**



**M14-3**



**M14-4**

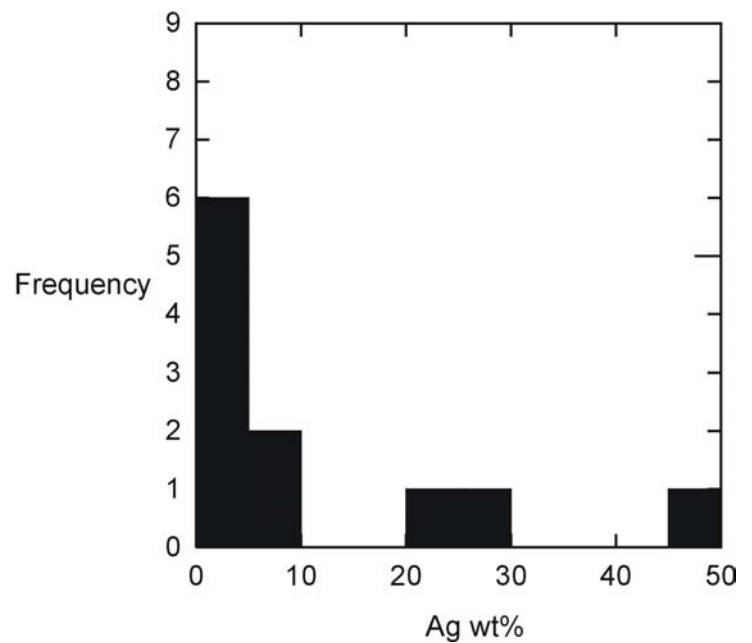
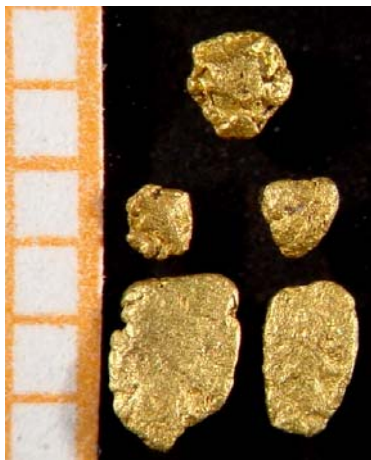


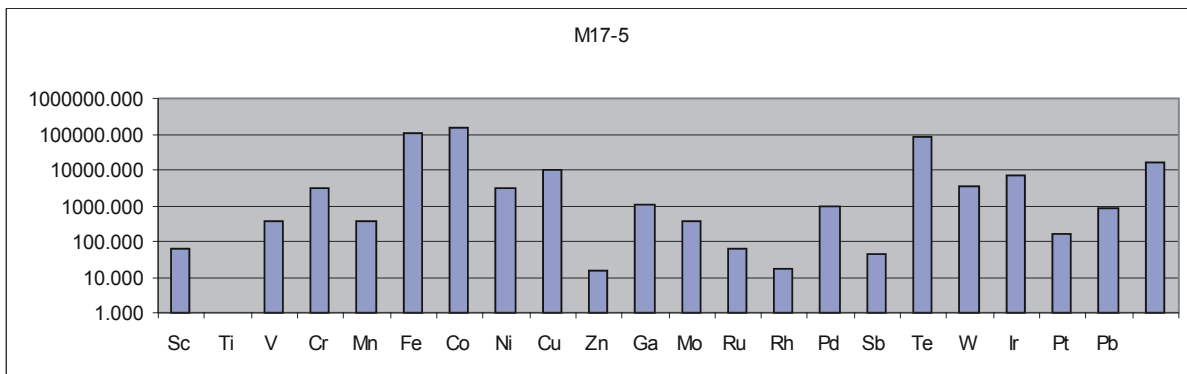
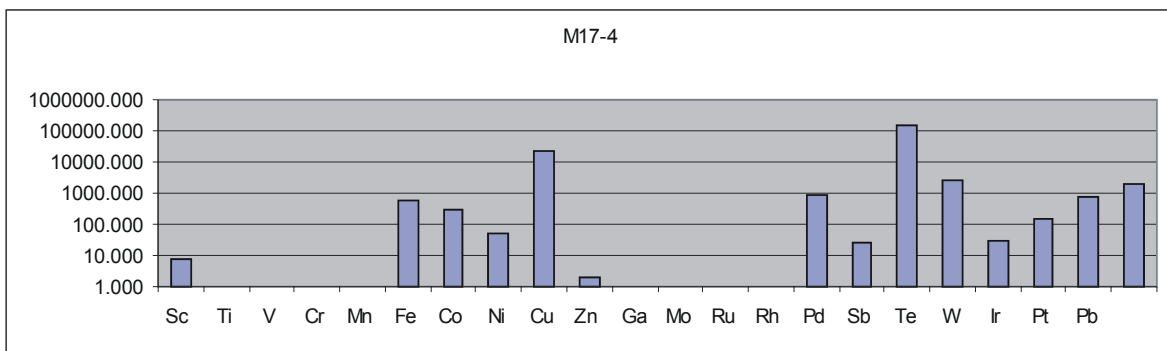
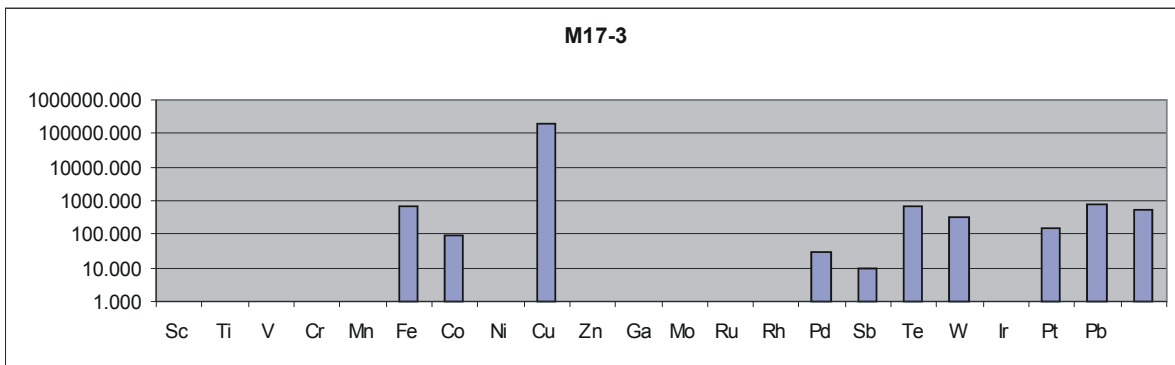
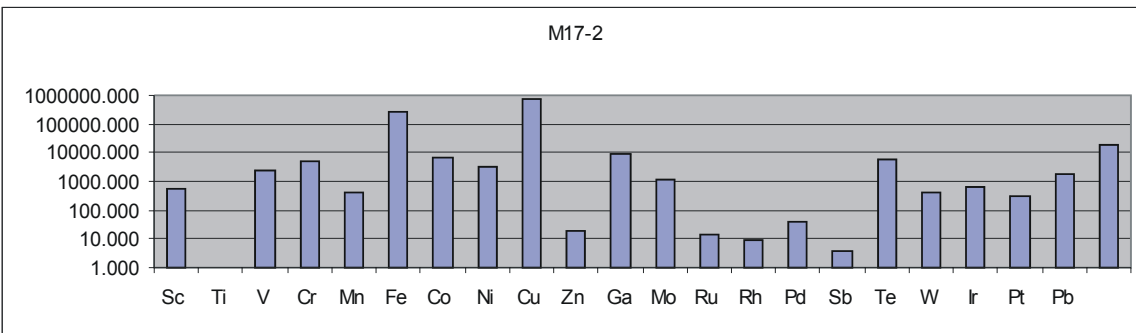
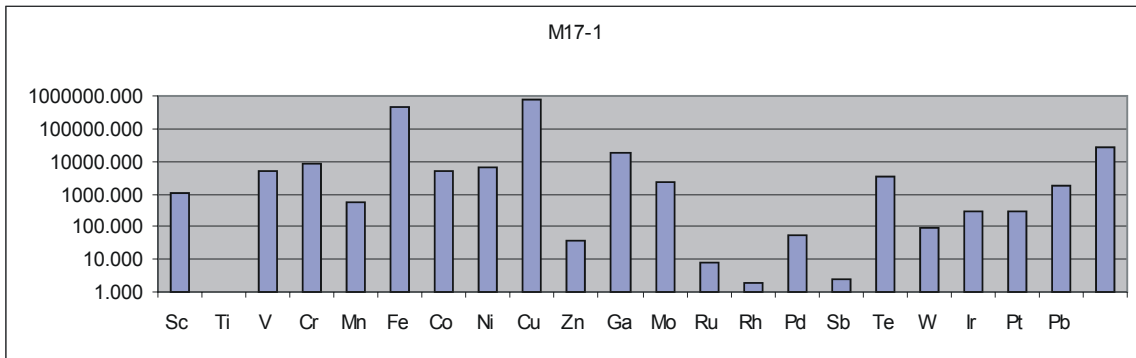
## M-17: Schwarza, Thüringen

This is a very heterogeneous sample with two or three groups of grain morphologies and at least three groups based on the Ag contents. Two general groups of grain morphologies can be distinguished.

- 1) Irregular, equant to complex flitters of intermediate to thick, thickness, which range from less than 0.5mm to almost 3.0mm in size.
- 2) The angular grains with diameters of 1 to 1.5mm, showing signs of more recent removal from the primary lode.

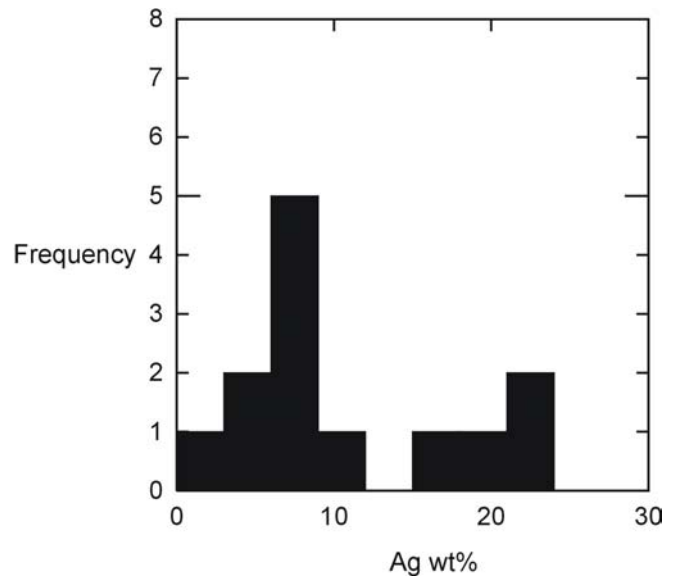
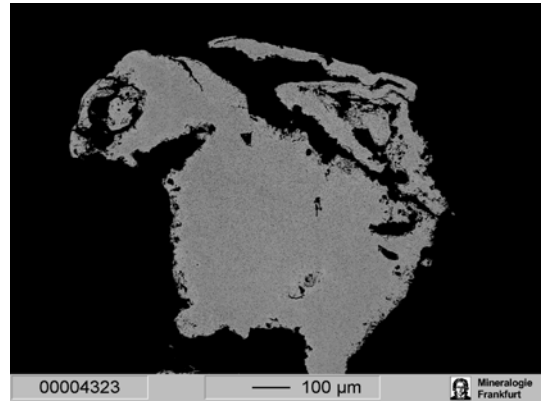
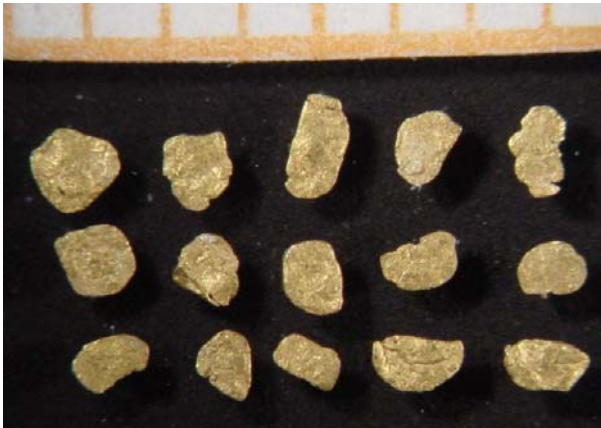
The trace elements show two definite groups characterised by the lack of Sc, Ti, V, Cr, Mn, Zn, Ga, Mo, Ru and Rh in subgroups; M17-3 and M17-4.



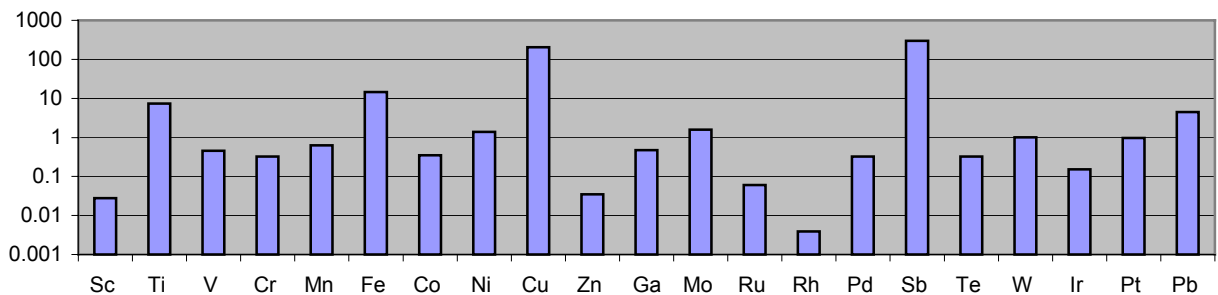


**M-18: Altrhein Rosenau**

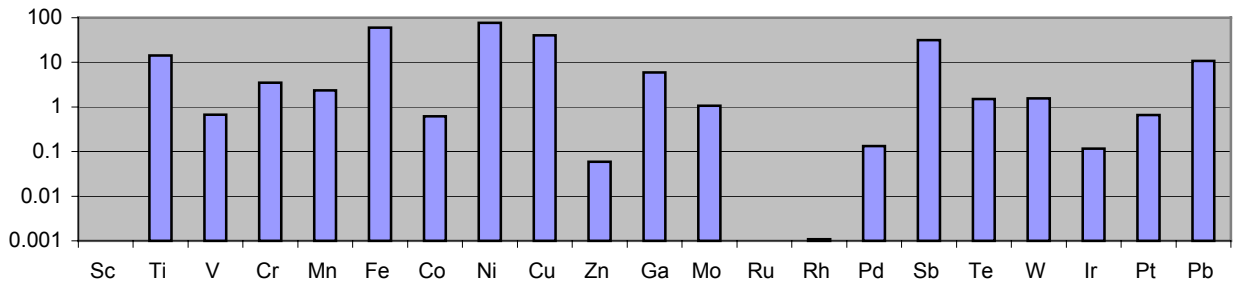
These irregular and equant flitters of intermediate thickness are between 1-2mm in size and display no rimming. Some folding can be seen on the photos below. Two broad groups can be seen on the Ag histogram. The sample as a whole can be distinguished from the other Rhine gold samples by its high Cu and Sb and low Pb. There seems to be one main trace element group containing M18-1, M18-3 and M18-4 while M18-2 has lower Cu concentrations.



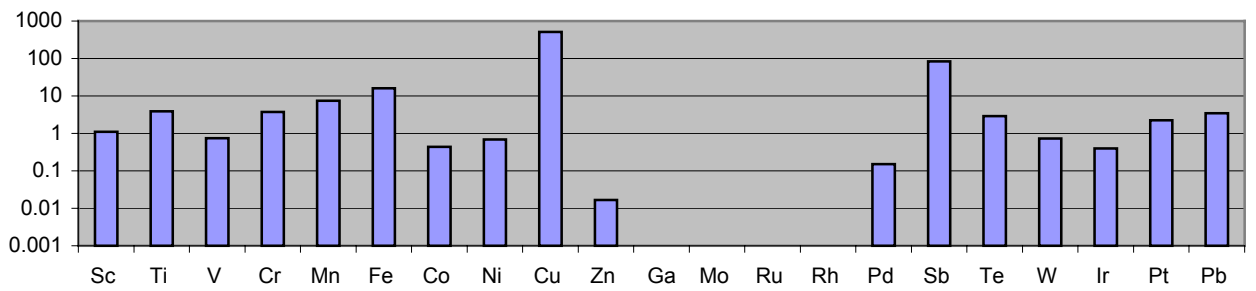
**M18-1**



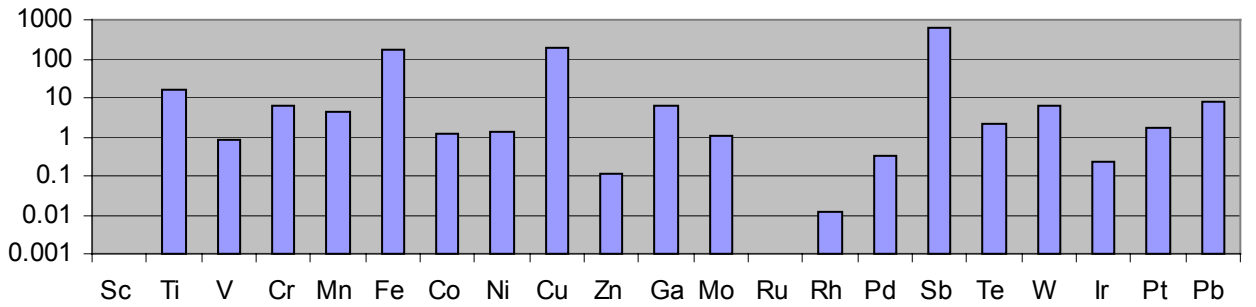
M18-2



M18-3



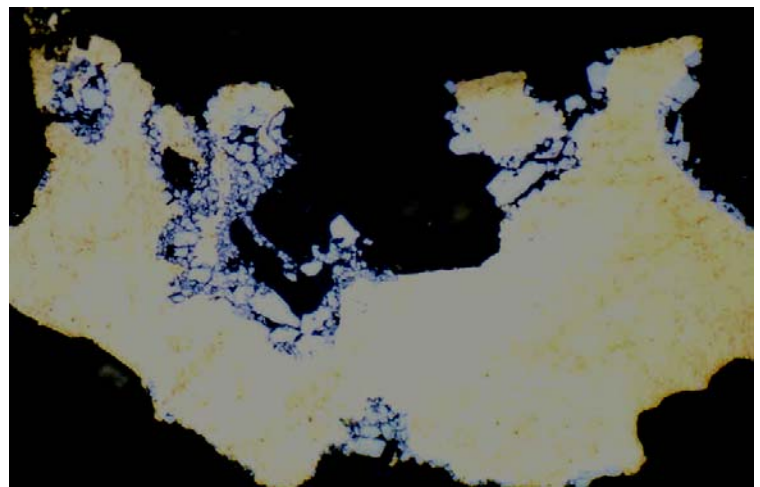
M18-4



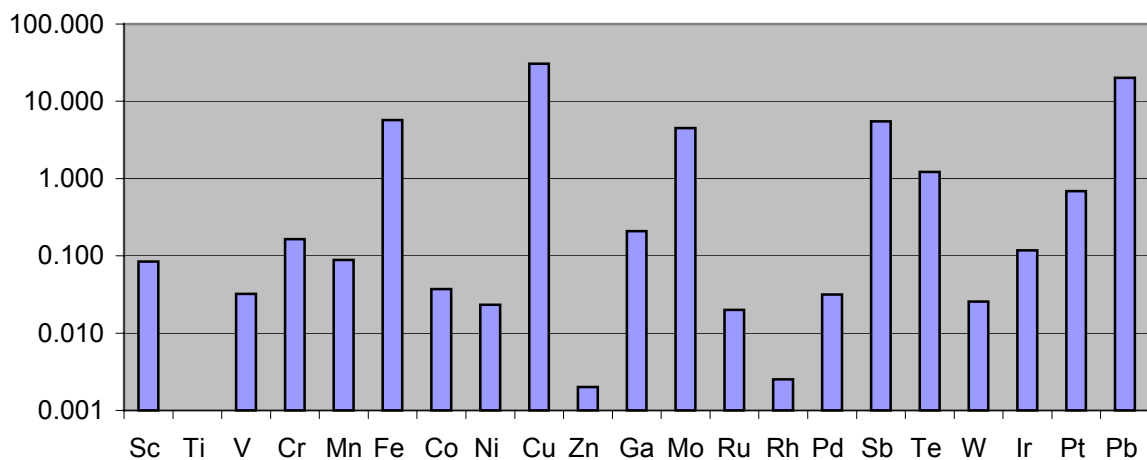
## Br-1: Laurieras, Limousin; French Massif Central

Gold crystals collected from quartz veins from an ancient mine, which is known to be of Celtic Origin. Gangue minerals include arsenopyrite, pyrite, fahlore, galena and sphalerite. Arsenopyrite and pyrite are the most common and appear to encrust the gold flakes. In the second photo on the right pyrite occurs as large white euhedral crystals and arsenopyrite as much smaller crystals surrounding the gold. Within the gold, sphalerite inclusions were found with Cu contents of up to 0.5wt%.

As expected for a lode gold sample it has a very consistent trace element pattern, considering tri-plots of W, Ir & Pd and Pt, Cu & Pb (Gold Chapter). One grain shows a higher Cu concentration and this probably reflects the ablation of one of the sphalerite inclusions mentioned above. Of note is the total lack of Ti from the total trace element pattern below.



Br-1

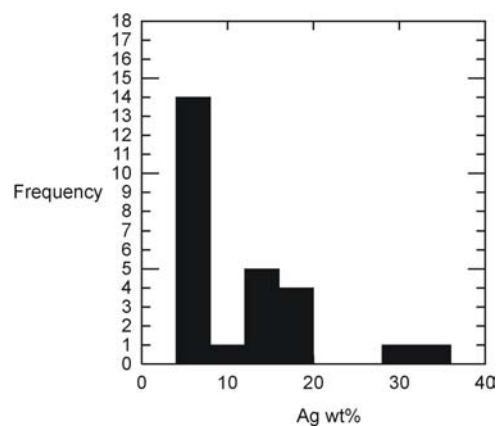
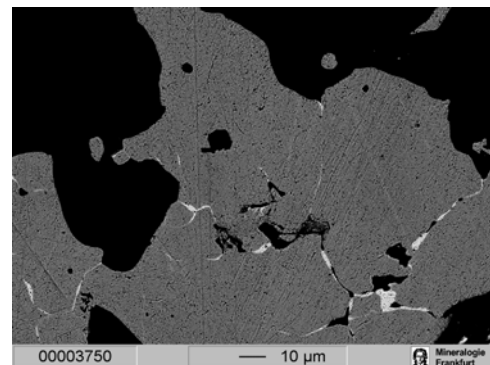
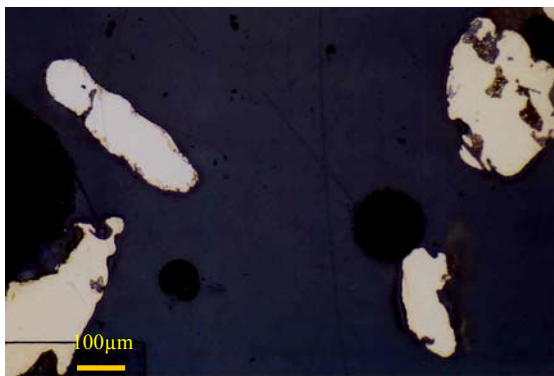
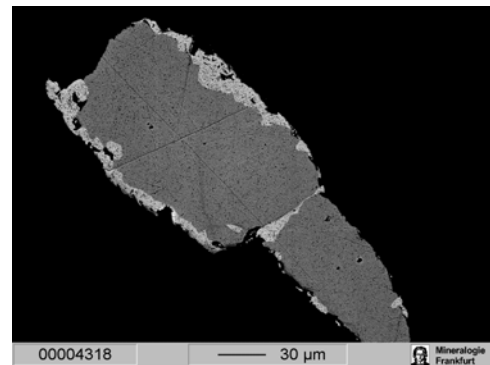
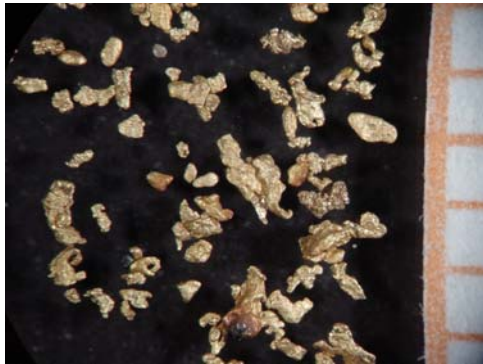




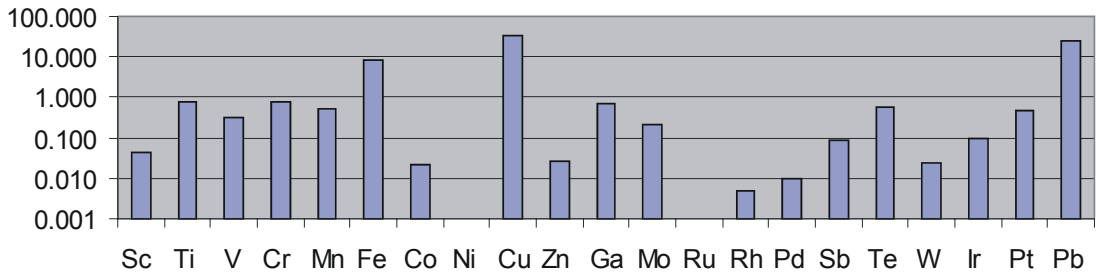
## Br-2: Kergal –Bretagne; Armorican Massif

Rounded thin flitters and grains with elongate and complex shapes from 0.1 to 1.0mm in size. Many grains contain inclusions of quartz within them, which may relate to the primary mineralisation, with many other quartz, feldspar and Fe-oxide inclusions embedded around the edges. Most display rimming although it is generally patchy. The grains with higher silver contents have the most well developed rimming. Higher silver grains appear starkly white in comparison to the more gold rich grains under a reflected light microscope. There are three main groups based on the Au/Ag ratios (histogram below).

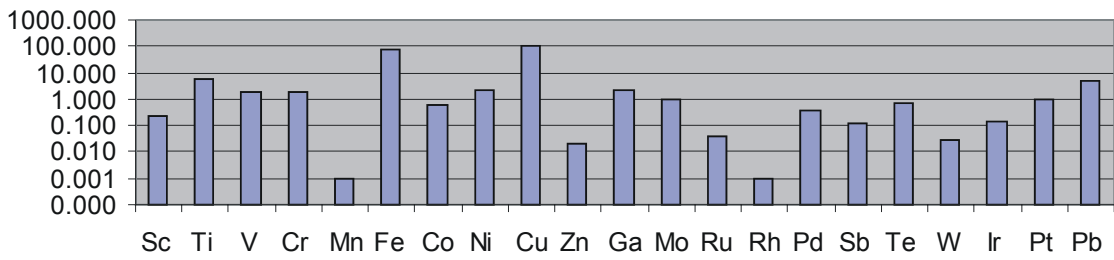
The trace elements form a reasonably characteristic group on the W, Ir & Pb tri-plot (with two different subgroups) while on the Pt, Cu, Pb triplot they all appear more variable. The total trace element patterns (below) show that the Ag rich group (30% Ag) is the most different, lacking the lighter elements Sc, Ti, Cr and Mn that are present in the others.



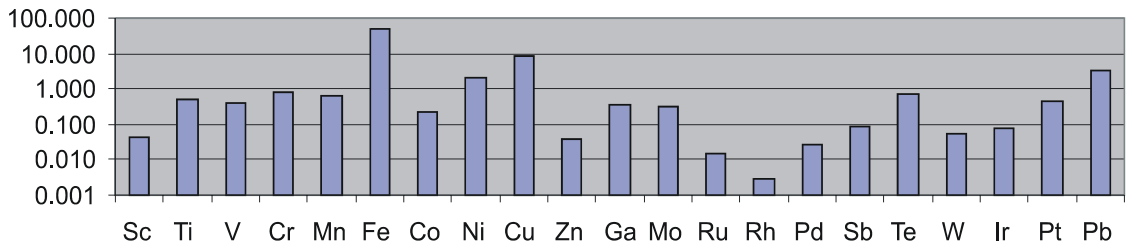
Br2-1 5% Ag



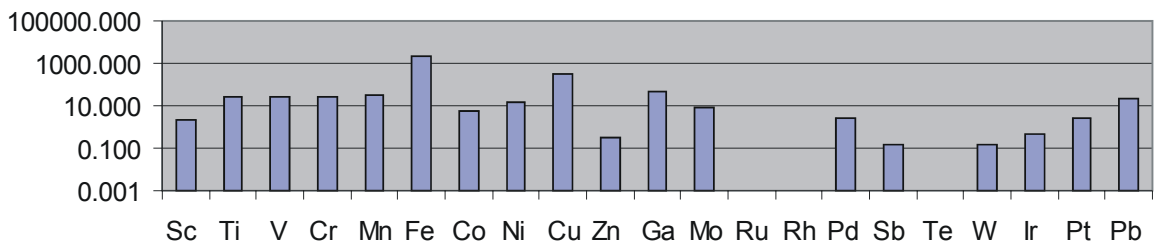
Br2-2 7% Ag



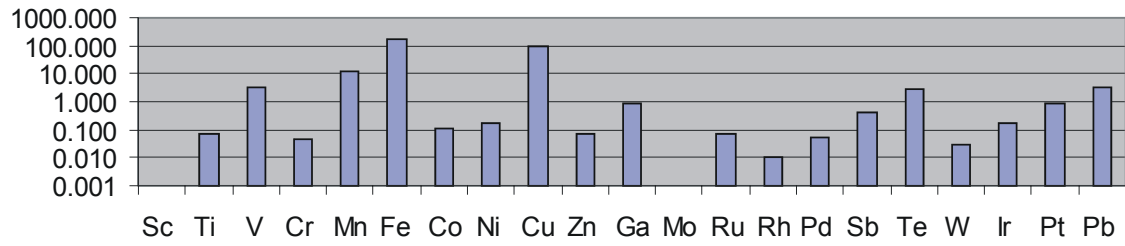
Br2-3 8%Ag



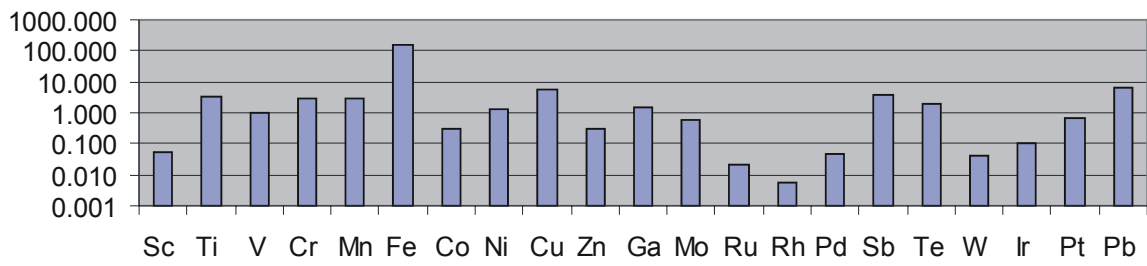
Br2-4 13% Ag



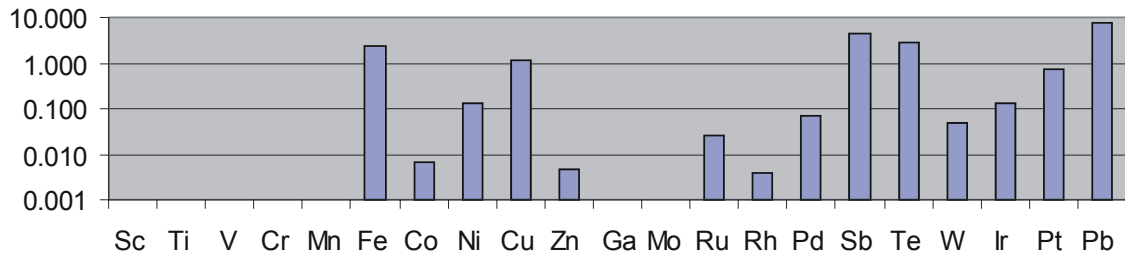
Br2-5 16% Ag



Br2-6 19% Ag

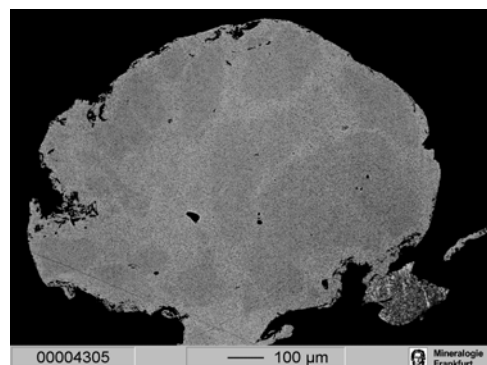
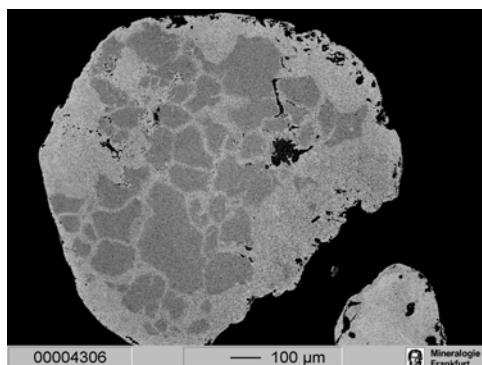
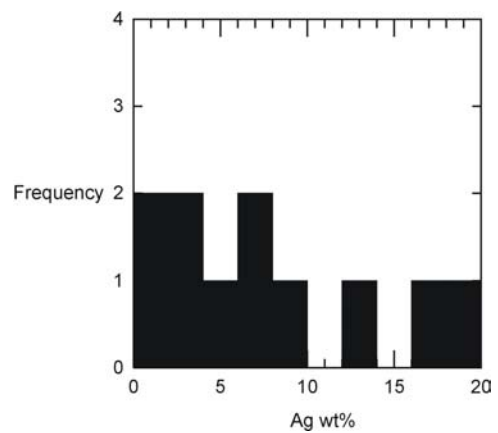
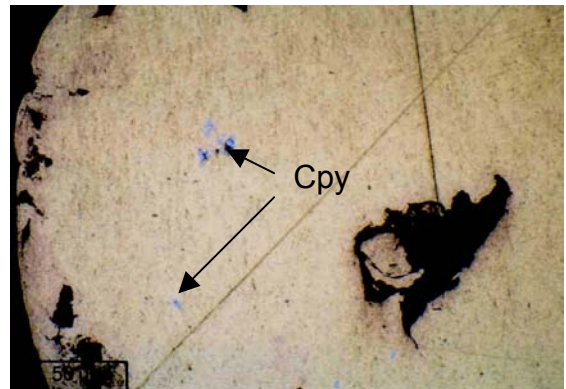
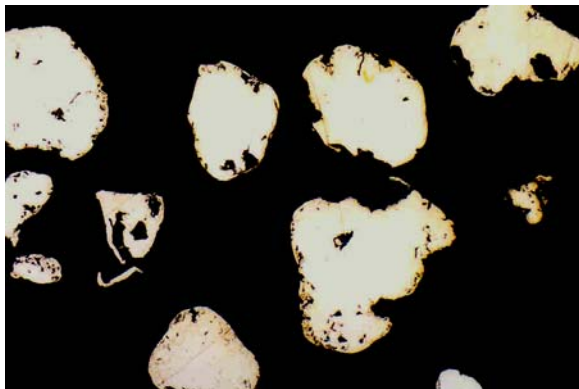


Br2-7 30% Ag

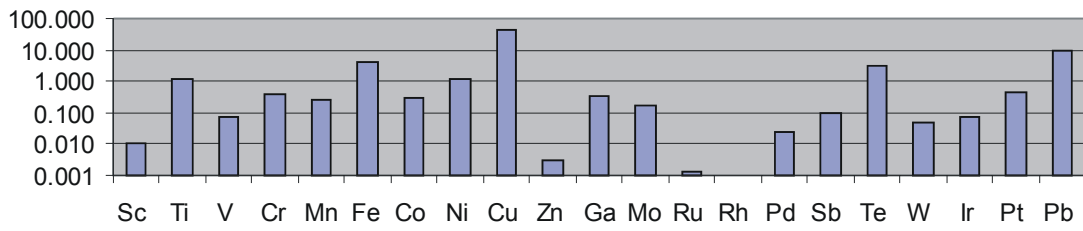


### Br-3: Céze, Gard (RocheGude); flows from French Massif Central

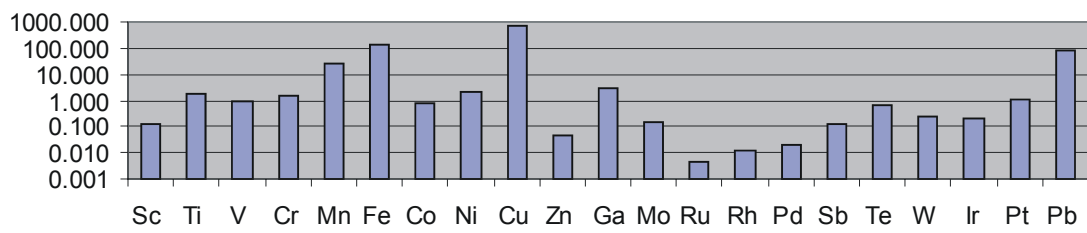
This sample is composed of thin rounded flitters with equant and complex habit. They all show rimming and many contain pyrite and chalcopyrite inclusions. The histogram of the Ag wt% shows up to four possible groups. This sample shows a fairly consistent signature on the W, Ir, Pd tri plot (Gold Chapter), with two distinctly different subgroups; Br3-4 and Br3-6. Considering the total trace element patterns (next page) Br3-4 is obviously different with a lack of Sc, Ti, V and Cr compared to the other subgroups. Br3-6 does not appear much different, possessing most of the elements that the other subgroups have, but it is the most Ag rich (24% Ag).



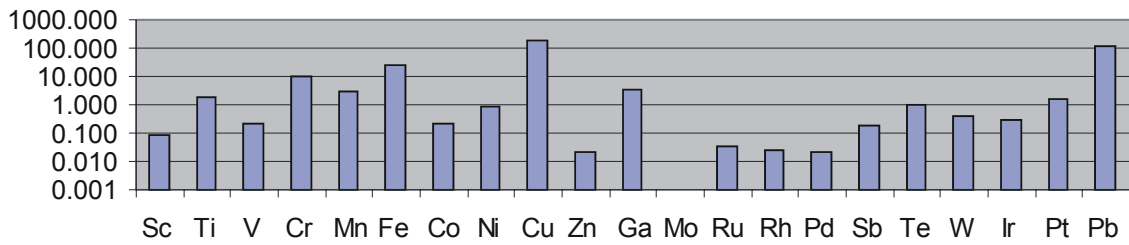
Br3-1 2% Ag



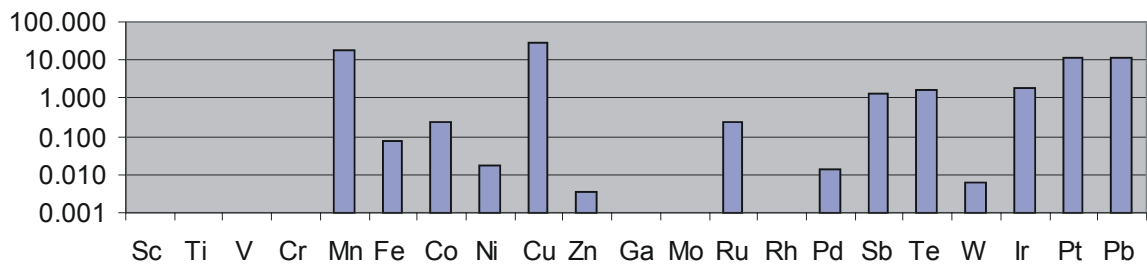
Br3-2 6% Ag



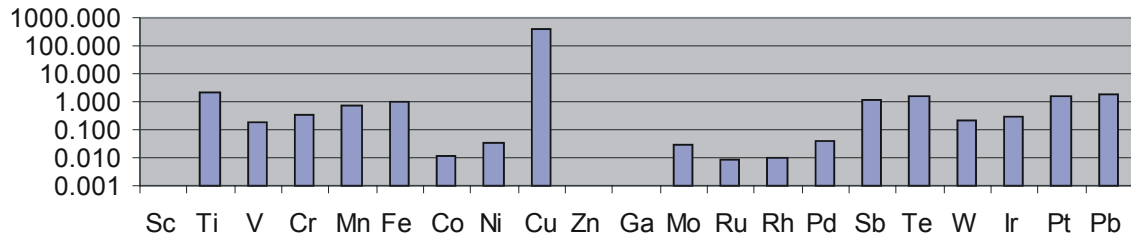
Br3-3 9% Ag



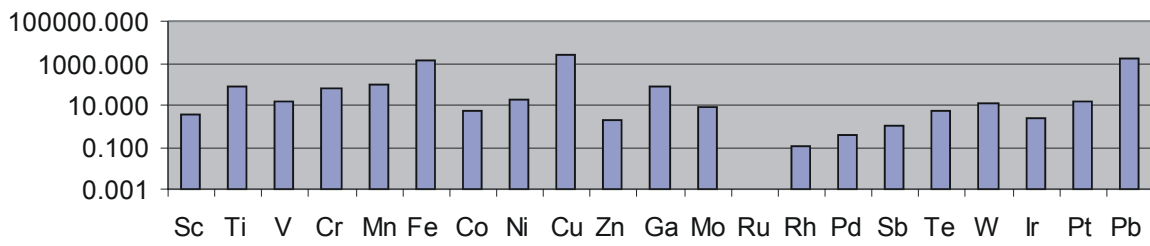
Br3-4 11% Ag



Br3-5 16% Ag

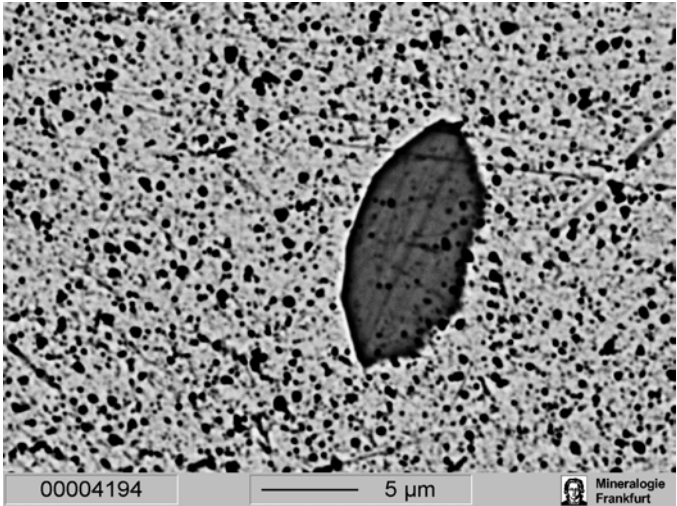


Br3-6 24% Ag

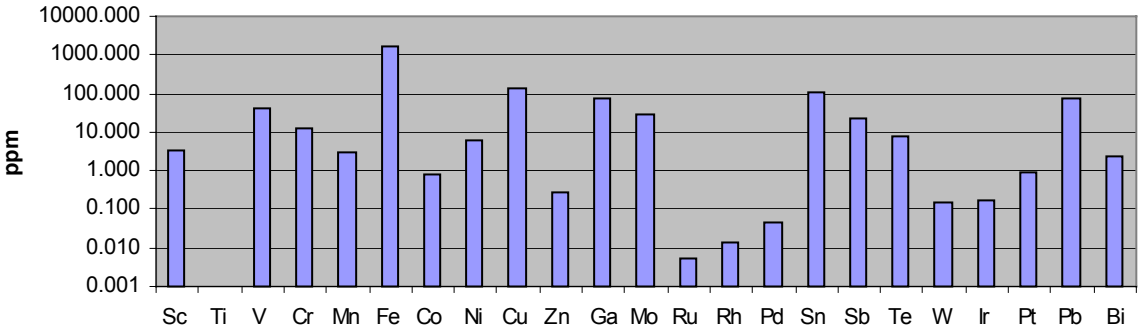


**Br-4 Massotais -Les Tailles (Baraque Fraiture)**

From quartz veins in an ancient mine dated to the late roman period ~450AD but with architecture thought to be of Celtic origin (pers comm. Dr. Veronique Hurt). Inclusions of telluride and pyrite.



Telluride Inclusion



## Br-5: Gardon Lézan -Gard      Flows from the French Massif Central

Contains rounded thin equant and complex grains 0.3 to 1.5mm with well developed rimming. Inclusions of galena (Fig. 3) were observed in four of the grains. One main group is shown on the histogram representing Ag wt% compositions of ~ 7-11 wt% with a possible subgroup of more Au-rich grains ~2 % Ag. One grain is distinct with a Ag composition of 22.5wt% Ag.

On the W, Ir, Pb Triplot this sample forms a group, which overlaps with Br-3 in a W rich field. The trace element patterns pictured on the next page appear very similar.

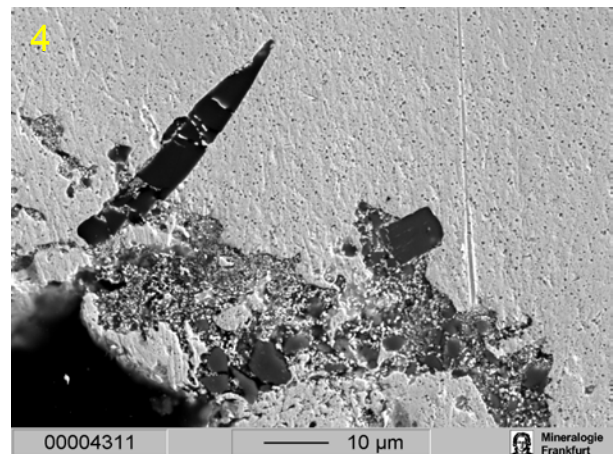
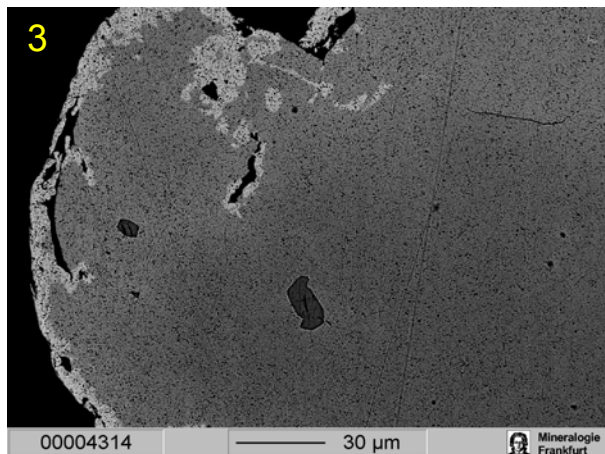
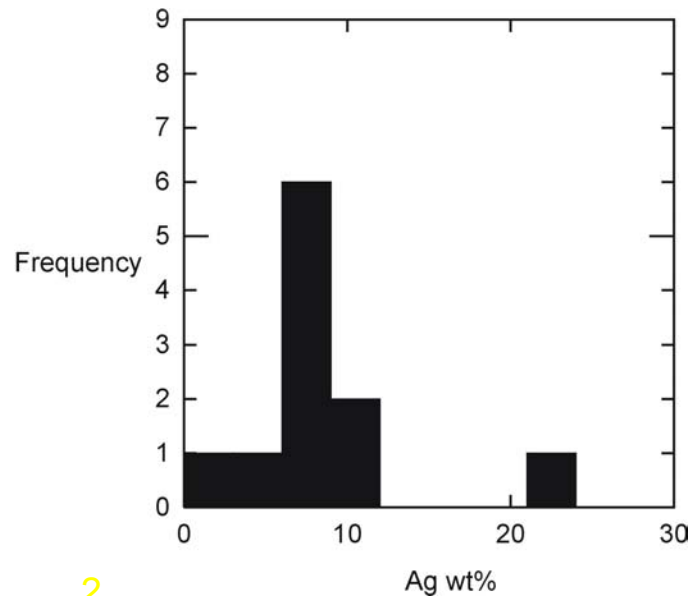
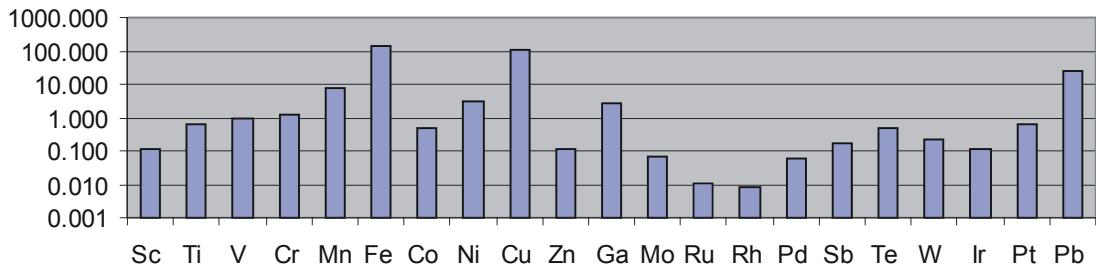


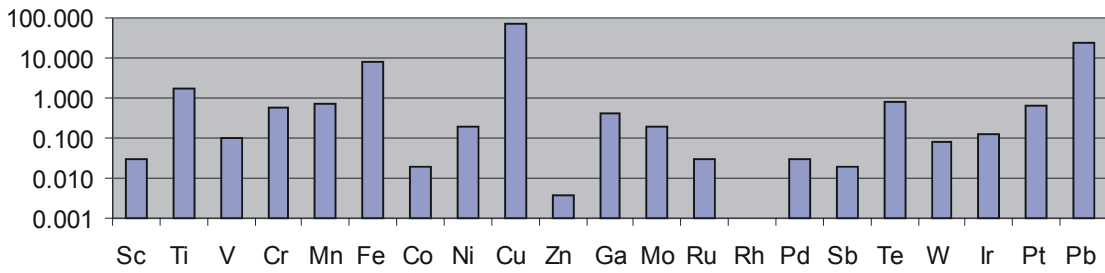
Fig 3 & 4: show inclusions of galena (3) rutile and quartz (4).



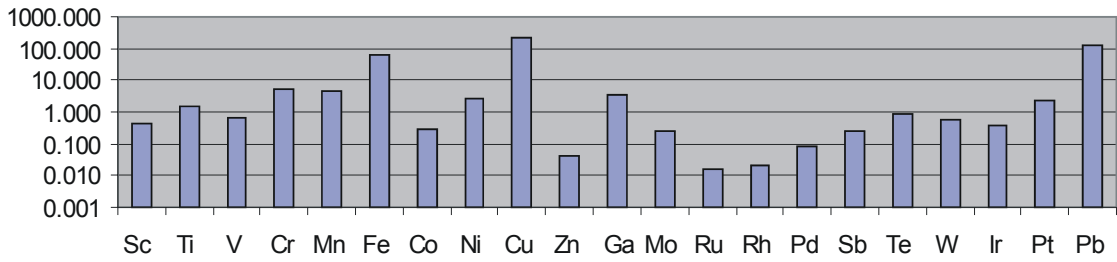
Br5-1 4% Ag



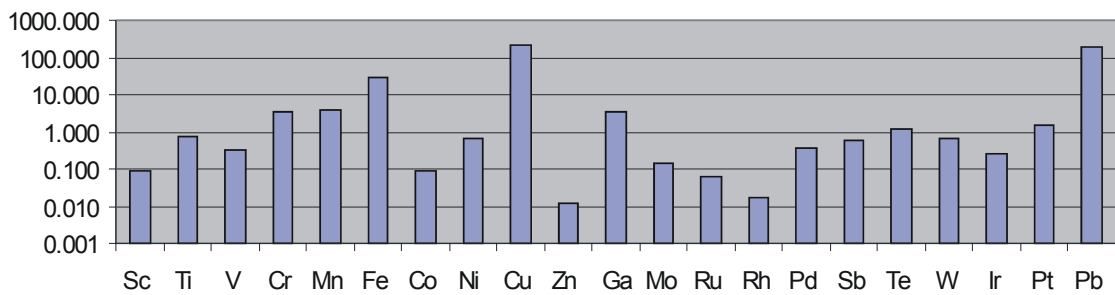
Br5-2 7% Ag



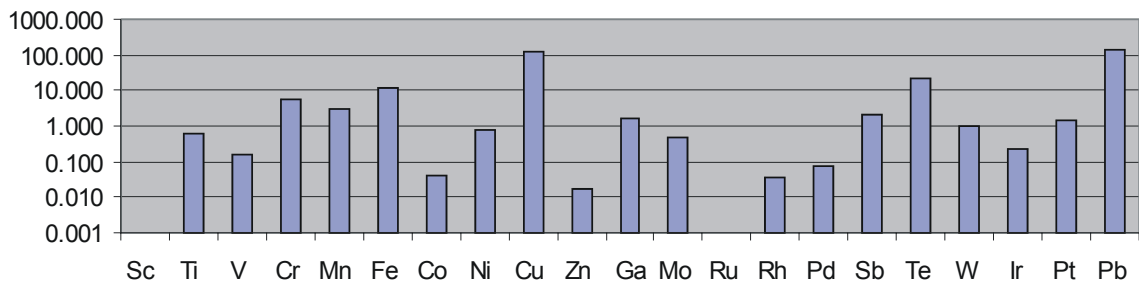
Br5-3 8% Ag



Br5-4 11% Ag



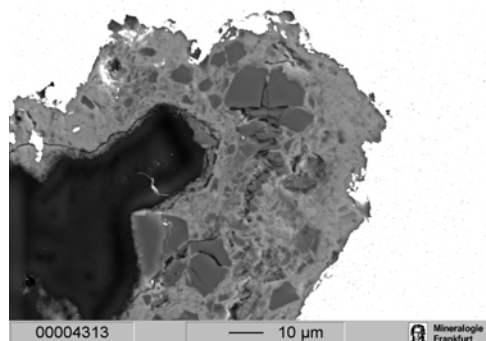
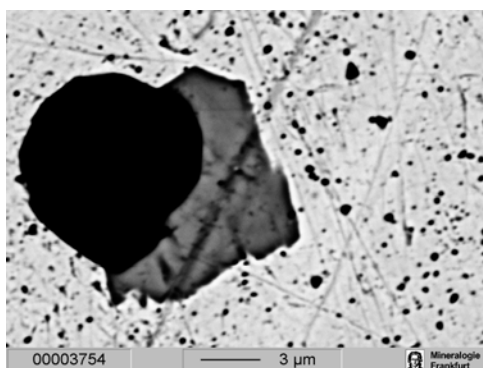
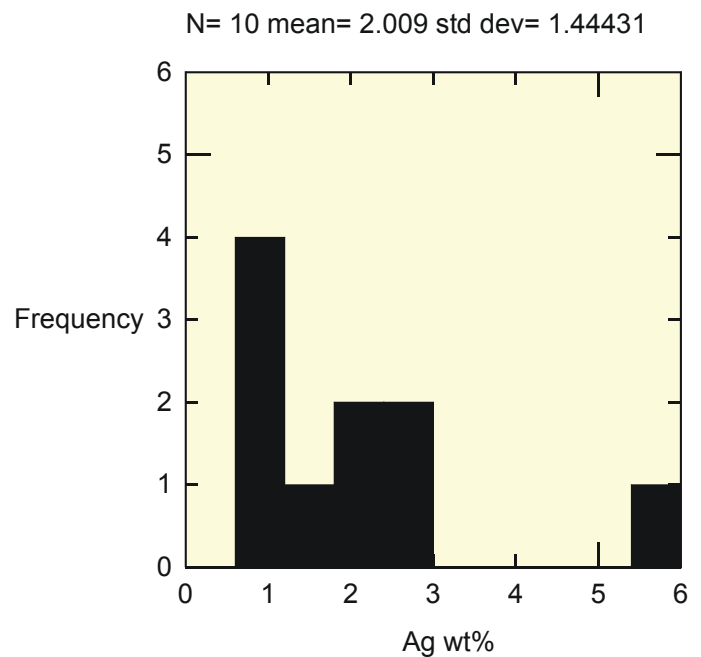
Br5-5 23% Ag



## Br-6: Ru De Poteau, Recht

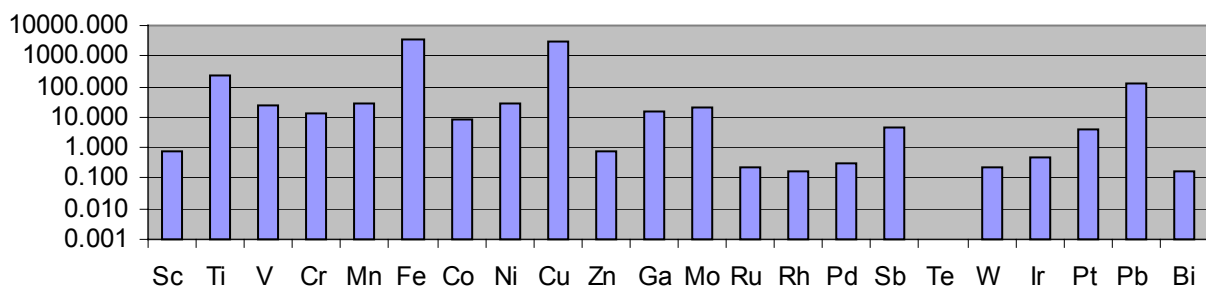
These irregular to rounded grains have complex and some slightly branched outlines and are 0.2 to 1.0 mm in size. Two, perhaps three groups are possible considering the Ag compositions (Histogram). The grains contain galena inclusions and show features on the edge of the grains, which have the form of pyrite or galena but are now filled with Fe-oxide and quartz.

The triplot of Pt, Cu and Pb shows that Br6-2 and Br2-3 are very similar, that Br6-4 contains a little bit more Pb or less Cu and that Br6-1 is very different. This reflected perfectly by the trace element patterns below.

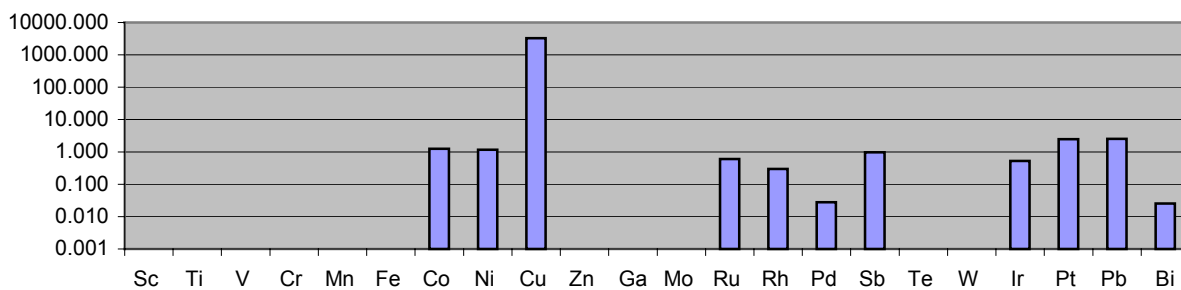


The compositional scans shown here show galena (left) and Fe-oxides with quartz embedded in them (right). The form of the Fe-oxides suggests that they are the weathering products of sulphides, possibly pyrite.

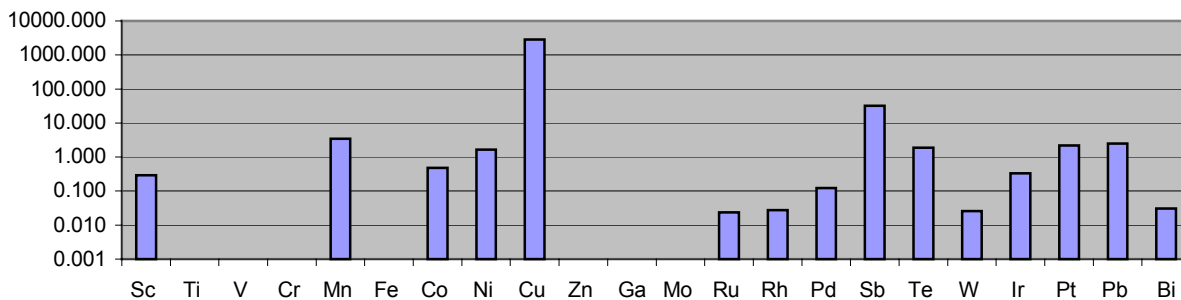
Br6-1



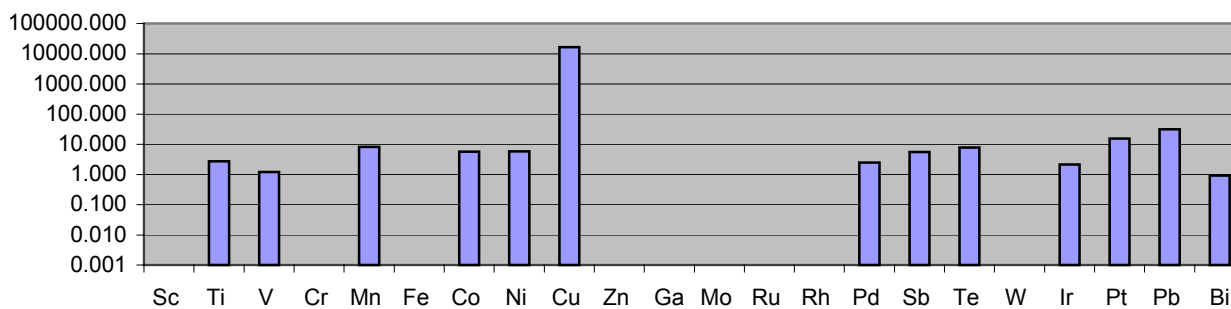
Br6-2



Br6-3

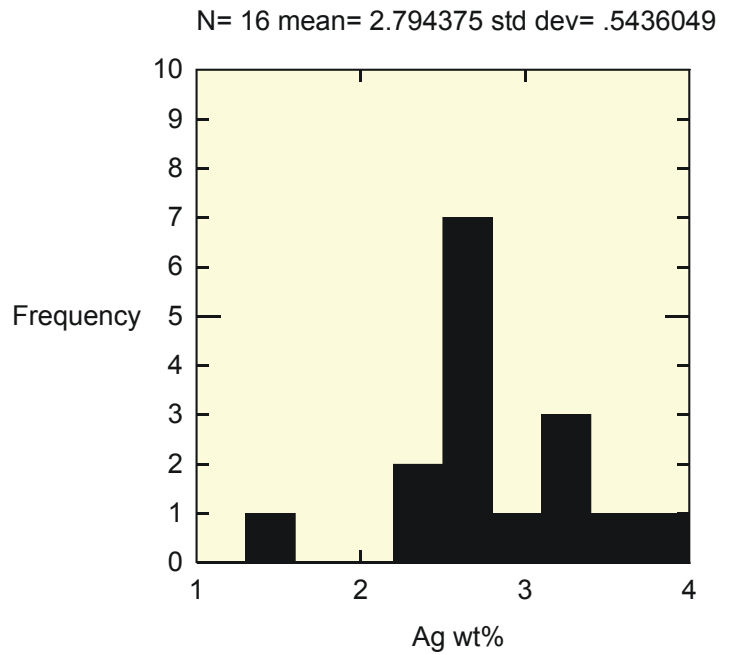


Br6-4

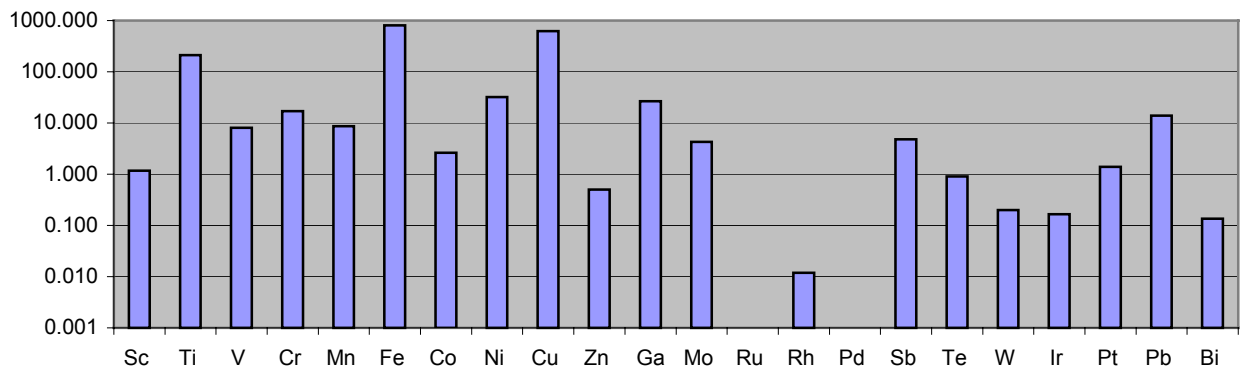


**Br-7: Schinderbach, Amel.**

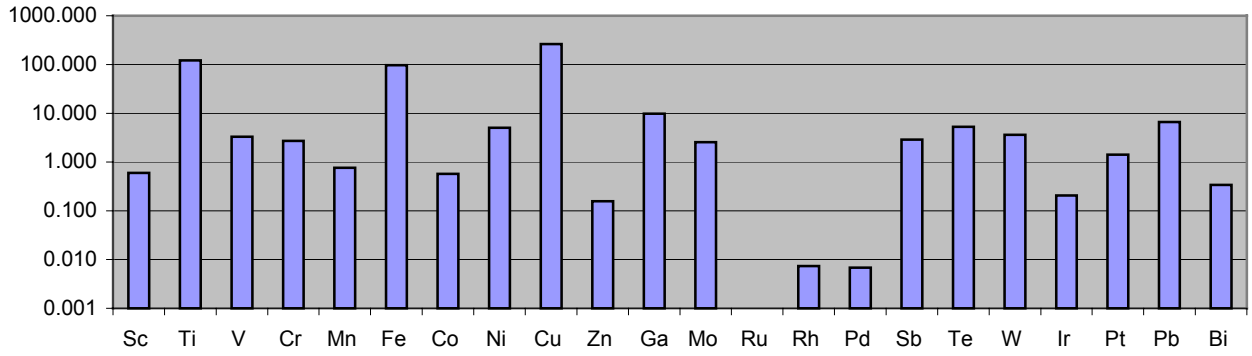
Irregular grains with elongate and complex shapes, they display no rimming. Inclusions include feldspar, quartz and rutile embedded in the edges. There could be two or three groups represented by their silver compositions. Trace element analysis has revealed three groups. On a tri-plot of Cu, Pt and Pb sample Br-7 is shown to form a loose group of three points (including two very similar points) while the fourth contains more copper. Visual comparisons of their entire trace element pattern reveals that groups Br7-1 and Br7-2 look very similar. Br7-3 looks similar to the first two but it lacks Cr, Ga, Mo and Ni. Br7-4 is the most different with no Ti, V, Cr, Mn, Fe, Ni, Ga, Mo, Rh and W.



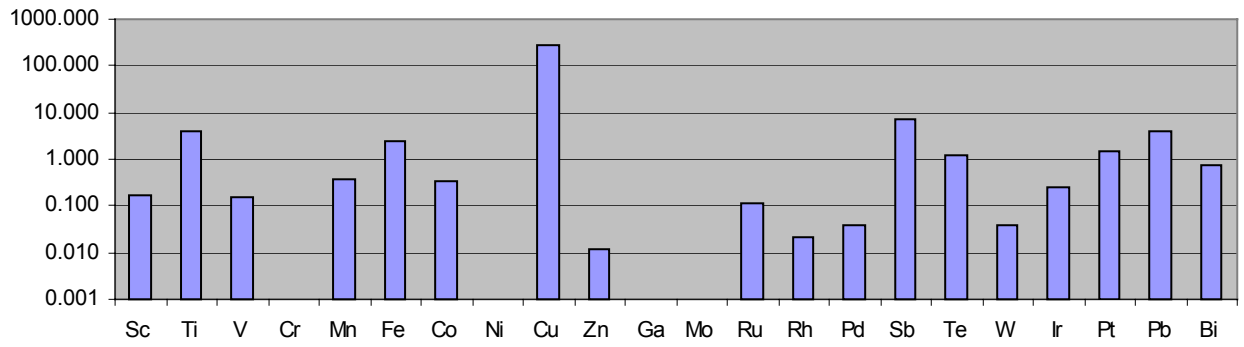
**Br7-1**



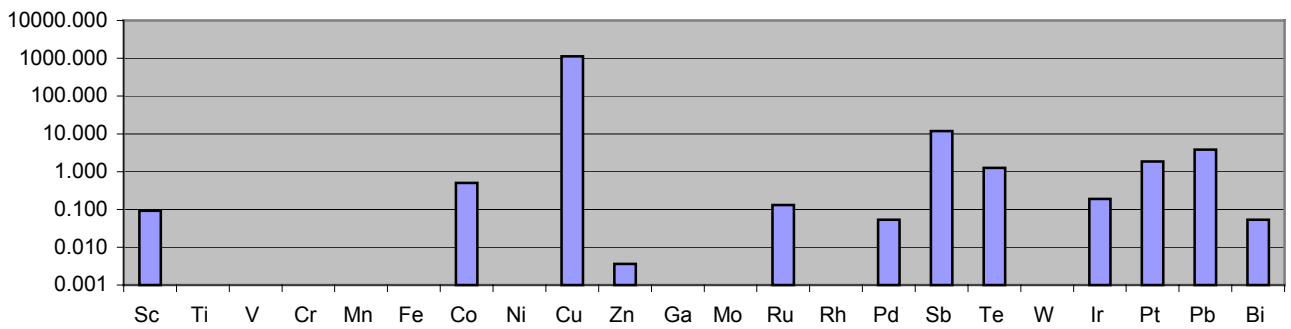
**Br7-2**



**Br7-3**



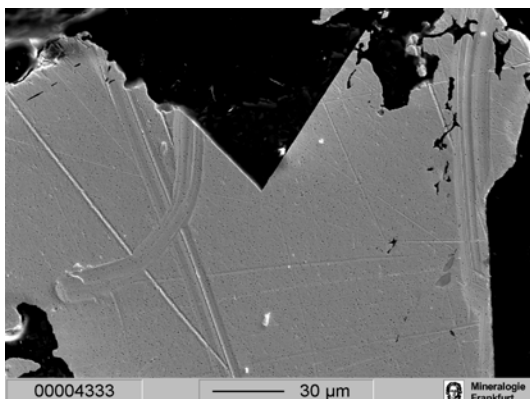
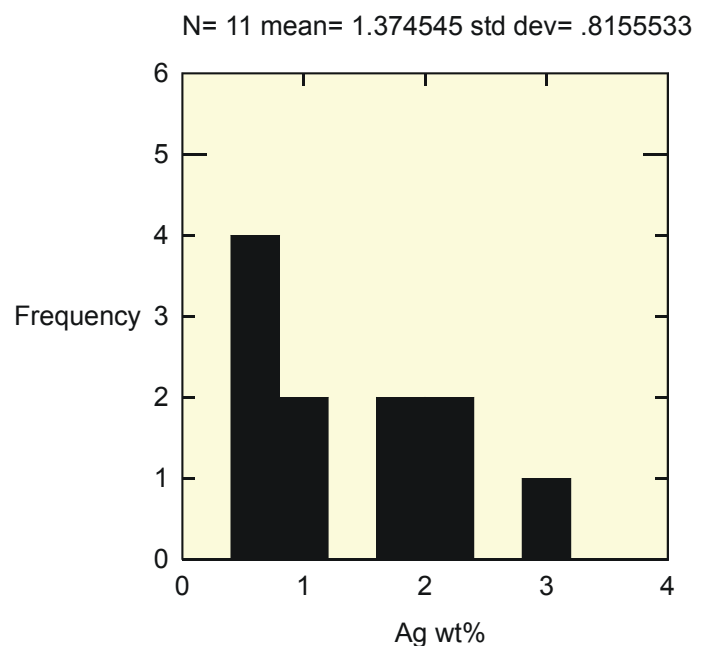
**Br7-4**



## Br-8: Vague Des Gommets ( Rau Du Moulin) –Suxy

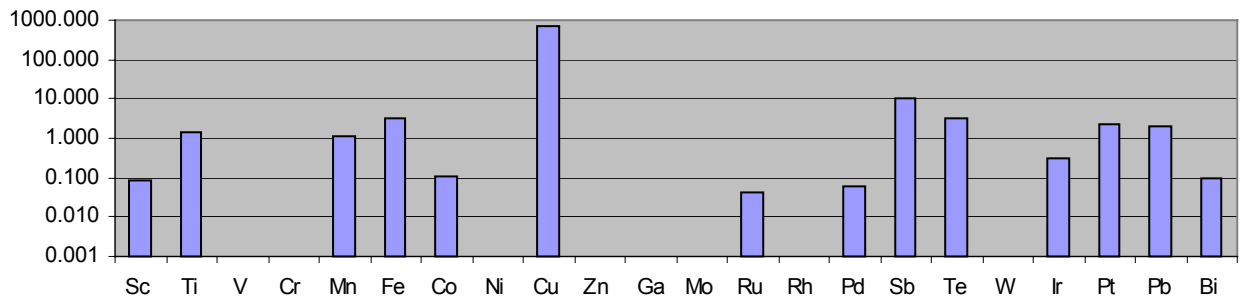
The surface is very friable and the angular to irregular flitters and grains display complex and branched outlines. Many of the grains contain sulphides, mostly galena, and one grain shows where a galena was probably removed from the edge (see SEM photo below). There is no rimming developed and the overall impression is one of very limited transport.

There appears to be three groups of grains within a limited range of silver compositions and these three groups are also characterised by the trace element patterns. Group Br8-1 can be characterised as containing no V, Cr, Ni, Zn, Ga, Mo, Rh or W while Br8-2 contains all the elements (except with lower Ru and Pd) while Br8-3 is typified by its lack of the lighter elements Sc, Ti, V, Cr, Mn and Fe.

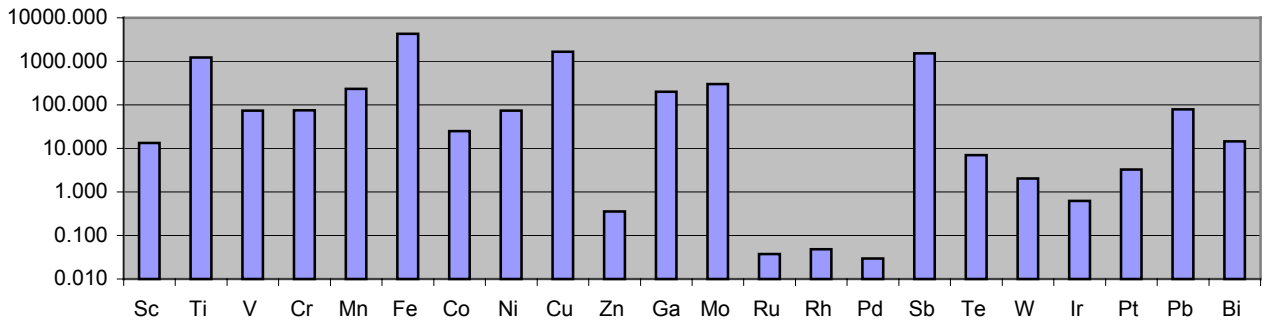


The sharp angle on the edge of this grain indicates that a sulphide mineral (galena or pyrite) once resided in this space.

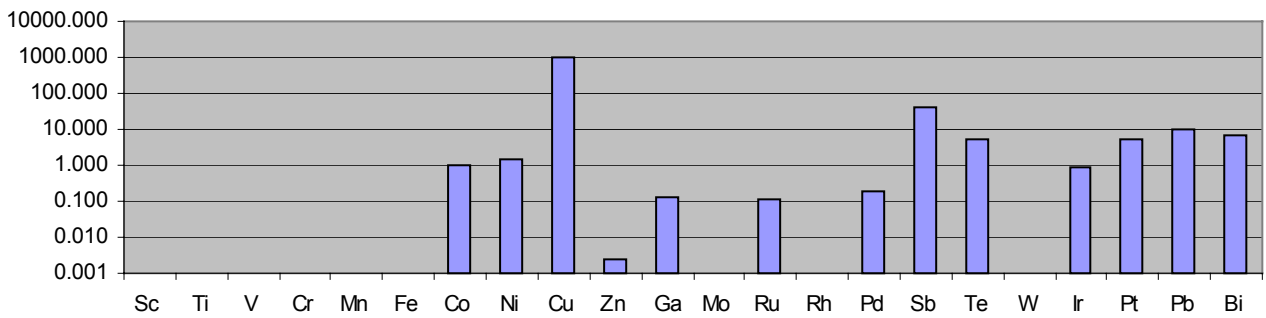
**Br8-1**



**Br8-2**

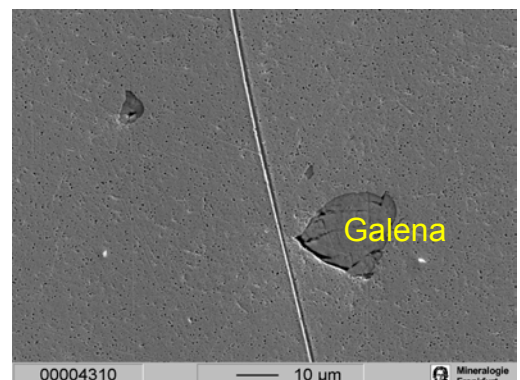
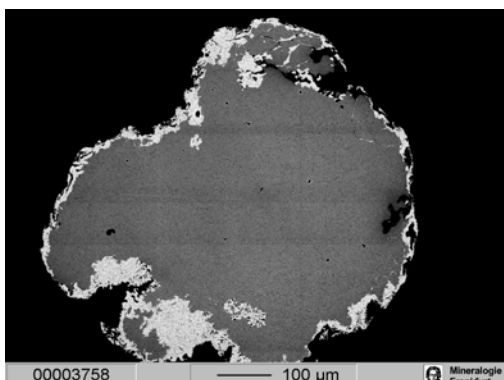
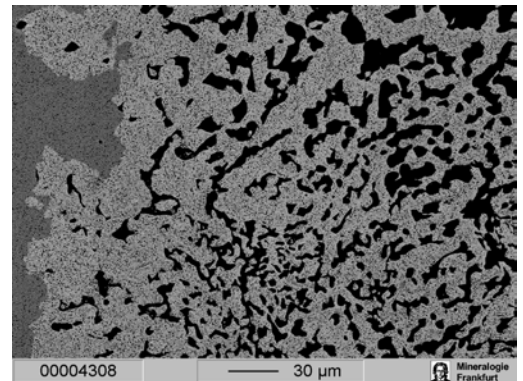
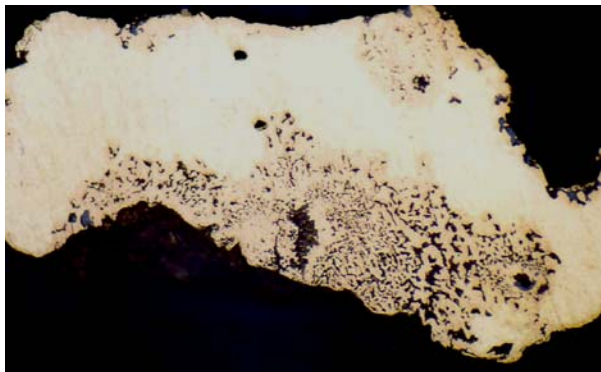
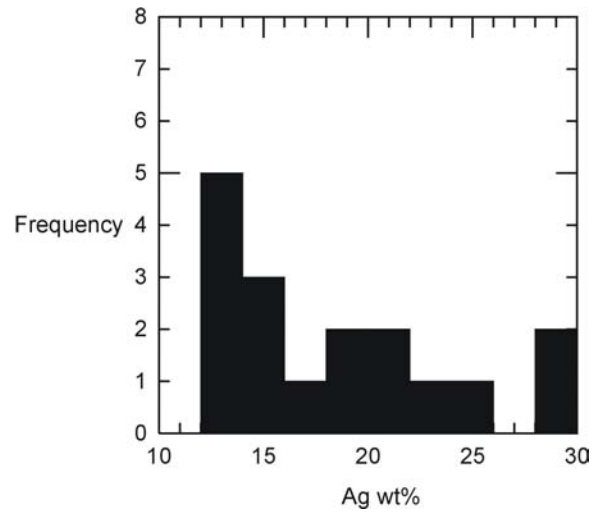


**Br8-3**



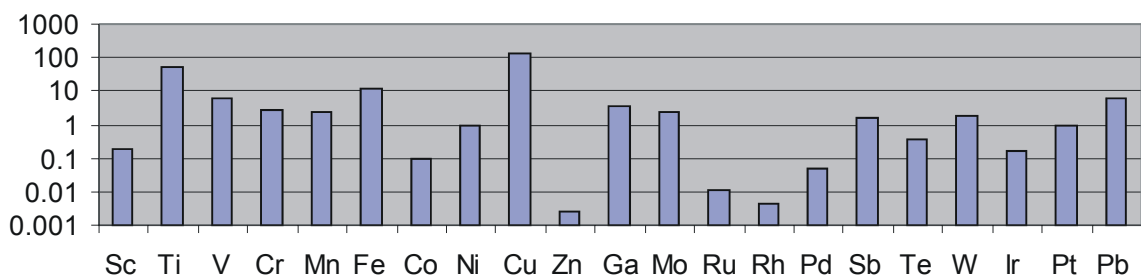
## Br-9 : Kildonan Burn.

These rounded to irregular flitters and grains have equant, complex and elongate shapes which are thin to intermediate in thickness and display well developed rimming. Inclusions include galena, feldspar, rutile and quartz. They can be distinguished by their relatively high W concentrations, which may also represent two subgroups.

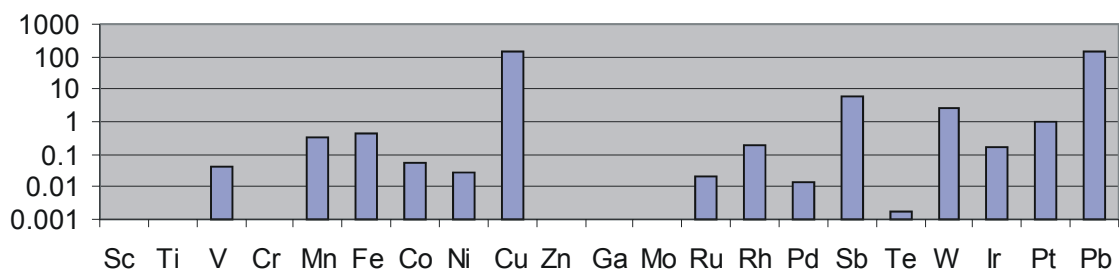




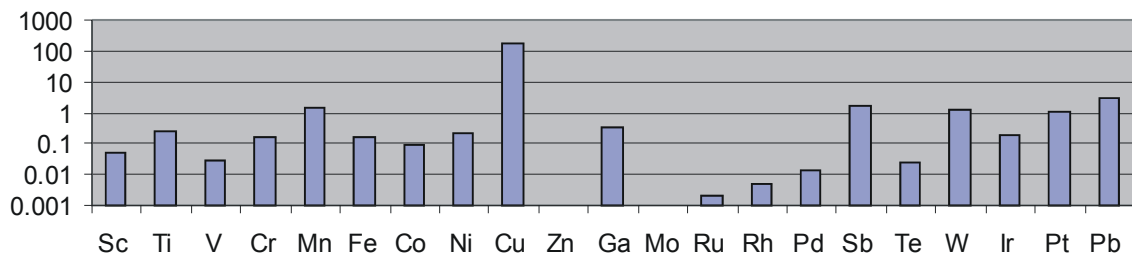
Br9-1



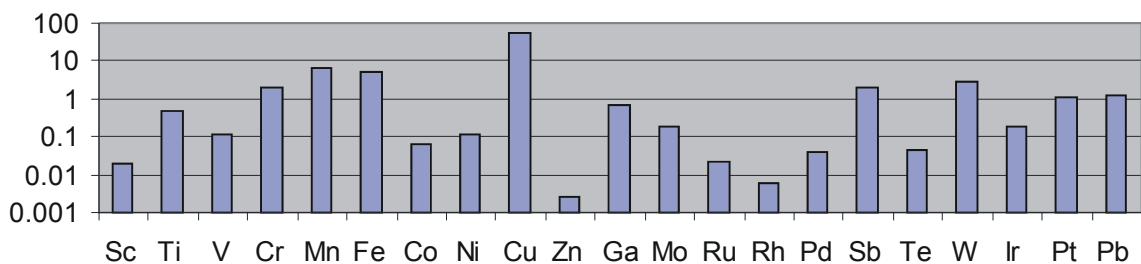
Br9-2



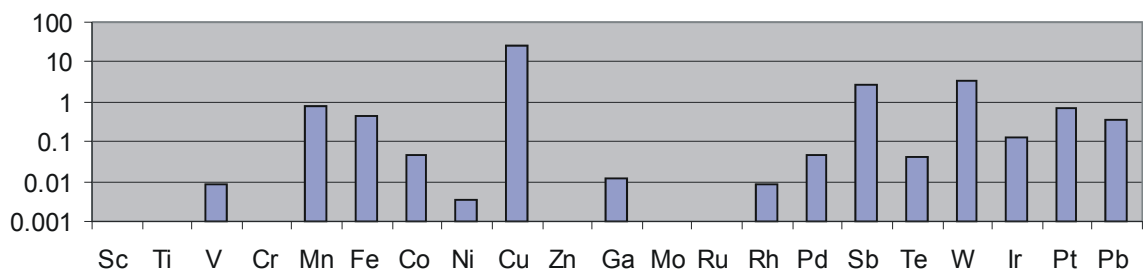
Br9-3



Br9-4



Br9-5



## Samples supplied by the Natural History Museum, Bern, Switzerland

Sample B7112: two polished sections from the Lukmanier Schlucht near Disentis, Swiss Alps. B7112A is a single grain, which contains inclusions of boulangerite.

Samples Gfont; 28 and 34: From Grosse Fontanne river, Napf area, Molasse Basin, Central Switzerland. Detrital gold in tertiary sediments.

Sample Ratoche41: A single large gold grain from the Rotache River, near Thun, Switzerland. Found in the same geological association as samples 28 and 34.

Samples Camedo; 20, 21 and 22: These samples are made up of small gold grains from Camedo, Centovalli, Ticino, Southern Switzerland. This gold maybe partially derived from the ultramafic Ivrea complex. The group 2 gold grains from Comedo 20 are Cu-Au alloys which also display high Pt concentrations of over 18.5ppm Pt.

Sample	Au	Ag	Cu
B7112A	82,27	17,72	b.d.
B7112B	81,37	18,62	0,01
Ratoche41	91,19	8,73	0,08
Gfont28	97,34	2,36	0,30
Gfont34	95,67	4,31	0,03
Camedo21	92,00	7,95	0,05
group 1	95,98	3,94	0,08
group 2	93,53	6,44	0,03
group 3	84,34	15,63	0,01
Camedo20	88,56	3,81	7,64
group 1	90,44	9,53	0,04
group 2	86,68	0,37	12,96
Camedo22	82,02	7,96	0,02
group 1	90,40	9,59	0,01
group 2	94,77	5,19	0,04
group 3	79,52	20,48	b.d.

Table 1. Quantitative measurements of the Au, Ag and Cu concentrations (given as % composition) produced on the electron microprobe. The figures shown here are an average of 10 analyses made on each sample. The Camedo samples are made up of a number of gold grains, which form groups based on composition, and which are shown separately with their aggregate compositions represented along side the sample name.

**Appendix 3: Averaged EPMA results of the coin alloy measurements. (Wt%)**

<b>Coin</b>	<b>Au</b>	<b>1<math>\sigma</math></b>	<b>Ag</b>	<b>1<math>\sigma</math></b>	<b>Cu</b>	<b>1<math>\sigma</math></b>	<b>Sn</b>	<b>1<math>\sigma</math></b>	<b>Pb</b>	<b>1<math>\sigma</math></b>
Sch23Rob	71.51	2.19	22.22	1.53	6.11	1.24	0	0	0	0
fo166	72.63	0.27	19.59	0.7	7.6	0.71	0.02	0.01	0.02	0.01
Fo117	79.58	0.18	15.47	0.26	4.77	0.16	0	0	0	0
FUG122	27.37	1.29	43.57	4.6	28.91	3.38	0	0	0.05	0.1
FUG121	34.93	0.98	42.15	3.8	22.83	2.82	0	0	0	0
fo105	26.51	5.46	45.52	7.36	27.65	11.91	0	0	0.15	0.21
2950	35.72	1.12	43.49	2.56	20.66	2.13	0	0	0	0
3321	27.55	0.86	45.86	1.06	26.41	0.54	0	0	0.07	0.11
stw4	33.38	2.13	43.56	4.31	22.98	2.51	0	0	0	0
87150	0.91	0.16	67.29	7.34	27.65	7.84	3.34	1.67	0.19	0.16
FUG93	25.13	4.76	67.39	4.05	6.87	2.01	0	0	0.41	0.35
Sch16G77	16.75	1.77	50.18	10.89	32.84	9.16	0.08	0.17	0.08	0.08
9800b	23.53	0.97	70.43	0.99	5.84	0.77	0	0	0.04	0.09
stw4a	31.24	1.95	63.66	1.78	4.9	0.89	0	0	0.02	0.03
regen	47.62	2.52	38	1.67	14.34	2.04	0	0	0.03	0.04
SFLAN1045	70.3	0.4	21.04	1.1	8.4	0.93	0.09	0.05	0	0
Fo124	52.22	0.38	35.89	1.33	11.76	1.18	0	0	0.01	0.01
8543	52.46	0.75	32.01	1.39	15.38	1.12	0	0	0	0
6124	64.82	0.37	23.59	1	11.46	0.94	0	0	0	0
22011	40.46	2.16	31.55	2.87	27.93	0.86	0	0	0.06	0.11
SFLAN507	51.55	0.38	33.75	2.16	14.65	1.91	0	0	0	0
LT8799	47.46	2	38.4	4.53	14	2.69	0	0	0	0.01
Lux7	44.56	0.32	42.19	0.95	13.14	0.68	0	0	0	0
22807	43.89	5.76	40.29	6.88	14.17	3.7	0	0	0.02	0.05
22809	41.41	1.9	44.89	6.14	13.63	4.44	0	0	0	0
30IVG176	40.46	0.44	41.32	3.5	17.97	2.98	0	0	0.12	0.09
30IV586	43.8	4.03	41.86	7.02	14.18	3.17	0	0	0.05	0.04
30IV329	37.69	0.66	43.47	3.37	18.57	2.72	0	0	0.1	0.05
30IV582	41.97	0.32	34.82	0.41	23.02	0.19	0	0	0.02	0.04
30IV575	36.99	0.79	39.88	4.45	22.83	3.59	0	0	0.14	0.09
87149	42.29	0.33	42.48	1.78	15.1	1.53	0	0	0.03	0.03
32243	21.38	7.51	50.43	27.69	28.09	20.84	0	0	0.03	0.04
32243	20.72	0.93	55.96	3.99	23.62	3.38	0	0	0.01	0.01
30V542	36.58	1.22	41.23	3.09	21.99	2.23	0	0	0.06	0.05

Coin	Au	1 $\sigma$	Ag	1 $\sigma$	Cu	1 $\sigma$	Sn	1 $\sigma$	Pb	1 $\sigma$
31087	37.82	1.66	40.15	4.69	22	3.25	0	0	0.03	0.03
Fo106	33.34	0.73	44.13	3.74	22.24	3.19	0.1	0.08	0.07	0.08
28323	34.9	1.53	41.8	4.54	22.29	3.32	0	0	0.21	0.17
22007	32.94	1.18	43.29	4.81	22.91	4.16	0	0	0.08	0.11
20163	33.45	0.81	40.45	1.25	25.55	0.85	0	0	0.06	0.1
22009	33.28	0.81	39.83	1.24	26.88	0.7	0	0	0.01	0.02
6719	35.77	0.82	37.09	1.2	27.02	0.6	0	0	0.02	0.03
lux3	34.03	1.42	38.48	2.02	27.15	1.09	0	0	0.16	0.37
30VG179	35.77	2.2	36.15	4.59	27.82	2.82	0.02	0.05	0.11	0.15
lux4	35.71	0.85	36.07	2.86	28.1	1.99	0	0	0	0
20409	37.42	1.26	32.88	4.04	29.68	3.1	0.02	0.05	0	0.01
12325	35.4	1.88	33.57	3.74	30.81	2.37	0	0	0.08	0.09
LuxV2	34.14	1.42	34.57	5.56	31	4.39	0	0	0.14	0.22
30V549	33.6	2.57	34.22	8.78	31.86	6.4	0	0	0.13	0.15
26827	35.39	2.7	30.73	6.74	32.51	4.71	0	0	0.1	0.11
22006	33.71	2.74	32.14	7.19	32.57	5.03	0	0	0.16	0.16
22113	34.83	2.09	32.3	6.6	32.64	4.73	0	0	0.24	0.16
22010	36.89	4.22	29.33	7.63	33.4	4.84	0	0	0.06	0.08
Lux5	33.77	1.24	31.55	5.81	34.14	4.7	0	0	0.18	0.13
19697	28.52	1.49	32.62	6.02	38.48	4.65	0	0	0.38	0.21
19698	30.26	1.6	27.88	6.69	41.6	5.48	0	0	0.26	0.23
8544	28.18	1.8	25.71	4.88	45.2	4.09	0.47	0.09	0.13	0.09
21931	19.28	0.77	24.29	5.09	51.94	5.17	4.34	1.22	0.16	0.13
22008	18.57	0.5	16.43	6.61	63.29	6.68	2.05	0.76	0.08	0.09
8544	0.05	0.04	0.82	1.07	98.54	1.01	0.38	0.05	0.05	0.08
26227	34.33	1.57	36.29	6.59	30.33	6.04	0	0	0.19	0.09
30449	36.98	1.47	24.46	5.1	38.53	3.73	0	0	0.04	0.07
20397	35.1	2.03	21.57	7.63	43.2	5.78	0	0	0.13	0.18
LuxVI1	35.05	0.88	23.21	3.77	41.47	2.99	0	0	0.02	0.05
LUX6	17.48	5.07	17.92	5.51	64.25	6.85	0.03	0.03	0.03	0.05
SFLAN3000	90.21	0.14	7	0.2	2.45	0.25	0.08	0.03	0	0
SFLAN1148	50.35	0.9	30.33	1.96	19.14	2.57	0	0	0.01	0.01
Flan	53.12	0.4	31.01	1.1	15.23	0.93	0	0.05	0	0.01
26227	33.12	6.65	32.1	24.25	34.51	17.69	0.06	0.02	0.11	0.15

**Appendix 4: EPMA results of gold samples**

<b>Sample</b>	<b>Sb</b>	<b>1<math>\sigma</math></b>	<b>As</b>	<b>1<math>\sigma</math></b>	<b>Pb</b>	<b>1<math>\sigma</math></b>	<b>Cu</b>	<b>1<math>\sigma</math></b>	<b>Bi</b>	<b>1<math>\sigma</math></b>
M1-1	0.03	0.04	0.01	0.02	0	0	0.01	0.01	0.12	0.04
M1-2	0.02	0.01	0	0.02	0	0	0.01	0.01	0.12	0.02
M1-3	0.04		50.32		0.02		0		0.07	
M1-4	0.01	0	0	0	0.02	0	0.01	0.01	0.13	0.03
M1-5	0.08	0.02	0.01	0.02	0.11	0.15	0.01	0	0.14	0.01
M1-6	0.05	0.02	0.01	0.01	0.09	0.1	0.01	0.01	0.09	0.03
M1-12	0.06	0	0	0	0	0	0	0	0.11	0.04
M12-1	0	0.01	0.01	0	0	0	0.01	0.01	0.1	0.02
M12-2	0.01	0.01	0	0	0.07	0.03	0.03	0.04	0.08	0.03
M12-3	0.06	0.02	0	0	0.09	0.05	0	0	0.12	0.01
M12-4	0.04	0.02	0	0	0.04	0.06	0.02	0.01	0.11	0.07
M12-5	0.03	0.01	0.01	0	0.13	0.02	0.01	0.02	0.1	0.08
M12-6	0.01	0.02	0	0	0.01	0.01	0.01	0.01	0.16	0.01
M12-7	0.05	0.03	0	0	0	0	0.11	0.04	0.07	0
M12-8	0.05	0.01	0	0	0	0	0.66	0.02	0.07	0.07
M12-9	0.04	0	0	0.01	0	0	0.01	0.02	0.09	0.04
M4-1	0.01	0.01	0	0	0	0	0	0	0.06	0.01
M4-2	0.01	0.01	0	0	0	0	0.02	0.03	0.08	0.02
M5-1	0.06	0.02	0	0	0	0	0.05	0	0.16	0.04
M5-2	0.02	0.03	0	0.01	0.01	0.02	0.05	0.01	0.14	0.01
M5-3	0.02	0.01	0.01	0.01	0	0	0.03	0.01	0.11	0.1
M5-4	0.05	0.04	0.01	0.01	0	0	2.38	0.25	0.17	0.01
M5-5	0.05		0		0		1.95		0.03	
M5-6	0.03	0.02	0.01	0	0	0	0.01	0	0.07	0.03
M9-1	0.02	0.02	0.01	0.01	0	0	0.37	0.02	0.13	0.05
M9-2	0.04	0.01	0	0	0	0	0.04	0.02	0.15	0.07
M9-3	0.03	0.02	0	0	0.01	0.02	0.02	0.01	0.11	0.02
M9-4	0.05	0.02	0	0	0.07	0.03	0	0	0.11	0.01
M9-5	0.04	0.03	0	0.01	0.09	0	0.02	0	0.06	0.06
Br4-1	0		0.02		0.1		0		0.1	
Br4-2	0.03	0.02	0	0	0.05	0.05	0.02	0.02	0.14	0.01
Br4-3	0.05	0	0	0	0.01	0.01	0.03	0	0.13	0.03
Br4-4	0.03	0.03	0	0	0.05	0.01	0.02	0	0.15	0.04
Br4-5	0.02	0.02	0	0	0	0	0.04	0.01	0.11	0.11

Sample	Sb	1σ	As	1σ	Pb	1σ	Cu	1σ	Bi	1σ
M17-1	0		0		84.23		0		0.63	
M17-2	0.01	0.01	0	0	0.09	0.06	0.01	0.01	0.11	0.08
M17-3	0.01	0.01	0	0.01	0	0	0.01	0.01	0.09	0.01
M17-4	0.07	0.02	0	0	0.2	0.25	0.01	0.02	0.13	0.01
M17-5	0.05	0.03	0	0	0.08	0.09	0.1	0.05	0.16	0.02
M17-6	0.04	0.02	0	0	0.05	0.07	0.08	0.01	0.1	0.04
M17-7	0.06	0	0.01	0.01	0.13	0.09	0.02	0	0.12	0.02
M17-8	0.04	0.04	0	0	0.13	0.01	0.03	0.03	0.1	0
M17-9	0.01	0.01	0	0	0.03	0.05	0	0	0.08	0
M17-10	0.03	0	0	0	0.09	0.07	0.01	0.01	0.12	0.06
M17-11	0.04	0.01	0.01	0.01	0.11	0.01	0.06	0.04	0.16	0
M17-12	0.01	0.01	0.01	0.01	0	0	0.05	0.02	0.17	0.08
Br1-1	0.04		18.48		0.04		0.02		0.11	
Br1-2	0.02	0.02	0	0	0	0	0.01	0.01	0.14	0.05
Br1-3	0.04	0.02	0	0	0.13	0.1	0.01	0.01	0.12	0.05
Br1-4	0.02	0.02	0.01	0	0	0	0	0	0.14	0.01
Br1-5	0.04	0.04	0	0	0	0	0.01	0.01	0.14	0.02
Br1-6	0.01	0.01	0	0	0	0	0.02	0.02	0.1	0.05
Br1-7	0.01	0.01	0	0	0.02	0.02	0	0	0.15	0.07
Br1-8	0		0.35		0.22		0.42		0.08	
Br3-1	0.06	0.03	0	0	0	0	0	0	0.15	0.04
Br3-2	0.06	0.03	0	0	0	0	0.04	0.04	0.09	0
Br3-3	0.01	0.01	0	0	0	0	0.02	0.02	0.18	0.09
Br3-4	0.03	0.02	0	0	0	0	0.02	0	0.13	0
Br3-5	0.03	0	0	0	0	0	0.01	0.01	0.07	0.02
Br3-6	3		0.81		11.69		1.2		0.42	
Br3-7	0.07	0.03	0	0	0	0	0.01	0.01	0.13	0.07
Br3-8	0.03	0	0	0	0	0	0.03	0.02	0.13	0.01
Br3-9	0.06	0.01	0	0	0.01	0.01	0.02	0.01	0.12	0.01
Br3-10	0.02	0	0	0	0	0	0	0	0.15	0.05
Br3-11	0.07	0.01	0	0	0	0	0.01	0	0.17	0.01
Br9-1	0.01	0.01	0	0	0	0	0.02	0.01	0.14	0.02
Br9-2	0	0	0	0	0	0	0.01	0.01	0.14	0.02
Br9-3	0.04	0.03	0	0	0	0	0.01	0.01	0.15	0.01
Br9-4	0		0.05		0		0		0.13	

Sample	Sb	1σ	As	1σ	Pb	1σ	Cu	1σ	Bi	1σ
Br9-5	0.01	0.01	0	0	0	0	0.01	0.01	0.05	0.03
Br9-6	0.02	0	0	0	0	0	0.01	0.01	0.11	0.03
Br9-7	0	0	0.01	0	0	0	0.03	0.01	0.2	0.01
Br9-8	0.01	0.01	0.01	0.01	0	0	0	0	0.15	0.07
Br9-9	0.01	0.01	0	0	0	0	0.02	0.03	0.09	0.01
Br9-10	0.02	0.01	0	0	0.02	0.02	0.01	0.02	0.18	0.06
Br9-11	0	0	0	0	0	0	0.01	0.01	0.16	0.08
Br9-12	0	0	0	0	0	0	0	0	0.14	0.03
Br9-13	0		0		0.01		0		0.08	
Br9-14	0	0	0	0	0	0	0	0	0.13	0.01
Br9-15	0.01	0.02	0	0.01	0.01	0.01	0.02	0.03	0.11	0.15
Br9-16	0.04	0.01	0	0	0.02	0.03	0.01	0.01	0.17	0.02
Br9-17	0	0	0	0	0.03	0.04	0.01	0.01	0.11	0.07
Br5-1	0.06	0	0	0	0	0	0.03	0	0.08	0.01
Br5-2	0.05	0.04	0.01	0	0.03	0.05	0.02	0	0.15	0.07
Br5-3	0.06	0.01	0.01	0.01	0.1	0.14	0.03	0	0.15	0
Br5-4	0.02	0	0	0	0	0	0.02	0	0.15	0.03
Br5-5	0.06	0.01	0.01	0.02	0.16	0.06	0.01	0.01	0.16	0.02
Br5-6	0.04	0.03	0	0	0.16	0.03	0.02	0.03	0.08	0.04
Br5-7	0.06	0.01	0.01	0.01	0.04	0.01	0.01	0.01	0.16	0.03
Br5-8	0.04	0.03	0.01	0.01	0.03	0.04	0	0	0.08	0.05
Br5-9	0.04	0.03	0	0	0	0	0.02	0.01	0.17	0.04
Br5-10	0.02	0.01	0	0	0.01	0.01	0.03	0.03	0.15	0.04
Br5-11	0.03		0		0.19		0		0.04	
Br5-12	0.02	0.03	0.01	0	0.08	0.01	0	0	0.1	0
Br2-1	0.02	0.01	0.01	0.01	0	0	0.01	0.01	0.12	0.04
Br2-2	0.13	0.16	0.01	0	0	0	0	0	0.08	0.03
Br2-3	0.03	0.02	0.01	0	0	0	0	0.01	0.07	0.04
Br2-4	0.01	0	0	0.01	0	0	0.03	0.02	0.1	0.05
Br2-5	0.02	0.02	0	0	0	0	0.02	0.01	0.15	0.01
Br2-6	0.01	0.01	0	0	0	0	0	0	0.08	0.01
Br2-7	0.04	0.03	0	0	0	0	0.01	0.01	0.1	0.08
Br2-8	0.01	0	0	0	0	0	0	0	0.11	0
Br2-9	0.02	0.03	0.01	0.01	0	0	0.01	0.01	0.17	0.01
Br2-10	0.03	0.02	0	0	0	0	0.01	0.01	0.11	0.03

Sample	Sb	1σ	As	1σ	Pb	1σ	Cu	1σ	Bi	1σ
Br2-11	0.02	0.02	0.01	0.01	0	0	0	0	0.14	0.07
Br2-12	0.03	0.01	0.01	0.01	0	0	0.02	0	0.09	0.07
Br2-13	0.05	0.05	0	0	0	0	0	0.01	0.15	0.05
Br2-14	0.01	0	0	0	0	0	0.01	0	0.09	0.03
Br2-15	0.01	0.01	0.01	0.01	0	0	0	0	0.13	0.03
Br2-16	0.04	0.01	0	0.01	0	0	0	0.01	0.16	0.01
Br2-17	0	0	0	0	0	0	0.01	0.01	0.15	0.02
Br2-18	0.01	0.01	0	0	0	0	0.01	0.01	0.13	0.07
Br2-19	0.04	0.03	0.01	0	0	0	0.02	0.02	0.14	0.06
Br2-20	0	0	0.01	0.01	0	0	0.01	0	0.1	0
Br2-21	0	0	0	0	0	0	0.01	0.01	0.1	0.02
Br2-22	0.02	0.02	0	0	0	0	0.01	0.01	0.12	0.01
Br2-23	0.05	0.01	0	0	0	0	0.01	0	0.06	0.02
Br2-24	0.02	0.01	0.01	0.01	0	0	0.01	0.01	0.16	0.01
Br2-25	0	0	0	0	0	0	0.01	0.01	0.16	0.03
Br2-26	0.02	0.03	0	0	0	0	0.02	0	0.1	0.06
M11-1	0.05	0.01	0	0	0	0	0.02	0.02	0.11	0.04
M11-2	0.02	0.02	0	0	0	0	0.01	0.01	0.13	0.04
M11-3	0.02	0.02	0	0	0	0	0.02	0.01	0.16	0.02
M11-4	0.07	0.02	0	0	0	0	0	0	0.18	0.08
M11-5	0.06	0.03	0	0	0	0	0.02	0.02	0.14	0.04
M11-6	0.04	0.01	0	0	0	0	0	0	0.07	0.01
M11-7	0.01	0.01	0	0	0	0	0	0.04	0.12	0.15
M11-8	0.04	0.02	0	0	0	0	0.06	0.02	0.1	0.01
M11-9	0.03	0.01	0.01	0	0	0	0.02	0.03	0.09	0.09
M11-10	0.03	0.04	0	0	0	0	0	0	0.13	0.07
M11-11	0.01	0	0	0	0	0	0.02	0.01	0.14	0.03
M11-12	0	0	0	0	0	0	0	0	0.07	0.06
M11-13	0.03	0.04	0	0	0	0	0.02	0.02	0.07	0.09
M11-14	0		16.08		0		59.53		0	
M11-15	0.48		14.04		0		61.96		0	
M11-16	0.04	0.01	0	0	0	0	0.03	0	0.11	0.05
M11-17	1.41		69.86		0		25.32		0	
M11-18	0.68		70.8		0		25.72		0	
M11-19	0.08	0.03	0	0	0	0	0.01	0	0.14	0.13



Sample	Sb	1σ	As	1σ	Pb	1σ	Cu	1σ	Bi	1σ
M11-20	0.05	0.01	0	0	0	0	0.01	0.02	0.15	0.01
M11-21	0.02	0.01	0	0	0	0	0.02	0	0.08	0.04
M11-22	0.02	0.02	0	0	0	0	0.02	0.01	0.08	0.08
M11-23	0.01	0.01	0	0	0	0	0.01	0.01	0.08	0.01
M14-1	0.03	0.04	0	0.01	0	0	0.01	0	0.13	0
M14-2	0.02	0.03	0	0	0	0	0.03	0.03	0.15	0.02
M14-3	0	0	0	0	0	0	0	0	0.12	0.01
M14-4	0.05	0.04	0	0	0	0	0.01	0.01	0.07	0
M14-5	0.01	0.01	0	0	0	0	0.01	0.01	0.13	0.04
M14-6	0.02	0.02	0	0	0	0	0.01	0.01	0.08	0.05
M14-7	0.01	0.01	0.01	0.01	0	0	0.14	0.02	0.05	0.04
M14-8	0	0	0.01	0.01	0	0	0.02	0.01	0.03	0.04
M14-9	0.1	0.03	0.01	0	0	0	0	0	0.14	0.05
M14-10	0.07	0.01	0	0	0	0	0	0	0.07	0.04
M14-11	0.01	0.02	0	0	0	0	0.02	0	0.17	0.04
M14-12	0		0.22		0.14		0.23		0.15	
M14-13	0.03	0.03	0	0	0	0	0	0.01	0.14	0.03
M10-1	0.03	0	0	0	0.02	0.03	0	0.01	0.09	0.01
M10-2	0.07	0.02	0	0	0.02	0.01	0	0	0.14	0.02
M10-3	0.05	0	0	0	0.06	0.06	0	0	0.15	0.03
M10-4	0.05	0.03	0.01	0	0.02	0.03	0.01	0.01	0.08	0.06
M10-5	0.04	0.01	0	0	0.02	0.01	0	0	0.07	0.01
M10-6	0.03	0.02	0	0	0	0	0	0.01	0.09	0.05
M10-7	0.08	0.02	0	0	0.09	0.13	0	0	0.13	0.03
M10-8	0.02	0.03	0	0	0	0	0.03	0.01	0.11	0.01
M10-9	0.04	0	0	0	0.02	0.03	0.01	0.02	0.09	0.12
M10-10	0.03	0.02	0	0	0	0	0.01	0	0.12	0.06
M10-11	0		0		0		0.01		0.09	
M18-1	0.09	0.01	0.01	0	0	0	0.02	0.02	0.17	0.05
M18-2	0.01	0.02	0.01	0.01	0.03	0.05	0.27	0.13	0.11	0.06
M18-3	0.05	0.02	0.01	0	0	0	0	0	0.15	0.04
M18-4	0.01	0	0	0	0.06	0.08	0.04	0.02	0.1	0
M18-5	0.05	0.03	0	0	0.02	0.03	0.03	0	0.17	0.01
M18-6	0.03	0.04	0	0	0.01	0.01	0	0	0.03	0.02
M18-7	0.02	0	0.01	0.01	0	0	0.01	0.01	0.12	0.01

Sample	Sb	1σ	As	1σ	Pb	1σ	Cu	1σ	Bi	1σ
M18-8	0.05	0.02	0.02	0.01	0.04	0.05	0.04	0	0.05	0.06
M18-9	0.05	0.02	0.01	0	0	0	0.03	0.03	0.13	0.04
M18-10	0.01	0.01	0	0	0	0	0.03	0.01	0.05	0.04
M18-11	0.01	0.01	0	0	0	0	0.01	0.01	0.18	0.01
M18-12	0.03	0	0	0	0.05	0	0.08	0.01	0.1	0.01
M8-1	0.04	0.01	0	0	0.02	0.02	0.01	0.01	0.09	0.07
M8-2	0.04	0.02	0	0	0.01	0.03	0.01	0.01	0.11	0.06
Br6-1	0.04	0	0	0.01	0	0	0.03	0.03	0.06	0.09
Br6-2	0.04	0.01	0.01	0.01	0	0	0.05	0.01	0.04	0
Br6-3	0.02	0.01	0.01	0	0	0	0.59	0	0	0
Br6-4	0.06	0.05	0.01	0	0	0	1.99	0.01	0.02	0.02
Br6-5	0.06	0.01	0.01	0	0	0	0.76	0.03	0.03	0.03
Br6-6	0.01	0.02	0	0	0.07	0.09	0.06	0.02	0.06	0.03
Br6-7	0.05	0.07	0.02	0	0	0	0.02	0.03	0.07	0.01
Br6-8	0.04	0.01	0	0	0	0	0.15	0.03	0.04	0.04
Br6-9	16.406		0		10.417		0		2.083	
Br6-10	0.02	0.03	0	0.01	0	0	0.03	0.01	0.05	0.02
Br6-11	0.05	0.01	0.01	0	0.02	0.03	0.06	0	0.02	0
Br7-1	0.05	0.01	0	0	0	0	0.01	0	0.06	0.05
Br7-2	0.02	0.03	0	0	0	0	0.02	0.02	0.09	0
Br7-3	0.03	0.01	0	0	0	0	0.06	0	0	0
Br7-4	0.03	0.04	0.01	0.01	0	0	0.05	0.01	0.03	0.04
Br7-5	0.06	0.01	0.01	0.01	0	0	0.17	0.03	0.04	0.01
Br7-6	0.04	0.01	0	0	0	0	0.05	0.01	0.08	0.06
Br7-7	0.04	0.01	0	0	0.05	0.08	0.02	0.03	0.03	0.04
Br7-8	0.04	0	0.01	0.01	0	0	0.03	0	0.11	0.02
Br7-9	0.08	0.03	0.01	0	0	0	0.03	0.02	0.06	0.01
Br7-10	0.04	0	0.01	0.01	0	0	0.04	0	0.05	0.07
Br7-11	0.05	0.02	0	0	0	0	0.04	0	0.06	0.01
Br7-12	0.04	0.06	0.01	0.02	0	0	0.02	0.01	0.08	0
Br7-13	0.02	0.03	0.01	0.01	0	0	0.08	0.02	0.02	0
Br7-14	0.05	0.04	0	0	0	0	0.04	0	0.05	0
Br7-15	1.34	1.79	0.31	0.43	4.2	5.65	0.14	0.13	0.02	0.03
Br7-16	0.04	0.01	0	0	0	0	0.1	0.01	0.07	0.05
Br7-17	0.01	0.01	0	0	0	0	0.06	0.02	0.01	0.02

Sample	Sb	1σ	As	1σ	Pb	1σ	Cu	1σ	Bi	1σ
Br8-1	0.05	0	0.01	0.01	0	0	0.01	0.02	0.01	0.02
Br8-2	0.03	0	0.02	0.01	0	0	0.34	0.32	0.03	0.04
Br8-3	0.05	0.01	0	0	0	0	0.1	0.07	0.02	0.01
Br8-4	0.05	0.01	0	0.01	0	0	0.02	0.02	0.08	0.07
Br8-5	0.01	0.01	0	0.01	0	0	0.14	0.13	0.04	0.04
Br8-6	0.04	0.03	0	0	0	0	0.04	0	0.05	0.02
Br8-7	0.04	0	0.01	0.01	0	0	0.03	0.04	0.08	0.02
Br8-8	0.07	0	0.01	0	0	0	0.02	0.01	0	0
Br8-9	0.04	0.01	0.01	0.01	0	0	0.05	0.06	0.07	0.07
Br8-10	0.03	0.01	0.02	0.01	0	0	0.05	0.01	0.03	0.04
Br8-11	0.06	0.03	0	0.01	0	0	0.09	0.01	0.01	0.01
M7-1	0.03	0.02	0.01	0.01	0	0	0.01	0.01	0.05	0.05
M7-2	0.03	0.04	0	0	0	0	0.05	0.02	0.03	0.03
M7-3	0.03	0	0	0.01	0	0	0.08	0.04	0.04	0.01
M7-4	0.02	0.03	0.01	0.01	0	0	0.02	0.01	0.03	0.05
M7-5	0.02	0.02	0	0	0	0	0.04	0.03	0.05	0.05
M7-6	0.03	0	0	0	0	0	0.02	0.01	0.07	0.03
M7-7	0.04	0.02	0	0	0	0	0	0	0.09	0.02
M7-8	0.02	0.03	0	0	0	0	0.07	0.06	0.02	0
M7-9	0.03	0.03	0	0	0	0	0.05	0.01	0.04	0.03
M7-10	0.02	0.01	0	0	0	0	0.02	0.03	0.07	0
M7-11	0.02	0	0.02	0.01	0	0	0.01	0	0.13	0.04
M7-12	0.04	0.02	0.01	0.01	0	0	0.01	0.01	0.05	0.02
M7-13	0.03	0.01	0.01	0.01	0	0	0.01	0.01	0.1	0.01
M7-14	0.05	0.01	0.01	0.02	0	0	0.01	0.01	0.03	0.04
M7-15	0.04	0.02	0	0	0	0	0.07	0.06	0	0
M7-16	0.04	0.05	0.01	0.01	0	0	0.03	0.02	0.04	0.03
M7-17	0.28	0.35	0	0	0.01	0.02	0	0	0.09	0.05
M7-18	0.02	0.02	0.01	0.01	0	0	0.04	0.01	0.02	0.03
M7-19	0.04	0	0.01	0	0	0	0.02	0	0.04	0.05
M7-20	0.04	0.01	0	0	0	0	0.01	0.01	0.03	0.04
M7-21	0.05	0.03	0.01	0	0	0	0	0	0	0
M7-22	0.04	0.04	0.01	0.01	0	0	0.06	0.06	0.08	0.03
M7-23	0.05	0.04	0.01	0.01	0	0	0.02	0.02	0.02	0.02
M7-24	0	0	0.01	0.01	0	0	0.01	0	0	0

Sample	Sb	1σ	As	1σ	Pb	1σ	Cu	1σ	Bi	1σ
M7-25	0	0.01	0	0.01	0	0	0.03	0.01	0.07	0.03
M7-26	0.02	0.02	0	0	0	0	0.01	0.02	0.09	0.01
M7-27	0.02	0.01	0.01	0.01	0	0	0.03	0.01	0.04	0.04
M7-28	0.04	0.01	0.01	0.01	0	0	0.03	0.02	0.06	0.09
M7-29	0.01	0	0.01	0.01	0	0	0.02	0.02	0.06	0.08
M7-30	0.02	0.03	0	0	0	0	0.06	0.03	0.1	0.05
M7-31	0.04	0.02	0	0	0	0	0.02	0.02	0.04	0.06
M7-32	0.03	0.04	0.01	0	0	0	0.01	0	0.07	0.1
M7-33	0.04	0.01	0.01	0.01	0	0	0.03	0.02	0.06	0.06
M7-34	0.03	0.02	0.01	0.01	0	0	0	0	0.05	0.06
M7-35	0.03	0.02	0.02	0	0	0	0.04	0	0	0
M7-36	0	0	0	0.01	0	0	0.03	0.01	0.07	0.01
M7-37	0.05	0.01	0	0	0	0	0.01	0.02	0.01	0.01
M7-38	0.03	0.02	0.01	0.01	0	0	0.02	0.02	0.01	0.02
M7-39	0.07	0.04	0	0	0	0	0.01	0.02	0.02	0.03
M13-1	0.04	0.05	0.01	0	0	0	0	0	0.04	0.04
M13-2	0.03	0.01	0	0	0	0	0.2	0.23	0.1	0.08
M13-3	0.03	0.01	0.01	0	0	0	0.02	0.02	0	0.01
M13-4	0.03	0.01	0.02	0	0	0	0	0.01	0.06	0.02
M13-5	0.03	0.03	0.01	0.01	0	0	0.61	0.01	0.07	0
M13-6	0.03	0.01	0.01	0	0	0	0	0	0.05	0.04
M13-7	0.03	0.04	0	0	0	0	0.05	0.01	0.09	0.03
M13-8	0.02	0.01	0.01	0.01	0	0	0.02	0.01	0.03	0.05
M13-9	0.01		0.04		0.04		0.02		0.13	
M13-10	0.03	0.02	0	0	0	0	0.02	0.03	0.09	0.06
M13-11	0.05	0	0	0.01	0	0	0.01	0.01	0.05	0.02
M13-12	0.06	0.02	0.01	0	0	0	0	0	0.06	0
M13-13	0.03	0.01	0	0.01	0	0	0.02	0	0.07	0.05
M13-14	0.02	0	0	0	0	0	0.01	0.01	0.01	0.01
M3-1	0.03	0.02	0	0.01	0	0	0.02	0.02	0.06	0.02
M3-2	0.04	0.02	0	0	0	0	0.12	0.16	0.04	0
M3-3	0.05	0.03	0	0	0	0	0.02	0.01	0.07	0.03
M3-4	0.03	0.01	0	0	0	0	0	0.01	0	0
M3-5	0.02	0.01	0	0	0	0	0	0	0.07	0
M3-6	0.04	0	0.01	0.02	0	0	0.01	0.01	0.07	0.02

<b>Sample</b>	<b>Sb</b>	<b>1<math>\sigma</math></b>	<b>As</b>	<b>1<math>\sigma</math></b>	<b>Pb</b>	<b>1<math>\sigma</math></b>	<b>Cu</b>	<b>1<math>\sigma</math></b>	<b>Bi</b>	<b>1<math>\sigma</math></b>
<b>M3-7</b>	0.09	0.04	0	0	0	0	0	0	0.03	0.04
<b>M3-8</b>	0.04	0.01	0.01	0.01	0	0	0.01	0.01	0.07	0.04
<b>M3-9</b>	0.06	0.01	0	0	0	0	0	0.01	0.06	0.02
<b>M3-10</b>	0.05	0.02	0	0.01	0	0	0.17	0.23	0.08	0.01

Appendix 4: EPMA results of gold samples

Sample	S	1 $\sigma$	Fe	1 $\sigma$	Ag	1 $\sigma$	Au	1 $\sigma$	Hg	1 $\sigma$
M1-1	0.01	0	0	0	27.07	1.24	72.46	1.15	0.29	0.04
M1-2	0.02	0	0.01	0	17.24	7.56	82.25	7.48	0.34	0.07
M1-3	30.21		18.72		0.02		0.55		0.05	
M1-4	0.01	0.01	0	0	23.7	0.1	75.66	0.07	0.46	0.01
M1-5	0.01	0	0.01	0.02	23.65	0.1	75.47	0.05	0.51	0.01
M1-6	0.01	0.01	0	0	25.26	0.1	74.19	0.22	0.3	0.01
M1-12	0.01	0.01	0	0	17.47	0.17	82.05	0.09	0.31	0.03
M12-1	0.02	0.01	0.01	0	21.96	0.89	77.56	0.87	0.34	0.01
M12-2	0	0	0	0	13.19	0.07	85.94	0.07	0.68	0.05
M12-3	0.02	0	0	0	18.85	0.19	80.46	0.12	0.41	0.02
M12-4	0.02	0.01	0.01	0.01	18.83	0.05	80.49	0.07	0.44	0.03
M12-5	0.02	0.01	0	0	8.95	0.63	90.38	0.73	0.37	0.06
M12-6	0.01	0	0	0	19.4	0.12	79.94	0.12	0.46	0.02
M12-7	0.02	0.01	0	0	2.89	0.01	96.42	0.05	0.43	0.02
M12-8	0	0	0	0	2.46	0	95.87	0.02	0.9	0.06
M12-9	0.02	0	0.01	0.01	16.81	0.09	82.71	0.1	0.31	0.04
M4-1	0.02	0	0	0	33.15	0.06	66.41	0.07	0.34	0.01
M4-2	0	0	0.01	0.01	24.36	0.05	75.25	0.02	0.28	0.02
M5-1	0.02	0.02	0	0	3.19	0.07	96.06	0.11	0.46	0.07
M5-2	0.02	0.01	0	0	5.93	3.81	93.42	3.79	0.41	0.01
M5-3	0.01	0	0	0	8.46	0.06	90.8	0.11	0.57	0.05
M5-4	0	0	0	0	0.93	0.16	95.16	0.45	1.31	0
M5-5	0		0		6.51		89.88		1.58	
M5-6	0	0	0.01	0.01	12.25	0.24	87.06	0.25	0.56	0.06
M9-1	0	0	0.01	0.01	9.27	0.13	89.33	0.07	0.87	0.02
M9-2	0.01	0.01	0	0	5.52	0.27	93.72	0.25	0.52	0.05
M9-3	0.02	0.01	0	0	11.34	0.16	88.01	0.09	0.45	0.05
M9-4	0.01	0.01	0.01	0	11.53	0.08	87.83	0.16	0.41	0.09
M9-5	0.02	0.01	0	0	11.42	0.04	87.89	0.06	0.46	0.07
Br4-1	40.18		58.78		0.02		0.77		0	
Br4-2	0.01	0	0	0	4.12	0.09	95.23	0.13	0.39	0.03
Br4-3	0.02	0.01	0	0	4.1	0.06	95.15	0.05	0.5	0.06
Br4-4	0.02	0	0.01	0.01	4.02	0.1	95.2	0.07	0.51	0.02
Br4-5	0.02	0.02	0.01	0	5.38	0.01	93.97	0.1	0.45	0.02

Sample	S	1σ	Fe	1σ	Ag	1σ	Au	1σ	Hg	1σ
<b>M17-1</b>	12.73		0		0.46		1.95		0	
<b>M17-2</b>	0.01	0	0	0	29	3.58	70.35	3.63	0.42	0.04
<b>M17-3</b>	0.01	0	0.01	0.01	45.01	0.56	54.23	0.59	0.63	0.02
<b>M17-4</b>	0.01	0	0	0	2.87	0.08	95.9	0.25	0.81	0.13
<b>M17-5</b>	0.02	0.01	0.01	0.01	1.19	0.02	97.75	0.16	0.65	0.02
<b>M17-6</b>	0.01	0	0.02	0.01	2.08	0.06	97.01	0.13	0.61	0.02
<b>M17-7</b>	0.01	0	0	0	3.41	0.07	95.61	0.06	0.63	0.01
<b>M17-8</b>	0.01	0	0	0	4.97	0.01	94.18	0	0.54	0.08
<b>M17-9</b>	0.01	0	0	0	22.22	0.07	77.23	0.15	0.41	0.03
<b>M17-10</b>	0.02	0	0	0	9.44	0.08	89.82	0.15	0.47	0.08
<b>M17-11</b>	0.03	0.01	0	0	1.32	0.13	97.73	0.09	0.53	0.05
<b>M17-12</b>	0.02	0	0	0	5.66	0	93.62	0.03	0.46	0.08
<b>Br1-1</b>	10.91		14.63		5.66		49.83		0.29	
<b>Br1-2</b>	0.02	0	0.01	0.01	10.09	0.04	89.35	0.12	0.37	0.01
<b>Br1-3</b>	0.03	0.01	0	0	10.55	0.06	88.75	0.12	0.38	0.06
<b>Br1-4</b>	0.04	0.04	0.02	0.02	11.06	0.09	88.27	0.18	0.44	0.02
<b>Br1-5</b>	0.04	0	0.01	0	10.91	0.04	88.39	0.14	0.46	0.02
<b>Br1-6</b>	0.03	0	0	0	10.5	0.06	89	0.05	0.34	0.01
<b>Br1-7</b>	0.03	0.01	0.01	0.01	15.92	0.02	83.49	0.11	0.38	0.04
<b>Br1-8</b>	40.31		16.16		0.77		3.06		0.06	
<b>Br3-1</b>	0.01	0	0	0	1.1	0.46	98.1	0.6	0.57	0.22
<b>Br3-2</b>	0.01	0.02	0	0	3.65	0.9	94.27	2.44	1.89	1.54
<b>Br3-3</b>	0.02	0.01	0.01	0.01	16.03	0.12	83.27	0.04	0.47	0.05
<b>Br3-4</b>	0	0	0	0	6.02	0.1	92.75	0.39	1.05	0.28
<b>Br3-5</b>	0	0	0	0.01	9.3	0.06	89.95	0.14	0.64	0.1
<b>Br3-6</b>	4.91		0.01		6.32		71.15		0.5	
<b>Br3-7</b>	0	0	0	0	7.98	6.32	89.42	5.17	2.39	1.25
<b>Br3-8</b>	0	0	0.01	0	6.89	0.65	92.23	0.37	0.68	0.29
<b>Br3-9</b>	0.01	0.01	0	0	4.95	0.11	94.25	0.11	0.58	0.06
<b>Br3-10</b>	0.01	0.01	0	0	19.66	0.2	79.84	0.25	0.32	0.1
<b>Br3-11</b>	0.02	0	0.01	0.01	1.48	0.9	97.64	1.15	0.6	0.27
<b>Br9-1</b>	0.02	0.01	0	0	15.93	0.02	83.58	0.03	0.3	0.03
<b>Br9-2</b>	0.03	0.01	0.01	0	28.95	0.41	70.59	0.42	0.27	0
<b>Br9-3</b>	0.02	0.01	0	0	14.25	0.04	85.16	0.05	0.37	0.1
<b>Br9-4</b>	5.51		3.31		19.1		71.67		0.24	

Sample	S	1σ	Fe	1σ	Ag	1σ	Au	1σ	Hg	1σ
Br9-5	0.03	0.01	0	0	22.64	1.5	77.02	1.39	0.24	0.07
Br9-6	0.01	0.01	0	0	16.02	0.79	83.54	0.75	0.29	0.03
Br9-7	0.02	0	0.01	0.01	13.2	0.2	86.18	0.15	0.35	0.05
Br9-8	0.02	0	0	0.01	21.92	1.41	77.6	1.29	0.29	0.04
Br9-9	0.01	0	0.01	0.01	12.95	1.44	86.56	1.47	0.35	0.02
Br9-10	0.02	0.01	0.01	0.01	12.46	0.19	86.87	0.24	0.42	0.01
Br9-11	0.01	0.01	0.01	0	14.55	0.19	84.9	0.32	0.35	0.03
Br9-12	0.02	0	0	0	29.52	0.53	69.96	0.6	0.36	0.03
Br9-13	0.03		0		40.57		59.12		0.19	
Br9-14	0.02	0.01	0	0	21.25	0.05	78.25	0.03	0.33	0.11
Br9-15	0.01	0.01	0	0	13.1	0.08	86.48	0.12	0.26	0.09
Br9-16	0.02	0	0	0	12.99	0.65	86.39	0.65	0.34	0.05
Br9-17	0.02	0	0	0	25.7	0.39	73.8	0.39	0.34	0.02
Br5-1	0.02	0	0	0	3.38	0.05	95.99	0.01	0.43	0.04
Br5-2	0.02	0	0.01	0.01	7.89	0.01	91.48	0.1	0.35	0.04
Br5-3	0.02	0	0	0	2.66	0.02	96.48	0.1	0.49	0.09
Br5-4	0.01	0	0	0	8.25	0.07	91.16	0.01	0.39	0.03
Br5-5	0.01	0.01	0.01	0.01	6.29	0.07	92.86	0.05	0.44	0.07
Br5-6	0.02	0.01	0	0	7.84	0.02	91.45	0	0.39	0.04
Br5-7	0.02	0	0.01	0.01	11.12	0.1	88.16	0.05	0.43	0
Br5-8	0.01	0	0	0	10.45	0.08	88.91	0.17	0.48	0.07
Br5-9	0.01	0	0	0	8.27	0.11	91.09	0.15	0.4	0.05
Br5-10	0.01	0.01	0	0	7.87	0.02	91.47	0.01	0.44	0.02
Br5-11	0.02		0		14.58		84.73		0.41	
Br5-12	0.02	0.02	0	0	22.46	0.7	76.91	0.56	0.39	0.09
Br2-1	0.06	0.09	0.08	0.13	4.78	0.03	94.5	0.25	0.43	0.03
Br2-2	0.04	0	0.01	0.01	35.63	3.53	63.85	3.71	0.27	0
Br2-3	0.02	0.01	0	0	6.49	0.02	92.94	0.09	0.44	0.08
Br2-4	0.03	0.01	0	0	7.07	0.08	92.37	0.02	0.39	0.02
Br2-5	0.02	0	0.01	0.02	5.93	0	93.44	0.08	0.41	0.04
Br2-6	0.02	0	0.01	0.01	18.81	1.15	80.68	1.13	0.39	0.02
Br2-7	0.02	0	0	0	5.89	0.01	93.55	0.08	0.4	0.03
Br2-8	0.03	0	0	0	15.53	2.19	83.98	2.17	0.34	0.01
Br2-9	0.01	0.01	0	0.01	5.54	0.23	93.79	0.33	0.45	0.1
Br2-10	0.01	0	0.01	0.02	4.16	0.03	95.2	0.1	0.47	0.12



Sample	S	1σ	Fe	1σ	Ag	1σ	Au	1σ	Hg	1σ
Br2-11	0.01	0.01	0	0.01	18.57	0.06	80.86	0.17	0.39	0
Br2-12	0.02	0	0	0	4.14	0.02	95.28	0.08	0.41	0.04
Br2-13	0.02	0.01	0.01	0.01	7.61	0.05	91.77	0.15	0.39	0.02
Br2-14	0.03	0	0	0	7.55	0.07	91.89	0.04	0.43	0.07
Br2-15	0.02	0.01	0	0	18.22	0.07	81.2	0.06	0.42	0.02
Br2-16	0.03	0	0	0	8.01	0.38	91.28	0.29	0.47	0.08
Br2-17	0.02	0	0	0	19.04	0.01	80.43	0.08	0.36	0.06
Br2-18	0.03	0.01	0	0	5.82	0.06	93.52	0.11	0.49	0.05
Br2-19	0.03	0	0.01	0.02	15.12	0.87	84.26	0.73	0.38	0.01
Br2-20	0.02	0.01	0	0	13.29	0.33	86.17	0.32	0.4	0
Br2-21	0.03	0.01	0	0	14.6	0.98	84.8	1.02	0.46	0.04
Br2-22	0.02	0	0	0	6.38	0.02	93	0.04	0.46	0.01
Br2-23	0.01	0.01	0	0	6.68	0.01	92.74	0.03	0.45	0
Br2-24	0.03	0	0.01	0.01	14.14	0.01	85.21	0.04	0.42	0.04
Br2-25	0.03	0.01	0	0	29.79	0.72	69.75	0.63	0.26	0.05
Br2-26	0.02	0.01	0	0	7.74	0.04	91.68	0.17	0.41	0.03
M11-1	0.03	0	0.01	0.01	5.58	0.1	93.64	0.14	0.57	0.03
M11-2	0.02	0	0	0	11.14	0.02	88.09	0.06	0.61	0.06
M11-3	0.02	0	0	0	13.81	0.11	85.57	0.14	0.4	0.03
M11-4	0.02	0.01	0	0	0.61	0.42	98.63	0.41	0.49	0.11
M11-5	0.03	0.01	0	0	3.48	1.3	95.77	1.31	0.51	0.02
M11-6	0.02	0	0	0	11.05	0.11	88.39	0.07	0.42	0.02
M11-7	0.02	0.01	0	0	6.82	3.71	92.6	95.39	0.43	0.67
M11-8	0.01	0	0	0	1.74	0.01	97.26	0.1	0.79	0.08
M11-9	0.02	0	0	0	1.53	0.03	97.74	0.06	0.56	0.1
M11-10	0.02	0.01	0	0.01	4.69	2.73	94.73	2.54	0.4	0.06
M11-11	0.02	0.01	0.01	0.01	12.9	0.04	86.53	0.05	0.39	0.05
M11-12	0	0	0	0	17.6	0.86	79.32	0.9	3.01	0.02
M11-13	0.02	0	0.01	0.01	1.81	0.03	97.4	0.07	0.63	0.01
M11-14	0		22.9		1.49		0		0	
M11-15	0		22.33		1.2		0		0	
M11-16	0	0	0	0.01	4.97	0.26	93.44	0.3	1.4	0.11
M11-17	0		3.19		0.22		0		0	
M11-18	0		2.8		0		0		0	
M11-19	0.02	0.01	0.04	0.05	0.14	0.02	99.11	0.11	0.47	0.02

Sample	S	1 $\sigma$	Fe	1 $\sigma$	Ag	1 $\sigma$	Au	1 $\sigma$	Hg	1 $\sigma$
M11-20	0.03	0	0.01	0	1.55	0.61	97.76	0.6	0.45	0
M11-21	0	0	0	0	13.17	0.42	85.48	0.29	1.23	0.07
M11-22	0.01	0.01	0.01	0.01	3.46	0.02	95.7	0.09	0.7	0
M11-23	0.02	0.02	0	0	11.73	0.01	87.72	0.03	0.43	0.02
M14-1	0.04	0.01	0	0	0.8	0.73	98.51	0.7	0.48	0.01
M14-2	0.02	0.01	0	0	15.09	0.21	84.07	0.21	0.62	0.01
M14-3	0.02	0	0.01	0.01	21.21	6.25	78.24	6.25	0.41	0
M14-4	0.03	0.01	0	0	27.33	0.22	72.16	0.23	0.35	0.04
M14-5	0.02	0.01	0	0	13.41	0.11	86.03	0.16	0.39	0.05
M14-6	0.01	0	0.01	0.02	0.38	0.14	99.01	0.07	0.48	0.03
M14-7	0.03	0.01	0	0	6.96	0.06	92.38	0.01	0.43	0.05
M14-8	0.02	0	0.01	0.01	18.31	0.08	81.24	0.01	0.37	0.02
M14-9	0.03	0.01	0	0	23.06	0.51	76.35	0.54	0.32	0.02
M14-10	0.03	0.01	0	0	0.12	0.06	99.25	0.07	0.46	0.05
M14-11	0.02	0	0	0	15.56	0.97	83.73	0.89	0.48	0.05
M14-12	53.17		45.25		0.01		0.8		0	
M14-13	0.04	0.02	0.01	0.01	0.33	0.12	98.95	0.12	0.5	0.03
M10-1	0.02	0.02	0.01	0.02	0.61	0.37	98.74	0.36	0.46	0.01
M10-2	0.03	0.01	0	0	0.89	0.06	98.33	0.08	0.51	0.11
M10-3	0.02	0.01	0.01	0	1.52	0.35	97.63	0.38	0.56	0.07
M10-4	0.02	0	0	0.01	1.53	0.23	97.81	0.3	0.48	0.07
M10-5	0.03	0.01	0	0	1.6	0.17	97.69	0.23	0.54	0.06
M10-6	0.01	0	0	0	9.67	0.59	89.74	0.62	0.45	0.03
M10-7	0.03	0.01	0	0	0.28	0.09	98.87	0.04	0.53	0.01
M10-8	0.02	0	0	0	10.67	0.24	88.69	0.08	0.46	0.1
M10-9	0.03	0.01	0	0	0.39	0	98.89	0.15	0.53	0.03
M10-10	0.01	0.01	0	0	0.69	0.37	98.58	0.3	0.56	0
M10-11	0.02		0.01		19.97		79.59		0.33	
M18-1	0.01	0	0.01	0.01	16.09	0.04	83.24	0.16	0.35	0.09
M18-2	0.02	0.01	0.03	0	5.86	2.09	93.21	2.19	0.45	0.01
M18-3	0.01	0.01	0	0.01	5.73	0.13	93.34	0.19	0.72	0
M18-4	0.02	0.01	0	0	10.33	0.01	89.03	0.14	0.43	0.02
M18-5	0.02	0.01	0	0	7.94	0.05	91.23	0.05	0.52	0.05
M18-6	0.02	0	0	0	22.75	0.02	76.54	0.04	0.63	0.01
M18-7	0.01	0	0	0	22.86	0.07	76.45	0	0.53	0.07

Sample	S	1 $\sigma$	Fe	1 $\sigma$	Ag	1 $\sigma$	Au	1 $\sigma$	Hg	1 $\sigma$
M18-8	0	0	0	0	8.34	0.12	90.57	0.24	0.9	0.11
M18-9	0	0.01	0.01	0.01	0.33	0.08	98.71	0.25	0.73	0.16
M18-10	0	0	0	0	8.38	0.26	90.66	0.39	0.87	0.1
M18-11	0.01	0	0	0	19.03	0.35	80.42	0.28	0.34	0.05
M18-12	0.03	0.01	0	0	8.25	0.71	91	0.76	0.46	0.06
M8-1	0.02	0	0.01	0.01	4.75	0.98	94.5	1.16	0.56	0.13
M8-2	0.02	0.01	0	0.01	16.69	0.63	82.73	0.69	0.4	0.04
Br6-1	0.01	0.01	0.01	0.01	2	0.02	96.58	0.08	1.27	0.01
Br6-2	0	0	0	0	1.83	0.07	96.04	0.02	1.99	0.03
Br6-3	0.01	0	0	0	2.9	0.02	95.45	0.07	1.01	0.1
Br6-4	0.01	0.01	0	0.01	1.02	0.04	96.07	0.1	0.83	0.01
Br6-5	0.02	0	0.01	0.01	0.87	0.03	97.28	0.04	0.98	0.04
Br6-6	0	0.01	0	0.01	2.66	0.02	95.69	0.06	1.44	0.05
Br6-7	0.01	0.01	0	0	1.26	0.79	96.8	2.09	1.76	1.35
Br6-8	0	0	0	0.01	0.89	0.02	97.53	0.1	1.34	0.06
Br6-9	0.781		0		0		70.312		0	
Br6-10	0	0	0	0	5.56	0.03	93.21	0.19	1.12	0.12
Br6-11	0.01	0.01	0	0	1.1	0	97.94	0.02	0.79	0.02
Br7-1	0.01	0	0	0	2.62	0.03	95.93	0.1	1.32	0.04
Br7-2	0	0	0.01	0.01	3.63	0.03	95.2	0	1.02	0.01
Br7-3	0.01	0	0.01	0.01	2.55	0.01	96.46	0.04	0.88	0.03
Br7-4	0.01	0.01	0.01	0.01	2.66	0.19	96.25	0.22	0.97	0.1
Br7-5	0.01	0.01	0	0	2.38	0.06	95.99	0.38	1.36	0.41
Br7-6	0.01	0.01	0	0	3.15	0.71	95.8	0.86	0.88	0.08
Br7-7	0.01	0.01	0.01	0.01	1.49	0.99	97.17	1.73	1.17	0.78
Br7-8	0.02	0.01	0.01	0.01	3.17	0.05	95.84	0.16	0.77	0.1
Br7-9	0.02	0	0	0	2.56	0.05	96.3	0.09	0.96	0.03
Br7-10	0.01	0.01	0	0	3.11	0.06	95.79	0.08	0.96	0.06
Br7-11	0.02	0.01	0	0	2.99	0	95.65	0.04	1.2	0
Br7-12	0.01	0.01	0	0	2.49	0.54	96.54	0.5	0.8	0.04
Br7-13	0	0	0.01	0.01	3.87	0.01	93.95	0	2.05	0.03
Br7-14	0.02	0.01	0	0	2.73	0.04	96.15	0.03	0.97	0.02
Br7-15	0.09	0.09	10.74	15.02	2.42	0.82	79.99	22.16	0.49	0.48
Br7-16	0	0	0.01	0.01	2.65	0	96.29	0.05	0.85	0.12
Br7-17	0.01	0.01	0.01	0.01	2.66	0.02	96.35	0.14	0.88	0.1

Sample	S	1σ	Fe	1σ	Ag	1σ	Au	1σ	Hg	1σ
Br8-1	0.03	0.01	0.01	0.02	2.06	0.5	96.97	0.55	0.85	0
Br8-2	0.01	0.02	0	0.01	1.12	0.15	97.53	0.03	0.92	0.19
Br8-3	0.01	0.01	0.07	0.1	2.24	1.48	96.66	1.24	0.84	0.26
Br8-4	0.01	0.01	0	0	1.64	1.14	97.33	1.25	0.88	0.01
Br8-5	0.01	0.01	0	0	3.04	0.78	95.89	0.83	0.85	0.11
Br8-6	0.01	0	0.01	0.01	1.62	1.12	97.35	1.13	0.88	0
Br8-7	0.02	0	0	0.01	0.83	0	98.02	0.04	0.97	0.1
Br8-8	0.01	0	0	0	0.63	0.25	98.2	0.09	1.07	0.34
Br8-9	0.02	0	0	0	0.53	0.02	98.39	0.12	0.9	0.01
Br8-10	0.01	0	0	0	0.67	0.19	98.16	0.13	1.03	0.3
Br8-11	0.03	0.01	0.02	0	0.74	0.18	98.31	0.24	0.74	0
M7-1	0.02	0	0	0	0.08	0.01	99	0.01	0.8	0
M7-2	0	0	1.4	1.98	11.02	0.44	86.79	2.44	0.68	0.02
M7-3	0.01	0	0	0	9.74	0.56	89.39	0.51	0.72	0.08
M7-4	0.01	0	0	0	1.57	1.53	97.47	1.57	0.85	0.06
M7-5	0.01	0.01	0	0	1.52	2.06	97.52	2.07	0.83	0.02
M7-6	0.02	0.01	0.03	0.03	7.63	1.96	91.49	1.9	0.7	0.09
M7-7	0.02	0.02	0.02	0.02	1.13	1.04	97.86	0.98	0.84	0.02
M7-8	0.01	0	0	0.01	6.75	4	92.32	3.78	0.82	0.14
M7-9	0	0	0	0	3.39	2.24	95.65	2.33	0.82	0.08
M7-10	0.02	0.01	0	0	1.37	1.08	97.73	1.12	0.77	0.07
M7-11	0.03	0.03	0.03	0.04	4.55	4.2	94.41	4.06	0.81	0.05
M7-12	0.02	0.01	0.01	0.01	2.85	2.42	96.22	2.4	0.79	0.01
M7-13	0.01	0	0.01	0.01	1.61	2.09	97.36	2.07	0.86	0.01
M7-14	0.02	0	0.01	0	6.18	8.58	92.87	8.62	0.82	0.03
M7-15	0.01	0	0	0	4.43	2.53	94.66	2.46	0.78	0.01
M7-16	0.02	0.01	0.01	0.02	4.47	6.18	94.61	6.03	0.76	0.09
M7-17	0.21	0.25	2.28	3.15	2	2.51	94.43	6.13	0.69	0.19
M7-18	0.01	0.01	0	0	7.35	6.09	91.73	6.1	0.81	0.06
M7-19	0.01	0	0	0.01	2.16	2.85	96.89	2.89	0.83	0.01
M7-20	0.02	0	0.04	0.03	0.13	0.02	98.95	0.01	0.8	0.04
M7-21	0.01	0	0	0	0.23	0.15	98.84	0.03	0.86	0.08
M7-22	0.01	0	0.01	0.01	2.65	0.46	96.3	0.32	0.85	0.07
M7-23	0.02	0.01	0.01	0.02	0.66	0.77	98.39	0.79	0.82	0.07
M7-24	0.01	0.01	0.01	0.01	23.72	0.17	75.57	0.14	0.67	0.03

Sample	S	1σ	Fe	1σ	Ag	1σ	Au	1σ	Hg	1σ
M7-25	0.01	0.01	0.01	0.01	8.12	4.55	90.94	4.54	0.82	0.03
M7-26	0.01	0.01	0	0	5.4	2.68	93.65	2.76	0.81	0.07
M7-27	0.01	0.01	0	0	5.83	0.26	93.3	0.36	0.76	0.02
M7-28	0.02	0	0.02	0.02	6.98	1.95	92.15	1.87	0.7	0.01
M7-29	0	0	0.02	0.03	8.03	1.04	90.79	1.13	1.05	0.01
M7-30	0.02	0	0.01	0	2.64	1.94	96.21	2	0.94	0.11
M7-31	0.02	0.01	0	0	0.18	0.12	98.9	0.09	0.8	0.04
M7-32	0.02	0	0	0	2.08	0.54	97.02	0.38	0.76	0.01
M7-33	0.01	0.01	0	0	7.99	2.4	90.99	2.37	0.88	0.08
M7-34	0.01	0	0	0	0.2	0.07	98.81	0.08	0.9	0.06
M7-35	0	0	0.01	0.01	7.3	0.43	91.85	0.34	0.75	0.06
M7-36	0.01	0.01	0.01	0	9.96	1.16	89.03	1.11	0.89	0.04
M7-37	0.03	0.01	0	0	1.87	1.53	97.23	1.55	0.8	0.02
M7-38	0.02	0.02	0	0	3.07	0.3	96.02	0.32	0.82	0.03
M7-39	0.03	0	0.01	0.01	0.19	0.05	98.85	0.12	0.82	0.01
M13-1	0.02	0.01	0.01	0.01	20.87	0.14	78.2	0.22	0.82	0.08
M13-2	0.03	0.01	0	0	0.4	0.02	98.4	0.5	0.85	0.18
M13-3	0.01	0	0	0	8.49	0.38	90.62	0.36	0.83	0.04
M13-4	0	0	0	0	11.06	0.06	87.03	0.03	1.8	0.07
M13-5	0	0	0	0	4.32	0.04	93.43	0.09	1.53	0
M13-6	0.01	0	0	0	6.58	0.19	92.44	0.15	0.88	0.07
M13-7	0.01	0	0	0	12.39	0.03	86.59	0.04	0.84	0
M13-8	0	0	0	0	13.48	0.12	85.3	0.09	1.14	0.06
M13-9	35.62		26.66		4.5		32.58		0.42	
M13-10	0.01	0	0	0	4.84	0.01	94	0.1	1.02	0.01
M13-11	0.01	0	0	0	10.2	0.41	88.95	0.39	0.72	0.01
M13-12	0.01	0	0	0	22.49	0.19	76.68	0.23	0.7	0.01
M13-13	0.01	0.01	0	0	4.18	0.12	94.85	0.01	0.83	0.09
M13-14	0.01	0.01	0	0	1.93	2.1	97.08	2.32	0.94	0.2
M3-1	0.01	0.01	0	0.01	0.39	0.01	98.71	0.04	0.78	0.01
M3-2	0.01	0.01	0.01	0.01	0.78	0.12	98.23	0.07	0.78	0.05
M3-3	0.02	0.01	0	0	0.63	0	98.49	0.1	0.74	0.05
M3-4	0.01	0.02	0	0	0.96	0.94	98.21	0.89	0.77	0.04
M3-5	0.02	0	0	0.01	0.75	0.54	98.36	0.49	0.78	0.03
M3-6	0.02	0	0	0	0.12	0	98.91	0.04	0.82	0.06

<b>Sample</b>	<b>S</b>	<b>1<math>\sigma</math></b>	<b>Fe</b>	<b>1<math>\sigma</math></b>	<b>Ag</b>	<b>1<math>\sigma</math></b>	<b>Au</b>	<b>1<math>\sigma</math></b>	<b>Hg</b>	<b>1<math>\sigma</math></b>
<b>M3-7</b>	0.03	0.01	0	0	0.17	0.16	98.8	0.04	0.88	0.01
<b>M3-8</b>	0.02	0.01	0	0	0.4	0.4	98.66	0.39	0.8	0.03
<b>M3-9</b>	0.01	0.01	0	0	0.84	0.41	98.28	0.41	0.74	0.04
<b>M3-10</b>	0.02	0.01	0	0	0.05	0.01	98.86	0.25	0.77	0.06

**Appendix 5: Trace element data; Gold coins.**

Coin	Ti47	1 $\sigma$	%RSD	V51	1 $\sigma$	%RSD	Cr52	1 $\sigma$	%RSD
Sch23Rob	0.000	0.000	231	0.000	0.000	134	0.004	0.006	151
2950	0.028	0.024	85	0.002	0.003	135	0.005	0.004	95
FUG122	0.000	0.000	200	0.001	0.001	94	0.019	0.020	103
FUG121	0.000	0.000	200	0.000	0.000	127	0.001	0.002	165
3321	0.010	0.010	97	0.001	0.001	88	0.003	0.003	87
STW4	0.006	0.001	15	0.000	0.000	200	0.003	0.006	173
87150	0.030	0.010	34	0.050	0.015	29	0.020	0.018	91
FUG93	0.005	0.007	147	0.004	0.001	31	0.006	0.006	93
STW4a	0.175	0.016	9	0.003	0.000	8	0.018	0.006	33
9800b	0.017	0.006	35	0.001	0.001	95	0.005	0.004	87
FUG77	0.002	0.004	200	0.000	0.000	123	0.004	0.006	141
6124	0.005	0.005	86	0.000	0.000	200	0.005	0.001	27
Rbogen	0.002	0.003	200	0.001	0.001	112	0.010	0.007	75
8543	0.001	0.002	173	0.000	0.000	200	0.002	0.003	132
LT8799611	0.002	0.005	200	0.000	0.000	77	0.009	0.009	105
LUX7	0.125	0.204	164	0.000	0.000	200	0.002	0.002	102
30IV586	0.000	0.000	200	0.004	0.007	195	0.005	0.004	90
30IVG176	0.000	0.000	200	0.000	0.000	108	0.002	0.002	90
22809	0.005	0.006	107	0.000	0.000	115	0.001	0.001	87
30IVWall	0.002	0.002	91	0.001	0.001	78	0.002	0.002	93
22807	0.028	0.021	75	0.001	0.001	141	0.000	0.000	200
30IV575	0.002	0.002	102	0.000	0.000	79	0.006	0.004	65
87149	0.003	0.005	173	0.000	0.000	200	0.004	0.003	87
22007	0.001	0.002	134	0.000	0.000	200	0.000	0.000	200
30IV582	0.000	0.000	200	0.000	0.000	105	0.011	0.010	91
30VG179	0.002	0.002	121	0.003	0.002	81	0.002	0.003	147
22007	0.008	0.008	103	0.000	0.000	141	0.002	0.003	141
30V542	0.014	0.010	73	0.000	0.001	124	0.012	0.011	89
22007	0.000	0.000	173	0.000	0.000	173	0.002	0.003	119
Lux3	0.002	0.002	92	0.015	0.013	91	0.004	0.004	97
20409	0.012	0.015	123	0.016	0.011	69	0.004	0.003	87
6719	0.008	0.012	149	0.001	0.002	173	0.002	0.003	173
30V549	0.032	0.064	200	0.008	0.004	47	0.013	0.012	93
Lux4	0.003	0.003	115	0.406	0.434	107	0.012	0.006	52
Lux2	0.003	0.002	87	0.001	0.001	103	0.005	0.004	88
12325	0.003	0.006	173	0.006	0.002	30	0.003	0.002	87
30449	0.001	0.002	173	0.000	0.000	173	0.005	0.005	87

Coin	Ti47	1 $\sigma$	%RSD	V51	1 $\sigma$	%RSD	Cr52	1 $\sigma$	%RSD
Lux5	0.000	0.000	200	0.072	0.044	60	0.008	0.006	68
8544	0.138	0.037	27	0.296	0.386	130	0.055	0.061	112
21931	0.002	0.003	125	0.000	0.000	95	0.007	0.006	89
Lux1	0.002	0.003	145	0.000	0.000	173	0.005	0.005	104
LUX6	0.005	0.009	173	0.000	0.000	200	0.007	0.002	31
SFLAN3000	0.003	0.002	59	0.000	0.000	70	0.002	0.001	87
Flan	0.000	0.000	200	0.000	0.000	173	0.003	0.002	87
SFLAN1148	0.000	0.001	173	0.000	0.000	173	0.005	0.000	8
22010	0.002	0.003	103	0.000	0.000	173	0.004	0.001	36
SFLAN1045	0.000	0.001	173	0.000	0.000	0	0.011	0.006	51
SFLAN507	0.005	0.003	63	0.000	0.000	0	0.005	0.004	69
Fo124	0.002	0.002	111	0.000	0.000	0	0.005	0.004	86
Fo106	0.001	0.002	173	0.001	0.000	44	0.003	0.002	70
Fo105	0.068	0.049	71	0.018	0.021	115	0.016	0.014	91
Fo117	0.021	0.016	76	0.000	0.000	0	0.018	0.011	61
Fo116	0.004	0.004	102	0.001	0.002	173	0.009	0.005	59
22009	0.010	0.009	83	0.002	0.002	149	0.006	0.003	51
32243	0.001	0.001	146	0.000	0.000	90	0.001	0.001	107
20163	0.002	0.003	123	0.000	0.000	117	0.002	0.002	101
26827	0.004	0.005	125	0.003	0.002	66	0.003	0.003	92
20397	0.009	0.007	79	0.001	0.001	134	0.004	0.002	45
28323	0.000	0.000	0	0.004	0.006	160	0.003	0.002	74
22006	0.001	0.001	79	0.001	0.001	133	0.007	0.001	19
22011	0.000	0.001	109	0.000	0.000	104	0.005	0.003	54
31433	0.241	0.235	98	0.012	0.011	86	0.014	0.009	65
22008	0.004	0.006	141	0.000	0.001	141	0.001	0.001	141
31087	0.081	0.134	166	0.004	0.004	118	0.009	0.005	59
26228	3.131	3.125	100	0.117	0.116	99	0.101	0.097	96
19698	0.003	0.000	10	0.001	0.000	43	0.002	0.002	100
22113	0.004	0.002	62	0.007	0.009	133	0.001	0.002	170
26227	0.003	0.004	165	0.003	0.001	31	0.007	0.004	60



**Appendix 5: Trace element data; Gold coins.**

Coin	Mn55	1 $\sigma$	%RSD	Fe57	1 $\sigma$	%RSD	Co59	1 $\sigma$	%RSD
Sch23Rob	0.040	0.005	14	0.075	0.008	11	0.014	0.001	4
2950	0.207	0.301	145	0.318	0.405	127	0.009	0.008	93
FUG122	0.084	0.082	98	0.210	0.131	63	0.014	0.011	76
FUG121	0.029	0.004	15	0.060	0.008	14	0.002	0.000	8
3321	0.024	0.022	92	0.070	0.063	90	0.004	0.002	48
STW4	0.022	0.008	35	0.031	0.005	17	0.004	0.001	14
87150	0.386	0.210	54	0.221	0.110	50	0.086	0.023	27
FUG93	0.179	0.159	89	0.305	0.171	56	0.009	0.005	60
STW4a	0.356	0.001	0	0.614	0.112	18	0.010	0.003	29
9800b	0.031	0.027	86	0.039	0.018	48	0.015	0.005	36
FUG77	0.013	0.013	102	0.011	0.013	115	0.001	0.000	11
6124	0.008	0.002	24	0.026	0.020	75	0.002	0.001	76
Rbogen	0.073	0.136	187	0.018	0.016	89	0.002	0.001	55
8543	0.017	0.005	31	0.023	0.015	66	0.008	0.000	6
LT8799611	0.017	0.007	42	0.047	0.009	19	0.013	0.003	19
LUX7	0.017	0.004	26	0.023	0.004	16	0.004	0.000	5
30IV586	0.015	0.010	69	0.022	0.016	74	0.005	0.001	25
30IVG176	0.015	0.008	56	0.017	0.008	48	0.003	0.001	18
22809	0.020	0.017	87	0.022	0.004	18	0.004	0.001	31
30IVWall	0.028	0.017	62	0.005	0.005	94	0.003	0.001	30
22807	0.010	0.015	141	0.028	0.017	61	0.005	0.001	25
30IV575	0.008	0.001	8	0.065	0.038	58	0.002	0.000	19
87149	0.004	0.004	106	0.007	0.001	12	0.006	0.001	10
22007	0.009	0.010	119	0.008	0.004	51	0.008	0.001	18
30IV582	0.013	0.009	64	0.025	0.024	95	0.008	0.011	130
30VG179	0.212	0.115	54	0.020	0.005	26	0.004	0.001	18
22007	0.008	0.011	141	0.008	0.001	16	0.009	0.002	18
30V542	0.023	0.031	135	0.072	0.041	57	0.008	0.000	6
22007	0.015	0.004	24	0.011	0.002	20	0.006	0.002	31
Lux3	0.041	0.005	11	0.081	0.010	12	0.083	0.014	17
20409	0.011	0.003	22	0.012	0.003	26	0.002	0.001	30
6719	0.009	0.011	120	0.011	0.007	68	0.001	0.000	24
30V549	0.080	0.053	67	0.061	0.082	135	0.011	0.007	66
Lux4	0.182	0.249	137	0.025	0.025	100	0.006	0.002	33
Lux2	0.005	0.004	77	0.017	0.007	39	0.001	0.000	53
12325	0.031	0.025	81	0.006	0.003	55	0.002	0.001	43
30449	0.029	0.011	38	0.055	0.020	36	0.004	0.001	35

Coin	Mn55	1 $\sigma$	%RSD	Fe57	1 $\sigma$	%RSD	Co59	1 $\sigma$	%RSD
Lux5	0.009	0.005	57	0.040	0.014	34	0.023	0.004	16
8544	0.054	0.016	29	0.117	0.009	8	0.018	0.004	21
21931	0.001	0.001	88	0.117	0.011	9	0.422	0.056	13
Lux1	0.012	0.011	89	0.022	0.004	20	0.012	0.004	34
LUX6	0.001	0.001	111	0.037	0.020	54	0.003	0.000	7
SFLAN3000	0.123	0.003	2	0.297	0.010	3	0.015	0.002	12
Flan	0.003	0.002	56	0.007	0.005	72	0.002	0.001	46
SFLAN1148	0.022	0.007	31	0.039	0.004	10	0.006	0.000	4
22010	0.001	0.001	173	0.004	0.005	126	0.006	0.002	28
SFLAN1045	0.272	0.011	4	0.649	0.013	2	0.752	0.010	1
SFLAN507	0.007	0.002	23	0.006	0.004	65	0.000	0.001	128
Fo124	0.005	0.002	44	0.008	0.004	54	0.003	0.004	130
Fo106	0.003	0.001	37	0.031	0.017	55	0.005	0.000	10
Fo105	0.190	0.135	71	4.296	4.815	112	0.011	0.003	28
Fo117	0.298	0.130	44	0.372	0.182	49	0.069	0.005	8
Fo116	0.056	0.016	29	0.120	0.022	18	0.040	0.001	4
22009	0.006	0.004	71	0.017	0.012	67	0.002	0.001	63
32243	0.001	0.001	60	0.002	0.001	57	0.000	0.000	173
20163	0.002	0.003	138	0.008	0.006	81	0.012	0.001	7
26827	0.060	0.025	42	0.016	0.011	69	0.002	0.001	28
20397	0.038	0.059	157	0.020	0.014	68	0.002	0.001	61
28323	0.112	0.179	159	0.011	0.004	38	0.006	0.000	5
22006	0.003	0.001	48	0.003	0.003	100	0.002	0.001	54
22011	0.004	0.002	52	0.042	0.053	125	0.004	0.001	26
31433	0.026	0.012	47	0.157	0.146	93	0.006	0.002	36
22008	0.001	0.001	94	0.017	0.001	7	0.020	0.003	14
31087	0.025	0.032	130	0.189	0.213	113	0.012	0.005	43
26228	0.407	0.373	92	18.734	18.639	99	0.011	0.010	90
19698	0.006	0.001	12	0.072	0.027	38	0.003	0.000	0
22113	0.005	0.002	34	0.003	0.002	70	0.002	0.001	33
26227	0.003	0.002	84	0.005	0.005	91	0.000	0.000	115

Coin	Ni60	1 $\sigma$	%RSD	Cu63	1 $\sigma$	%RSD	Cu65	1 $\sigma$	%RSD
Sch23Rob	0.313	0.007	2	39601.875	765.977	2	13603.190	146.502	1
2950	0.480	0.281	58	71377.255	45697.392	64	29335.953	18694.678	64
FUG122	0.788	0.504	64	85581.352	29676.134	35	29992.223	10490.960	35
FUG121	0.197	0.039	20	141816.944	15157.492	11	50620.953	5120.710	10
3321	0.201	0.056	28	151707.161	61849.354	41	64912.018	26665.887	41
STW4	0.274	0.044	16	167020.585	12336.256	7	66645.617	3612.517	5
87150	0.452	0.304	67	275713.265	86277.818	31	117869.589	39170.497	33
FUG93	0.316	0.153	49	44215.817	7106.834	16	15389.235	2568.174	17
STW4a	0.391	0.079	20	38534.969	11055.687	29	16112.085	4882.837	30
9800b	0.078	0.020	26	43826.348	1108.176	3	18056.802	280.907	2
FUG77	0.234	0.304	130	83234.779	52281.083	63	28807.677	17763.378	62
6124	0.077	0.048	62	78093.438	6442.243	8	31016.912	3042.100	10
Rbogen	0.227	0.025	11	94562.734	8471.780	9	32584.823	2895.349	9
8543	0.258	0.024	9	104710.752	3435.592	3	43821.456	729.753	2
LT8799611	0.918	0.138	15	102987.671	7581.147	7	34542.134	2442.320	7
LUX7	0.435	0.018	4	101979.264	3599.899	4	39832.744	1605.123	4
30IV586	0.209	0.025	12	95554.762	4993.695	5	32328.736	1669.382	5
30IVG176	0.249	0.039	16	99789.058	8123.852	8	34669.853	2946.979	9
22809	0.167	0.085	51	94657.266	14872.385	16	40857.554	5654.861	14
30IVWall	0.162	0.024	15	96683.927	11597.579	12	42046.254	4215.646	10
22807	0.173	0.067	38	102147.958	4609.406	5	42736.468	514.994	1
30IV575	0.387	0.068	18	120394.462	7910.354	7	42762.876	2725.419	6
87149	0.145	0.009	6	125303.758	15957.562	13	48945.941	6266.659	13
22007	0.560	0.088	16	142044.890	16210.592	11	49199.010	4312.108	9
30IV582	0.215	0.224	104	151531.644	4039.278	3	52159.659	1064.073	2
30VG179	0.666	0.092	14	174139.272	13015.971	7	61577.264	4424.374	7
22007	0.389	0.056	14	159052.060	10511.919	7	69273.918	2881.758	4
30V542	2.130	0.144	7	141992.434	7725.888	5	50798.923	2204.074	4
22007	0.317	0.018	6	148660.850	10135.250	7	64277.774	5669.257	9
Lux3	3.080	1.017	33	179722.533	7290.363	4	76095.218	2699.411	4
20409	1.246	0.174	14	176935.152	10037.038	6	76395.589	5083.555	7
6719	0.884	0.211	24	193572.933	17410.600	9	78484.346	4869.904	6
30V549	3.534	0.437	12	228175.423	14418.477	6	78563.156	5267.215	7
Lux4	1.928	0.728	38	192993.592	47371.574	25	82924.647	19408.914	23
Lux2	1.743	0.755	43	205675.750	29850.280	15	85713.960	11849.156	14
12325	1.673	0.499	30	213047.187	33357.449	16	87358.421	13813.565	16
30449	1.457	0.377	26	202804.252	21236.168	10	88875.408	9215.448	10

Coin	Ni60	1 $\sigma$	%RSD	Cu63	1 $\sigma$	%RSD	Cu65	1 $\sigma$	%RSD
Lux5	1.948	0.263	13	258439.944	15317.560	6	111231.137	8311.095	7
8544	3.170	0.648	20	298766.281	40637.613	14	119412.826	15303.869	13
21931	1.961	0.159	8	378090.006	17209.267	5	163912.747	9315.612	6
Lux1	3.591	1.124	31	281997.071	32131.988	11	118563.836	12577.933	11
LUX6	4.537	0.383	8	437744.899	5700.927	1	176671.647	3052.711	2
SFLAN3000	0.115	0.024	21	13421.960	1225.896	9	5914.115	677.367	11
Flan	0.083	0.008	10	101064.858	8076.967	8	43657.796	2573.419	6
SFLAN1148	0.445	0.026	6	99561.376	4207.912	4	44019.257	1745.984	4
22010	1.792	0.476	27	113464.928	13043.638	11	52097.113	5423.645	10
SFLAN1045	0.517	0.031	6	108013.333	3709.423	3	48503.300	1403.337	3
SFLAN507	0.102	0.010	10	95993.208	9837.886	10	43017.567	4373.237	10
Fo124	0.146	0.006	4	68506.510	431.650	1	30760.024	345.813	1
Fo106	0.712	0.060	8	66327.130	3660.230	6	29621.492	1760.504	6
Fo105	1.737	0.742	43	20104.504	16652.207	83	9128.718	7606.311	83
Fo117	0.863	0.096	11	97551.819	8941.586	9	44661.661	3595.968	8
Fo116	0.713	0.052	7	95981.532	18035.418	19	44374.403	8386.432	19
22009	0.474	0.381	80	75475.304	2774.244	4	34643.578	1346.558	4
32243	0.034	0.011	32	30856.934	1310.080	4	14131.537	614.509	4
20163	0.239	0.015	6	69498.707	922.529	1	32283.435	393.622	1
26827	1.071	0.289	27	106391.437	14607.738	14	48822.375	6733.752	14
20397	1.893	0.468	25	116514.097	16926.518	15	55038.206	7847.699	14
28323	0.199	0.051	26	58192.820	9763.823	17	27462.718	4571.017	17
22006	1.028	0.287	28	84196.688	9313.585	11	39625.783	4431.018	11
22011	0.574	0.166	29	105704.443	12339.654	12	49065.225	5478.610	11
31433	0.485	0.069	14	74972.796	2042.155	3	35216.219	998.151	3
22008	0.765	0.081	11	83808.105	4147.786	5	38834.665	2204.470	6
31087	0.570	0.137	24	62855.389	5207.255	8	29765.332	2452.082	8
26228	0.065	0.062	95	7610.411	3487.839	46	3636.669	1684.644	46
19698	0.645	0.076	12	176615.713	16526.925	9	83509.006	8034.783	10
22113	0.847	0.313	37	78921.569	8770.324	11	37482.392	4368.846	12
26227	0.813	0.142	17	137141.914	9926.096	7	64874.304	4812.251	7

Coin	Zn66	1 $\sigma$	%RSD	Ga69	1 $\sigma$	%RSD	Mo96	1 $\sigma$	%RSD
Sch23Rob	0.027	0.001	3	0.007	0.002	27	0.004	0.002	54
2950	0.003	0.002	77	0.006	0.002	37	0.002	0.001	39
FUG122	0.019	0.008	43	0.006	0.004	73	0.003	0.002	61
FUG121	0.015	0.002	11	0.021	0.002	12	0.002	0.000	25
3321	0.004	0.001	32	0.003	0.000	3	0.003	0.003	90
STW4	0.002	0.001	26	0.009	0.003	32	0.001	0.001	119
87150	0.003	0.001	30	0.075	0.056	76	0.043	0.020	47
FUG93	0.016	0.006	41	0.007	0.002	31	0.001	0.000	34
STW4a	0.015	0.003	23	0.014	0.002	15	0.003	0.002	49
9800b	0.007	0.002	22	0.003	0.001	39	0.001	0.001	88
FUG77	0.006	0.002	30	0.004	0.002	50	0.001	0.000	27
6124	0.002	0.001	68	0.006	0.006	100	0.001	0.000	43
Rbogen	0.017	0.005	29	0.003	0.003	84	0.001	0.001	70
8543	0.006	0.000	2	0.002	0.001	40	0.001	0.001	112
LT8799611	0.050	0.005	9	0.042	0.009	21	0.002	0.002	108
LUX7	0.006	0.001	13	0.002	0.001	65	0.001	0.000	5
30IV586	0.029	0.004	14	0.002	0.004	197	0.001	0.002	179
30IVG176	0.293	0.043	15	0.005	0.003	56	0.001	0.000	19
22809	0.016	0.002	13	0.003	0.001	40	0.001	0.001	44
30IVWall	0.021	0.004	20	0.004	0.001	21	0.001	0.000	31
22807	0.033	0.009	27	0.006	0.000	5	0.002	0.000	1
30IV575	0.111	0.022	20	0.006	0.003	42	0.001	0.000	52
87149	0.003	0.000	17	0.003	0.001	26	0.001	0.000	40
22007	0.116	0.019	16	0.003	0.004	105	0.002	0.001	34
30IV582	0.015	0.012	76	0.026	0.033	129	0.001	0.001	83
30VG179	0.051	0.029	57	0.009	0.011	121	0.002	0.001	62
22007	0.024	0.004	17	0.002	0.001	51	0.001	0.001	141
30V542	0.860	0.102	12	0.007	0.006	79	0.001	0.000	47
22007	0.018	0.002	12	0.002	0.002	63	0.001	0.001	87
Lux3	0.004	0.001	18	0.012	0.001	8	0.002	0.001	40
20409	0.002	0.000	16	0.004	0.001	26	0.002	0.001	52
6719	0.001	0.000	8	0.002	0.001	42	0.001	0.001	110
30V549	0.077	0.027	36	0.007	0.003	38	0.002	0.001	62
Lux4	0.008	0.003	31	0.005	0.003	50	0.002	0.001	45
Lux2	0.001	0.000	36	0.003	0.001	35	0.002	0.002	101
12325	0.003	0.000	11	0.003	0.000	15	0.003	0.002	58
30449	0.008	0.000	5	0.042	0.012	28	0.001	0.001	90

Coin	Zn66	1 $\sigma$	%RSD	Ga69	1 $\sigma$	%RSD	Mo96	1 $\sigma$	%RSD
Lux5	0.797	0.034	4	0.003	0.001	23	0.002	0.002	71
8544	0.012	0.000	1	0.107	0.031	29	0.010	0.002	19
21931	0.006	0.001	15	0.005	0.001	17	0.002	0.002	86
Lux1	0.011	0.002	15	0.008	0.001	12	0.003	0.001	26
LUX6	0.013	0.002	16	0.005	0.002	43	0.003	0.002	64
SFLAN3000	0.007	0.001	15	0.008	0.002	28	0.001	0.000	14
Flan	0.002	0.001	35	0.001	0.001	87	0.000	0.001	128
SFLAN1148	0.024	0.002	9	0.004	0.001	35	0.000	0.000	135
22010	0.170	0.025	15				0.001	0.001	105
SFLAN1045	0.026	0.006	21				0.003	0.004	144
SFLAN507	0.014	0.002	17				0.002	0.002	119
Fo124	0.021	0.003	14				0.002	0.002	120
Fo106	0.047	0.003	7				0.001	0.001	74
Fo105	0.080	0.089	110				0.003	0.003	116
Fo117	0.175	0.080	46				0.008	0.004	53
Fo116	0.068	0.013	19				0.003	0.005	173
22009	0.022	0.015	67				0.001	0.001	102
32243	0.003	0.001	29				0.000	0.001	171
20163	0.007	0.002	26				0.001	0.000	36
26827	0.010	0.003	28				0.001	0.001	173
20397	0.021	0.003	17				0.001	0.002	159
28323	0.065	0.011	16				0.002	0.001	66
22006	0.009	0.002	22				0.003	0.002	88
22011	0.024	0.002	7				0.000	0.001	173
31433	0.048	0.011	22				0.013	0.011	88
22008	0.148	0.006	4				0.001	0.001	139
31087	0.200	0.043	22				0.003	0.003	110
26228	0.068	0.061	90				0.058	0.057	98
19698	0.034	0.006	16				0.001	0.001	83
22113	0.010	0.001	9				0.000	0.000	173
26227	0.015	0.001	4				0.001	0.000	30

Coin	Ru101	1 $\sigma$	%RSD	Rh103	1 $\sigma$	%RSD	Pd105	1 $\sigma$	%RSD
Sch23Rob	0.005	0.003	60	0.020	0.000	1	0.018	0.001	3
2950	0.002	0.000	23	0.024	0.012	48	0.020	0.000	1
FUG122	0.003	0.002	75	0.030	0.010	33	0.022	0.006	26
FUG121	0.002	0.000	18	0.048	0.005	10	0.031	0.011	37
3321	0.005	0.003	63	0.044	0.017	39	0.025	0.006	26
STW4	0.002	0.000	15	0.045	0.003	8	0.024	0.001	5
87150	0.002	0.000	19	0.076	0.025	33	0.033	0.011	34
FUG93	0.001	0.000	29	0.014	0.002	13	0.009	0.001	6
STW4a	0.003	0.001	36	0.016	0.002	10	0.018	0.000	1
9800b	0.001	0.000	62	0.012	0.001	5	0.008	0.001	10
FUG77	0.001	0.000	25	0.024	0.014	59	0.014	0.005	38
6124	0.001	0.000	15	0.024	0.002	6	0.122	0.016	13
Rbogen	0.001	0.000	43	0.028	0.002	7	0.030	0.002	7
8543	0.001	0.001	60	0.030	0.000	1	0.046	0.002	4
LT8799611	0.002	0.000	23	0.030	0.001	3	0.038	0.003	7
LUX7	0.001	0.000	20	0.029	0.000	1	0.032	0.000	1
30IV586	0.001	0.000	18	0.028	0.002	8	0.032	0.000	1
30IVG176	0.002	0.000	21	0.031	0.002	7	0.052	0.002	3
22809	0.001	0.000	32	0.028	0.005	19	0.032	0.002	5
30IVWall	0.001	0.000	10	0.029	0.003	11	0.031	0.002	8
22807	0.001	0.000	5	0.031	0.002	7	0.029	0.000	1
30IV575	0.002	0.000	28	0.043	0.003	8	0.044	0.002	4
87149	0.001	0.000	55	0.035	0.004	10	0.033	0.001	2
22007	0.002	0.001	44	0.047	0.003	7	0.037	0.002	5
30IV582	0.002	0.001	41	0.045	0.001	2	0.045	0.002	4
30VG179	0.002	0.001	38	0.058	0.005	9	0.044	0.006	14
22007	0.002	0.000	13	0.049	0.002	5	0.038	0.001	1
30V542	0.002	0.000	22	0.052	0.002	3	0.049	0.002	4
22007	0.002	0.000	9	0.048	0.007	15	0.036	0.002	6
Lux3	0.001	0.000	28	0.050	0.002	4	0.035	0.006	17
20409	0.002	0.001	27	0.051	0.004	8	0.043	0.004	8
6719	0.002	0.000	27	0.054	0.005	9	0.045	0.006	13
30V549	0.003	0.001	46	0.063	0.003	5	0.044	0.003	7
Lux4	0.003	0.001	33	0.055	0.013	24	0.047	0.010	22
Lux2	0.002	0.000	26	0.057	0.008	14	0.043	0.012	27
12325	0.002	0.001	58	0.059	0.011	18	0.039	0.007	19
30449	0.002	0.000	11	0.060	0.005	9	0.040	0.005	13

Coin	Ru101	1 $\sigma$	%RSD	Rh103	1 $\sigma$	%RSD	Pd105	1 $\sigma$	%RSD
Lux5	0.003	0.001	21	0.075	0.005	7	0.049	0.004	8
8544	0.002	0.000	3	0.081	0.012	15	0.047	0.005	11
21931	0.003	0.000	13	0.106	0.008	8	0.056	0.003	6
Lux1	0.003	0.001	29	0.076	0.010	13	0.050	0.008	17
LUX6	0.003	0.000	11	0.115	0.004	4	0.055	0.002	4
SFLAN3000	0.001	0.000	28	0.006	0.000	9	0.047	0.013	27
Flan	0.001	0.000	21	0.030	0.001	5	0.032	0.002	5
SFLAN1148	0.001	0.000	34	0.030	0.001	2	0.033	0.001	2
22010	0.002	0.001	65						
SFLAN1045	0.002	0.001	65						
SFLAN507	0.001	0.001	59						
Fo124	0.000	0.001	129						
Fo106	0.001	0.001	80						
Fo105	0.002	0.002	94						
Fo117	0.013	0.006	44						
Fo116	0.014	0.011	78						
22009	0.001	0.001	95						
32243	0.000	0.000	100						
20163	0.001	0.001	87						
26827	0.001	0.001	78						
20397	0.002	0.001	58						
28323	0.001	0.001	55						
22006	0.002	0.001	33						
22011	0.002	0.001	30						
31433	0.002	0.002	100						
22008	0.000	0.001	141						
31087	0.002	0.002	94						
26228	0.000	0.000	100						
19698	0.002	0.000	1						
22113	0.001	0.001	101						
26227	0.003	0.001	37						



Coin	Pd106	1 $\sigma$	%RSD	Pd108	1 $\sigma$	%RSD	Pd110	1 $\sigma$	%RSD
Sch23Rob	0.022	0.001	3	0.024	0.000	0	0.007	0.000	2
2950	0.020	0.009	42	0.026	0.009	36	0.009	0.003	36
FUG122	0.020	0.008	38	0.027	0.008	27	0.009	0.002	22
FUG121	0.019	0.013	68	0.025	0.013	52	0.008	0.003	43
3321	0.016	0.002	13	0.019	0.002	13	0.007	0.001	9
STW4	0.013	0.002	13	0.017	0.001	9	0.006	0.000	8
87150	0.006	0.001	10	0.012	0.002	18	0.005	0.001	16
FUG93	0.009	0.001	10	0.018	0.001	5	0.007	0.000	2
STW4a	0.022	0.003	15	0.027	0.003	10	0.009	0.001	8
9800b	0.009	0.001	11	0.016	0.002	10	0.006	0.000	7
FUG77	0.011	0.002	23	0.019	0.003	17	0.007	0.001	12
6124	0.170	0.023	13	0.162	0.023	14	0.044	0.007	16
Rbogen	0.031	0.003	10	0.034	0.002	6	0.010	0.000	5
8543	0.053	0.001	3	0.055	0.001	2	0.017	0.000	2
LT8799611	0.042	0.002	5	0.045	0.002	5	0.013	0.001	5
LUX7	0.033	0.001	3	0.036	0.001	2	0.011	0.000	2
30IV586	0.036	0.001	2	0.041	0.001	3	0.012	0.000	1
30IVG176	0.064	0.000	0	0.069	0.001	2	0.019	0.000	2
22809	0.032	0.002	7	0.035	0.001	2	0.010	0.001	8
30IVWall	0.030	0.002	5	0.031	0.000	1	0.010	0.000	3
22807	0.027	0.001	4	0.028	0.001	3	0.009	0.000	4
30IV575	0.043	0.001	1	0.048	0.000	1	0.014	0.000	2
87149	0.031	0.002	8	0.033	0.003	9	0.010	0.001	7
22007	0.031	0.003	8	0.036	0.002	4	0.011	0.000	4
30IV582	0.044	0.002	5	0.047	0.002	4	0.013	0.001	5
30VG179	0.034	0.007	20	0.038	0.006	16	0.011	0.002	15
22007	0.028	0.002	5	0.031	0.002	7	0.010	0.000	4
30V542	0.045	0.002	5	0.050	0.001	2	0.014	0.001	4
22007	0.027	0.003	11	0.031	0.002	8	0.010	0.001	11
Lux3	0.023	0.007	31	0.027	0.007	27	0.009	0.001	17
20409	0.032	0.001	2	0.033	0.002	5	0.011	0.001	6
6719	0.037	0.007	20	0.040	0.007	16	0.012	0.002	15
30V549	0.030	0.005	15	0.033	0.005	14	0.010	0.001	11
Lux4	0.039	0.008	20	0.043	0.007	17	0.013	0.002	13
Lux2	0.036	0.019	52	0.035	0.010	29	0.010	0.003	32
12325	0.028	0.007	25	0.029	0.005	17	0.009	0.001	13
30449	0.025	0.004	17	0.027	0.004	14	0.008	0.001	13

Coin	Pd106	1 $\sigma$	%RSD	Pd108	1 $\sigma$	%RSD	Pd110	1 $\sigma$	%RSD
Lux5	0.029	0.003	10	0.034	0.003	8	0.010	0.001	8
8544	0.024	0.001	3	0.026	0.001	3	0.008	0.000	5
21931	0.021	0.001	4	0.021	0.001	4	0.006	0.000	4
Lux1	0.029	0.007	24	0.030	0.005	17	0.009	0.002	18
LUX6	0.014	0.003	19	0.016	0.004	23	0.005	0.001	20
SFLAN3000	0.066	0.019	28	0.064	0.017	26	0.018	0.005	27
Flan	0.031	0.003	10	0.032	0.004	12	0.010	0.001	11
SFLAN1148	0.037	0.008	22	0.035	0.002	7	0.011	0.001	13
22010	0.017	0.004	25	0.019	0.003	16	0.005	0.001	16
SFLAN1045	0.009	0.001	9	0.015	0.001	4	0.011	0.000	4
SFLAN507	0.035	0.003	7	0.036	0.003	9	0.009	0.001	11
Fo124	0.038	0.001	2	0.041	0.001	2	0.014	0.006	40
Fo106	0.014	0.001	4	0.016	0.000	1	0.004	0.000	3
Fo105	0.012	0.004	34	0.011	0.002	19	0.003	0.001	21
Fo117	0.076	0.019	25	0.080	0.017	22	0.021	0.004	19
Fo116	0.050	0.011	23	0.054	0.012	22	0.015	0.003	18
22009	0.013	0.004	31	0.014	0.003	20	0.004	0.001	18
32243	0.005	0.001	13	0.006	0.000	8	0.002	0.000	11
20163	0.017	0.001	8	0.018	0.001	6	0.005	0.000	10
26827	0.019	0.004	18	0.020	0.003	17	0.005	0.001	16
20397	0.016	0.002	15	0.018	0.002	14	0.004	0.000	8
28323	0.013	0.000	2	0.016	0.000	3	0.004	0.000	3
22006	0.012	0.002	20	0.014	0.002	15	0.004	0.001	15
22011	0.017	0.004	25	0.019	0.004	23	0.005	0.001	15
31433	0.018	0.002	9	0.020	0.002	11	0.006	0.001	9
22008	0.005	0.002	48	0.005	0.002	37	0.001	0.000	36
31087	0.026	0.002	8	0.028	0.002	6	0.008	0.001	11
26228	0.010	0.001	12	0.018	0.000	2	0.007	0.000	7
19698	0.004	0.003	62	0.005	0.003	59	0.001	0.001	67
22113	0.015	0.003	23	0.018	0.004	22	0.005	0.001	17
26227	0.022	0.002	10	0.024	0.003	13	0.006	0.001	10

Coin	Ag107	1 $\sigma$	%RSD	Ag109	1 $\sigma$	%RSD	Sn118	1 $\sigma$	%RSD
Sch23Rob	119405.223	403.155	0	112277.508	878.543	1	39.852	1.971	5
2950	279322.938	29797.714	11	262753.933	35175.779	13	15.338	11.074	72
FUG122	314499.957	21827.168	7	296602.165	18394.257	6	23.458	18.865	80
FUG121	235500.584	10035.573	4	222719.074	10655.869	5	44.948	20.079	45
3321	257092.429	47548.189	18	250780.617	40973.701	16	9.337	6.133	66
STW4	224300.050	7381.361	3	208218.489	9021.002	4	13.757	2.091	15
87150	303157.719	65940.229	22	294039.503	59522.624	20	38.236	8.040	21
FUG93	356373.722	6760.903	2	332150.775	3710.020	1	66.538	20.835	31
STW4a	340539.459	8682.018	3	292395.958	7257.876	2	17.170	1.747	10
9800b	358289.932	2055.832	1	344496.387	3089.222	1	19.153	7.630	40
FUG77	372077.718	37300.772	10	348290.197	33125.087	10	53.581	22.856	43
6124	125819.408	4594.004	4	116879.404	4903.287	4	4.259	1.959	46
Rbogen	207013.914	6723.487	3	192233.235	4765.321	2	20.341	7.885	39
8543	166139.017	2058.962	1	160656.290	3179.722	2	54.926	8.716	16
LT8799611	201375.463	5604.986	3	186418.435	4625.339	2	41.847	7.239	17
LUX7	215680.864	2643.854	1	196898.453	2749.257	1	20.225	3.361	17
30IV586	233361.813	3455.249	1	220264.099	3243.879	1	18.652	1.863	10
30IVG176	234758.384	6247.104	3	226183.584	4837.488	2	26.873	2.795	10
22809	235759.264	6562.978	3	214626.151	15139.665	7	15.742	3.948	25
30IVWall	252848.913	6263.978	2	231496.007	9725.446	4	21.538	12.580	58
22807	218053.360	1396.767	1	198172.653	3737.566	2	26.822	9.459	35
30IV575	243338.962	6799.982	3	226413.069	3987.441	2	75.054	8.597	11
87149	210376.809	12247.892	6	192464.764	10298.839	5	9.977	2.262	23
22007	246169.067	12625.161	5	230953.854	8276.788	4	17.681	3.342	19
30IV582	198326.188	1634.058	1	184996.981	3535.841	2	50.641	32.460	64
30VG179	211222.449	9840.838	5	196963.654	8227.791	4	90.472	23.026	25
22007	230625.336	7279.595	3	211612.010	6134.704	3	15.927	6.533	41
30V542	228556.251	5880.150	3	215716.802	4206.306	2	77.445	9.321	12
22007	239619.004	4805.817	2	218009.442	12246.584	6	6.217	1.276	21
Lux3	206230.902	7225.438	4	197588.110	3155.335	2	16.840	8.517	51
20409	192598.138	9627.939	5	179863.761	5382.763	3	19.466	9.796	50
6719	190424.598	8993.525	5	179802.868	13344.431	7	3.933	1.177	30
30V549	183979.592	10106.842	5	174044.365	9958.068	6	108.506	80.347	74
Lux4	185400.840	33081.187	18	181475.751	33643.948	19	75.554	46.959	62
Lux2	190694.434	21603.517	11	176478.062	20127.566	11	3.680	1.097	30
12325	175994.990	20889.075	12	169573.407	26357.989	16	10.985	1.626	15
30449	176628.636	15495.336	9	161843.046	14877.613	9	27.189	5.308	20

Coin	Ag107	1 $\sigma$	%RSD	Ag109	1 $\sigma$	%RSD	Sn118	1 $\sigma$	%RSD
Lux5	147029.138	12540.646	9	145509.681	10952.102	8	59.460	6.992	12
8544	154251.281	25928.039	17	145716.883	30004.403	21	22.087	0.422	2
21931	137885.069	13124.729	10	127240.558	13397.899	11	55.545	7.102	13
Lux1	126803.957	22445.287	18	122068.134	21832.781	18	46.642	12.154	26
LUX6	108522.807	3402.109	3	102189.748	5530.996	5	33.282	14.410	43
SFLAN3000	40598.222	943.784	2	37876.769	977.306	3	96.366	4.558	5
Flan	167764.332	5689.799	3	156297.445	4939.595	3	36.459	17.622	48
SFLAN1148	182655.901	2405.970	1	170222.513	3601.104	2	37.892	5.416	14
22010	104745.906	9367.007	9	98587.175	8936.888	9			
SFLAN1045	282203.335	4255.558	2	264322.997	892.809	0			
SFLAN507	195027.309	7762.012	4	181462.158	6571.262	4			
Fo124	217623.049	902.472	0	205341.529	648.328	0			
Fo106	122681.857	2809.689	2	114841.762	2647.945	2			
Fo105	121621.899	12432.806	10	114284.792	11864.896	10			
Fo117	337581.352	6140.835	2	316012.587	6393.507	2			
Fo116	303213.498	14153.244	5	282800.134	12259.115	4			
22009	114722.140	1753.309	2	107984.492	2365.035	2			
32243	85489.536	796.411	1	79996.394	1126.603	1			
20163	119895.438	741.684	1	112819.777	749.589	1			
26827	102827.389	11369.493	11	95815.096	9964.160	10			
20397	91963.612	12668.178	14	87454.060	12085.905	14			
28323	135595.717	7005.869	5	127764.955	7346.199	6			
22006	109984.437	7076.322	6	103298.913	6647.842	6			
22011	128532.526	8997.930	7	121318.706	8805.440	7			
31433	151712.581	1531.969	1	143313.958	1517.020	1			
22008	32344.902	3103.179	10	30705.602	3253.017	11			
31087	146602.092	3902.946	3	138998.448	3834.032	3			
26228	397782.847	3981.843	1	379749.465	1217.974	0			
19698	21906.441	12648.202	58	20522.613	11935.137	58			
22113	118885.208	6699.663	6	112934.582	6449.695	6			
26227	69366.758	7471.683	11	65828.315	7265.715	11			

Coin	Sb121	1 $\sigma$	%RSD	Te125	1 $\sigma$	%RSD	W182	1 $\sigma$	%RSD
Sch23Rob	0.003	0.000	9	0.022	0.002	9	0.000	0.000	137
2950	0.348	0.155	44	0.030	0.005	16	0.001	0.000	43
FUG122	0.006	0.006	95	0.039	0.008	20	0.000	0.000	78
FUG121	0.003	0.001	20	0.037	0.003	9	0.001	0.000	68
3321	0.359	0.215	60	0.035	0.008	22	0.000	0.000	28
STW4	0.201	0.046	23	0.033	0.007	22	0.000	0.000	57
87150	21.689	7.455	34	0.099	0.014	14	0.001	0.000	7
FUG93	0.008	0.004	43	0.060	0.012	20	0.001	0.000	32
STW4a	0.260	0.033	13	0.053	0.001	1	0.000	0.000	20
9800b	0.473	0.107	23	0.050	0.009	17	0.001	0.000	35
FUG77	0.006	0.003	59	0.042	0.009	21	0.001	0.001	112
6124	0.072	0.034	47	0.017	0.003	16	0.000	0.000	27
Rbogen	0.011	0.004	34	0.027	0.003	11	0.000	0.000	81
8543	1.351	0.400	30	0.047	0.013	28	0.000	0.000	33
LT8799611	0.040	0.009	23	0.020	0.010	51	0.000	0.000	169
LUX7	0.954	0.152	16	0.028	0.001	4	0.000	0.000	1
30IV586	0.008	0.001	15	0.029	0.001	4	0.000	0.000	79
30IVG176	0.030	0.005	16	0.028	0.001	5	0.000	0.000	37
22809	0.826	0.344	42	0.027	0.003	12	0.000	0.000	49
30IVWall	0.505	0.156	31	0.026	0.003	13	0.000	0.000	48
22807	0.774	0.094	12	0.026	0.003	12	0.001	0.000	44
30IV575	0.037	0.007	19	0.034	0.004	11	0.000	0.000	12
87149	0.375	0.210	56	0.030	0.003	9	0.000	0.000	42
22007	0.056	0.009	17	0.036	0.010	29	0.000	0.000	124
30IV582	0.026	0.005	21	0.027	0.005	17	0.000	0.000	94
30VG179	0.046	0.022	47	0.028	0.007	26	0.000	0.000	31
22007	5.095	2.965	58	0.039	0.004	11	0.000	0.000	39
30V542	0.060	0.013	21	0.031	0.002	7	0.000	0.000	16
22007	3.372	1.599	47	0.048	0.015	32	0.000	0.000	14
Lux3	7.535	5.047	67	0.029	0.006	19	0.000	0.000	1
20409	1.719	0.405	24	0.017	0.005	29	0.001	0.000	52
6719	3.501	1.279	37	0.025	0.003	13	0.000	0.000	30
30V549	0.130	0.017	13	0.022	0.004	16	0.001	0.000	41
Lux4	6.861	2.664	39	0.039	0.019	49	0.001	0.000	22
Lux2	6.969	4.130	59	0.031	0.011	36	0.001	0.000	86
12325	8.002	2.208	28	0.022	0.003	13	0.000	0.000	30
30449	12.155	3.130	26	0.031	0.001	5	0.000	0.000	59

Coin	Sb121	1 $\sigma$	%RSD	Te125	1 $\sigma$	%RSD	W182	1 $\sigma$	%RSD
Lux5	7.940	1.132	14	0.029	0.005	18	0.000	0.000	38
8544	18.530	0.371	2	0.036	0.003	9	0.000	0.000	44
21931	6.186	1.390	22	0.062	0.014	23	0.000	0.000	104
Lux1	16.021	4.400	27	0.020	0.004	22	0.000	0.000	84
LUX6	21.841	1.583	7	0.023	0.002	10	0.000	0.000	20
SFLAN3000	0.253	0.071	28	0.005	0.001	25	0.000	0.000	21
Flan	0.279	0.075	27	0.029	0.006	21	0.000	0.000	30
SFLAN1148	0.570	0.092	16	0.021	0.003	13	0.000	0.000	94
22010	2.392	0.697	29	0.008	0.005	59	0.000	0.000	112
SFLAN1045	0.958	0.154	16	0.047	0.009	19	0.003	0.005	161
SFLAN507	0.068	0.012	18	0.018	0.007	41	0.000	0.000	84
Fo124	0.283	0.014	5	0.018	0.006	32	0.000	0.000	29
Fo106	2.174	0.465	21	0.011	0.003	31	0.000	0.000	115
Fo105	0.173	0.096	56	0.007	0.006	90	0.000	0.000	140
Fo117	0.622	0.058	9	0.029	0.011	38	0.002	0.001	68
Fo116	0.861	0.064	7	0.053	0.013	25	0.001	0.001	71
22009	2.913	0.908	31	0.013	0.005	36	0.000	0.000	173
32243	0.066	0.041	63	0.006	0.002	37	0.000	0.000	92
20163	0.146	0.064	44	0.009	0.003	40	0.001	0.001	77
26827	5.654	0.891	16	0.012	0.002	18	0.000	0.000	109
20397	17.958	3.571	20	0.006	0.005	81	0.000	0.000	70
28323	2.079	0.910	44	0.015	0.005	36	0.000	0.000	136
22006	6.440	1.653	26	0.013	0.003	24	0.000	0.001	122
22011	1.741	0.592	34	0.016	0.005	33	0.000	0.000	79
31433	1.568	0.344	22	0.011	0.001	5	0.001	0.000	45
22008	2.037	0.392	19	0.008	0.003	32	0.000	0.000	141
31087	5.310	0.380	7	0.010	0.007	69	0.000	0.000	146
26228	0.043	0.019	45	0.031	0.004	13	0.005	0.004	79
19698	22.207	0.279	1	0.020	0.004	20	0.000	0.000	67
22113	7.140	2.933	41	0.013	0.006	43	0.000	0.000	54
26227	18.544	1.871	10	0.008	0.003	40	0.000	0.000	158

Coin	Os189	1 $\sigma$	%RSD	Ir193	1 $\sigma$	%RSD	Pt194	1 $\sigma$	%RSD
Sch23Rob	4.002	5.136	128	0.021	0.005	22	0.649	0.017	3
2950	0.539	0.261	48	0.012	0.007	61	0.527	0.302	57
FUG122	1.026	0.922	90	0.018	0.017	93	0.378	0.296	78
FUG121	0.353	0.089	25	0.007	0.002	24	0.205	0.031	15
3321	1.978	2.759	139	0.015	0.009	57	0.330	0.085	26
STW4	0.376	0.273	73	0.006	0.002	38	0.277	0.060	22
87150	0.291	0.148	51	0.001	0.000	41	0.009	0.004	41
FUG93	0.639	0.174	27	0.005	0.001	29	0.052	0.022	42
STW4a	0.694	0.265	38	0.013	0.005	39	0.720	0.307	43
9800b	0.431	0.293	68	0.001	0.001	39	0.059	0.031	52
FUG77	2.413	3.579	148	0.003	0.002	83	0.064	0.056	87
6124	0.327	0.311	95	0.020	0.007	33	0.456	0.044	10
Rbogen	0.305	0.128	42	0.005	0.001	15	0.160	0.013	8
8543	0.198	0.175	88	0.003	0.000	5	0.176	0.004	2
LT8799611	0.436	0.430	99	0.007	0.001	9	0.217	0.010	5
LUX7	0.378	0.171	45	0.005	0.000	3	0.235	0.006	3
30IV586	0.361	0.283	78	0.006	0.000	6	0.187	0.006	3
30IVG176	0.298	0.112	38	0.006	0.001	11	0.175	0.010	6
22809	0.342	0.082	24	0.005	0.001	12	0.236	0.009	4
30IVWall	0.633	0.411	65	0.005	0.000	6	0.197	0.012	6
22807	0.404	0.129	32	0.007	0.001	9	0.286	0.017	6
30IV575	0.451	0.139	31	0.006	0.001	16	0.164	0.017	10
87149	0.269	0.011	4	0.007	0.001	15	0.246	0.013	5
22007	0.716	0.246	34	0.006	0.002	29	0.192	0.041	21
30IV582	0.615	0.098	16	0.010	0.000	2	0.236	0.007	3
30VG179	0.377	0.087	23	0.005	0.002	46	0.189	0.068	36
22007	0.176	0.145	82	0.007	0.001	15	0.280	0.032	12
30V542	0.439	0.034	8	0.006	0.001	8	0.173	0.020	12
22007	1.482	2.032	137	0.005	0.001	19	0.227	0.035	16
Lux3	0.235	0.117	50	0.001	0.000	48	0.164	0.114	70
20409	3.108	5.255	169	0.005	0.002	50	0.228	0.066	29
6719	0.269	0.143	53	0.004	0.002	42	0.291	0.093	32
30V549	0.465	0.202	43	0.005	0.003	60	0.166	0.070	42
Lux4	1.873	2.225	119	0.007	0.004	56	0.328	0.160	49
Lux2	0.285	0.068	24	0.002	0.001	64	0.253	0.151	60
12325	0.139	0.082	59	0.005	0.002	44	0.214	0.089	41
30449	0.310	0.110	35	0.003	0.002	57	0.173	0.081	47

Coin	Os189	1 $\sigma$	%RSD	Ir193	1 $\sigma$	%RSD	Pt194	1 $\sigma$	%RSD
Lux5	0.548	0.263	48	0.015	0.004	25	0.308	0.070	23
8544	0.503	0.353	70	0.003	0.000	0	0.180	0.029	16
21931	0.722	0.222	31	0.006	0.001	18	0.179	0.025	14
Lux1	0.566	0.351	62	0.006	0.005	72	0.256	0.135	53
LUX6	0.790	0.693	88	0.003	0.002	47	0.125	0.062	50
SFLAN3000	0.321	0.230	72	0.005	0.001	16	0.376	0.085	23
Flan	0.251	0.056	22	0.005	0.000	4	0.246	0.010	4
SFLAN1148	0.454	0.515	113	0.004	0.000	1	0.247	0.002	1
22010	0.225	0.123	55	0.005	0.002	33	0.183	0.059	32
SFLAN1045	0.461	0.265	58	0.002	0.000	23	0.035	0.002	5
SFLAN507	0.101	0.141	139	0.004	0.000	7	0.239	0.007	3
Fo124	0.139	0.141	102	0.005	0.000	4	0.270	0.004	2
Fo106	0.065	0.047	72	0.002	0.000	10	0.086	0.005	6
Fo105	0.334	0.395	118	0.005	0.004	77	0.167	0.094	56
Fo117	3.774	2.986	79	0.057	0.019	34	3.616	0.658	18
Fo116	2.987	2.408	81	0.072	0.022	30	2.814	0.715	25
22009	0.035	0.047	134	0.001	0.001	68	0.080	0.045	56
32243	0.064	0.067	106	0.001	0.000	37	0.027	0.011	41
20163	0.022	0.029	131	0.001	0.000	25	0.126	0.015	12
26827	0.040	0.044	111	0.001	0.001	57	0.146	0.056	38
20397	0.042	0.036	86	0.003	0.001	29	0.131	0.046	35
28323	0.318	0.360	113	0.004	0.001	16	0.175	0.021	12
22006	0.095	0.100	105	0.002	0.001	56	0.089	0.040	45
22011	0.053	0.092	173	0.003	0.002	78	0.111	0.060	54
31433	0.115	0.115	100	0.003	0.001	34	0.130	0.027	21
22008	0.116	0.135	116	0.001	0.000	39	0.036	0.007	20
31087	0.439	0.238	54	0.003	0.002	44	0.132	0.034	26
26228	0.120	0.120	100	0.001	0.000	0	0.058	0.003	4
19698	0.066	0.066	100	0.001	0.001	79	0.032	0.025	80
22113	0.072	0.061	85	0.001	0.000	71	0.061	0.039	65
26227	0.191	0.169	88	0.007	0.002	22	0.273	0.060	22



Coin	Pb208	1 $\sigma$	%RSD
Sch23Rob	3.136	0.203	6
2950	0.618	0.076	12
FUG122	1.054	0.880	83
FUG121	0.831	0.208	25
3321	3.826	2.024	53
STW4	0.647	0.290	45
87150	41.027	16.109	39
FUG93	11.802	6.047	51
STW4a	3.014	1.371	45
9800b	10.688	1.609	15
FUG77	5.274	5.199	99
6124	0.424	0.202	48
Rbogen	9.697	0.561	6
8543	4.813	2.117	44
LT8799611	8.244	1.904	23
LUX7	3.099	0.501	16
30IV586	16.084	2.426	15
30IVG176	12.431	1.518	12
22809	5.347	1.535	29
30IVWall	5.083	0.736	14
22807	4.890	0.271	6
30IV575	2.806	2.545	91
87149	6.249	3.613	58
22007	8.359	7.630	91
30IV582	3.660	1.247	34
30VG179	9.882	6.028	61
22007	11.547	3.896	34
30V542	6.251	0.211	3
22007	11.730	6.426	55
Lux3	25.148	18.684	74
20409	1.366	0.398	29
6719	7.407	4.183	56
30V549	14.361	2.279	16
Lux4	12.778	8.473	66
Lux2	18.717	10.895	58
12325	10.051	3.164	31
30449	11.168	3.989	36

Coin	Pb208	1 $\sigma$	%RSD
Lux5	16.572	3.573	22
8544	13.003	4.255	33
21931	10.981	3.216	29
Lux1	11.449	5.400	47
LUX6	9.181	1.306	14
SFLAN3000	0.491	0.082	17
Flan	2.205	0.518	24
SFLAN1148	3.767	0.670	18
22010	7.921	2.911	37
SFLAN1045	5.913	1.036	18
SFLAN507	2.856	0.510	18
Fo124	11.979	0.610	5
Fo106	10.878	2.410	22
Fo105	1.644	2.577	157
Fo117	2.211	0.410	19
Fo116	10.372	4.442	43
22009	9.658	8.193	85
32243	2.487	1.917	77
20163	9.981	5.173	52
26827	12.310	3.416	28
20397	23.352	10.336	44
28323	16.641	5.495	33
22006	26.669	9.031	34
22011	10.420	5.044	48
31433	6.261	1.299	21
22008	9.192	1.951	21
31087	10.461	0.935	9
26228	3.436	1.181	34
19698	39.548	18.152	46
22113	36.549	17.068	47
26227	24.004	5.274	22

**Appendix 6: Trace element data; gold samples (ppm)**

Sample	Sc45	Ti47	V51	Cr52	Mn55	Fe57	Co59	Ni60	Cu ppm	Zn66	Ga69	Mo96	Ru101	Rh103	Pd105	Pd106
Br1-1	0.009	0.000	0.000	0.000	0.017	154.481	0.059	0.000	54.126	0.002	0.000	0.000	0.000	0.007	0.016	0.124
Br1-2	0.146	0.000	0.027	0.327	0.171	4.296	0.000	0.000	44.626	0.001	0.000	0.075	0.021	0.000	0.035	0.123
Br1-3	0.449	0.000	0.126	2.663	0.000	338.207	0.071	0.002	46.699	0.004	0.850	0.871	0.026	0.005	0.019	0.140
Br1-4	0.022	0.000	0.038	0.000	0.007	7.185	0.073	0.046	16.931	0.003	0.415	8.917	0.019	0.004	0.028	0.137
Br1-5	0.000	0.000	0.000	0.033	0.058	1.325	0.000	0.000	22.496	0.001	0.000	0.109	0.004	0.008	0.015	0.056
Br4-1	0.220	0.000	3.230	1.379	0.000	734.937	0.084	1.032	220.395	0.021	0.952	2.171	0.007	0.008	0.017	0.073
Br4-2	1.081	0.000	11.089	8.305	0.800	213.884	0.258	1.296	68.111	0.051	23.140	1.994	0.000	0.011	0.115	0.192
Br4-3	3.491	0.000	52.221	34.777	10.155	2599.229	1.867	10.087	119.274	0.936	40.884	109.118	0.015	0.018	0.006	0.089
Br4-5	8.141	0.000	106.280	5.165	0.976	2847.617	1.052	10.763	168.622	0.061	249.117	1.291	0.000	0.017	0.036	0.052
M17-1	0.000	0.000	0.000	0.000	0.000	0.000	0.480	0.099	11.099	0.003	0.000	0.000	0.000	0.000	1.215	1.634
M17-2	0.085	0.000	0.000	0.000	0.040	0.000	0.040	0.000	127.642	0.000	0.000	0.000	0.000	0.003	0.096	0.158
M17-3	0.015	0.000	0.000	0.000	0.000	1.133	0.121	0.000	36.266	0.001	0.000	0.000	0.000	0.000	0.641	0.927
M17-4	0.000	0.000	0.000	0.000	0.000	0.700	0.095	0.000	192.593	0.000	0.000	0.000	0.000	0.000	0.030	0.152
M17-5	0.000	0.000	0.000	0.000	0.101	0.000	0.182	0.000	1295.162	0.002	0.000	0.000	0.000	0.017	0.009	0.011
M17-7	0.000	0.000	0.000	0.000	0.145	0.000	0.201	0.000	373.109	0.000	0.118	0.334	0.033	0.009	0.023	0.061
M17-9	0.000	0.000	0.000	0.000	0.193	0.623	0.154	0.000	808.941	0.000	0.000	0.000	0.024	0.003	0.042	0.059
M17-10	0.000	0.000	0.000	0.000	0.103	50.805	0.131	0.000	906.544	0.000	0.000	0.000	0.019	0.024	0.002	0.099
M17-11	0.059	0.000	0.373	3.208	0.352	110.044	154.843	2.902	10.016	0.014	1.079	0.367	0.060	0.017	0.969	1.566
Br5-1	0.224	1.252	1.776	2.173	14.862	284.041	0.847	6.263	143.532	0.218	4.972	0.142	0.022	0.011	0.096	0.130
Br5-2	0.000	0.062	0.059	0.355	0.620	2.381	0.092	0.154	68.428	0.003	0.245	0.000	0.000	0.006	0.014	0.052
Br5-3	0.000	0.000	0.002	0.146	0.428	0.000	0.000	0.000	149.004	0.001	0.024	0.203	0.035	0.012	0.017	0.104
Br5-4	0.031	1.784	0.098	0.551	0.709	7.939	0.018	0.197	71.272	0.004	0.427	0.198	0.030	0.000	0.029	0.085
Br5-5	0.142	0.902	0.768	1.858	3.960	86.999	0.398	1.966	73.165	0.047	1.905	0.090	0.000	0.006	0.037	0.103
Br5-6	0.000	0.643	0.165	5.595	3.027	11.276	0.038	0.759	117.498	0.017	1.548	0.483	0.000	0.035	0.074	0.282
Br5-7	0.000	0.000	0.007	1.032	3.308	12.691	0.071	0.162	262.765	0.010	0.232	0.000	0.041	0.000	0.694	0.997
Br5-8	0.181	1.532	0.631	5.733	4.453	47.844	0.105	1.194	168.393	0.015	6.858	0.274	0.081	0.033	0.003	0.135
Br5-9	1.600	5.467	1.994	17.504	11.440	156.199	0.784	8.579	459.418	0.116	12.114	0.703	0.000	0.047	0.177	0.368
Br5-10	0.000	0.000	0.000	0.514	3.036	0.622	0.003	0.000	162.485	0.001	0.000	0.000	0.030	0.015	0.103	0.159
Br3-1	0.000	0.000	0.023	0.420	3.523	5.212	0.032	0.000	218.460	0.002	0.813	0.000	0.000	0.002	0.017	0.082
Br3-2	0.000	0.000	0.000	0.000	34.740	0.000	0.490	0.000	21.892	0.006	0.000	0.000	0.492	0.000	0.000	0.362
Br3-3	0.000	0.000	0.001	0.068	0.101	0.243	0.000	0.013	43.386	0.000	0.195	0.000	0.000	0.001	0.039	0.058
Br3-4	0.270	3.432	1.768	2.667	46.258	267.684	1.454	4.513	1129.105	0.091	5.178	0.316	0.009	0.024	0.022	0.070
Br3-5	0.080	1.929	0.204	10.796	2.841	26.339	0.209	0.874	174.053	0.021	3.450	0.000	0.035	0.026	0.020	0.108
Br3-6	0.000	0.000	0.000	0.000	0.223	0.150	0.000	0.036	36.023	0.001	0.000	0.000	0.005	0.002	0.029	0.128
Br3-7	0.020	2.452	0.141	0.664	0.423	7.611	0.576	2.436	40.363	0.006	0.452	0.351	0.003	0.000	0.007	0.026
Br3-9	0.000	0.000	0.000	0.120	1.267	0.178	0.001	0.063	22.493	0.000	0.000	0.059	0.017	0.002	0.045	0.217
Br3-10	0.000	4.001	0.396	0.593	0.320	1.869	0.023	0.000	738.339	0.001	0.000	0.000	0.000	0.019	0.037	0.184

Sample	Sc45	Ti47	V51	Cr52	Mn55	Fe57	Co59	Ni60	Cu ppm	Zn66	Ga69	Mo96	Ru101	Rh103	Pd105	Pd106
Br9-1	0.000	0.000	0.018	0.000	0.645	0.238	0.059	0.000	40.323	0.000	0.000	0.000	0.000	0.009	0.242	0.581
Br9-2	0.000	0.000	0.041	0.000	0.343	0.429	0.052	0.026	153.228	0.001	0.000	0.000	0.021	0.186	0.042	0.216
Br9-4	0.052	0.255	0.030	0.161	1.486	0.172	0.085	0.216	163.882	0.001	0.314	0.000	0.002	0.005	0.053	0.263
Br9-5	0.039	0.929	0.217	3.800	11.418	9.593	0.106	0.120	43.730	0.004	1.310	0.000	0.026	0.007	0.060	0.293
Br9-6	0.000	0.000	0.014	0.028	1.939	0.377	0.024	0.115	70.313	0.001	0.000	0.380	0.019	0.005	0.055	0.287
Br9-7	0.000	0.000	0.000	0.000	0.890	0.630	0.034	0.007	9.457	0.000	0.024	0.000	0.000	0.008	0.063	0.318
Br9-8	0.418	83.551	11.807	4.493	3.690	28.916	0.259	2.587	74.669	0.005	9.425	4.743	0.003	0.000	0.056	0.169
Br9-9	0.029	0.000	0.006	0.124	0.780	0.107	0.005	0.000	44.231	0.000	0.042	0.046	0.015	0.001	0.038	0.162
Br9-10	0.092	76.090	6.532	4.152	2.851	8.042	0.022	0.149	275.786	0.003	1.825	2.859	0.016	0.012	0.027	0.168
Br2-1	0.000	0.181	0.372	0.779	1.215	65.134	0.260	0.764	11.540	0.065	0.163	0.346	0.029	0.001	0.023	0.101
Br2-2	0.000	0.000	0.000	0.000	0.000	2.279	0.007	0.137	1.181	0.005	0.000	0.000	0.026	0.004	0.068	0.356
Br2-3	0.423	11.598	3.473	3.336	0.000	151.042	1.131	4.337	165.855	0.040	4.650	1.868	0.042	0.000	0.695	0.874
Br2-4	0.000	0.288	0.339	4.941	5.477	164.022	0.132	0.485	9.313	0.577	0.660	0.633	0.021	0.000	0.054	0.234
Br2-5	0.105	5.907	1.559	1.200	0.000	136.067	0.495	2.185	2.535	0.037	2.328	0.587	0.019	0.011	0.038	0.240
Br2-6	0.000	0.071	3.104	0.047	12.903	170.147	0.112	0.160	99.457	0.072	0.885	0.000	0.073	0.011	0.056	0.180
Br2-7	0.086	0.849	0.416	0.931	0.000	32.314	0.185	3.222	6.041	0.011	0.544	0.265	0.000	0.005	0.031	0.111
Br2-8	0.000	0.036	0.026	0.150	0.000	1.430	0.052	0.000	50.612	0.003	0.000	0.000	0.043	0.002	0.021	0.085
Br2-9	2.091	28.409	23.842	27.495	33.191	2006.940	5.514	15.255	342.245	0.313	45.479	7.724	0.000	0.000	2.465	3.143
Br2-10	0.045	0.792	0.322	0.739	0.505	7.996	0.023	0.000	32.983	0.027	0.694	0.212	0.000	0.005	0.010	0.045
M14-1	0.004	1.771	0.024	0.261	0.272	0.684	0.014	0.060	14.448	0.019	0.052	0.288	0.000	0.001	0.006	1.439
M14-2	0.000	3.383	5.853	4.480	3.337	16.038	0.314	0.744	13.573	0.414	0.795	0.637	0.092	0.031	0.000	0.109
M14-3	0.000	0.411	0.103	4.608	3.527	15.175	0.024	0.466	61.541	0.061	0.629	0.984	0.049	0.010	0.051	0.214
M14-4	0.000	0.093	0.003	0.894	0.000	1.262	0.059	0.091	63.161	0.026	0.000	0.000	0.000	0.013	0.017	0.101
M11-1	0.048	0.448	0.287	1.180	3.631	4.738	0.037	0.256	77.974	0.052	0.735	0.000	0.020	0.000	0.122	0.221
M11-2	1.089	8.879	3.779	11.467	22.171	104.736	0.599	3.920	411.093	0.088	7.207	1.167	0.107	0.000	0.152	0.186
M11-3	0.000	0.475	0.277	2.827	0.000	8.081	0.420	0.003	171.823	0.119	2.186	0.000	0.149	0.000	0.065	0.238
M9-1	0.000	0.000	0.025	0.000	2.538	0.532	0.084	0.023	133.622	0.000	0.000	0.000	0.000	0.016	0.064	0.156
M9-2	0.122	0.789	0.861	1.667	0.428	48.253	0.120	5.663	171.474	0.004	1.683	0.000	0.000	0.003	0.026	0.141
M9-3	0.000	0.189	0.197	0.079	3.467	83.583	0.060	0.980	419.604	0.000	0.000	0.219	0.011	0.000	0.013	0.083
M9-4	0.000	0.650	0.472	0.154	0.136	0.000	0.029	0.179	1265.880	0.000	0.000	0.256	0.000	0.033	0.037	0.438
M9-5	0.000	0.648	0.315	2.675	0.975	21.519	0.143	5.957	1489.573	0.001	1.163	0.000	0.000	0.030	0.053	0.384
M5-1	0.000	0.000	0.017	0.105	1.205	0.000	0.062	0.195	169.058	0.000	0.000	0.000	0.000	0.000	0.037	0.138
M5-3	0.805	17.206	7.742	4.198	0.000	195.137	0.690	16.026	1486.275	0.023	13.821	3.384	0.055	0.885	0.724	0.583
M5-4	0.000	0.037	0.012	0.000	0.000	0.251	0.048	0.041	261.429	0.000	0.000	0.352	0.000	0.000	0.013	0.148
M5-5	0.000	0.000	0.000	0.000	0.185	0.000	0.169	0.643	1847.917	0.000	0.000	0.000	0.040	0.000	0.244	0.372
M1-1	0.000	0.000	0.000	0.000	0.000	0.000	0.255	0.000	28.924	0.000	0.000	0.000	0.051	0.000	0.263	0.630
M1-2	0.000	0.000	0.000	0.000	0.832	0.000	0.117	0.000	25.954	0.000	0.000	0.000	0.009	0.000	0.407	0.503
M1-3	0.000	0.000	0.060	0.059	1.021	0.287	0.140	0.000	16.410	0.001	0.000	0.194	0.043	0.010	0.053	0.404
M1-4	0.115	0.000	0.113	0.000	0.341	0.550	0.136	0.109	87.600	0.000	0.000	0.000	0.012	0.000	0.239	0.481

Sample	Sc45	Ti47	V51	Cr52	Mn55	Fe57	Co59	Ni60	Cu ppm	Zn66	Ga69	Mo96	Ru101	Rh103	Pd105	Pd106
M1-5	0.000	0.000	0.000	0.000	0.162	0.179	0.148	0.000	19.357	0.000	0.000	0.162	0.012	0.000	0.134	0.325
M8-1	0.048	12.110	0.712	0.353	0.000	19.567	0.451	1.374	48.926	0.071	2.921	3.726	0.000	0.006	0.000	0.169
M8-2	0.261	9.373	0.489	3.254	2.157	114.682	0.327	0.536	20.620	0.129	0.961	0.000	0.000	0.000	0.038	0.205
M8-3	0.122	5.480	0.806	2.827	5.082	132.183	0.435	0.807	10.428	0.154	9.516	0.409	0.023	0.009	0.000	0.068
M18-2	0.083	2.784	0.258	0.000	0.000	4.589	0.241	0.216	121.349	0.016	0.047	0.000	0.118	0.002	0.071	0.072
M18-3	0.000	2.240	0.024	0.084	0.000	2.698	0.324	0.100	11.710	0.010	2.802	1.472	0.000	0.025	0.076	0.226
M18-4	0.000	28.268	1.634	13.133	8.921	321.063	2.107	2.616	376.873	0.224	9.367	0.762	0.000	0.000	0.593	0.339
M18-5	1.114	3.854	0.745	3.773	7.482	16.115	0.438	0.692	509.633	0.017	0.000	0.000	0.000	0.000	0.150	0.243
M18-6	0.000	14.784	0.721	0.701	1.330	26.707	0.546	2.440	68.662	0.074	1.381	3.243	0.062	0.009	0.800	1.071
M18-7	0.000	4.311	0.378	0.273	0.574	11.943	0.264	1.504	428.166	0.015	0.000	1.499	0.000	0.000	0.106	0.202
M18-8	0.000	14.237	0.669	3.507	2.349	60.264	0.617	76.688	40.230	0.060	5.924	1.065	0.000	0.001	0.133	0.260
M10-1	0.000	3.867	0.700	0.799	0.950	16.653	0.252	0.240	43.321	0.024	0.298	0.000	0.006	0.000	0.430	0.574
M10-3	0.241	34.294	1.163	0.890	3.970	25.747	0.173	0.388	5.989	0.013	2.438	29.128	0.000	0.005	0.020	0.034
M10-4	0.248	30.585	1.576	2.695	0.843	22.355	0.093	0.298	1.853	0.011	6.143	0.191	0.033	0.000	0.005	0.000
M10-5	0.155	6.289	0.000	0.326	0.000	29.815	0.793	2.069	9.658	0.128	0.000	0.000	0.000	0.045	0.000	0.023
M10-7	0.034	0.000	0.020	0.000	1.604	24.798	0.944	0.650	28.723	0.044	0.579	0.000	0.303	0.037	6.778	7.740
M10-9	0.000	0.814	0.016	0.053	0.002	0.501	0.035	0.106	7.080	0.003	0.000	0.053	0.000	0.000	0.005	0.020
M10-10	0.079	38.020	2.187	1.161	16.784	296.286	1.009	2.921	14.892	0.082	2.453	3.465	0.000	0.000	0.347	0.413
M13-1	0.000	10.278	0.074	6.125	0.000	39.843	0.797	2.720	362.974	0.173	0.000	0.000	0.000	0.038	0.034	0.201
M13-2	0.097	0.312	0.000	0.000	0.452	0.000	0.127	0.041	46.411	0.000	0.000	0.000	0.026	0.004	0.238	0.383
M13-3	1.219	2.089	0.502	3.971	0.000	19.186	0.652	1.053	122.830	0.029	6.866	0.000	0.081	0.000	0.111	0.289
M13-4	29.691	318.040	25.575	209.391	136.417	1484.819	32.486	103.216	82197.764	1.230	10.852	0.000	0.000	0.567	140.154	151.800
M13-5	0.000	0.654	0.428	2.608	3.365	42.534	0.454	0.069	74.799	0.028	1.322	0.000	0.043	0.000	0.037	0.176
M13-6	0.000	9.866	0.193	0.000	0.000	33.595	1.005	1.271	5592.692	0.027	0.020	0.000	0.000	0.097	7.669	9.277
M13-7	0.000	0.000	0.000	0.000	0.381	58.103	0.439	0.000	111.058	0.001	0.000	0.000	0.002	0.037	0.049	0.199
M13-8	0.030	5.319	0.098	0.334	0.198	8.578	0.079	0.130	14.136	0.006	0.097	0.160	0.000	0.000	0.016	0.032
M13-9	0.000	47.132	2.122	28.395	23.626	201.824	1.313	0.000	1033.559	0.130	0.000	0.000	0.000	0.000	0.000	0.840
M13-10	0.000	0.743	0.573	2.556	2.840	38.847	0.512	0.702	39.418	0.052	1.053	1.075	0.005	0.000	0.123	0.510
M3-1	0.115	0.000	0.188	0.955	7.891	9.416	0.562	1.067	1.664	0.013	0.000	0.000	0.000	0.030	2.089	2.553
M3-2	0.000	331.832	3.940	2.587	18.610	66.458	3.362	4.332	1678.962	0.044	7.592	44.111	0.000	0.031	0.016	0.000
M3-3	0.000	207.758	2.557	5.134	0.000	5022.214	19.147	9.576	25.380	0.011	0.025	0.000	0.000	0.000	0.236	0.079
M3-4	0.000	2.280	0.217	1.431	0.783	12.116	0.724	0.000	26.691	0.000	0.958	0.234	0.020	0.000	5.388	6.216
M3-5	0.325	49.997	1.789	3.638	15.676	44.675	0.423	0.000	4.321	0.007	3.749	0.000	0.000	0.000	0.118	0.108
M3-6	1.447	19.558	0.837	11.285	3.893	33.577	1.065	4.041	200.166	0.003	2.136	0.684	0.000	0.000	0.049	0.144
M7-1	14.158	0.000	127.614	293.461	1679.689	39998.257	117.359	420.562	824.495	6.127	0.000	1494.047	6.675	0.864	149.853	152.657
M7-2	2.173	603.441	32.463	47.999	7.983	3267.200	7.389	88.609	244.583	1.719	59.521	16.030	0.234	0.003	2.569	3.765
M7-3	0.000	72.290	7.109	18.004	17.811	240.113	1.595	6.446	112.281	0.218	11.981	0.000	0.000	0.000	15.009	17.853
M7-4	7.147	3686.613	40.736	60.318	0.000	716.884	5.919	79.449	836.845	0.454	21.965	36.823	0.116	0.122	1.576	1.203
M7-5	0.161	19.914	1.412	0.675	0.907	110.540	0.358	0.738	57.694	0.037	0.912	0.270	0.000	0.002	0.192	0.274

	M7-6	0.080	10.600	0.634	1.495	1.696	29.919	0.217	1.267	25.718	0.019	1.163	0.031	0.005	0.003	0.655	0.766
Sample	Sc45	Ti47	V51	Cr52	Mn55	Fe57	Co59	Ni60	Cu ppm	Zn66	Ga69	Mo96	Ru101	Rh103	Pd105	Pd106	
M4-1	0.000	1158.608	1.301	0.000	0.000	566.566	62.221	197.862	1563.848	0.450	153.018	124.765	0.000	0.317	52.365	65.119	
M4-2	0.032	0.000	0.000	0.000	0.743	2.151	0.179	0.000	47.356	0.001	0.000	0.000	0.064	0.013	0.058	0.426	
M4-3	0.000	0.000	0.099	0.000	0.000	2.303	0.227	0.000	17.841	0.001	1.160	0.000	0.026	0.000	0.142	0.408	
M4-4	0.000	0.000	0.195	0.000	0.489	0.000	0.205	0.218	14.830	0.001	0.000	0.000	0.000	0.019	0.127	0.363	
M12-1	0.000	0.000	0.066	0.039	1.397	10.044	0.307	0.199	32.755	0.029	0.000	0.000	0.072	0.012	0.000	0.137	
M12-2	0.000	44.236	2.784	3.190	11.003	152.338	0.976	4.173	5401.798	0.127	5.145	2.945	0.000	0.044	19.008	21.906	
M12-3	0.000	211.975	1.268	3.545	2.867	94.388	1.250	0.700	71.102	0.087	0.000	0.000	0.000	0.000	2.400	2.921	
M12-4	0.000	9.763	0.422	0.558	0.000	13.025	0.549	0.968	195.613	0.028	0.753	0.000	0.000	0.017	0.198	0.467	
M12-5	0.000	10.083	1.309	0.000	0.287	75.524	0.415	1.263	52.911	0.027	2.851	0.000	0.000	0.000	0.000	0.187	
Br6-1	0.000	7.572	0.000	0.000	3.600	0.000	1.126	0.228	6068.020	0.000	1.390	0.712	0.000	0.104	0.097	0.000	
Br6-2	0.000	0.000	0.000	0.000	0.000	0.000	1.253	1.149	3281.935	0.000	0.000	0.000	0.596	0.295	0.028	0.000	
Br6-3	1.425	483.043	45.514	25.871	49.258	6972.112	16.077	53.416	141.232	1.465	29.940	43.142	0.465	0.215	0.504	0.463	
Br6-4	0.000	2.772	1.186	0.000	8.180	0.000	5.726	5.919	16308.982	0.000	0.000	0.000	0.000	0.000	2.477	2.878	
Br6-7	0.589	0.000	0.000	0.000	0.000	0.000	0.577	2.467	6421.889	0.000	0.000	0.000	0.070	0.027	0.334	0.612	
Br6-8	0.284	0.000	0.000	0.000	0.000	0.000	0.355	0.000	91.870	0.000	0.000	0.000	0.000	0.004	0.035	0.143	
Br6-9	0.000	0.000	0.000	0.000	10.328	0.000	0.520	2.536	2068.229	0.001	0.000	0.000	0.000	0.051	0.000	0.455	
Br7-1	0.000	152.111	1.209	0.000	0.000	6.889	0.433	0.000	377.315	0.005	0.000	0.000	0.000	0.000	0.007	0.110	
Br7-2	0.000	0.000	0.000	0.000	0.000	0.000	0.153	0.000	156.743	0.000	0.000	0.000	0.000	0.022	0.014	0.054	
Br7-3	0.496	0.000	0.000	0.000	0.000	0.000	0.279	0.000	411.805	0.001	0.000	0.000	0.182	0.000	0.040	0.099	
Br7-4	1.805	212.958	8.679	8.204	2.278	284.952	1.137	15.122	256.172	0.467	29.662	7.702	0.000	0.000	0.000	0.056	
Br7-5	0.000	0.000	0.000	0.000	0.000	3.318	0.493	0.000	159.896	0.003	0.000	0.000	0.000	0.067	0.033	0.078	
Br7-6	0.000	12.509	0.448	0.000	1.147	4.127	0.256	0.000	272.256	0.032	0.000	0.000	0.172	0.000	0.041	0.187	
Br7-7	0.093	0.000	0.000	0.000	0.000	0.000	0.503	0.000	1123.736	0.004	0.000	0.000	0.131	0.000	0.054	0.203	
Br7-8	1.177	211.629	8.115	16.987	8.671	806.116	2.641	32.106	619.388	0.504	26.470	4.307	0.000	0.012	0.000	0.030	
Br8-1	0.594	119.434	3.379	3.814	12.154	188.886	1.601	3.910	773.627	0.032	7.983	2.764	0.058	0.018	0.000	0.039	
Br8-2	0.089	1.351	0.000	0.000	1.063	3.347	0.106	0.000	712.024	0.000	0.000	0.000	0.041	0.000	0.057	0.000	
Br8-3	36.064	3216.836	197.536	210.927	660.087	11917.702	43.212	180.626	1631.389	0.948	552.553	877.374	0.000	0.019	0.000	0.000	
Br8-5	0.000	0.000	0.000	0.000	0.000	0.000	0.959	1.436	1003.269	0.003	0.130	0.000	0.109	0.000	0.185	0.000	
Br8-6	3.567	357.698	21.466	10.388	25.410	744.479	29.565	35.077	2608.764	0.093	45.150	19.277	0.055	0.108	0.086	0.057	
Cam21-1	0.000	0.000	1.253	0.000	2.305	154.712	28.536	17.848	35.941	0.007	0.527	0.971	0.055	0.001	0.014	0.059	
Cam21-2	0.039	0.000	0.091	0.000	2.149	0.445	0.274	0.373	586.770	0.000	0.847	0.000	0.000	0.000	0.030	0.030	
Grf28-1	0.000	1.139	0.000	0.000	0.000	0.000	0.127	0.330	0.826	0.000	0.409	0.417	0.002	0.000	0.016	0.051	
Grf28-2	0.309	6.770	1.196	0.000	1.597	34.906	1.255	0.000	1.650	0.023	7.805	0.000	0.626	0.000	0.194	0.243	
Grf28-3	0.000	0.000	0.000	0.000	0.260	0.000	0.106	0.000	60.234	0.000	0.000	0.000	0.000	0.000	0.022	0.063	
Grf28-4	1.026	246.914	11.075	8.793	194.188	925.389	5.754	23.309	11892.936	0.090	12.818	20.245	0.000	0.090	0.319	0.268	
Grf28-5	0.000	0.000	0.000	0.000	0.098	0.253	0.766	0.000	282.871	0.009	0.000	0.000	0.000	0.000	0.231	0.252	
Grf28-6	0.000	22.170	0.000	3.467	28.180	120.180	2.751	0.000	10.160	0.124	5.847	21.308	0.000	0.182	0.000	0.142	
Grf28-7	0.000	40.128	0.729	0.000	8.267	77.793	1.877	0.000	307.642	0.005	2.934	3.121	0.097	0.000	5.330	6.116	

<b>Sample</b>	<b>Sc45</b>	<b>Ti47</b>	<b>V51</b>	<b>Cr52</b>	<b>Mn55</b>	<b>Fe57</b>	<b>Co59</b>	<b>Ni60</b>	<b>Cu ppm</b>	<b>Zn66</b>	<b>Ga69</b>	<b>Mo96</b>	<b>Ru101</b>	<b>Rh103</b>	<b>Pd105</b>	<b>Pd106</b>
<b>Cam20-1</b>	0.000	0.000	0.000	0.000	2.188	0.335	0.428	0.011	399.343	0.000	0.000	0.000	0.070	0.029	0.049	0.133
<b>Cam20-2</b>	0.000	0.000	0.000	0.000	0.000	0.000	35.141	6617.659	31673.323	0.077	0.000	71.054	0.000	26.784	11.170	6.932
<b>Grf34-1</b>	0.000	24.252	0.579	0.000	0.000	26.198	0.715	0.000	204.486	0.045	9.110	13.037	0.041	0.000	0.000	0.058
<b>Grf34-2</b>	0.034	0.514	0.000	0.000	0.000	0.000	0.135	0.408	153.532	0.003	0.215	0.433	0.011	0.000	1.055	1.235
<b>Grf34-3</b>	0.000	5.998	0.000	0.000	0.000	0.775	1.229	2.112	121.943	0.013	0.000	3.638	0.000	0.013	0.070	0.073
<b>Grf34-4</b>	0.052	0.000	0.000	0.000	0.000	0.094	0.130	0.385	22.978	0.000	0.000	0.053	0.000	0.003	1.956	2.287
<b>Grf34-5</b>	0.000	0.000	0.000	0.000	0.000	0.000	0.000	0.000	209.529	0.003	0.000	0.000	0.042	0.000	0.000	0.039
<b>Rat31-1</b>	0.000	2.516	0.000	0.000	0.000	0.000	0.414	0.575	601.141	0.006	0.000	2.104	0.074	0.000	0.000	0.155
<b>Rat31-2</b>	0.081	0.000	0.018	0.000	0.806	0.000	0.140	0.000	596.741	0.002	0.784	0.661	0.045	0.004	0.000	0.139
<b>Cam22-1</b>	0.091	0.000	0.000	0.000	0.000	1.570	0.456	0.694	335.297	0.001	0.000	0.000	0.000	0.000	0.015	0.064
<b>Cam22-2</b>	0.118	0.000	0.000	0.000	0.758	0.293	0.001	0.168	137.075	0.003	0.822	0.000	0.112	0.000	0.008	0.148

## Appendix 6: Trace element data; gold samples (ppm)

Sample	Pd108	Pd110	Ag ppm	Sn118	Sb121	Te125	W182	Os189	Ir193	Pt194	Tl205	Pb208	Bi209	AuAr+
Br1-1	0.368	0.134	109654.639	71.729	8.850	1.098	0.009	0.000	0.149	0.819	0.007	96.218	3.802	21587
Br1-2	0.381	0.134	109918.669	45.099	2.652	1.237	0.025	0.000	0.138	0.830	0.003	3.679	1.883	26635
Br1-3	0.375	0.143	109469.043	100.893	63.961	0.709	0.016	0.000	0.124	0.680	0.005	52.218	3.762	30262
Br1-4	0.365	0.138	109910.076	36.442	8.344	1.203	0.026	0.000	0.097	0.543	0.003	36.501	0.436	24513
Br1-5	0.164	0.065	49875.537	19.100	3.602	0.305	0.007	0.000	0.061	0.412	0.002	78.214	6.982	32700
Br4-1	0.153	0.090	49150.847	51.013	5.625	0.686	0.025	0.000	0.126	0.754	0.005	48.092	0.377	23793
Br4-2	0.318	0.088	49911.926	53.134	3.701	0.563	0.186	0.000	0.203	1.072	0.030	25.826	0.151	27772
Br4-3	0.184	0.090	47032.710	85.458	72.017	14.926	0.383	0.000	0.169	0.983	0.102	168.614	1.698	23769
Br4-5	0.176	0.063	46491.963	233.731	9.318	15.757	0.013	0.000	0.162	0.939	0.250	70.023	6.751	19606
M17-1	2.038	0.601	228038.578	54.538	30.475	2.293	0.017	0.000	0.125	0.607	0.003	2.514	0.042	14090
M17-2	0.187	0.115	22705.446	21.988	0.207	0.000	0.000	0.000	0.064	0.404	0.001	0.603	0.002	21058
M17-3	1.522	0.489	296778.191	87.117	258.558	2.706	0.046	0.000	0.173	0.991	0.005	1.297	0.328	13704
M17-4	0.342	0.133	101798.778	55.437	0.712	0.337	0.000	0.000	0.146	0.779	0.004	0.557	0.012	16750
M17-5	0.102	0.040	43690.599	133.086	1.827	0.562	0.033	0.000	0.479	2.500	0.002	6.887	0.024	20246
M17-7	0.171	0.059	48287.954	69.359	10.986	0.717	0.019	0.000	0.300	1.582	0.007	1.222	0.128	20385
M17-9	0.126	0.041	30256.262	59.641	0.698	0.272	0.025	0.000	0.194	1.365	0.005	1.688	0.002	20563
M17-10	0.239	0.115	64995.410	72.218	7.986	1.128	0.039	0.000	0.286	1.565	0.004	3.517	15.217	17038
M17-11	2.488	0.762	458753.472	104.024	83.063	3.497	7.016	0.000	0.153	0.809	0.004	16.406	0.045	12197
Br5-1	0.208	0.110	35205.264	42.074	0.031	0.606	0.322	1.807	0.149	0.844	0.003	32.296	0.232	29453
Br5-2	0.130	0.085	40011.038	39.957	0.325	0.372	0.103	1.551	0.081	0.471	0.003	15.872	0.058	28371
Br5-3	0.280	0.182	85362.412	50.029	0.330	1.173	0.028	2.445	0.150	0.866	0.000	0.885	0.095	26509
Br5-4	0.225	0.141	72336.116	46.305	0.019	0.835	0.077	1.002	0.122	0.642	0.002	23.526	0.043	27154
Br5-5	0.292	0.182	85175.978	40.280	0.145	1.080	0.067	2.172	0.101	0.610	0.001	36.963	0.400	26634
Br5-6	0.778	0.430	231020.354	469.681	2.119	21.822	1.005	4.517	0.237	1.433	0.004	138.776	129.307	20433
Br5-7	1.152	0.491	111056.188	86.174	0.392	1.087	0.086	1.254	0.202	1.258	0.002	21.212	0.056	23129
Br5-8	0.393	0.357	115185.469	3084.726	0.811	1.267	1.221	0.795	0.343	1.880	0.024	351.146	0.507	22861
Br5-9	0.430	0.493	88505.391	1059.690	0.465	0.000	2.058	10.775	1.137	6.469	0.077	494.863	0.622	23863
Br5-10	0.334	0.179	85537.839	56.818	0.075	1.108	0.020	2.880	0.220	1.130	0.001	1.082	0.332	25065
Br3-1	0.198	0.118	61416.578	59.139	0.064	0.746	0.029	2.162	0.142	0.805	0.002	22.479	0.043	34113
Br3-2	0.253	0.275	113066.865	617.116	1.067	2.411	0.000	21.786	3.829	21.907	0.014	21.106	0.116	32397
Br3-3	0.098	0.047	19538.035	17.374	0.131	5.996	0.005	0.563	0.053	0.293	0.000	6.048	2.305	37430
Br3-4	0.198	0.126	56804.384	1029.570	0.197	0.517	0.466	1.662	0.270	1.441	0.007	141.727	0.558	35112
Br3-5	0.282	0.172	84576.565	214.284	0.192	0.944	0.405	4.774	0.279	1.708	0.007	108.911	0.126	30553
Br3-6	0.324	0.197	101200.114	32.149	1.551	0.943	0.012	1.345	0.083	0.476	0.000	1.461	0.007	30399
Br3-7	0.072	0.041	23534.056	40.493	0.057	0.184	0.087	0.594	0.097	0.555	0.001	14.080	0.039	35296
Br3-9	0.599	0.309	168315.935	53.848	1.918	1.901	0.023	4.329	0.149	0.859	0.001	0.766	0.023	28378
Br3-10	0.488	0.267	151032.860	139.190	0.377	1.148	0.442	0.973	0.412	2.496	0.002	2.844	0.715	29019



<b>Br9-1</b>	1.172	0.628	294053.650	79.853	0.020	2.891	0.038	4.344	0.132	0.801	0.000	0.452	0.008	19209
<b>Sample</b>	<b>Pd108</b>	<b>Pd110</b>	<b>Ag ppm</b>	<b>Sn118</b>	<b>Sb121</b>	<b>Te125</b>	<b>W182</b>	<b>Os189</b>	<b>Ir193</b>	<b>Pt194</b>	<b>Tl205</b>	<b>Pb208</b>	<b>Bi209</b>	<b>AuAr+</b>
<b>Br9-2</b>	0.514	0.408	150635.990	60.820	0.014	5.746	0.002	2.493	0.167	1.033	0.023	144.471	19.058	25101
<b>Br9-4</b>	0.628	0.365	198767.036	66.299	0.013	1.695	0.024	1.191	0.181	1.030	0.001	2.855	0.015	23276
<b>Br9-5</b>	0.683	0.403	223900.804	95.863	0.060	1.537	0.070	4.060	0.212	1.147	0.002	1.512	0.150	20177
<b>Br9-6</b>	0.711	0.399	217402.704	86.272	0.015	2.552	0.017	1.576	0.176	1.051	0.001	0.874	0.044	20414
<b>Br9-7</b>	0.826	0.465	262092.874	56.986	0.070	2.547	0.041	2.715	0.112	0.610	0.001	0.263	0.058	19516
<b>Br9-8</b>	0.394	0.248	134255.885	86.682	0.012	1.543	0.451	1.411	0.262	1.575	0.001	14.907	0.431	45961
<b>Br9-9</b>	0.430	0.246	138165.738	30.174	0.109	1.202	0.013	1.750	0.074	0.435	0.000	0.388	0.508	26378
<b>Br9-10</b>	0.412	0.238	135758.653	62.802	0.017	2.005	0.564	2.564	0.158	0.934	0.011	2.322	1.231	30895
<b>Br2-1</b>	0.264	0.166	87199.396	43.581	0.096	0.775	0.016	1.336	0.075	0.458	0.001	1.895	0.043	17423
<b>Br2-2</b>	0.911	0.505	302534.154	79.770	4.479	2.775	0.047	4.428	0.136	0.757	0.001	7.689	0.018	12679
<b>Br2-3</b>	0.925	0.407	69938.284	71.588	0.084	0.693	0.046	1.994	0.179	1.195	0.001	8.802	0.113	18868
<b>Br2-4</b>	0.621	0.368	192945.949	102.621	1.137	1.681	0.028	4.675	0.132	0.821	0.001	4.714	0.062	13996
<b>Br2-5</b>	0.585	0.342	195589.850	51.518	6.144	2.046	0.057	2.821	0.085	0.502	0.001	7.442	0.031	13851
<b>Br2-6</b>	0.469	0.305	160410.007	75.833	0.415	2.664	0.029	1.349	0.171	0.928	0.000	3.261	1.021	14956
<b>Br2-7</b>	0.248	0.153	82440.234	33.403	0.083	0.738	0.094	1.095	0.072	0.394	0.000	4.412	0.026	17771
<b>Br2-8</b>	0.198	0.121	64867.301	41.240	0.141	0.754	0.014	2.348	0.114	0.683	0.000	1.552	0.049	19258
<b>Br2-9</b>	2.959	1.161	135681.786	230.542	0.147	0.000	0.141	12.191	0.473	2.609	0.004	19.622	0.262	15955
<b>Br2-10</b>	0.142	0.118	47140.704	31.103	0.088	0.554	0.024	0.000	0.092	0.484	0.000	24.174	0.132	19481
<b>M14-1</b>	0.042	0.031	14598.502	571.215	0.053	0.131	0.038	0.475	0.027	0.177	0.001	6.467	0.045	21633
<b>M14-2</b>	0.058	0.220	9502.280	248.424	0.568	1.555	0.155	2.584	0.323	2.443	0.004	188.433	0.453	22002
<b>M14-3</b>	0.422	0.331	140065.392	386.126	0.587	1.983	0.042	11.019	0.219	1.223	0.003	23.397	0.597	16403
<b>M14-4</b>	0.236	0.135	76124.059	52.971	3.889	0.906	0.015	0.000	0.075	0.467	0.000	6.421	0.024	18859
<b>M11-1</b>	0.315	0.183	63628.222	108.361	2.306	0.760	0.069	3.208	0.096	0.554	0.001	25.798	0.294	17231
<b>M11-2</b>	0.460	0.307	136388.690	630.522	24.262	1.892	0.774	2.091	0.713	3.278	0.007	93.570	4.405	15081
<b>M11-3</b>	0.643	0.367	206734.610	404.314	5.312	1.454	0.177	9.880	0.302	1.375	0.001	50.966	4.630	12701
<b>M9-1</b>	0.444	0.226	135260.463	79.496	0.007	1.381	0.020	1.029	0.179	0.927	0.001	1.145	0.002	12933
<b>M9-2</b>	0.330	0.189	105563.467	66.381	0.412	0.800	0.034	5.612	0.148	0.942	0.001	1.560	0.175	16523
<b>M9-3</b>	0.203	0.148	65632.158	60.687	0.242	0.824	0.000	4.047	0.189	1.135	0.000	1.229	0.033	20020
<b>M9-4</b>	0.527	2.499	105925.476	68.117	0.043	0.825	0.019	3.128	0.143	0.931	0.000	1.193	0.002	17333
<b>M9-5</b>	0.489	2.400	102838.950	69.517	0.091	0.391	0.029	2.271	0.164	0.934	0.001	0.883	0.008	17219
<b>M5-1</b>	0.292	0.182	93468.151	42.872	0.905	1.323	0.018	0.000	0.105	0.666	0.000	0.394	0.001	17848
<b>M5-3</b>	0.728	0.435	100508.618	223.103	1.082	10.168	0.097	15.096	0.889	5.759	0.004	185.111	0.871	18492
<b>M5-4</b>	0.295	0.174	103016.515	70.114	0.869	1.082	0.031	6.970	0.173	0.962	0.001	0.707	0.002	15093
<b>M5-5</b>	0.592	0.305	127509.170	197.157	0.016	3.301	0.000	4.108	0.611	3.619	0.000	3.038	0.026	11747
<b>M1-1</b>	1.018	0.318	260036.728	35.402	2547.862	2.100	0.000	9.032	0.126	0.777	0.017	0.364	1.317	8501
<b>M1-2</b>	0.961	0.253	177993.622	36.006	247.531	1.382	0.000	6.301	0.141	0.776	0.001	0.562	0.123	11492
<b>M1-3</b>	0.865	0.306	274679.983	35.058	721.849	2.707	0.039	40.555	0.103	0.653	0.011	0.679	0.310	7855
<b>M1-4</b>	0.855	0.310	242746.999	53.182	2539.458	1.858	0.026	0.000	0.209	1.159	0.000	0.952	0.136	8561

<b>M1-5</b>	0.804	0.285	242051.887	37.164	1878.879	1.727	0.003	29.878	0.118	0.682	0.004	0.194	0.069	9668
<b>Sample</b>	<b>Pd108</b>	<b>Pd110</b>	<b>Ag ppm</b>	<b>Sn118</b>	<b>Sb121</b>	<b>Te125</b>	<b>W182</b>	<b>Os189</b>	<b>Ir193</b>	<b>Pt194</b>	<b>Tl205</b>	<b>Pb208</b>	<b>Bi209</b>	<b>AuAr+</b>
<b>M8-1</b>	0.184	0.112	35702.888	6267.042	575.875	0.000	0.257	0.000	0.179	1.533	0.189	65.727	0.683	11184
<b>M8-2</b>	0.362	0.147	105225.460	114.301	232.377	0.896	0.059	0.000	0.127	0.752	0.061	23.409	0.170	10279
<b>M8-3</b>	0.131	0.050	41252.554	75.987	92.164	0.276	0.029	1.110	0.065	0.389	0.028	17.486	0.206	11292
<b>M18-2</b>	0.166	0.076	53175.951	3283.105	12.950	0.016	0.406	19.469	0.104	0.764	0.049	2.623	0.498	10875
<b>M18-3</b>	0.600	0.212	196290.997	970.994	1156.409	1.341	0.290	6.515	0.143	0.656	0.010	1.611	0.540	6494
<b>M18-4</b>	0.973	0.279	198963.655	36487.589	101.993	2.765	12.443	0.000	0.300	2.641	0.169	13.327	6.701	4547
<b>M18-5</b>	0.575	0.282	167964.724	1094.466	84.282	2.883	0.727	24.036	0.397	2.247	0.071	3.473	0.352	7445
<b>M18-6</b>	0.983	0.439	79720.414	14549.762	771.084	0.745	2.177	11.318	0.183	1.068	0.064	7.830	2.009	8323
<b>M18-7</b>	0.318	0.119	64944.692	2170.674	111.879	0.215	0.465	20.069	0.174	1.065	0.059	3.097	0.384	10330
<b>M18-8</b>	0.462	0.148	105912.385	3909.273	31.316	1.517	1.558	17.724	0.117	0.664	0.107	10.805	0.594	7767
<b>M10-1</b>	0.584	0.159	40212.623	74.284	1.948	0.554	0.029	1.296	0.093	0.571	0.030	9.292	0.228	8527
<b>M10-3</b>	0.022	0.007	4655.966	8994.680	34.566	0.000	1.003	0.000	0.128	0.966	0.031	27.955	0.038	14737
<b>M10-4</b>	0.050	0.026	14927.844	129.783	2.331	0.146	0.079	4.654	0.288	1.976	0.022	2.232	0.068	14065
<b>M10-5</b>	0.109	0.027	30955.910	10972.852	128.104	2.651	0.043	0.000	0.515	3.007	0.055	10.867	0.184	12646
<b>M10-7</b>	7.304	1.653	19674.926	2258.988	49.580	1.699	0.027	44.955	0.560	3.434	0.032	7.036	0.051	13100
<b>M10-9</b>	0.051	0.017	16427.722	352.413	2.120	0.149	0.071	2.136	0.031	0.208	0.002	0.509	0.003	13191
<b>M10-10</b>	0.395	0.096	6974.791	5200.574	70.256	0.105	0.059	0.000	0.358	2.456	0.128	6.044	0.161	15108
<b>M13-1</b>	0.491	0.193	135657.094	109.654	1.586	2.433	0.104	4.436	0.167	1.785	0.048	26.354	0.119	6719
<b>M13-2</b>	0.365	0.146	69465.116	26.538	365.019	0.944	0.002	11.759	0.083	0.519	0.012	0.798	0.384	8275
<b>M13-3</b>	0.523	0.282	131636.521	107.136	179.481	2.216	0.044	0.000	0.280	1.542	0.000	5.683	0.426	6776
<b>M13-4</b>	137.109	30.160	126964.502	3348.611	36.846	37.100	1.682	634.176	9.096	45.378	3.678	336.127	11.769	5451
<b>M13-5</b>	0.350	0.134	97452.062	71.177	1.738	1.054	0.011	19.212	0.224	1.487	0.008	4.728	1.027	7539
<b>M13-6</b>	8.894	2.063	101551.897	81.517	3.406	0.438	0.000	0.000	0.352	2.091	0.058	5.121	0.079	7726
<b>M13-7</b>	0.371	0.122	118342.922	30.494	0.326	1.535	0.000	23.169	0.122	0.701	0.012	25.798	0.008	7454
<b>M13-8</b>	0.083	0.033	28962.150	8.790	350.201	0.276	0.005	0.325	0.037	0.191	0.014	1.001	0.054	8613
<b>M13-9</b>	1.059	0.452	246769.101	366.252	16.991	10.187	0.014	0.000	1.494	8.891	0.000	22.124	0.600	5123
<b>M13-10</b>	0.638	0.266	219891.362	103.950	1.648	2.341	0.013	13.340	0.210	1.063	0.051	11.039	0.050	5295
<b>M3-1</b>	2.109	0.551	16346.333	129.888	301.484	2.738	0.006	12.483	0.465	2.583	0.059	37.202	1.898	8953
<b>M3-2</b>	0.000	0.000	10063.495	235.070	670.217	0.998	0.607	33.157	0.444	2.394	0.030	64.313	1.628	10872
<b>M3-3</b>	0.106	0.065	9476.018	139.184	579.949	0.608	2.650	0.000	0.349	2.252	0.037	48.750	1.719	9594
<b>M3-4</b>	5.660	1.155	11865.926	154.146	476.443	2.144	0.000	2.714	0.487	2.769	0.000	44.538	2.098	11390
<b>M3-5</b>	0.133	0.150	8042.039	266.549	1165.875	0.150	0.109	0.000	0.526	3.583	0.178	136.007	4.327	14594
<b>M3-6</b>	0.227	0.065	17000.174	229.046	547.346	6.573	0.114	109.378	0.688	3.599	0.034	67.530	3.000	7481
<b>M7-1</b>	149.343	32.462	9215.269	5470.323	160.740	156.409	7.565	0.000	25.340	146.934	220.266	859.385	88.511	9794
<b>M7-2</b>	3.913	0.822	82522.751	150.841	18.378	10.636	0.948	18.518	0.511	4.205	0.193	210.936	6.136	9577
<b>M7-3</b>	16.485	3.708	161658.691	317.816	5.678	32.075	0.217	33.079	0.926	7.199	0.203	21.919	0.603	8042
<b>M7-4</b>	2.405	0.680	245440.511	346.516	22.370	73.354	4.980	122.101	1.086	37.351	0.658	288.056	6.766	5772
<b>M7-5</b>	0.278	0.077	24885.600	27.956	2.212	2.632	0.924	6.404	0.068	0.831	0.029	40.349	0.111	12082

<b>M7-6</b>	0.703	0.161	10259.539	5.906	0.372	1.734	0.024	2.000	0.030	1.562	0.023	9.603	0.116	13595
<b>Sample</b>	<b>Pd108</b>	<b>Pd110</b>	<b>Ag ppm</b>	<b>Sn118</b>	<b>Sb121</b>	<b>Te125</b>	<b>W182</b>	<b>Os189</b>	<b>Ir193</b>	<b>Pt194</b>	<b>Tl205</b>	<b>Pb208</b>	<b>Bi209</b>	<b>AuAr+</b>
<b>M4-1</b>	52.166	11.977	242865.374	5070.858	1006.163	0.000	10.612	1553.983	14.514	100.648	0.375	664.606	23.577	11497
<b>M4-2</b>	0.867	0.288	298999.628	46.550	969.743	2.438	0.008	175.490	0.401	1.075	0.000	0.374	0.096	7794
<b>M4-3</b>	1.011	0.338	339975.163	97.051	237.555	2.913	0.130	0.000	0.162	0.767	0.022	2.426	0.204	6024
<b>M4-4</b>	0.951	0.305	335853.248	49.043	232.623	2.550	0.000	9.339	0.131	0.688	0.007	1.587	0.125	6433
<b>M12-1</b>	0.268	0.075	96835.705	407.835	2.314	0.340	0.056	2.280	0.092	0.926	0.014	2.058	0.085	8539
<b>M12-2</b>	18.779	4.478	38488.580	6072.127	27.621	0.000	14.489	32.184	0.631	4.365	0.948	27.498	0.314	11435
<b>M12-3</b>	3.121	0.833	224743.871	529.577	13.201	1.249	0.563	28.460	0.358	1.756	0.392	8.116	0.228	4951
<b>M12-4</b>	0.547	0.118	146565.869	321.437	13.944	1.025	0.086	8.414	0.247	1.505	0.022	4.919	0.000	7673
<b>M12-5</b>	0.508	0.218	176058.595	1277.063	1498.038	3.256	0.011	13.290	0.260	1.575	0.122	2.939	0.749	6962
<b>Br6-1</b>	0.038	0.039	23614.363	61.783	0.116	0.000	0.000	0.000	0.392	2.062	0.000	1.650	0.000	7124
<b>Br6-2</b>	0.234	0.012	33541.511	111.958	0.974	0.000	0.000	26.217	0.518	2.469	0.008	2.510	0.025	6348
<b>Br6-3</b>	0.000	0.068	18991.111	285.394	9.255	0.000	0.467	0.000	0.613	5.699	0.183	251.357	0.331	6703
<b>Br6-4</b>	3.323	0.788	150467.060	491.912	5.532	7.819	0.000	890.980	2.163	15.681	0.274	31.077	0.910	5012
<b>Br6-7</b>	0.517	0.164	51882.523	62.309	0.499	0.444	0.069	0.000	0.218	1.869	0.000	2.269	0.079	3922
<b>Br6-8</b>	0.207	0.105	43844.119	36.616	42.855	0.709	0.000	0.000	0.132	0.666	0.008	0.924	0.000	4873
<b>Br6-9</b>	0.174	0.301	45295.269	136.024	52.036	4.487	0.008	0.000	0.643	4.047	0.000	4.288	0.013	4566
<b>Br7-1</b>	0.145	0.086	45470.067	66.992	3.232	0.000	10.637	3.095	0.194	1.633	0.016	7.178	0.647	7067
<b>Br7-2</b>	0.112	0.074	43938.743	49.779	0.420	15.865	0.002	37.717	0.215	1.113	0.000	3.517	0.074	7385
<b>Br7-3</b>	0.196	0.302	53800.107	60.270	8.074	0.000	0.002	22.635	0.287	1.511	0.014	2.001	0.035	6514
<b>Br7-4</b>	0.137	0.121	46109.237	94.270	5.047	0.000	0.257	0.000	0.210	1.524	0.036	9.301	0.304	6939
<b>Br7-5</b>	0.138	0.149	51832.330	59.521	6.804	0.000	0.112	3.580	0.217	1.366	0.011	6.017	2.216	5704
<b>Br7-6</b>	0.190	0.093	53911.604	63.886	5.842	3.488	0.000	22.358	0.232	1.668	0.003	4.016	0.000	6284
<b>Br7-7</b>	0.228	0.177	72951.161	48.507	11.968	1.255	0.000	7.702	0.189	1.853	0.018	3.855	0.054	7834
<b>Br7-8</b>	0.148	0.168	35325.938	56.054	4.821	0.905	0.199	0.000	0.166	1.384	0.041	13.852	0.136	8336
<b>Br8-1</b>	0.095	0.038	35075.900	42.985	2.837	0.795	0.101	26.830	0.152	0.965	0.005	5.468	1.303	6811
<b>Br8-2</b>	0.027	0.046	19271.997	77.563	10.734	3.240	0.000	10.939	0.297	2.367	0.016	2.123	0.092	8001
<b>Br8-3</b>	0.119	0.051	24745.683	408.399	2411.447	2.381	2.832	0.000	0.763	3.583	1.548	144.625	4.982	5444
<b>Br8-5</b>	0.081	0.063	40990.961	189.007	38.760	5.609	0.000	0.000	0.845	5.528	0.004	10.618	6.441	7319
<b>Br8-6</b>	0.160	0.206	39428.258	251.344	2186.244	17.759	3.170	7.359	0.939	5.314	0.096	86.014	37.441	7762
<b>Cam21-1</b>	0.137	0.061	49615.393	34.780	6.133	0.834	0.318	0.000	0.067	0.361	0.004	1.918	4.296	5520
<b>Cam21-2</b>	0.238	0.156	49390.238	66.421	0.734	0.000	0.000	9.349	0.166	0.973	0.005	3.891	0.100	5460
<b>Grf28-1</b>	0.108	0.037	29994.971	6.397	2.345	0.009	0.005	3.410	0.020	0.100	0.002	0.126	0.003	4664
<b>Grf28-2</b>	0.061	0.113	30350.022	348.491	4.902	0.000	0.000	48.118	0.850	4.195	0.165	41.100	0.131	6682
<b>Grf28-3</b>	0.114	0.047	29960.720	23.763	0.191	0.000	0.000	15.939	0.083	0.425	0.000	0.906	0.009	4059
<b>Grf28-4</b>	0.266	0.082	17467.867	596.009	14.090	1.420	0.458	122.254	0.691	4.704	0.026	55.271	0.633	6650
<b>Grf28-5</b>	0.344	0.029	29562.832	223.875	1.184	2.789	0.000	25.427	0.378	2.874	0.108	54.196	0.032	5694
<b>Grf28-6</b>	0.048	0.000	23756.245	7233.307	76.666	0.308	0.042	0.000	1.575	9.465	0.109	489.531	4.506	6530
<b>Grf28-7</b>	5.300	1.163	29450.403	166.121	3.997	0.000	0.416	81.636	0.737	4.296	0.068	36.480	1.393	6407

<b>Sample</b>	<b>Pd108</b>	<b>Pd110</b>	<b>Ag ppm</b>	<b>Sn118</b>	<b>Sb121</b>	<b>Te125</b>	<b>W182</b>	<b>Os189</b>	<b>Ir193</b>	<b>Pt194</b>	<b>Tl205</b>	<b>Pb208</b>	<b>Bi209</b>	<b>AuAr+</b>
<b>Cam20-1</b>	0.297	0.120	99508.135	75.414	104.290	1.180	0.007	0.000	0.159	0.838	0.016	2.120	0.785	6207
<b>Cam20-2</b>	1.360	7.243	104380.068	1506.932	124.153	0.000	1.775	0.000	4.247	36.131	0.377	35.526	0.259	3820
<b>Grf34-1</b>	0.143	0.079	41597.121	258.857	31.968	0.000	0.036	28.100	0.489	2.898	0.001	87.118	13.091	9283
<b>Grf34-2</b>	1.154	0.270	41675.080	43.044	12.603	0.549	0.018	0.000	0.119	0.540	0.003	10.082	0.017	7507
<b>Grf34-3</b>	0.100	0.053	39854.008	141.803	4.970	0.000	0.000	0.000	0.331	3.271	0.000	36.703	0.331	6470
<b>Grf34-4</b>	2.082	0.461	39943.429	22.649	6.555	0.259	0.000	6.226	0.056	0.315	0.006	2.803	0.167	5279
<b>Grf34-5</b>	0.092	0.041	40089.375	26.957	1.381	0.000	0.000	0.000	0.069	0.308	0.009	2.000	0.001	3093
<b>Rat31-1</b>	0.300	0.158	88046.872	554.508	818.973	0.357	0.056	12.519	0.151	0.782	0.000	2.636	0.247	6356
<b>Rat31-2</b>	0.218	0.183	88312.087	208.328	919.135	1.062	0.096	24.204	0.151	0.864	0.000	1.861	0.276	5811
<b>Cam22-1</b>	0.205	0.071	59659.803	71.291	0.585	1.305	0.016	0.000	0.180	0.992	0.002	4.091	0.106	7215
<b>Cam22-2</b>	0.244	0.401	59782.067	72.015	86.596	1.124	0.032	0.000	0.075	0.484	0.006	1.784	0.539	6325

Appendix 7:Pb isotope data acquired by solution and Laser Ablation MC-ICPMS, for gold, silver and copper coins and gold samples.

Gold Coins	206Pb/204Pb	1s	207Pb/204Pb	1s	208Pb/204Pb	1s	207/206	1s
2950	9.60235	0.013797	8.111754	0.004799	20.034784	0.010361	0.844768	0.000861
3321	13.570191	0.002409	11.443633	0.008019	28.271806	0.022503	0.843292	0.000376
6124	3.223595	0.011483	2.706507	0.010241	6.714131	0.028528	0.839593	0.000062
6719	17.962987	0.000759	15.151715	0.000417	37.498683	0.001435	0.843496	0.000016
8543	17.241445	0.002766	14.486107	0.003474	35.893589	0.012522	0.840191	0.000061
8544	18.194343	0.006475	15.310323	0.002094	37.946526	0.00814	0.841488	0.000288
12325	18.498876	0.003033	15.544134	0.003602	38.560769	0.01202	0.840275	0.000055
20163	15.513933	0.001001	13.119784	0.000855	32.432325	0.003027	0.845677	0.000018
26227	16.166565	0.001519	13.702622	0.001176	33.815839	0.004257	0.84759	0.000028
26228	0.601584	1.115743	0.506316	0.946036	1.25316	2.359523	0.841639	0.000099
28323	18.134568	0.001769	15.245505	0.002095	37.797878	0.00675	0.840687	0.000036
87149	16.749394	0.001623	14.081275	0.001572	34.936281	0.00528	0.840704	0.000048
20397a	18.23858	0.000854	15.432434	0.001447	38.126856	0.003859	0.846142	0.00004
20397b	18.254535	0.001097	15.447739	0.001405	38.166052	0.00388	0.846241	0.000051
20397c	17.855107	0.001297	15.108486	0.001677	37.33016	0.005296	0.846172	0.000038
21931a	18.38132	0.001435	15.440209	0.001294	38.284791	0.004355	0.839995	0.000045
21931b	17.0517	0.001375	14.323183	0.001144	35.514918	0.00497	0.839986	0.000014
22006a	16.33031	0.003349	13.749043	0.003665	34.066393	0.010229	0.841934	0.000053
22007a	18.264378	0.000929	15.362396	0.00136	38.075867	0.004437	0.841113	0.000032
22007b	18.134696	0.001828	15.253566	0.001868	37.807953	0.006225	0.841126	0.00002
22007a2	17.420615	0.002349	14.653976	0.002528	36.324872	0.008634	0.841186	0.000034
2200b2	18.532311	0.002341	15.588739	0.002267	38.640334	0.008001	0.841165	0.000028
22010a	17.922939	0.001063	15.079804	0.001287	37.373492	0.003006	0.841369	0.00003
22010surface	13.814361	0.00421	11.622242	0.00401	28.804055	0.011403	0.841316	0.000053
22113line	18.395765	0.002258	15.491092	0.002036	38.31685	0.020896	0.842101	0.000082
22113spot	18.477442	0.000866	15.55791	0.001379	38.548478	0.004111	0.841995	0.000049
22809a	17.839566	0.00134	14.990565	0.001228	37.184949	0.003883	0.840299	0.000016
2950b	9.799178	0.008043	8.265628	0.004671	20.431906	0.01229	0.843502	0.000184

Gold Coins	206Pb/204Pb	1s	207Pb/204Pb	1s	208Pb/204Pb	1s	207/206	1s
2950c	9.467955	0.005313	7.985674	0.004073	19.742675	0.011744	0.843442	0.000095
30449a	18.112002	0.001549	15.272697	0.00171	37.805568	0.005249	0.843236	0.000033
30449b	17.77596	0.001443	14.988591	0.001559	37.100905	0.004423	0.843194	0.000027
30IV575	10.327376	0.006252	8.690409	0.005195	21.520185	0.0176	0.841492	0.000021
30IV582	7.417371	0.00279	6.235937	0.002925	15.463279	0.008348	0.840721	0.000031
30IV586	13.806763	0.002086	11.596958	0.001743	28.771687	0.003882	0.839948	0.000015
30IVwall	18.426146	0.000854	15.486177	0.000528	38.431433	0.001593	0.840446	0.00006
30V542	11.718926	0.001527	9.851324	0.001518	24.423042	0.00544	0.840634	0.000027
30V549	9.953072	0.011436	8.383359	0.010004	20.764153	0.024028	0.842289	0.000034
30VG179	6.363487	0.00997	5.353203	0.00878	13.270324	0.02189	0.841237	0.000034
6124b	4.208828	0.009844	3.533905	0.00723	8.767411	0.016236	0.839641	0.000104
9800b	18.050156	0.001554	15.247266	0.002124	37.697031	0.005924	0.844717	0.000044
flanb	13.754732	0.002928	11.567858	0.003126	28.683248	0.009485	0.841009	0.000034
fo105	11.980889	0.004707	10.006866	0.004563	24.787762	0.012004	0.835236	0.000039
Fo106	12.980601	0.000387	10.923547	0.000809	27.065488	0.003385	0.841529	0.000038
FO116	12.249672	0.002234	10.266114	0.002964	25.400159	0.008542	0.838073	0.00006
FO116b	12.706456	0.003763	10.650083	0.004038	26.349728	0.010788	0.838163	0.000058
FO117	4.278939	0.005534	3.589647	0.003928	8.871881	0.011062	0.838911	0.000086
Fo124	11.440103	0.000969	9.62137	0.001071	23.854712	0.004061	0.841021	0.000033
FUG121	1.809516	0.046158	1.523671	0.038181	3.769902	0.09593	0.842032	0.00009
FUG122	16.706266	0.006774	14.082072	0.00866	34.826077	0.028686	0.842922	0.000177
FUG77	13.302923	0.003625	11.207146	0.004211	27.720402	0.007302	0.842457	0.000083
FUG93	17.878423	0.001497	15.068614	0.002538	37.25543	0.006771	0.842838	0.000086
G176	4.185273	0.028689	3.517529	0.024149	8.722837	0.058784	0.840454	0.000013
Lt8799611	8.922762	0.002651	7.499704	0.002408	18.597188	0.007178	0.840514	0.000018
lux1	17.412617	0.001215	14.685843	0.00095	36.344689	0.004654	0.843402	0.000011
lux2	18.28068	0.001449	15.37461	0.002004	38.120111	0.006203	0.841031	0.000045
lux3	17.961419	0.003131	15.108049	0.003562	37.470037	0.012654	0.841139	0.00005
lux4	18.223727	0.000706	15.342006	0.001259	38.012689	0.003564	0.84187	0.000035

Gold Coins	206Pb/204Pb	1s	207Pb/204Pb	1s	208Pb/204Pb	1s	207/206	1s
lux5	18.226611	0.002414	15.379293	0.002427	38.060422	0.008831	0.843782	0.000028
lux6	18.113786	0.001076	15.384425	0.001133	37.929172	0.002965	0.849321	0.000034
lux7	17.36048	0.003166	14.641132	0.002284	36.235347	0.009016	0.84336	0.000111
FlanA	16.654932	0.001571	14.005933	0.002384	34.725298	0.008086	0.840948	0.000067
Sch23Robiano	11.294752	0.001401	9.534827	0.001331	23.510392	0.004341	0.844182	0.000025
SFLAN1045	17.687287	0.00365	14.830321	0.003785	36.80599	0.013114	0.838473	0.000049
SFLAN1148	14.447391	0.004332	12.156034	0.004734	30.137035	0.015019	0.8414	0.000058
SFLAN3000	4.877775	0.004557	4.104546	0.003762	10.164633	0.01129	0.841479	0.000129
SFLAN507	15.529366	0.004841	13.057652	0.003783	32.386592	0.008017	0.840836	0.000041
Stw4	12.211034	0.006045	10.297742	0.006032	25.448622	0.015419	0.843315	0.000057
STW4a	17.31174	0.004535	14.586351	0.004544	36.10499	0.013443	0.84257	0.000051
Stw4bb	8.014061	0.008948	6.757917	0.007909	16.705638	0.019874	0.843257	0.000024
30IVWALL	18.644504	0.000369	15.666657	0.000357	38.864433	0.000838	0.840283	0.000004
22007	18.62104	0.000321	15.660785	0.000276	38.810873	0.000634	0.841026	0.000002
19697	18.653476	0.000895	15.680793	0.001003	38.889326	0.002805	0.840636	0.000008
19698	18.670032	0.000275	15.681302	0.000419	38.908516	0.001326	0.839918	0.000001
20397	18.507772	0.000611	15.65951	0.000296	38.6915	0.000828	0.846105	0.000008
20409	18.610166	0.001182	15.65759	0.001326	38.797093	0.004359	0.841346	0.000017
21931	18.646941	0.000778	15.669125	0.000612	38.845487	0.00198	0.840305	0.000014
21932	18.601797	0.001447	15.679214	0.001155	38.806268	0.003415	0.842887	0.000006
22008	18.57799	0.000182	15.667488	0.000145	38.779988	0.000557	0.843336	0.000007
22009	18.599779	0.000463	15.661229	0.000525	38.798403	0.001603	0.842012	0.000008
22010	18.619025	0.001041	15.664437	0.00087	38.824135	0.00235	0.841313	0.000013
22011	18.459602	0.000836	15.65762	0.001322	38.641522	0.002666	0.84821	0.000022
22113	18.605046	0.000864	15.664197	0.000786	38.813731	0.002321	0.841933	0.000004
26827	18.578721	0.001147	15.664098	0.00149	38.779238	0.004612	0.84312	0.000021
31087	18.650696	0.000516	15.664199	0.000608	38.860886	0.002386	0.839872	0.000001
32243	18.654573	0.000748	15.676855	0.001043	38.875102	0.001789	0.840376	0.000006
30IVWALL	18.644504	0.000369	15.666657	0.000357	38.864433	0.000838	0.840283	0.000004

<b>22007</b>	<b>18.62104</b>	0.000321	<b>15.660785</b>	0.000276	<b>38.810873</b>	0.000634	<b>0.841026</b>	0.000002
<b>Gold Samples</b>	<b>206Pb/204Pb</b>	1 $\sigma$	<b>207Pb/204Pb</b>	1 $\sigma$	<b>208Pb/204Pb</b>	1 $\sigma$	<b>207/206</b>	1 $\sigma$
Br1	<b>18.093338</b>	1.50E-03	<b>15.583051</b>	2.55E-03	<b>38.117739</b>	5.88E-03	<b>0.861259</b>	6.60E-05
Br1.2	<b>18.100865</b>	1.50E-03	<b>15.588263</b>	2.55E-03	<b>38.132279</b>	5.88E-03	<b>0.861189</b>	6.60E-05
Br2	<b>18.264203</b>	2.64E-03	<b>15.615978</b>	2.08E-03	<b>38.283302</b>	5.33E-03	<b>0.855005</b>	2.66E-05
Br2.2	<b>18.247888</b>	4.16E-03	<b>15.600306</b>	3.67E-03	<b>38.249546</b>	8.82E-03	<b>0.85491</b>	2.06E-05
Br3	<b>18.330097</b>	1.91E-03	<b>15.629596</b>	2.00E-03	<b>38.387628</b>	6.01E-03	<b>0.852674</b>	2.29E-05
Br4	<b>18.327901</b>	6.42E-04	<b>15.620327</b>	5.52E-04	<b>38.284039</b>	1.62E-03	<b>0.85227</b>	1.24E-05
Br5	<b>18.414525</b>	6.66E-04	<b>15.64199</b>	8.82E-04	<b>38.394075</b>	2.59E-03	<b>0.849438</b>	1.75E-05
Br6	<b>18.444516</b>	3.07E-03	<b>15.658701</b>	1.95E-03	<b>38.410622</b>	6.40E-03	<b>0.848962</b>	2.07E-04
Br7	<b>18.18366</b>	2.20E-04	<b>15.578973</b>	3.55E-04	<b>38.00891</b>	1.21E-03	<b>0.856757</b>	8.02E-06
Br8	<b>18.262931</b>	2.25E-04	<b>15.589036</b>	2.65E-04	<b>38.112063</b>	7.11E-04	<b>0.853589</b>	6.71E-06
Br9	<b>16.957653</b>	1.53E-03	<b>15.264896</b>	1.81E-03	<b>36.922209</b>	5.56E-03	<b>0.900177</b>	2.16E-05
M1	<b>18.504118</b>	7.81E-04	<b>15.668576</b>	7.74E-04	<b>38.640124</b>	2.04E-03	<b>0.846762</b>	1.56E-05
M2	<b>18.144755</b>	1.21E-02	<b>15.613599</b>	1.56E-02	<b>38.29587</b>	1.89E-02	<b>0.860502</b>	4.81E-03
M3	<b>18.43279</b>	2.64E-02	<b>15.660163</b>	2.99E-02	<b>38.48032</b>	3.46E-02	<b>0.849582</b>	3.53E-03
M5	<b>18.550981</b>	4.97E-02	<b>15.795157</b>	4.36E-02	<b>38.936426</b>	1.07E-01	<b>0.851446</b>	1.55E-04
M8	<b>18.314601</b>	2.57E-03	<b>15.707917</b>	3.19E-03	<b>38.379012</b>	7.47E-03	<b>0.857672</b>	6.22E-05
M8.2	<b>18.298259</b>	3.09E-03	<b>15.694289</b>	2.58E-03	<b>38.346192</b>	6.56E-03	<b>0.857693</b>	2.78E-05
M9	<b>18.378143</b>	6.44E-03	<b>15.68179</b>	5.40E-03	<b>38.405811</b>	1.23E-02	<b>0.853285</b>	2.61E-05
br2	<b>18.391543</b>	0.002704	<b>15.602546</b>	0.002092	<b>38.258294</b>	0.004834	<b>0.848354</b>	0.00004
br9	<b>18.759964</b>	0.004106	<b>15.678018</b>	0.003599	<b>38.362691</b>	0.008781	<b>0.835717</b>	0.000018
m11	<b>18.602081</b>	0.001734	<b>15.598832</b>	0.001824	<b>38.489579</b>	0.003812	<b>0.838553</b>	0.000034
m7	<b>18.271271</b>	0.000758	<b>15.601614</b>	0.00074	<b>38.28513</b>	0.001565	<b>0.853888</b>	0.000007
M5	<b>18.406548</b>	0.001826	<b>15.615495</b>	0.001547	<b>38.44323</b>	0.004251	<b>0.848366</b>	0.000016
m13	<b>18.129075</b>	0.000888	<b>15.586057</b>	0.000816	<b>38.084531</b>	0.002314	<b>0.859727</b>	0.000007
m10	<b>18.054453</b>	0.014688	<b>15.462047</b>	0.012464	<b>37.79824</b>	0.030472	<b>0.856412</b>	0.000055
m10b	<b>17.997071</b>	0.011415	<b>15.412953</b>	0.009192	<b>37.680046</b>	0.025357	<b>0.856415</b>	0.000079
M14	<b>18.826372</b>	0.009466	<b>15.591235</b>	0.008068	<b>38.430904</b>	0.020194	<b>0.828159</b>	0.000028
M8	<b>18.251548</b>	0.008668	<b>15.59366</b>	0.007464	<b>38.219465</b>	0.017772	<b>0.854375</b>	0.000036



M18	<b>18.543113</b>	0.006943	<b>15.739314</b>	0.005937	<b>38.707763</b>	0.014725	<b>0.848796</b>	0.000051
M18b	<b>18.53089</b>	0.008843	<b>15.727511</b>	0.007357	<b>38.683733</b>	0.018568	<b>0.848719</b>	0.000068
M12	<b>25.710231</b>	0.034922	<b>16.273348</b>	0.024789	<b>77.975071</b>	0.109066	<b>0.632952</b>	0.000083
M12b	<b>25.217174</b>	0.073733	<b>16.180655</b>	0.045637	<b>75.538034</b>	0.225643	<b>0.641652</b>	0.000084

**Silver and Copper alloys**

	<b>206Pb/204Pb</b>	1 $\sigma$	<b>207Pb/204Pb</b>	1 $\sigma$	<b>208Pb/204Pb</b>	1 $\sigma$	<b>207/206</b>	1 $\sigma$
20794	<b>18.59046</b>	0.000242	<b>15.666302</b>	0.000278	<b>38.797906</b>	0.000718	<b>0.842707</b>	0.000006
20160	<b>18.627609</b>	0.000447	<b>15.660467</b>	0.000395	<b>38.832377</b>	0.000991	<b>0.840713</b>	0.000003
15654	<b>18.651565</b>	0.000528	<b>15.667798</b>	0.000509	<b>38.85512</b>	0.001122	<b>0.840026</b>	0.000005
20791	<b>18.716277</b>	0.000918	<b>15.677344</b>	0.000833	<b>38.977731</b>	0.00215	<b>0.837632</b>	0.000005
15666	<b>18.618903</b>	0.000447	<b>15.654324</b>	0.000442	<b>38.814135</b>	0.001125	<b>0.840776</b>	0.000006
20988	<b>18.710023</b>	0.000281	<b>15.671386</b>	0.000302	<b>38.956507</b>	0.000723	<b>0.837593</b>	0.000006
20792	<b>18.662741</b>	0.000326	<b>15.668148</b>	0.00035	<b>38.888919</b>	0.000705	<b>0.839542</b>	0.000005
20793	<b>18.648671</b>	0.000675	<b>15.667497</b>	0.000533	<b>38.878734</b>	0.001477	<b>0.84014</b>	0.000004
20411	<b>18.399243</b>	0.000291	<b>15.667044</b>	0.000255	<b>38.548661</b>	0.000642	<b>0.851505</b>	0.000002
20165	<b>18.686119</b>	0.000312	<b>15.676287</b>	0.000263	<b>38.869818</b>	0.000675	<b>0.838927</b>	0.000002
20143	<b>18.695916</b>	0.000657	<b>15.672082</b>	0.000629	<b>38.945534</b>	0.001541	<b>0.838262</b>	0.000007
23039	<b>18.473614</b>	0.000293	<b>15.671488</b>	0.000248	<b>38.696545</b>	0.000551	<b>0.848317</b>	0.000003
SFLAN1451	<b>18.63328</b>	0.001036	<b>15.675512</b>	0.00075	<b>38.852621</b>	0.001666	<b>0.841264</b>	0.000001
SFLAN617b	<b>18.704308</b>	0.000291	<b>15.682143</b>	0.000254	<b>38.903048</b>	0.000682	<b>0.838424</b>	0.000005
SFLAN617	<b>18.706017</b>	0.000243	<b>15.683767</b>	0.000149	<b>38.907715</b>	0.000497	<b>0.838434</b>	0.000005
1299	<b>18.584475</b>	0.00038	<b>15.750163</b>	0.000361	<b>38.900751</b>	0.001188	<b>0.84749</b>	0.000008
19696	<b>2.370276</b>	0.01322	<b>3.641193</b>	0.016465	<b>5.567935</b>	0.022231	<b>1.536189</b>	0.003438
20186	<b>2.393257</b>	0.00843	<b>3.684145</b>	0.011342	<b>5.635699</b>	0.014823	<b>1.539385</b>	0.003254
20189	<b>2.378746</b>	0.006897	<b>3.656987</b>	0.008577	<b>5.593335</b>	0.014933	<b>1.537359</b>	0.002466
20411	<b>18.737381</b>	0.000149	<b>15.954609</b>	0.000398	<b>39.260588</b>	0.001902	<b>0.851486</b>	0.000009
20416	<b>18.618581</b>	0.000208	<b>15.835576</b>	0.000303	<b>38.986225</b>	0.000867	<b>0.850525</b>	0.000008
21825	<b>18.86613</b>	0.000982	<b>15.952324</b>	0.001177	<b>39.433479</b>	0.003404	<b>0.845554</b>	0.000002
23039	<b>18.44407</b>	0.001282	<b>15.647993</b>	0.001438	<b>38.641526</b>	0.004956	<b>0.848402</b>	0.000019
23039b	<b>2.365712</b>	0.020295	<b>3.626279</b>	0.032783	<b>5.535353</b>	0.042999	<b>1.532849</b>	0.0125

23040	<b>18.776629</b>	0.000548	<b>15.781721</b>	0.000583	<b>39.154601</b>	0.001814	<b>0.840498</b>	0.000008
24619	<b>18.7304</b>	0.000456	<b>15.789641</b>	0.000421	<b>39.054826</b>	0.001309	<b>0.842995</b>	0.000013
<b>Silver and Copper alloys</b>								
	<b>206Pb/204Pb</b>	1 $\sigma$	<b>207Pb/204Pb</b>	1 $\sigma$	<b>208Pb/204Pb</b>	1 $\sigma$	<b>207/206</b>	1 $\sigma$
24829	<b>19.846782</b>	0.001373	<b>16.675847</b>	0.001109	<b>41.364943</b>	0.002678	<b>0.840229</b>	0.000016
24829b	<b>18.761899</b>	0.000424	<b>15.766253</b>	0.000573	<b>39.103898</b>	0.002028	<b>0.840334</b>	0.000016
24861	<b>18.597442</b>	0.000397	<b>15.835356</b>	0.000411	<b>38.966267</b>	0.001554	<b>0.85148</b>	0.000011
26657	<b>19.309052</b>	0.001276	<b>16.453405</b>	0.00109	<b>40.525629</b>	0.003039	<b>0.852108</b>	0.000013
29476	<b>18.840969</b>	0.001262	<b>15.798871</b>	0.001342	<b>39.199</b>	0.004132	<b>0.838538</b>	0.000014
29867	<b>24.493326</b>	0.002585	<b>20.526096</b>	0.001968	<b>50.984065</b>	0.005708	<b>0.838028</b>	0.000032

**Appendix 7:Pb isotope data acquired by solution and Laser Ablation MC-ICPMS, for gold, silver and copper coins and gold samples.**

<b>Gold Coins</b>	<b>208/206</b>	<b>1s</b>
2950	2.086446	0.001026
3321	2.083376	0.001045
6124	2.082809	0.000292
6719	2.087553	0.000076
8543	2.08182	0.000354
8544	2.085622	0.000486
12325	2.084492	0.000297
20163	2.090529	0.000051
26227	2.091715	0.00007
26228	2.083101	0.000429
28323	2.0843	0.000169
87149	2.085824	0.000212
20397a	2.090451	0.000111
20397b	2.090771	0.000105
20397c	2.090727	0.000147
21931a	2.08281	0.000081
21931b	2.082779	0.000122
22006a	2.086084	0.000173
22007a	2.084707	0.000134
22007b	2.084841	0.000134
22007a2	2.085166	0.00021
2200b2	2.085025	0.000167
22010a	2.085232	0.000042
22010surface	2.085081	0.000173
22113line	2.082917	0.001206
22113spot	2.086245	0.000135
22809a	2.084409	0.000088
2950b	2.085063	0.000702

<b>Gold Coins</b>	<b>208/206</b>	<b>1s</b>
2950c	2.08521	0.000121
30449a	2.087321	0.000109
30449b	2.087139	0.00008
30IV575	2.0838	0.000297
30IV582	2.084739	0.000135
30IV586	2.083884	0.000044
30IVwall	2.085701	0.000157
30V542	2.084068	0.000154
30V549	2.086206	0.000091
30VG179	2.085385	0.000137
6124b	2.083101	0.000389
9800b	2.08846	0.000142
flanb	2.085337	0.000179
fo105	2.068942	0.000128
Fo106	2.085072	0.000176
FO116	2.073538	0.000211
FO116b	2.073728	0.000199
FO117	2.073384	0.00013
Fo124	2.085183	0.000208
FUG121	2.083376	0.000095
FUG122	2.084612	0.000857
FUG77	2.083783	0.000226
FUG93	2.083821	0.000221
G176	2.084174	0.000102
Lt8799611	2.084241	0.000106
lux1	2.087262	0.000117
lux2	2.085268	0.000172
lux3	2.08614	0.000326
lux4	2.08589	0.00011

<b>Gold Coins</b>	<b>208/206</b>	<b>1s</b>
lux5	2.088179	0.0002
lux6	2.09394	0.0001
lux7	2.087232	0.000206
FlanA	2.084986	0.000273
Sch23Robiano	2.081532	0.000181
SFLAN1045	2.080929	0.000306
SFLAN1148	2.085985	0.000315
SFLAN3000	2.083867	0.000585
SFLAN507	2.085506	0.000194
Stw4	2.084068	0.000146
STW4a	2.085578	0.000214
Stw4bb	2.084541	0.000085
30IVWALL	2.084498	0.00001
22007	2.084248	0.000006
19697	2.08483	0.000048
19698	2.084009	0.00004
20397	2.090554	0.00002
20409	2.084726	0.000098
21931	2.08321	0.000034
21932	2.086157	0.000034
22008	2.087416	0.000013
22009	2.08596	0.000035
22010	2.085186	0.000047
22011	2.093302	0.000065
22113	2.086194	0.000015
26827	2.087293	0.000107
31087	2.083616	0.000058
32243	2.083945	0.000025
30IVWALL	2.084498	0.00001

<b>22007</b>	<b>2.084248</b>	0.000006
--------------	-----------------	----------

**Gold Samples**

	<b>208/206</b>	1 $\sigma$
Br1	<b>2.106728</b>	1.42E-04
Br1.2	<b>2.106655</b>	1.42E-04
Br2	<b>2.096084</b>	5.54E-05
Br2.2	<b>2.096108</b>	4.82E-05
Br3	<b>2.09424</b>	1.26E-04
Br4	<b>2.088839</b>	4.04E-05
Br5	<b>2.084989</b>	6.29E-05
Br6	<b>2.082496</b>	1.53E-04
Br7	<b>2.090278</b>	3.19E-05
Br8	<b>2.086854</b>	2.16E-05
Br9	<b>2.177318</b>	1.19E-04
M1	<b>2.088191</b>	4.53E-05
M2	<b>2.110575</b>	9.62E-03
M3	<b>2.087602</b>	6.38E-03
M5	<b>2.098888</b>	4.82E-04
M8	<b>2.095542</b>	1.53E-04
M8.2	<b>2.09562</b>	5.88E-05
M9	<b>2.089755</b>	5.16E-05
br2	<b>2.080211</b>	0.000187
br9	<b>2.044923</b>	0.000057
m11	<b>2.069101</b>	0.000068
m7	<b>2.095373</b>	0.00002
M5	<b>2.088563</b>	0.000026
m13	<b>2.100743</b>	0.000048
m10	<b>2.093569</b>	0.000123
m10b	<b>2.093677</b>	0.000091
M14	<b>2.041334</b>	0.0001
M8	<b>2.09404</b>	0.000051

M18	<b>2.087447</b>	0.00011
M18b	<b>2.087527</b>	0.000038
M12	<b>3.032842</b>	0.000335
M12b	<b>2.9955</b>	0.000601
<b>Silver and Copper alloys</b>		
	<b>208/206</b>	1 $\sigma$
20794	<b>2.086979</b>	0.000016
20160	<b>2.084668</b>	0.000012
15654	<b>2.08321</b>	0.000017
20791	<b>2.082558</b>	0.000018
15666	<b>2.084663</b>	0.000014
20988	<b>2.08212</b>	0.000012
20792	<b>2.083773</b>	0.000013
20793	<b>2.084799</b>	0.000007
20411	<b>2.095122</b>	0.000003
20165	<b>2.080144</b>	0.000003
20143	<b>2.083104</b>	0.000016
23039	<b>2.094693</b>	0.000007
SFLAN1451	<b>2.08512</b>	0.000022
SFLAN617b	<b>2.079898</b>	0.000013
SFLAN617	<b>2.079957</b>	0.000011
1299	<b>2.093185</b>	0.000028
19696	<b>2.349066</b>	0.007058
20186	<b>2.354824</b>	0.006915
20189	<b>2.35138</b>	0.005274
20411	<b>2.095308</b>	0.000064
20416	<b>2.093942</b>	0.000025
21825	<b>2.090173</b>	0.000076
23039	<b>2.095065</b>	0.000125
23039b	<b>2.339826</b>	0.022728

23040	<b>2.085284</b>	0.000039
-------	-----------------	----------

24619	<b>2.085104</b>	0.000045
-------	-----------------	----------

**Silver and Copper alloys**

<b>208/206</b>	$1\sigma$
----------------	-----------

24829	<b>2.084214</b>	0.000034
-------	-----------------	----------

24829b	<b>2.084218</b>	0.000056
--------	-----------------	----------

24861	<b>2.095249</b>	0.000054
-------	-----------------	----------

26657	<b>2.098789</b>	0.000051
-------	-----------------	----------

29476	<b>2.080519</b>	0.000064
-------	-----------------	----------

29867	<b>2.081549</b>	0.000096
-------	-----------------	----------



**Appendix 8: Cu isotope data acquired by solution and Laser Ablation MC-ICPMS, for the gold, silver and copper coins and the gold samples.**

**Gold Coins**

<b>Sample</b>	<b>δCu65 with Ni spike</b>	<b>1s</b>	<b>δCu65 without Ni spike</b>	<b>1s</b>
<b>26228</b>	-0.5735	0.00002	-0.33035	0.00006
<b>Fo116</b>	-2.14113	0.00004	-2.20157	0.00004
<b>Fo117</b>	0.23341	0.00009	-0.44057	0.00022
<b>Fo117surface</b>	-0.28886	0.00002	-0.25088	0.00003
<b>Fo116b surface</b>	-2.0577	0.0001	-2.12661	0.00014
<b>Sch23rob</b>	-0.25512	0.00005	-0.33416	0.00007
<b>22011-3</b>	0.31994	0.01132	0.19047	0.00881
<b>22011-1</b>	0.13644	0.00755	0.16628	0.00961
<b>22011-2</b>	0.20318	0.01418	0.20119	0.01064
<b>FUG93</b>	-1.04777	0.00006	-0.65256	0.00014
<b>FUG121</b>	0.21463	0.00001	0.01261	0.00002
<b>32243-1</b>	0.18233	0.0094	0.21483	0.01162
<b>32243-2</b>	0.12806	0.01486	0.2125	0.00987
<b>32243-3</b>	0.22818	0.01586	0.25066	0.01031
<b>22809a</b>	1.0198	0.00002	1.44576	0.00008
<b>30IV329</b>	0.86809	0.00619	0.86937	0.01823
<b>30IV575</b>	-1.46168	0.00004	-1.13419	0.00008
<b>30IV586</b>	0.17987	0.00007	0.18471	0.00006
<b>30V542</b>	-0.53936	0.00004	-0.28556	0.00004
<b>30VG179</b>	-0.25039	0.00003	0.04432	0.00003
<b>20409</b>	0.18866	0.00001	0.22422	0.00002
<b>22006</b>	0.03757	0.00014	0.5044	0.00009
<b>26827</b>	0.89746	0.00002	0.79581	0.00002
<b>31087</b>	0.16516	0.00003	0.32366	0.00005
<b>21931a</b>	-1.17435	0.00002	-1.3369	0.00002
<b>21931b</b>	0.04406	0.01005	-0.07988	0.01036
<b>22007a</b>	0.69766	0.00004	0.9265	0.00006
<b>22007b</b>	1.30898	0.00002	1.11652	0.00002
<b>22007c</b>	1.03066	0.00002	0.45497	0.00007
<b>28323polished</b>	0.1806	0.00001	0.00549	0.00001
<b>28323surface</b>	-0.216	0.00004	-0.41611	0.00005
<b>26827</b>	0.22386	0.01083	0.09024	0.00727
<b>22010</b>	0.83618	0.01114	0.7053	0.0106
<b>20409</b>	1.64247	0.01061	1.54718	0.01006
<b>21932</b>	0.75179	0.0112	1.02587	0.00558
<b>22113</b>	1.81974	0.01135	1.65271	0.01286
<b>22009</b>	2.11157	0.01441	1.91691	0.01424
<b>22008</b>	0.20861	0.01503	0.0311	0.00839
<b>21087-3</b>	0.10663	0.01222	0.14979	0.00954
<b>31087-1</b>	0.04868	0.00873	0.09954	0.01044
<b>31087-2</b>	0.04129	0.01785	0.09915	0.01157
<b>20397a</b>	0.28871	0.01299	0.13773	0.01011
<b>20397b</b>	0.44116	0.00005	0.7566	0.00004
<b>26227</b>	0.36793	0.00005	0.46396	0.00007
<b>30449</b>	0.91769	0.00003	0.66352	0.00003

**Silver coins**

<b>Sample</b>	<b>δCu65 with Ni spike</b>	<b>1s</b>	<b>δCu65 without Ni spike</b>	<b>1s</b>
<b>20794</b>	0.3314	0.00851	0.31244	0.01458
<b>15666</b>	1.25936	0.01133	1.17921	0.01465
<b>15654-1</b>	0.9478	0.0135	0.78437	0.01272

<b>15654-2</b>	0.77384	0.01251	0.77556	0.01756
<b>20143</b>	0.24311	0.01329	0.21638	0.01262
<b>20791</b>	0.15272	0.01033	0.11995	0.01528
<b>20988</b>	0.36987	0.00917	0.36351	0.0149
<b>20160</b>	0.92391	0.01027	0.87993	0.01106
<b>20792</b>	0.81547	0.01201	0.77677	0.0161
<b>20793</b>	0.56698	0.00878	0.51665	0.01377
<b>Copper alloys</b>				
<b>20165-1</b>	1.74716	0.00549	1.73283	0.01449
<b>20165-3</b>	1.67811	0.0045	1.73424	0.01577
<b>20411</b>	1.78325	0.01452	1.81101	0.01384
<b>23039-1</b>	0.14799	0.00721	0.13525	0.00854
<b>23039-2</b>	0.09115	0.00761	0.10643	0.01128
<b>23039-3</b>	0.06953	0.0082	0.14003	0.0104
<b>SF1451</b>	-0.05984	0.0074	-0.00822	0.01243
<b>SF617</b>	0.18372	0.00716	0.26397	0.00883
<b>19697</b>	0.23621	0.01038	0.026	0.01026
<b>19698</b>	0.35624	0.00971	0.2768	0.00969
<b>Gold Samples</b>				
<b>M9</b>	0.45754	0.02158	-0.96019	0.01046
<b>M15</b>	0.39792	0.00593	0.34395	0.01794
<b>M13</b>	0.64705	0.00676	0.53698	0.0134
<b>M8</b>	-0.09362	0.0049	-0.09733	0.0167
<b>Br7</b>	0.62962	0.0059	0.61657	0.01881
<b>M10</b>	-0.40445	0.0114	-0.40829	0.01345
<b>M14</b>	0.30548	0.01091	0.35333	0.0149
<b>M5</b>	1.335	0.00769	1.27149	0.01858
<b>Br2</b>	0.91438	0.00959	0.80057	0.01088
<b>M17</b>	0.78844	0.00608	0.58453	0.01891
<b>M11</b>	0.31322	0.00419	0.34106	0.00959
<b>M18</b>	1.92123	0.0057	1.8966	0.01404
<b>Br4</b>	1.03867	0.00695	0.70345	0.01175
<b>Br5</b>	0.64773	0.00795	0.63598	0.00891
<b>Br2</b>	1.45257	0.02598	1.35099	0.01722
<b>M9</b>	0.43695	0.00618	-0.11079	0.00703
<b>M8</b>	0.36584	0.03319	0.25378	0.01049
<b>Br3</b>	-2.86621	0.01751	0.66784	0.01456
<b>Br1</b>	0.63638	0.03707	0.78553	0.00716
<b>M2</b>	2.29495	0.01558	1.50354	0.01296
<b>Br7</b>	0.72787	0.01281	0.57526	0.01141
<b>M3</b>	-0.32142	0.0257	-0.24629	0.0089
<b>Br9</b>	0.72303	0.01165	-0.63089	0.00928
<b>M1</b>	1.53675	0.02827	1.59733	0.01073
<b>Br6</b>	0.17576	0.01968	-0.07874	0.00892
<b>M5</b>	1.27066	0.01764	-0.04923	0.00845